Conducting Research to Better Define the Sequestration Options in Eastern Ohio and the Appalachian Basin

by

Christopher J. Perry, Matthew S. Erenpreiss, Timothy E. Leftwich,
Ronald A. Riley, Gregory A. Schumacher, Michael P. Solis, and Mark E. Wolfe

Open-File Report 2013-2
Columbus 2022

Graphic design & layout:
Jeremy E. Gladden

Front Cover:
Zoomed-in view showing partial section of the project's area of review. Green and reddish areas represent oil & gas fields. Blue, green, and orange points represent CO2 sources. Red line represents the boundary of the area of review. Brown line represents the boundary of the Appalachian Basin. See fig. 2 for the original map.

RECOMMENDED CITATION:

Perry, C.J., Erenpreiss, M.S., Leftwich, T.E., Riley, R.A., Schumacher, G.A., Solis, M.P., and Wolfe, M.E., 2013 [2022], Conducting Research to Better Define the Sequestration Options in Eastern Ohio and the Appalachian Basin: Columbus, Ohio Department of Natural Resources, Division of Geological Survey Open File Report 2013-2, 111 p.

FOREWORD

Carbon Capture, Utilization, and Storage (CCUS) is the process by which carbon dioxide (CO_2) is removed from industrial sources, transported, and either stored for further commercial use or injected underground for long-term geologic sequestration. In Ohio, coal-fired power plants, steel mills, and fertilizer plants generate the largest amounts of carbon dioxide. Many scientists consider efficient and economic management of CO_2 emissions as being essential if the nation and the world continue to depend on combustion of coal, oil, and natural gas for generation of electricity. Soon, management of greenhouse-gas emissions through geologic sequestration may become a major consideration for Ohio's industries.

The Division of Geological Survey has established itself as a leader in Ohio for CCUS research over the last 20 years. In the early 2000s, Ohio was involved in one of the first CO_2-sequestration projects in the world, Midcontinent Interactive Digital Carbon Atlas and Relational database (MIDCARB). From 2003 through 2020, Ohio was part of a very influential partnership called the Midwest Regional Carbon Sequestration Partnership (MRCSP). The MRCSP was managed by Battelle Memorial Institute with Ohio initially serving as the geologic team lead in the eight-state region, which also included Indiana, Kentucky, Maryland, Michigan, New York, Pennsylvania, and West Virginia. MRCSP conducted regional and site-specific characterization for geologic CO_2-sequestration, along with performing small-scale CO_2-injection tests in Ohio. Starting in 2020, Ohio entered into a new expanded partnership, the Midwest Region Carbon Initiative (MRCI). This new partnership, encompassing 20 states and led by Battelle Memorial Institute, has a goal to accelerate CCUS deployment in the Midwestern and Northeastern United States. MRCI builds upon more than 20 years of CCUS experience from the MIDCARB and MRCSP partnerships, with plans on advancing CCUS research and large-scale deployment throughout the region.

In 2010, the ODGS entered into a research agreement with the Ohio Coal Development Office (OCDO) to produce a series of reports on CCUS potential in Ohio. The first report of the project involved inventorying all available relevant data and summarizing all the potential sequestration targets for Ohio. While the report was finished in 2013, the data inventory and analyses in the report is still relevant for CCUS activities in Ohio.

This report is significant for several reasons. There is a new emphasis on large scale CCUS implementations in the United States. The report provides a comprehensive inventory of subsurface geologic data to start the process of site selection and implementation of CCUS in Ohio. In addition, the data outlined in this report can be used for oil and gas exploration, enhanced oil and gas recovery projects, solution mining projects (U.S. EPA Class III injection wells), natural gas liquid (NGL) storage projects, exploration for rare earth elements and critical minerals, and oil-field brine (U.S. EPA Class II injection wells) and hazardous and industrial waste disposal (U.S. EPA Class I injection wells). Because of the increased emphasis in CCUS and due to the potential multiple uses of this report, we feel that the report is of great use and should be released to the public.

James McDonald, February 2022

Final report

on

Conducting Research to Better Define the Sequestration Options in Eastern Ohio and the Appalachian Basin

Grant Agreement No. CDO/D-10-07b

This project was funded in part by the
Ohio Coal Development Office of the Ohio Development Services Agency,
Office of Energy, State of Ohio

Project co-funded by Ohio Department of Natural Resources
State of Ohio

Christopher J. Perry, Project Manager
Energy Resources Group Supervisor
ODNR Division of Geological Survey
2045 Morse Rd., Bldg. C-2
Columbus, Ohio 43229-6693
(614) 265-6576

Written by
Christopher Perry, Matthew Erenpreiss, Tim Leftwich,
Ron Riley, Greg Schumacher, Michael Solis, and Mark Wolfe

Submitted on January 31, 2013
Period of Performance: June 1, 2010–January 31, 2013

ACKNOWLEDGMENTS

The authors thank the Ohio Coal Development Office within the Ohio Air Quality Development Authority for funding this project. We also thank Battelle for being our collaborators on this project.

Special thanks go to Dean Martin, Chuck Salmons, Lisa Van Doren, and Joe Wells of the Technology Transfer Group at the ODNR Division of Geological Survey for their patience and skill in helping compile this report and their assistance to team members as this study progressed. Finally, thanks go to Division Chief Thomas J. Serenko for his thoughtful review of this document.

DISCLAIMER

This report was prepared by Ohio Department of Natural Resources, Division of Geological Survey as a result of research performed and funded through a grant from the Ohio Coal Development Office of the Ohio Air Quality Development Authority (OCDO/OAQDA). Neither the State of Ohio nor any of its agencies, nor any person acting on behalf of the State:

(1) Make any warranty or representation, express or implied, with respect to the accuracy, completeness, or usefulness of the information contained in this report, or that the use of any information, apparatus, method, or process disclosed in this report may not infringe privately-owned rights; or

(2) Assume any liabilities with respect to the use of, or for damages resulting from the use of, any information, apparatus, method or process disclosed in this report.

Reference herein to any specific commercial product, process, or service by trade name trademark, manufacturer, or otherwise, does not necessarily constitute or imply its endorsement, recommendation, or favoring; nor do the views and opinions of authors expressed herein necessarily state or reflect those of the State of Ohio or its agencies.

NOTICE TO JOURNALISTS AND PUBLISHERS: Please feel free to quote and borrow from this report; however, please include a statement noting the Ohio Coal Development Office's support for the project.

EXECUTIVE SUMMARY

This report summarizes the results by the Ohio Department of Natural Resources (ODNR), Division of Geological Survey (the Survey) to identify and evaluate geologic sequestration options for CO_2 emissions in eastern Ohio and the upper Ohio River Valley (UORV) area. The research summarized herein represents Step 1 of a three-step process, funded by the Ohio Coal Development Office (OCDO), to support the development of a regional strategy for sequestering CO_2. This research primarily supports the coal-burning electric-power industry along with other large, industrial point-source CO_2 emitters in the area that collectively provide affordable energy, valuable jobs, and significant economic input for the region.

During this project, the Survey successfully collected, digitized, and evaluated all pertinent geologic data archived at the Survey's offices and those of the ODNR Division of Oil and Gas Resources Management (DOGRM). Stratigraphic intervals were interpreted and location maps were created for all data types. New regional cross sections and structure maps were generated to better define the stratigraphic and structural framework of Ohio's subsurface geology. Data from four "Piggyback" wells drilled during this project were incorporated into these maps and cross sections. In collaboration with Battelle, preliminary interpretations were made of 280 miles (mi) of seismic reflection data. Also, CO_2-enhanced oil recovery (EOR) potential from the state's first CO_2 injection test, in the East Canton oil field, was evaluated for its sequestration and secondary oil recovery potential.

Archived data collected and mapped during this project include:

250,000 drillers' well cards.
5,066 well (rock) cuttings and 845 cores.
74,400 suites of oil and gas geophysical logs.
307 wells with porosity and permeability analyses.
8,251 wells with formation and well pressure data.
203 Class I and Class II disposal injection well data points.
569 reservoir brine geochemical data points.
4 published reports with interpreted lineaments.
Statewide coverage of gravity and magnetic geophysical data.
488 wells with datasets for bottom-hole temperature.
555 mi of public domain seismic reflection data.
280 mi of newly acquired seismic reflection data.

Four types of CO_2 sequestration targets are considered important for eastern Ohio and the UORV: (1) deep saline formations, (2) oil and gas fields, (3) unmineable coal beds, and (4) carbonaceous shales. Geologic formations greater than 2,500 feet (ft) deep are primary targets because pressure at such depth is sufficient to keep the CO_2 under supercritical (liquid) conditions. At these depths there are also adequate confining intervals to protect the deepest underground sources of drinking water. Deep saline formations, the primary focus of this project, collectively possess the largest volume of storage capacity to sequester CO_2. Oil and gas fields offer the potential to utilize injected CO_2 for EOR and these fields typically benefit from being well characterized, delineated, and possessing proven containment. Unmineable coal beds and carbonaceous shales offer the least sequestration potential. Depth to coals is less than 2,500 ft, and carbonaceous shales are actively being explored and produced for oil and gas.

Structure maps using over 50,000 well control points were constructed on the top of the Silurian Dayton Formation, the Middle Devonian Onondaga Limestone, and the Upper Devonian Berea Sandstone. These detailed structure maps illustrate regional and linear structural trends that are coincident on all maps. Mapping multiple horizons with such dense well control proved to be a good diagnostic tool for developing the structural framework in the subsurface. Piggyback wells and other new deep wells drilled in eastern Ohio have provided useful geophysical-log and hydraulic data, which was applied by the Survey and Battelle during this project to create updated regional cross sections of sub-Knox stratigraphy. For example, the Georgetown Marine well shows that eastern Belmont County apparently lacks laterally extensive target injection zones. Several of the other piggyback wells showed viable injection zones in the sub-Knox to Precambrian interval. The newly created map of brine disposal-well injection rates identifies areas of higher injectivity and will be useful for targeting reservoirs and geographic areas that could also be favorable for CO_2 sequestration. Finally, reservoir characterization and the 80-t cyclic-CO_2 test of the "Clinton" sandstone shows that this widely-present

and well-developed eastern Ohio reservoir exhibits favorable CO_2 injectivity and that CO_2 mixes with oil in the reservoir, increasing oil mobility and productivity.

Recommendations for future work include additional wireline logging, flow testing, and coring projects in areas where geologic data is lacking, as shown by maps of data distribution in this report. Additional work is needed to incorporate structure maps with recent seismic line acquisitions to develop a better understanding of the stratigraphic and structural framework. Larger-scale (10,000–20,000 metric tons [t]) injection testing also is recommended to better evaluate the efficacy of CO_2-EOR and sequestration in the "Clinton" and other reservoirs in eastern Ohio. Finally, continued assessment through detailed reservoir characterization and field studies of targeted reservoirs is needed to better evaluate the best sequestration options for eastern Ohio and the UORV.

Coal-fired power plants are the largest single stationary source contributor to CO_2 emissions in the United States, accounting for approximately 1.8 billion t per year. Long-term storage of CO_2 in deep geologic formations is the only known means for directly mitigating CO_2 emissions from industrial sources. Many scientists believe carbon capture and storage (CCS) is a necessary element in an overall worldwide strategy to mitigate the environmental effects of CO_2, which is thought to be a major factor in climate change. The geologic knowledge gained from this research should provide critical information necessary to support decision-making by policy makers and key shareholders in developing a long-term, cost-effective management strategy for eastern Ohio and the UORV region.

CONTENTS

FIGURES

TABLES

APPENDICES

UNIT ABBREVIATIONS USED IN THIS REPORT

Hydraulic conductivity (K)	
feet per day	ft/day
Length	
foot	ft
mile	mi
meter	m
kilometer	km
inch	in
centimeter	cm
Mass	
pound	lb
gram	g
metric ton (tonne)	t
million metric ton	MMt
Permeability	
millidarcy	md
Pressure	
pounds per square inch	psi
Production Rates	
barrels of oil per day	bopd
Time	
billion years	b.y.
million years	m.y.
hour	hr
Temperature	
degrees Celsius	˚C
Transmissivity	
square feet per day	ft^2/day
Volume	
cubic feet	ft^3
thousand cubic feet	MCF
million cubic feet	MMCF
million cubic feet per day	MMCF/d
billion cubic feet	BCF
barrel	bbl
million barrels	MMbbl
thousand standard cubic feet	MSCF
stock tank barrel of oil	STBO
million stock tank barrels of oil	MMSTBO
thousand stock tank barrels of oil	MSTBO
Water Quality	
parts per million	ppm

Conducting Research to Better Define the Sequestration Options in Eastern Ohio and the Appalachian Basin

INTRODUCTION

Background

This report presents results of research by the Ohio Department of Natural Resources (ODNR), Division of Geological Survey (the Survey) during Step 1 of a three-step characterization of geologic sequestration options in eastern Ohio and the upper Ohio River Valley (UORV) region (Table 1). The Survey, Battelle, and the OCDO, along with many industrial partners, have been investigating Ohio's options for geologic sequestration since 2003, mostly through funding from the U.S. Department of Energy (US DOE) via the Midwest Regional Carbon Sequestration Partnership (MRCSP).

Much understanding has been gained through research by the MRCSP; however, despite that work, eastern Ohio and the UORV Valley region in general, still lacks adequate characterization to properly define this area's options. The region has one of the largest concentrations of large CO_2 point sources in the United States, and because of this, it is an area requiring thorough evaluation. The eastern Ohio portion of the UORV contains nine potential deep saline formations, three of which are considered to be local targets. However, because of limited well penetrations, the areal extents and injectivity of these formations have been only minimally characterized.

The technology associated with long-term storage of CO_2 in deep geologic formations is commonly called *Carbon Capture and Geologic Storage* or CCS. The CO_2 targeted by CCS technology is largely that emitted by coal-burning power plants and other industrial operations prevalent in the UORV region. Long-term storage of CO_2 in deep geologic formations is the only known means for directly mitigating CO_2 emissions from industrial sources that are critical to the economic vitality of the region.

During CCS, the CO_2 first would be separated and captured from the exhaust gases of various point source industrial emissions, then transported by pipeline at supercritical pressure ($\geq$1,200 psi) to various deep wells, and finally injected into porous sandstone, dolomite, or limestone reservoirs at depths at or below 2,500 ft below ground surface. A minimum depth of 2,500 ft is needed to keep the CO_2 under enough pressure to maintain supercritical (or liquid) state. Far more CO_2 can be stored under such conditions than in a gaseous state. Many scientists and engineers view CCS technology as a necessary element in an overall national and worldwide strategy to reduce CO_2 emissions thought to be accelerating climate change.

A large number of depleted oil-and-gas fields are present in eastern Ohio and surrounding areas of the UORV. These fields provide an opportunity to synergistically sequester CO_2 in deep reservoirs while also enhancing oil production from these fields. The US DOE now recognizes that enhanced oil recovery (EOR) will play a vital role in the early deployment of CCS technology (Rogers, 2012). Such utilization will be possible within the broader scope of a CO_2 storage infrastructure. Utilizing CO_2 for EOR and sequestration is termed *Carbon Capture, Utilization, and Storage* or CCUS.

Coal-generated electric power is the single largest contributor to CO_2 emissions in the United States and largely to the world (US EPA, 2012). Coal is an important part of the Ohio economy and of the UORV region in general. The manufacturing-based UORV economy has evolved around coal in large part because of plentiful and affordable coal-generated electric power. Some of the largest and newest coal-fired electric plants have been constructed and now operate in the UORV.

TABLE 1.—*Outline of three-step program for eastern Ohio geologic characterization*

Activity	Step 1 Jun 2010–Jan 2013	Step 2 ~3 years	Step 3 ~4 years
Review existing data; compile regional maps and supporting data	• Search and analyze existing well logs in eastern Ohio • Purchase and reprocess selected existing seismic data focused in eastern Ohio	• Extend review and analysis of existing well logs to broader UORV region • Broaden search for acquisition and reprocessing of existing seismic data to the UORV region • Extend analysis to include EOR and other value-added options	• Conduct additional review of existing well logs and core data in the UORV beyond that in Steps 1 and 2 • An assessment of EOR potential in the region • Existing data will be used to guide piggyback and drilling activities
Piggybacking on commercial wells	• Conduct several piggyback projects focused in eastern Ohio	• Conduct three to four additional piggyback projects in selected areas of the broader UORV region	• Conduct several additional piggyback projects if available in strategic areas
Seismic acquisition		• Conduct one to two 3D surveys (~10 sq mi each) in targeted areas	• Conduct one to two additional 3D surveys in conjunction with purpose drilled wells
Drilled wells		• Plan for location and design of purpose-drilled wells in Step 3 • Conduct one EOR huff-n-puff at a selected site	• Implement several purpose-drilled wells in strategically selected locations not available by piggyback

Figure 1 shows the multistate UORV region that includes the eastern part of Ohio delineated as the Area of Review (AOR) for this study. This figure also shows the large CO_2 point sources within 50 and 75 miles (mi) of the Ohio River that might one day depend on geologic storage of CO_2 emissions in this region. Most of these sources are coal-fired power plants and collectively, they have an output of over 200 million metric tons (t) of CO_2 per year. Figure 2 shows the eastern Ohio AOR within the context of the entire State of Ohio; the figure also shows the western boundary of the Appalachian Basin and all oil and gas fields that have been identified and mapped within Ohio. Carbon capture, utilization, and storage potentially could be applied to many of these eastern Ohio oil and gas fields.

The UORV contains a number of potential deep saline formations that have been characterized and tested by only a very limited number of exploratory wells. Thus the areal extent and potential for CO_2 injectivity and storage for each of these deep saline formations requires additional study and testing. The area also contains hundreds of oil and gas fields that, through the deployment of EOR, may hold the potential to store very significant amounts of CO_2. However, unlike fields in other areas of the United States, these fields have not undergone secondary or tertiary oil recovery in the past, thus very little is known about how they will perform if CO_2-EOR is implemented.

This study began in June 2010 and was funded by the Ohio Coal Development Office under Grant/Agreement CDO/D-10-07b. It was undertaken due to the importance of coal-based energy in the region and the potential future value of CCUS to long-term viability of coal as a cost-effective energy source for Ohio. The Survey's work on this project has been carried out in coordination with complementary work performed by Battelle under a separate OCDO grant (Grant/Agreement CDO/D-10-07a). The Survey collaborated on several activities and interpretations presented in Battelle's report and similarly,

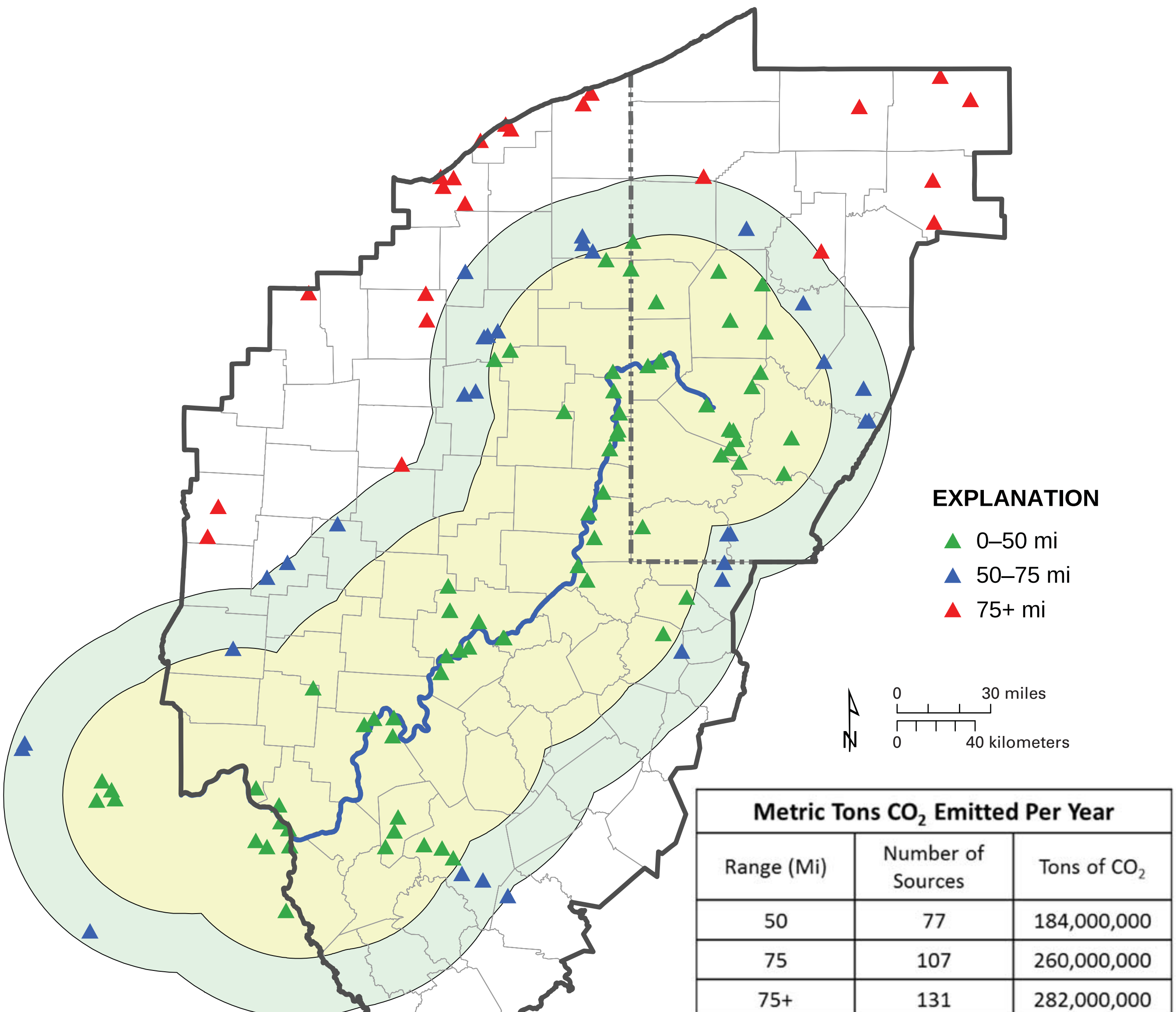

Metric Tons CO_2 Emitted Per Year		
Range (Mi)	Number of Sources	Tons of CO_2
50	77	184,000,000
75	107	260,000,000
75+	131	282,000,000

Source: U.S. EPA Greenhouse Gas Reporting Program 2010 Data

FIGURE 1.—CO_2 point sources within radiuses of 50 and 75 mi from the Ohio River.

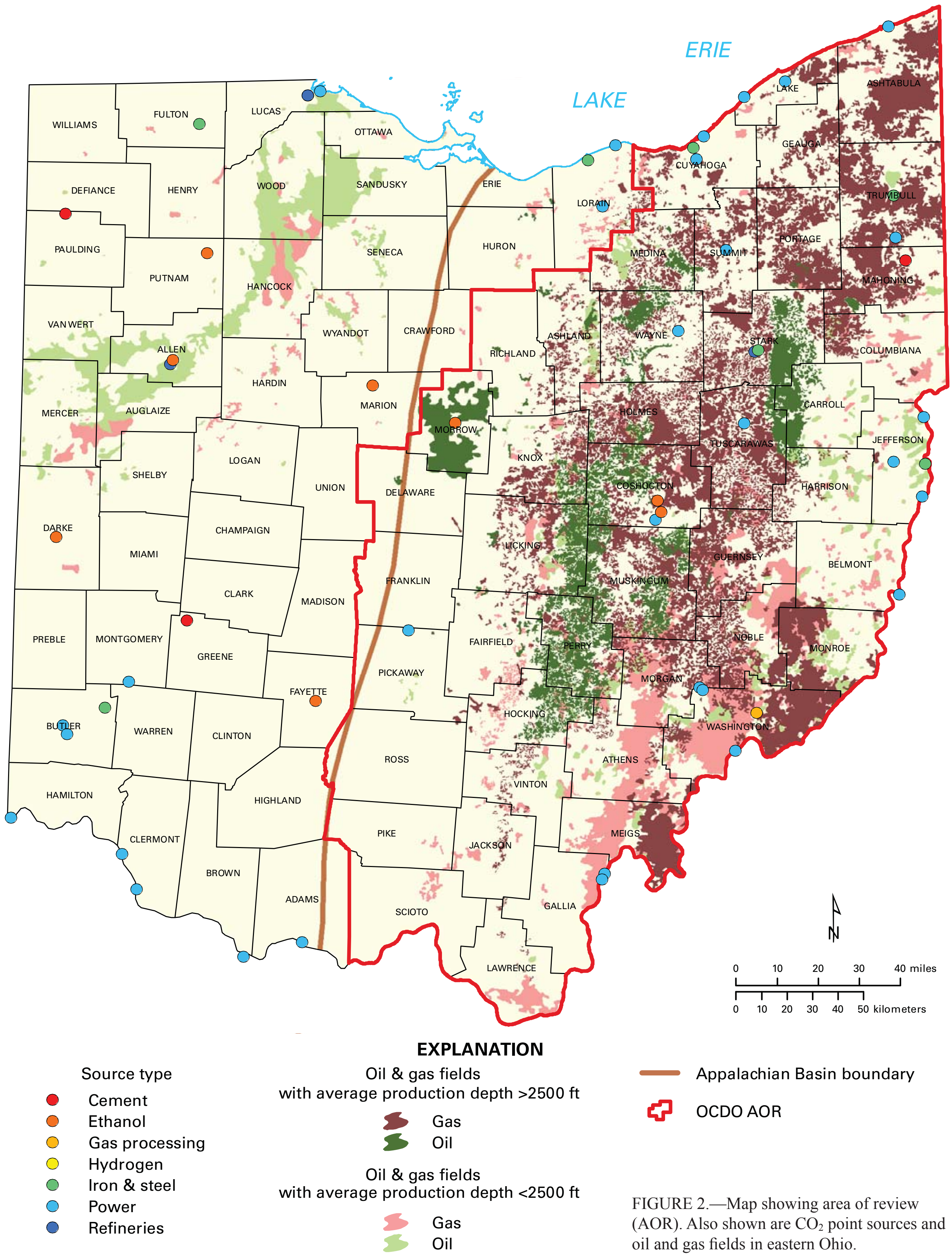

FIGURE 2.—Map showing area of review (AOR). Also shown are CO_2 point sources and oil and gas fields in eastern Ohio.

Battelle supported work presented in this report. The work described herein also was carried out in collaboration with complementary research being conducted by the MRCSP Phase III program (see **www.mrcsp.org** for more information).

Project Goal

The ultimate project goal is to develop the geologic knowledge needed to support decision-making by policy makers and key stakeholders in developing a long-term, cost-effective carbon management strategy for eastern Ohio and the UORV region. Eastern Ohio is a crucial area in which carbon sequestration options must be explored fully so that stakeholders may identify and understand the options and costs to advance CCS and CO_2-EOR (CCUS) technologies in the area.

Project Scope

The Survey's primary objective in Step 1was to identify, compile, and organize all pertinent geologic data into digital files for easier accessibility. This data was used to update and generate relevant geologic maps, cross sections, and interpretations for evaluating CO_2 sequestration potential. Many of the data sets evaluated and shown in this report have been previously inaccessible or not updated and therefore underutilized by both the Survey, the public, and industry. By digitizing and mapping these datasets, the Survey can better assist in addressing CCUS objectives and other geological uses. The Survey utilized select data, including "piggyback" wells, collected primarily by Battelle, to update our stratigraphic and structural interpretations by creating a set of detailed regional structure maps and cross sections. These maps and cross sections also will assist in identifying geographic areas and formations with favorable injectivity and storage potential. Results of these efforts are presented in the data mining (p. 14), regional cross sections (p. 63), and structure mapping (p. 71) sections of this report.

REGIONAL GEOLOGIC SETTING

Precambrian Framework

The Precambrian Era basement complex serves as the foundation for overlying Paleozoic Era (and younger) rocks of eastern North America. In general terms, the Precambrian complex of the region includes all rocks older than 600 million years (m.y.), and overlying Paleozoic rocks include rocks less than 600 m.y. old. A thorough understanding of the geologic structure, character, and history of the underlying Precambrian complex is necessary to understand the geologic framework of the overlying Paleozoic strata. Therefore, a very general description is provided here based on our interpretation of the limited available data.

The Precambrian basement complex of Ohio consists of portions of the Grenville Province, the East Continent Rift Basin System, and the Eastern Granite-Rhyolite Province (Fig. 3). The basement in the AOR lies within the Grenville Province. Uranium to Lead (U-Pb) age dates have not been determined for the Grenville Province in Ohio. However, regional geochronological investigations outside Ohio indicate it is approximately 1.0–1.2 billion years (b.y.) old (Culshaw and Dostal, 2002).

The Grenville Province is an extension of the Grenville metamorphic and igneous terrane exposed in southern Canada and consists of regionally metamorphosed igneous and sedimentary rocks formed during the Grenville Orogeny, a late Precambrian mountain-building event. In addition to underlying eastern Ohio, the Grenville Province also underlies adjacent Pennsylvania and West Virginia. To the west it is known to contain numerous fault blocks where it has overridden the East Continent Rift System in central and western Ohio. However, few deep-seated faults are known within the Precambrian in eastern Ohio.

During the Paleozoic Era, periodic structural adjustment occurred along pre-existing Precambrian faults and associated zones of weakness. This adjustment affected faulting, sedimentation, and depositional patterns during the Paleozoic (Beardsley and Cable, 1983; Riley and others, 1993).

Two regional structural features developed on the eastern Laurentian craton, which was the deeply eroded Grenville Province: the Rome Trough (McGuire and Howell, 1963) and the Appalachian Basin (Fig. 3). The Rome Trough, which was first described by Woodward (1961) as a "Cambrian coastal declivity," is considered an Early to Middle Cambrian-age failed interior rift (Harris, 1978). The Rome Trough is a regional, northeast-trending structure extending from southwestern Pennsylvania, where it is termed the Olin Basin (Wagner, 1976), to northern Tennessee and is very prominent on magnetic intensity maps (King and Zietz, 1978). Sparse deep-well data and seismic reflection data correlate to this magnetic trend and indicate the Rome Trough is an asymmetric failed-rift zone with the deepest portion on the northwest side (Ryder and others, 1998; Gao and others, 2000).

The Appalachian Basin did not begin to take on its present configuration until after Middle Cambrian time following the major movement of the Rome Trough. The Rome Trough is thought to have controlled, in part, the formation and orientation of the northern Appalachian Basin (Ammerman and Keller, 1979). The subsidence of the Appalachian Basin culminated with the Alleghenian Orogeny and development of the Allegheny structural front.

Paleozoic Stratigraphy and Geologic History

Regional and localized areas of recurrent crustal movement of the Precambrian basement followed by later regional uplifts, subsidence, and compressional forces affected the distribution, character, and thickness of Paleozoic rock units. Thickness of Paleozoic Appalachian Basin rock units in Ohio ranges from approximately 3,000 ft in central Ohio to more than 13,000 ft in southeastern Ohio. The Paleozoic stratigraphic column of Ohio ranges in age from Middle Cambrian to Early Permian (Slucher and others, 2006; Fig. 4). A range of sedimentary rock types, including carbonates,

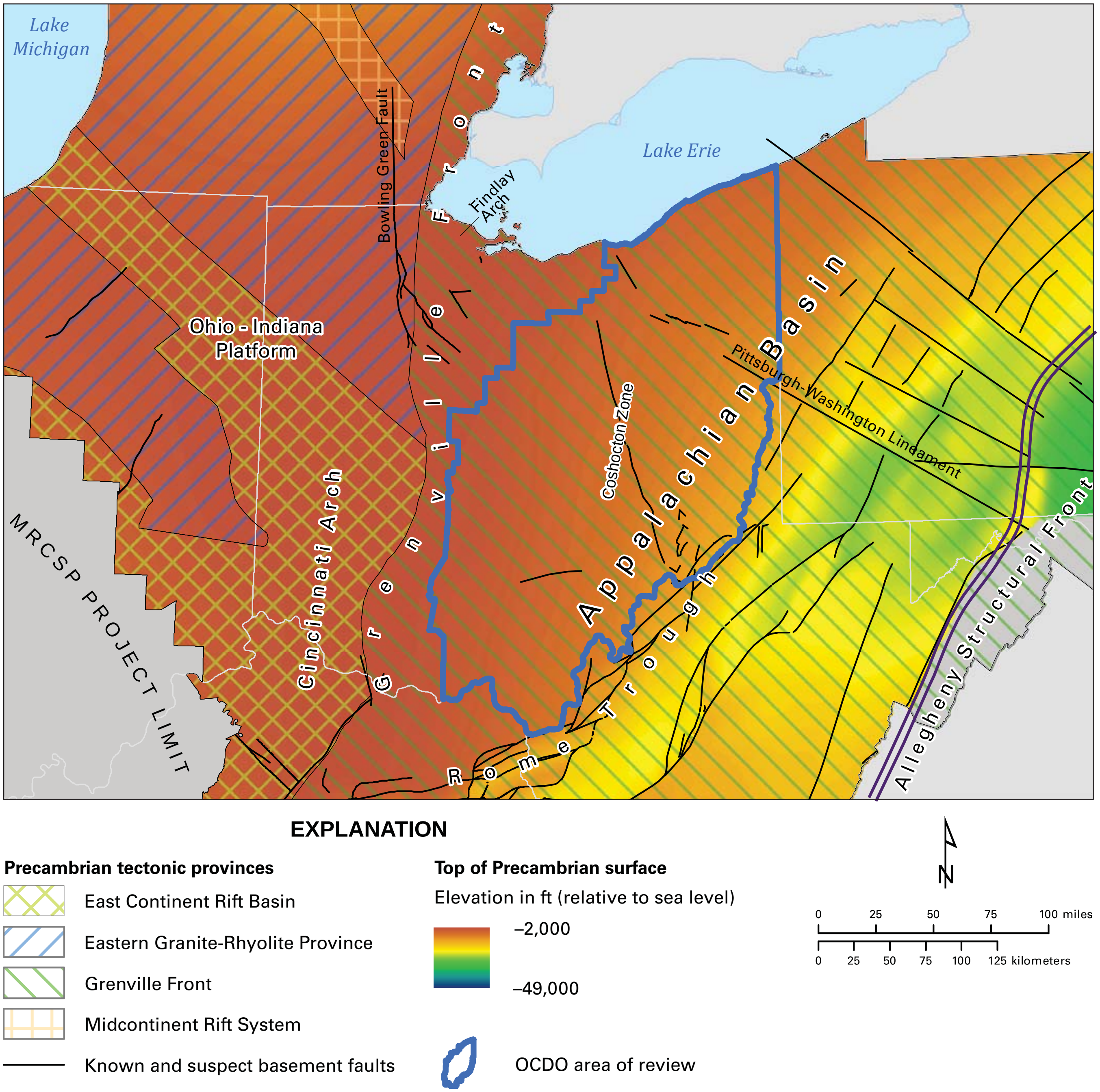

FIGURE 3.—Map showing Precambrian tectonic provinces, elevation on top of the Precambrian unconformity, major basement faults, and other structural features. Modified from Wickstrom and others (2005).

evaporites, shale, sandstone, siltstone, k-bentonites, and chert, are present throughout the state.

The stratigraphy of the Middle Cambrian in eastern Ohio is particularly problematic because of sparse deep-well data and a lack of nearby continuous cores. Another difficulty has been a lack of Cambrian paleontological studies to adequately constrain lithostratigraphic correlations (Babcock, 1994). A recent investigation of all available continuous cores and geophysical logs from deep wells across the state has resulted in an updated Cambrian nomenclature and stratigraphy, which is used in this report (Fig. 4). A stratigraphic correlation chart for eastern Ohio, comparing the Survey's present nomenclature to the previous nomenclature of Janssens (1973) and also to the stratigraphy of the Rome Trough present in areas immediately south of the Ohio River in northwestern West Virginia is shown in Figure 5. Important results from recent investigations show that (1) the Mount Simon Sandstone pinches out in central Ohio, (2) the Rome Formation is not present in Ohio, and (3) the Conasauga Formation (Janssens, 1973) has been redefined to the Conasauga group (Baranoski, in press).

The earliest record of sedimentation within the region is found within the Rome Trough sequence of rocks in West Virginia and Kentucky. Deposition of this sequence began with the lowermost Paleozoic basal sandstone (arkose) in the latest Precambrian-Early Cambrian time. Rifting of the eastern Laurentian continent resulted in the opening of the Iapetus Ocean (Harris, 1978; Scotese and McKerrow, 1991). Subsidence of the Rome Trough continued with deposition of the Shady Dolomite and Rome Formation during the Lower Cambrian and continued through Middle Cambrian with deposition of the Conasauga group. The pre-Knox section of the Rome Trough is older and greatly thickened when compared to the same intervals of the stable cratonic sequence. As much as 10,000 ft of pre-Knox sediments accumulated in the Rome Trough (Ryder, 1992; Ryder and others, 1996).

From late Precambrian through most of Middle Cambrian time, eastern Ohio remained an emergent area, a stable cratonic platform. During this time, erosion of the exposed Grenville basement complex in Ohio and northwestern West Virginia supplied clastic sediments to the Rome Trough while carbonate deposition dominated east of the trough. Scattered seismic reflection survey data in Ohio, collected from Class I well site characterization and oil and gas exploration, indicates local areas where Cambrian sediments older than the Conasauga group may be present in structurally low areas. Near the end of the Middle Cambrian, seas had completely transgressed the exposed Precambrian basement complex in Ohio resulting in near-shore to marginal marine deposition of Mount Simon Sandstone in western Ohio, while marginal marine and marine deposition of the Conasauga group occurred in eastern Ohio. The Mount Simon Sandstone, which is a 200- to 300-ft-thick, highly permeable, porous quartz sandstone in western Ohio, pinches out and/or is in facies transition with the Conasauga group in the eastern portion of Ohio. In northwestern West Virginia and the Rome Trough region, deposition of the Conasauga group continued into the Upper Cambrian with a minor marine regression represented by Nolichucky Shale, followed by a transgression resulting in deposition of the Maynardville Limestone.

Open-marine conditions continued with deposition of the Knox Dolomite. As used in this report, the Knox Dolomite is subdivided in ascending order into the Copper Ridge dolomite, the Rose Run sandstone, and the Beekmantown dolomite (Figs. 4 and 5). Minor regressions took place with input of clastics in the "B-zone" and to a greater degree, the Rose Run sandstone.

A major regression took place during the Middle Ordovician with the onset of the regional Knox unconformity. An extensive erosional surface developed on the emergent Knox carbonate platform (Riley and others, 1993). Paleotopography reached a maximum of about 150 ft on the karstic terrain of the Knox Dolomite (Janssens, 1973). Tropical seas returned to the Ohio region and inundated the subsiding Knox platform during the Middle Ordovician. The "St. Peter" sandstone and Wells Creek Formation represent the next major marine transgression; these units were deposited on the regional Knox unconformity. The "St. Peter" is a very fine-grained, well-sorted, quartz arenite that forms the basal part (where the unit is present) of the Wells Creek Formation. The "St. Peter" increases in thickness from the stable craton into the Rome Trough (Humphreys and Watson, 1996). The Wells Creek Formation is dolomitic shale that locally contains beds of limestone and sandy dolomite. In general, the Wells Creek provides a good seal unit above the Knox unconformity, as indicated by numerous oil and gas pools found within Knox erosional remnants throughout the region. Shallow-marine sedimentation continued through the Middle and Upper Ordovician with deposition of the Black River Group, Trenton Limestone, and the Cincinnati group of shales and limestones. The clastic sediments of the Cincinnati group were associated with the Taconic Orogeny of eastern North America, where compressional forces caused a deepening of the seas covering the region.

Marine sedimentation in the region temporarily ceased during Late Ordovician-Early Silurian time as another major regression began and a regional unconformity developed on top of the Cincinnati group. By the end of the Ordovician, the western margin of the Appalachian Basin was delineated by the Indiana-Ohio Platform and the Cincinnati and Findlay Arches. As Silurian time progressed, repeated fluctuations of sea level flooded and retreated from the coastal lowlands on the western flank of the Appalachian Basin. Silurian-age Tuscarora Sandstone and other clastic equivalents ("Clinton" and "Medina" sandstones) were deposited in near-shore to marginal marine environments on this unconformity surface at the onset of another marine transgression. A mixture of clastics and carbonates followed with deposition of the Rose Hill Formation and its equivalents and the overlying Lockport Dolomite, Salina Group, Bass Islands Dolomite and Helderberg Formation. Another period of regression is marked by an unconformity within Lower Devonian strata and is followed by a period of transgression and subsequent deposition of the Oriskany Sandstone; the overlying Onondaga Limestone; and shales of the Hamilton Group, including the Marcellus Shale (marking the onset of the Acadian Orogeny).

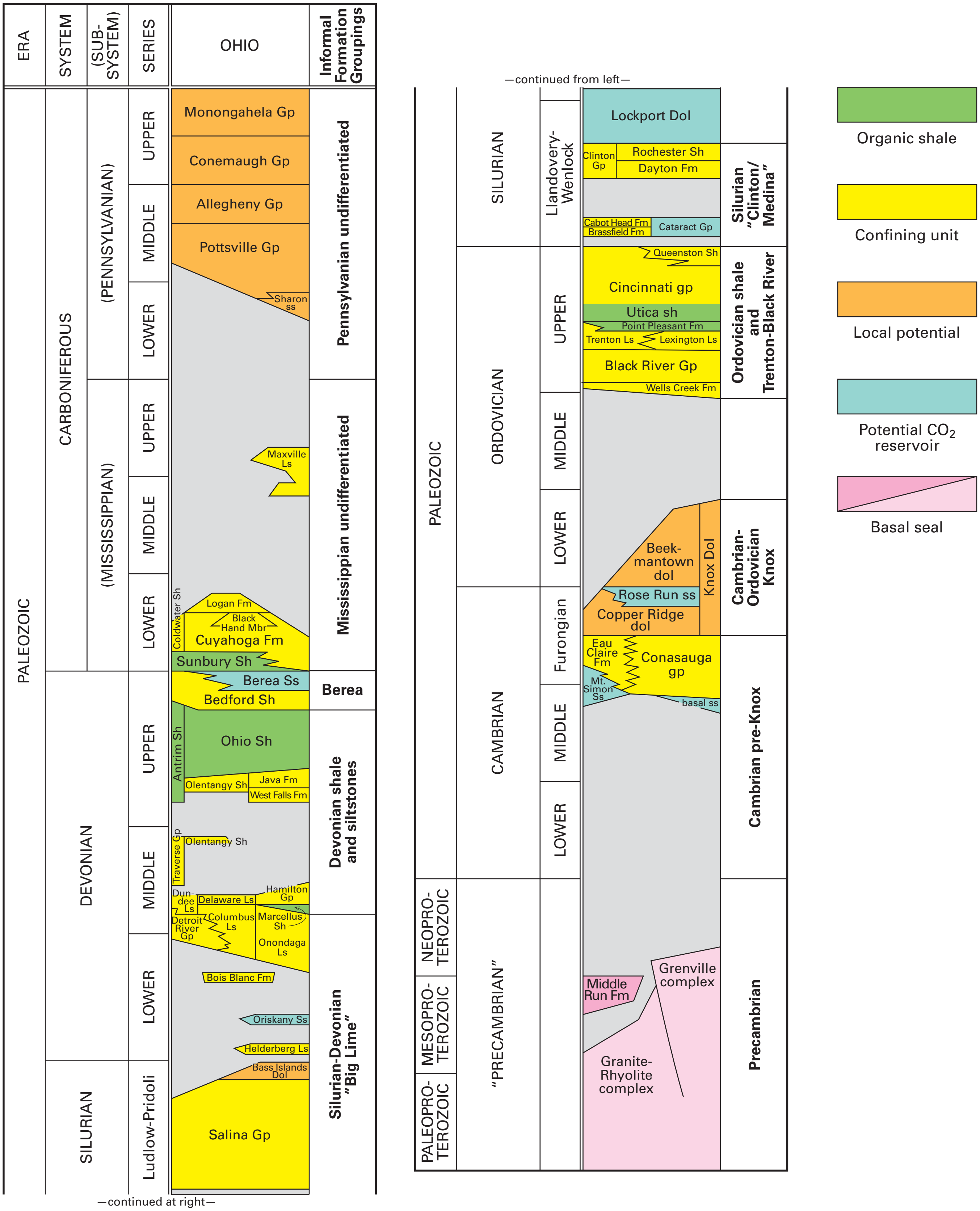

FIGURE 4.—Stratigraphic chart illustrating geologic units found beneath eastern Ohio. Rock units are color coded to illustrate potential injection zones, confining units, organic shales, and basal seals. Modified from Wickstrom and others (2005).

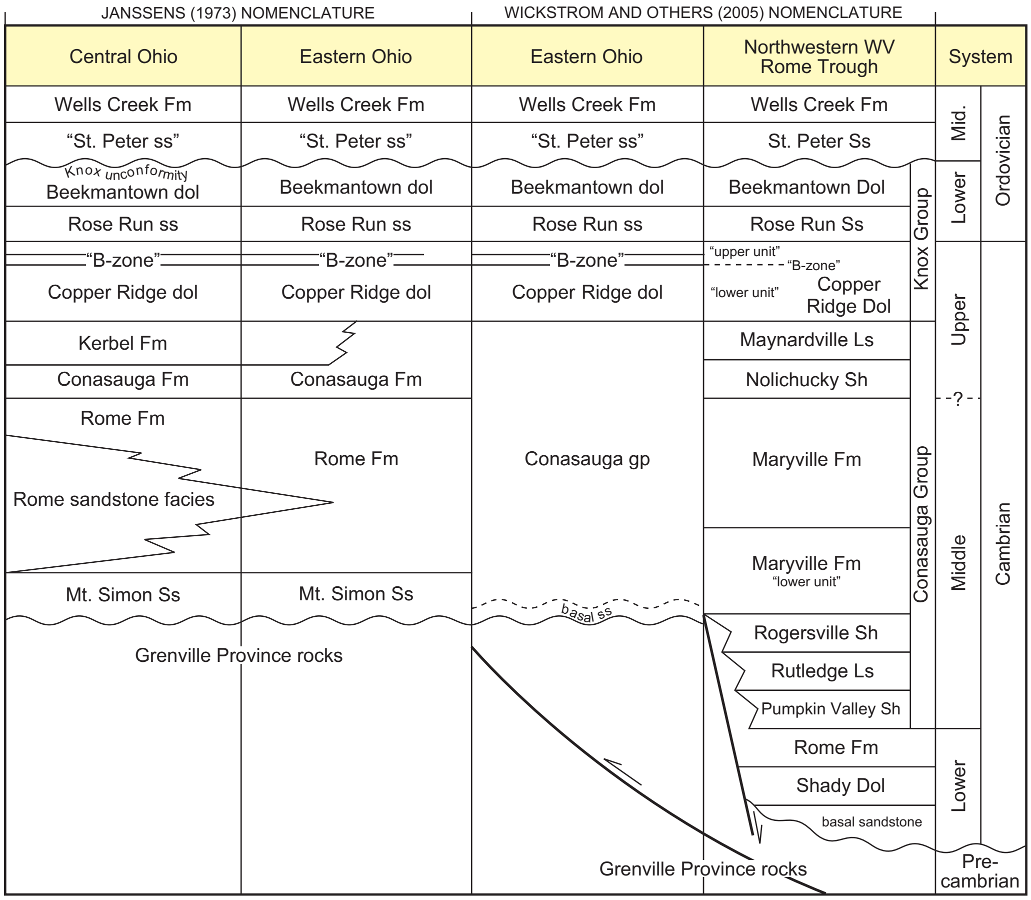

FIGURE 5.—Correlation chart for previous and existing stratigraphic nomenclature in eastern Ohio and for the Rome Trough.

During the Late Devonian Acadian Orogeny, tropical seas again inundated the region with deposition of the Sonyea and West Falls Formations, as well as the Ohio Shale in a partially restricted marine basin. The overlying Bedford Shale and Berea Sandstone represent the progradation of gray shales and sandstones over this restricted basin. An Early Mississippian marine transgression resulted in the deposition of the Sunbury Shale. Renewed mountain building in eastern North America during the Early Mississippian Alleghenian Orogeny resulted in delta progradation and the deposition of the Cuyahoga and Logan Formations, followed by a minor marine transgression with deposition of the Greenbrier Limestone and equivalents. Continued mountain building to the east resulted in extensive fluvial, clastic deposition, including coals with minor limestone accumulations throughout the Pennsylvanian.

POTENTIAL GEOLOGIC RESERVOIR TYPES

The U.S. Department of Energy has identified several categories of geologic reservoirs for potential CO_2 sequestration (US DOE, 1999, 2004, 2005). Of these categories, four are considered important for eastern Ohio: (1) deep saline formations, (2) oil and gas fields, (3) unmineable coal beds, and (4) carbonaceous shales.

Deep Saline Formations

Saline formations are natural saltwater-bearing intervals of porous and permeable rocks that typically occur at depths well below any levels of potable groundwater. Currently, 33 geologic units are used for waste-fluid disposal in Ohio for both Class I (hazardous and industrial-waste injection) and Class II (oil-and-gas brine or enhanced recovery injection) wells (Appendix A). Thus a long history of technical data and regulatory experience exists that could be applied to CO_2 injection/disposal. Saline formations are widespread and in close proximity to many large CO_2 sources in eastern Ohio and the upper Ohio River Valley region.

To maintain the injected CO_2 in supercritical (i.e., liquid) phase, the reservoir storage units must be approximately 2,500 ft or greater in depth. Maintaining the CO_2 in a liquid phase is desirable because, as a liquid, it takes up much less volume than when in the gaseous phase. One tonne of CO_2 at surface temperature and pressure (in gaseous phase) occupies approximately 18,000 cubic feet (ft^3). The same amount of CO_2, when injected to approximately 2,700 ft in depth, will occupy only 50 ft^3. Sequestration depths of at least 2,500 ft also ensure there is an adequate confining interval above the potential injection zones to protect the deepest underground source of drinking water (USDW).

The primary mechanisms for CO_2 sequestration in saline formations include solubility, hydrodynamic, and mineral trapping. *Solubility trapping* refers to CO_2 dissolved in formation waters. Up to 30 percent of CO_2 injected in saline formations dissolves over time in the formation water (Law and Bachu, 1996). In *hydrodynamic trapping*, CO_2 is trapped as a gas under low-permeability confining units similar to the mechanism for trapping natural gas. *Mineral trapping* occurs when CO_2 reacts with minerals, fluids, and organic matter in a geologic formation to precipitate carbonate minerals. Depth, permeability, injectivity, reservoir pressure, reservoir integrity, and water chemistry are some of the variables that control the sequestration potential of deep saline formations (Reichle and others, 1999; Bachu and Adams, 2003).

In addition to the properties of the injection zone or reservoir, an overlying confining interval is necessary. Injected CO_2 has a lower specific gravity, and thus is more buoyant, than the natural formation fluids and will therefore rise to the top of the porous zones. Hence all confining intervals must be relatively impermeable and sufficiently thick to arrest any appreciable vertical movement of the CO_2 within the sequestration interval, thereby trapping it in the deep subsurface. Storage of CO_2 can be in either subsurface traps or in unconfined strata. In subsurface traps, the more buoyant CO_2 will occupy the highest portions of any structural (e.g., anticline) or stratigraphic (e.g., pinch-out) feature. These same mechanisms of trapping are found in many of the natural gas and oil reservoirs (i.e., traps) that occur in eastern Ohio. Within such traps, only the pore volume available in the rock and the size of the trap limit the volume of CO_2 that can be injected. In unconfined storage reservoirs, CO_2 is injected in regional aquifers located in rocks without specific structural closures or stratigraphic traps. Once injected, the CO_2 will migrate to the highest portion of the saline aquifer where it accumulates against the cap rock, which prevents further vertical movement (Bentham and Kirby, 2005). At that point the injected CO_2 then will migrate laterally, following the normal hydrodynamic flow regime of the region (usually towards shallower areas). However, it must be emphasized that flow velocities in deep geologic systems occur at very slow rates, typically measured in ft per hundreds or thousands of years.

Oil and Gas Fields

Oil and gas fields represent known geologic traps (structural or stratigraphic) containing hydrocarbons within a confined reservoir with a known cap or seal (confining unit). In depleted or abandoned petroleum fields, CO_2 could be injected into the reservoir to fill the pore volume left after the extraction of oil or natural gas resources (Westrich and others, 2002). Injected CO_2 would be trapped by the limits of the reservoir (whether structural or stratigraphic) for secure storage. Some of the variables that control the sequestration potential of depleted oil and gas fields are volume, permeability, injectivity, pressure, reservoir integrity, water chemistry, the nature of the cap rock or reservoir seal, and the history of production (Reichle and others, 1999). This may be an attractive option because of the state's long history of oil and gas recovery, which is concentrated in eastern Ohio (Fig. 2). Sequestration would be targeting fields greater than 2,500 ft deep, where CO_2 would be in the supercritical phase. In addition, eastern Ohio includes 22 natural-gas storage fields that date back to the 1930s. Such large volumes of gas storage capacity strongly suggest that CO_2 gas can be successfully managed in subsurface reservoirs within the region.

As demonstrated in active oil fields throughout the United States, CO_2 can be used for EOR. In this process, some of the oil that remains in reservoirs after primary production is recovered by injecting CO_2 that either (1) repressurizes the reservoir and displaces and drives the remaining oil to a recovery well (a process called *immiscible flooding*) or (2) directly mixes and chemically interacts with the remaining oil as it pushes it to the producing well (*miscible flooding*). As a general rule, reservoirs below 2,500 ft are considered to be in the miscible range. Currently, there are 120 active CO_2-EOR projects in the United States demonstrating the effectiveness of this value-added sequestration option (Koottungal, 2012). Moreover, CO_2-EOR could provide an economic incentive to storage in eastern Ohio, where CO_2 sources are located near oil fields.

In 2008, the Survey, in cooperation with private industry, conducted a successful 80-t cyclic CO_2 test (or "Huff-n-Puff") in Stark County. This EOR project, discussed later in this report (p. 55), demonstrated that the Silurian-age "Clinton" sandstone would accept significant volumes (80 t) of injected CO_2, as well as mobilizing and producing additional oil in the East Canton oil field. This successful technique could have widespread application to many "Clinton" fields and other reservoirs throughout eastern Ohio and the surrounding region.

In addition to geological considerations, other concerns and limitations need to be considered when evaluating CO_2-EOR potential in a region, including: (1) locations and availability of CO_2 sources (e.g., power plants, steel mills, cement plants) and their proximities to oil reservoirs, (2) well spacing, (3) unitization issues, (4) location of improperly plugged wells and well-bore integrity, and (5) other economic considerations.

Within our region, naturally occurring sources of CO_2 for EOR are not readily available as they are in the West Texas fields. The future supply of CO_2 for EOR in our region will be controlled largely by proximity to power plants, utility demand, and emissions regulations. Proper well spacing and placement of injection wells is necessary to avoid or reduce early breakthrough of CO_2, thus bypassing hydrocarbons during EOR operations. Unitization issues (consolidation of lease interests covering a common source of supply) will need to be examined before large-scale CO_2-EOR projects can be conducted. In older, mature fields, all wells must be located and well-bore integrity must be evaluated prior to a CO_2 flood to avoid compromising the EOR or sequestration effort. Finally, other economic considerations must be evaluated prior to implementing a CO_2-EOR project. Feasibility to perform CO_2-EOR will depend largely on reservoir quality, price of oil, availability and cost of CO_2, and operation and design costs.

Unmineable Coal Beds

Eastern Ohio and the Ohio River Valley, including portions of Pennsylvania, West Virginia, and Kentucky, is one of the largest Pennsylvanian-age coal-producing regions in the world (EIA, 2012). Coal-bearing formations extend across the eastern third of the state and are situated within the northern Appalachian Basin (Fig. 6). Coal beds considered as potential targets for geologic CO_2 sequestration occur in Pennsylvanian-age rocks and are subdivided in ascending order into the Pottsville, Allegheny, Conemaugh, and Monongahela Groups (Fig. 4). It should be noted that depth to coal beds in Ohio is less than 2,500 ft, making these a less desirable sequestration target.

Similar to CO_2-EOR, unmineable coal beds provide the potential for value-added revenue for CO_2 storage because they could be used for enhanced coalbed methane (ECBM) recovery. Such a process could offset some of the costs of CO_2 injection, making unmineable coal beds an attractive CO_2 sequestration target. Furthermore, many coal-fired power plants—which are major CO_2 point sources—are located within the Ohio River Valley coal-producing area (Fig. 1).

Unlike its behavior in the previously described reservoir types, CO_2 injected into a coal bed would not only occupy pore space, but would bond, or *adsorb*, onto the carbon elements in the coal itself. The adsorption rate for CO_2 in coals is approximately twice that of methane; thus in theory, the injected CO_2 would displace methane, allowing for the potential of enhanced gas recovery (Reznik and others, 1982; Gale and Freund, 2001; Schroeder and others, 2002). Concerns of miscibility that occur in oil and gas reservoirs are not an issue because of the adsorption mechanism in coal. Thus the injection of CO_2 and resulting enhanced recovery of coalbed methane could occur at shallower depths than for depleted oil reservoirs. Hydrogeologic flow, water chemistry, coal thickness and quality, and subsurface temperature-pressure conditions are some of the variables that control the potential use of coal beds for CO_2 sequestration and ECBM recovery (Pashin and others, 2003).

Concerns for ECBM recovery with CO_2 include (1) depth, (2) coal swelling, (3) leakage or breakthrough issues in previously hydraulically fractured CBM wells, (4) wellbore integrity, (5) legal issues, (6) monitoring and verification, and (7) possible competing uses for deep unmineable coal beds (Greb and others, 2010). Additional testing is required to determine the impact of swelling in the eastern Ohio coal beds. Since most CBM wells are fractured, and the fractures may not be confined to the coal, leakage of any CO_2 that bypasses the coal reservoir through fractures may be an issue. Careful project design and monitoring of injection and producing wells should help to minimize leakage or early breakthrough. Most oil and conventional gas wells in potential CBM-producing parts of Ohio will penetrate the coal-bearing interval; wellbore integrity and well density will need to be considered in most areas of commercial CBM production. Legal issues such as liability, ownership, unitization, and mineral rights regarding CBM and injected CO_2 will need to be addressed. Methods need to be developed for monitoring and verifying injected CO_2 to ensure it remains in the reservoir. Because it is such an important commodity, coals for ECBM recovery must be chosen with care, specifically those coals that will not be mined in the future. Currently, low natural gas prices and an abundance of shale gas are limiting factors in the development of ECBM recovery.

Studies by MRCSP have concluded that unmineable Appalachian Basin coal faces both physical and economic hurdles that reduce attractiveness as potential CCS targets. Furthermore, unmineable Ohio coal may be relatively unattractive because it is located at shallower depths compared to other, more favorable unmineable Appalachian Basin coals. However, the ability of coal to adsorb CO_2 and displace methane gives unmineable Ohio coal the potential to serve as a future CCS target. Ohio coal may hold offsetting advantages relative to other Appalachian Basin coals because of its proximity to a large number of CO_2 point sources. Thus economical and logistical circumstances at any given time may dictate if unmineable Ohio coal may ever be utilized.

Carbonaceous Shales

Eastern Ohio contains widespread, thick deposits of carbonaceous shales in both the Devonian shale and the Upper Ordovician black shale intervals (Fig. 4). These shales are multifunctional, acting as confining intervals (seals) for underlying sequestration reservoirs and as source rocks for oil and gas reservoirs and are unconventional oil and gas reservoirs themselves. Analogous to sequestration in coal beds, CO_2 injection into unconventional carbonaceous shale reservoirs could be used to enhance existing gas production. In addition, carbonaceous shales would adsorb the CO_2 into the shale matrix, permitting long-term CO_2 storage, even at relatively shallow depths (Nuttall and others, 2005). Based on adsorption isotherm analyses, Eble and others (2010) estimated that the shales can hold approximately four times the amount of CO_2 as compared to the adsorption of methane.

Throughout the United States, the application of horizontal drilling combined with multistage hydraulic fracturing has resulted in a drilling boom for unconventional oil and gas production from organic-rich shale intervals. This technology has stimulated drilling activity and production in eastern Ohio and the Appalachian Basin for both the Devonian-age Marcellus Shale and the Ordovician-age Utica-Point Pleasant shale interval. These shale intervals currently are the most active oil and gas plays in the eastern United States.

The Marcellus Shale is the lowermost shale unit of the Devonian shale interval (Fig. 4). Thickness of the organic-rich portion of the Marcellus Shale in eastern Ohio ranges from 0 ft west of the pinchout edge to over 75 ft in extreme southeastern Ohio (Fig. 7). Marcellus oil and gas exploration has been concentrated in western Pennsylvania, where the shale interval is better developed and reaches thicknesses over 100 ft. However, portions of Belmont and Monroe Counties in eastern Ohio, where thickness exceeds 50 ft, also have been actively drilled. Areas in eastern Ohio where the Marcellus is greater than 20 ft thick are considered as potential targets for oil and gas exploration in this prolific shale gas play.

The Upper Ordovician Utica-Point Pleasant interval is present throughout Ohio, with thickness ranging from 100 to 250 ft in the AOR (Fig. 8). In southern Ohio, the Utica shale

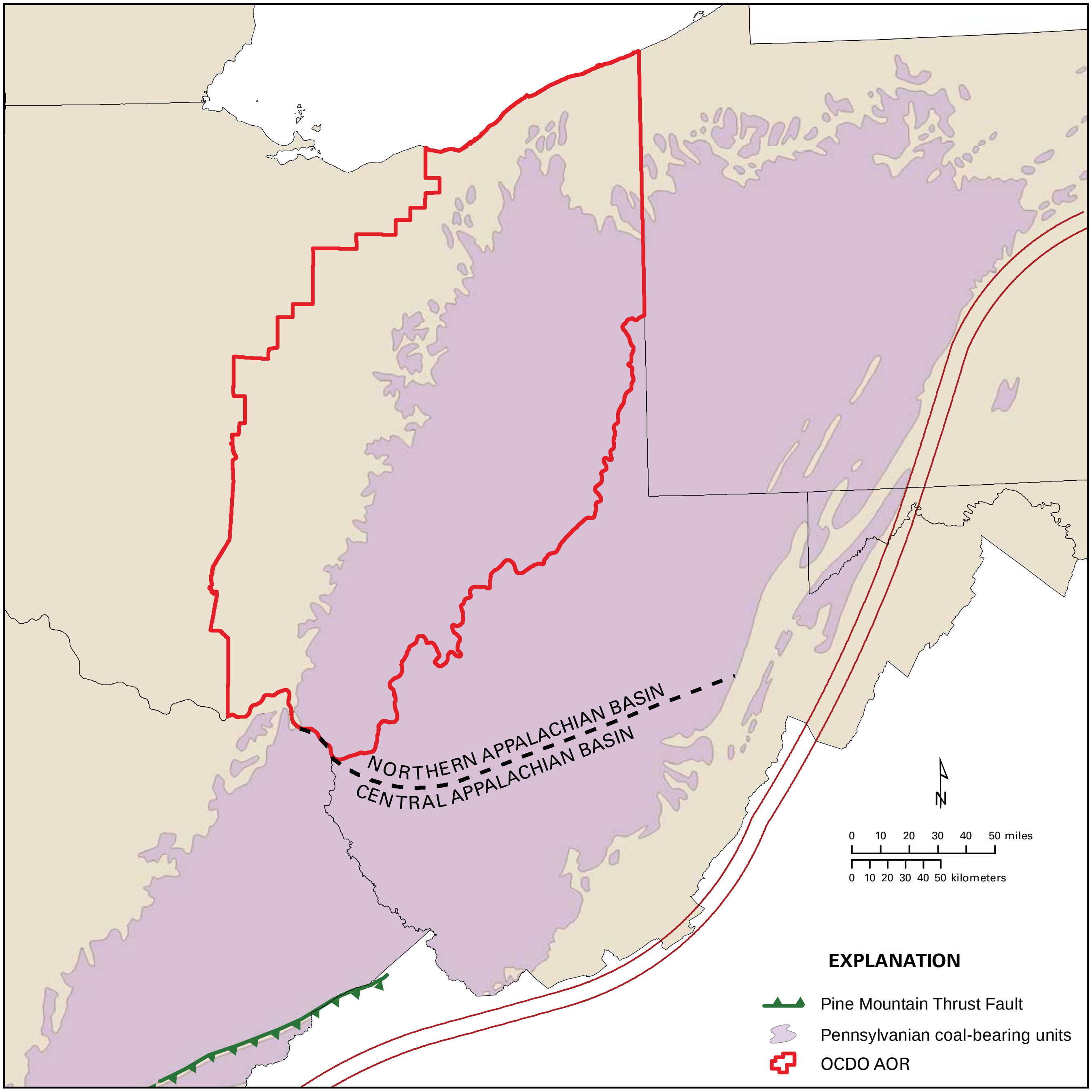

FIGURE 6.—Map showing the extent of coal-bearing formations in eastern Ohio and the Appalachian Basin. From Wickstrom and others (2005).

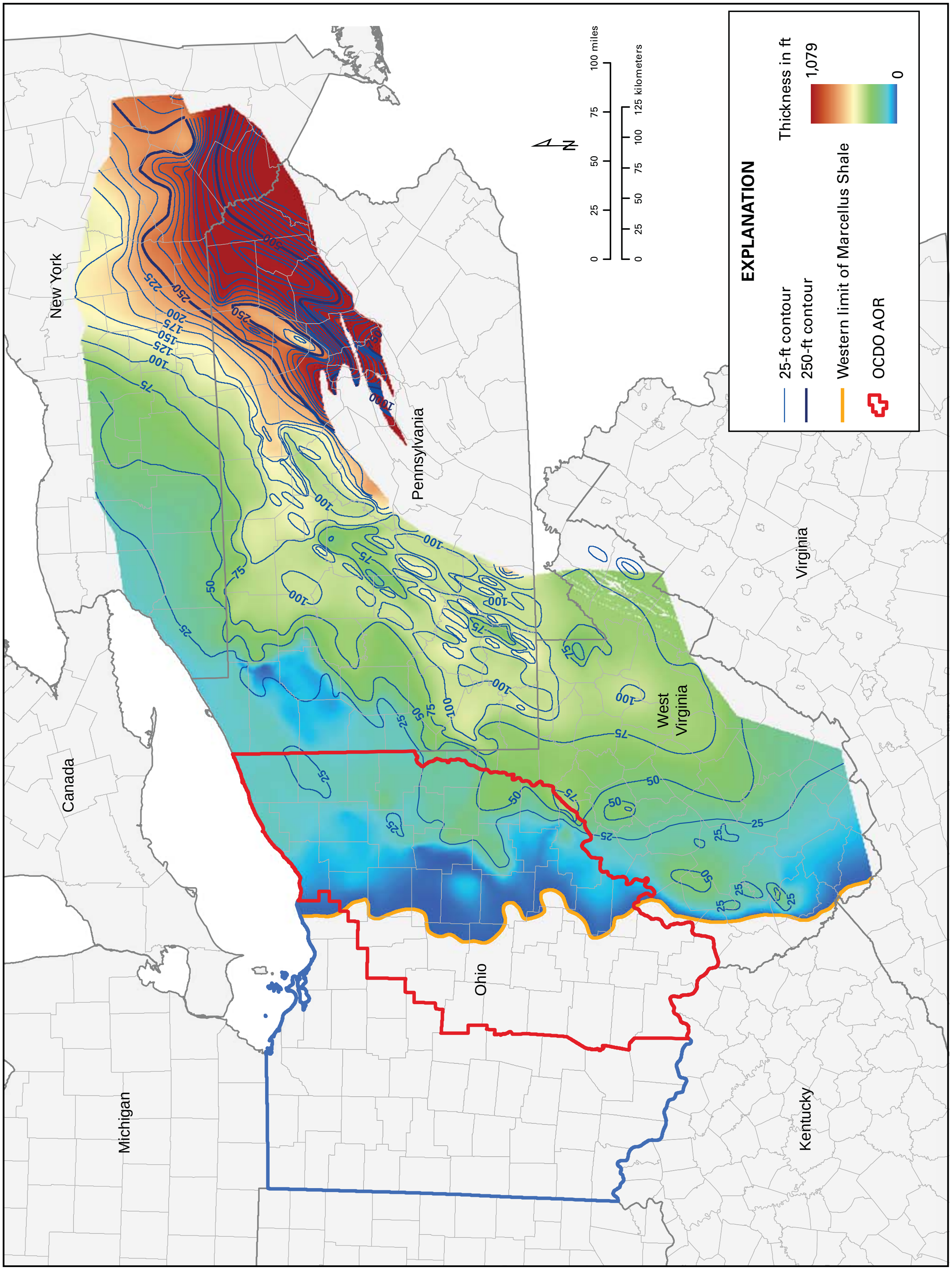

FIGURE 7.—Map showing organic-thickness of the Marcellus Shale. From Erenpreiss and others (2011).

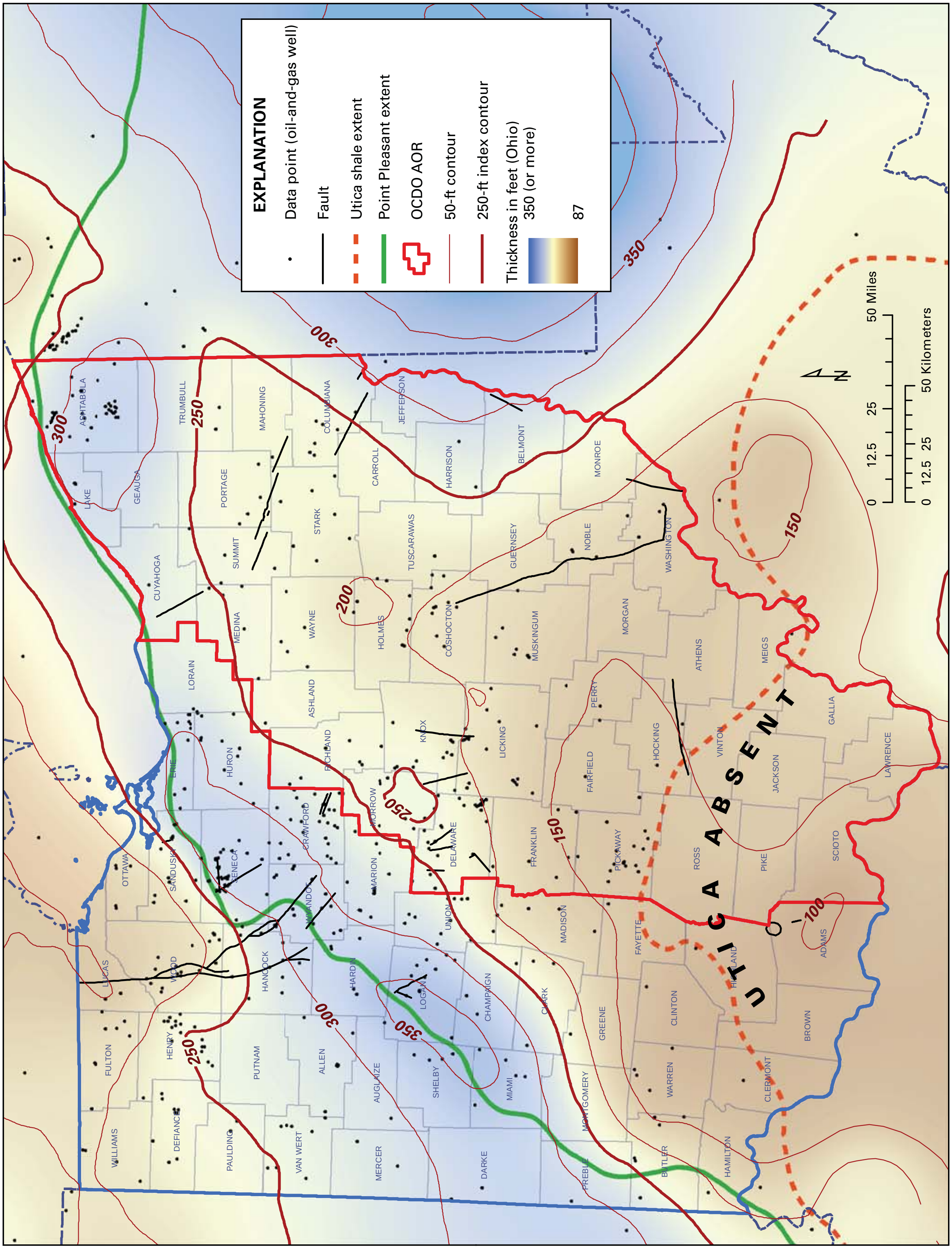

FIGURE 8.—Map showing interval thickness of the Utica shale to Trenton Limestone in Ohio. From Patchen and others (2006).

is absent through facies change as the dark brown-black, organic-rich Utica shale transitions to a less organic-rich gray shale. To date, Utica-Point Pleasant oil and gas exploration has been focused in Carroll, Columbiana, and Harrison Counties. Exploration wells also have been drilled as far west as Knox County, as far south as Noble County, and as far north as Geauga County. This increased activity in Ordovician shale drilling will provide additional deep well data with modern geophysical logs and analyses that will greatly add to our knowledge of these units as either confining intervals or potential sequestration targets.

Issues regarding the Devonian and Ordovician shale intervals include the co-location of deep saline sequestration targets with shale production. In areas where the shales have been hydraulically fractured, concerns have been raised that shale production may be in conflict with the use of shale formations as a caprock barrier to CO_2 migration. It should be noted that the portion of the productive shales that are targeted typically are only 50 to 100 ft thick. Above the hydraulically fractured zones are thousands of additional feet of shale and other low-permeability rock to serve as confining units. In other words, even if a small section of caprock is fractured, the overlying shale interval still could serve as a seal and will often have additional multiple seals above it.

Carbonaceous shales are not considered as primary sequestration targets because of low permeability and injection rates. However, their capacity to adsorb CO_2 is expected to increase the effectiveness of these shales for sequestration. Future economic factors, specifically the price of CO_2 and natural gas, will determine whether enhanced natural gas recovery from shale using CO_2 injection will be attempted on a commercial scale.

GEOLOGICAL AND GEOPHYSICAL DATA MINING AND RESULTS

The following sections describe the approach and results of the Survey's data mining effort, which consisted of two steps. The first step was to identify the types of data that have been archived at ODNR; this was data primarily held by the Survey and DOGRM. The second step was to develop a list of data types that would be useful for characterizing and mapping deep formations in eastern Ohio to identify areas and formations that may possess favorable injectivity and storage potential to sequester CO_2 and for CO_2-EOR or CCUS. Twelve data types were reviewed, collected, and compiled during this effort. Until the completion of this effort, a significant amount of these data had not been readily accessible to either Survey personnel or the public. A list of these twelve data types is shown in Table 2.

Once the various data sets were compiled and reviewed, a set of location or "spot" maps were created to depict the locations of various data types now available for characterization. Developing spot maps to depict data locations is useful, but such work also is necessary to identify the formation or formation interval(s) for which any given data set applies. To allow for this, the data locations maps employ symbols that indicate the deepest formation(s) or formation interval(s) associated with any given data location depicted on a map.

TABLE 2.—*Twelve data types collected and mapped during this study*

- Well cards
- Well rock cuttings and core
- Oil and gas geophysical logs
- Porosity and permeability data
- Formation and well pressure data
- Injection well data
- Reservoir brine geochemical data
- Lineament maps
- Gravity survey data and maps
- Magnetic survey data and maps
- Geothermal data and maps
- Seismic surveys

Formation Groups

The majority of the data collected for this project are stored within the Risk Based Data Management System (RBDMS), which is cooperatively managed by DOGRM and the Survey. Each agency is tasked with managing different aspects of the dataset. Any information regarding permitting, completion, production, and/or any regulated well activity is managed by DOGRM, whereas the Survey manages any non-regulated data, such as log scans, cuttings, core, and analyses. Data overlap or commonality occurs for some data types. An example of data overlap between each agency's data sets is formation tops. There are two sets of formation tops in the database, including "drillers' tops" managed by DOGRM and "geologic tops" managed by the Survey. Such overlap must be resolved either by verifying values using other data types, such as geophysical logs, or by using judgment. Furthermore, in addition to having two potentially incongruent datasets for the "same" geologic information, there can be other inherent problems associated with "formation tops" data. The most evident is that as geologists continue to gather new data as they study, correlate, and map various formations, formal formation names are subject to revision. Through the years, a single stratigraphic unit can have multiple names, depending on its history of use. This myriad of formal, informal, and driller formation names, and the evolution of these names, is inherent to the database.

Most of the other data types in the database are (or can be) solely tied to these stratigraphic "tops" and units. And due to the overall volume and diversity of data that has been collected for these countless units, a standardized format was needed to consistently display what is available. To address this need, the project staff decided to revise and reuse a technique that was utilized in the *Oil and Gas Fields Map of Ohio* (Riley and others, 2004) project by creating "formation groups". These groups were created using systemic boundaries combined with stratigraphic nomenclature derived on the *Generalized Column of Bedrock Units in Ohio* (Ohio Division of Geological Survey, 1990). This effort to categorize stratigraphically-grouped data resulted in the creation of nine generalized data groups (Table 3), providing map users knowledge of what information is available at a particular depth on a mapped "spot" location. An extended version of Table 3 that defines each formation group by individual formation name(s) is provided in Appendix B.

TABLE 3.—*Nine stratigraphic groups for mined data at mapped locations*

- Pennsylvanian undifferentiated
- Mississippian undifferentiated
- Berea
- Devonian shale and siltstones
- Silurian-Devonian "Big Lime"
- Silurian "Clinton/Medina"
- Ordovician shale and Trenton-Black River
- Cambrian-Ordovician Knox
- Cambrian pre-Knox and Precambrian

Well Completion Cards

Since the advent of oil-and-gas drilling in Ohio in the mid-1800s, of the approximately 250,000 oil and gas wells drilled to date, well records in the form of completion or "drillers" cards have been collected and are accessible for some 179,000 of those wells. These well completion cards often contain useful driller-reported formation tops, an often overlooked resource that, with the use of modern geostatistical and mapping software, can be used to efficiently create more detailed structural maps of key subsurface formations, including several that are relevant to ODCO objectives in eastern Ohio.

Many drillers work in Ohio for years and thus develop a strong understanding of subsurface stratigraphy. Such experience enables the drillers to record accurately the drilled depths, elevations, or "tops" of key formations. However, not all reported tops present on well cards are accurate. In an effort to enhance map accuracy by applying only valid well card tops, geostatistical methods can be used to sort through and discard a large number of poorly identified tops in a relatively expeditious way.

As a part of this study, the Survey mined the well completion card database and devised a method to cull and utilize valid available data to create a set of very useful structure maps. These structure maps are more detailed than similar maps developed earlier under previous MRCSP grants. The process details and the results of this effort are presented in the section describing regional cross sections and key mapped units for this report (p. 63–76).

Well Cuttings and Core

In the mid 1980s, the Survey began work on a long-term project to inventory and produce databases for the many collections of physical rock samples and paper records archived by the Survey. Initially, this effort concentrated on the many thousands of paper records housed at the Survey's main office located at the Fountain Square Complex in Columbus. Later, work was undertaken to inventory and develop databases for the fifteen major collections stored at the Survey's temporary sample and core repositories located in Columbus. Then in 1999, the H. R. Collins Laboratory (HRCL) core and sample repository, located at Alum Creek State Park in Delaware County, was opened. At the HRCL, many of the Survey collections were consolidated into a permanent location. Since 1999, progress has continued toward the goal of inventorying and developing databases that embody the well cutting samples, cores, strip logs, and twelve other major geoscience collections stored at the HRCL.

In June 2005, the Survey joined the U.S. Geological Survey (USGS) in a major cooperative effort to complete inventories and develop Microsoft Access databases for the fifteen major geoscience collections housed at the HRCL (Table 4). Funding for this effort was provided in part by the National Geological and Geophysical Data Preservation Program (NGGDPP) and matched with State of Ohio funding on a 1:1 basis. In 2010, the Survey completed inventories, developed databases, and generated metadata for the 95,756 geologic samples and paper records contained within the fifteen major geoscience collections housed at the HRCL.

In 2010, the Survey began work on this grant funded by the OCDO to mine data on the top and bottom (range) of the cuttings or core contained in the Survey collections and to identify cutting samples or core that were missing. Over the years, Survey staff members have placed a priority on recording the range of cutting or core samples collected from a borehole, as well as missing-intervals well cuttings and core, as part of the inventory process. However, because of limited staffing and time, some well cutting suites, cores, and cutting and paper strip log records did not have the range data or missing cutting or cored intervals captured in the Survey's Oil and Gas Field and Wells Database. The capture of this missing data was completed as part of this OCDO effort and allowed the Oil and Gas Field and Wells Database to be populated with this information.

The completion of this data mining effort now allows the rapid search of the Oil and Gas Field and Wells Database to determine what well cuttings, cores, and strip logs are available and what is present and what is missing for any geologic horizon of interest. This will streamline the process of determining which cuttings suites and cores can be sampled to assist the Survey and industry with ongoing CO_2 sequestration studies, to aid studies examining the geology and reservoir properties of eastern Ohio oil and gas horizons, and to assist in the development of potential underground storage fields and/or injection wells.

Data Mining Methods

Cuttings collection

The Survey's well cuttings collection consists of samples obtained from the drilling of 5,066 wells (Figs. 9 and 10). Also, duplicate sets of cuttings from over 1,200 wells provide additional material for examination, sampling, and geochemical analysis. The collection contains well cutting samples from all 88 Ohio counties but does not contain out-of- state cutting samples. Each cutting sample is stored either in a standard sand

TABLE 4.—*Collections housed at the ODNR Division of Geological Survey Horace R. Collins Laboratory and the number of samples or paper records in each collection*

54,009	USGS and USDA aerial photographs flown from 1949 through 1979
8,650	Unconsolidated Cenozoic-age sediment samples
6,932	Lake Erie sediment samples from the Dr. Thomas Lewis collection
6,205	Paper seismogram tracings recording earthquake events
5,066	Well sample cuttings suites, including 1,175 duplicate well sample suites
3,428	Paper strip logs of cores, oil and gas wells, and measured sections
2,778	Lake Erie bottom-sediment paper records
2,627	Geochemical analysis records for economic carbonate deposits and coal beds
1,318	Lake Erie soft-sediment core and grab samples from 1974 through 2005
955	Rock cores totaling over 300,000 ft (91,440 m)
736	Coastal Engineering Research Center core samples
629	Sand-and-gravel sieve analyses for samples collected from 12 Ohio counties
600	Well cutting strip logs
503	Ohio River boring records from engineering reports dating from 1911 through 1914
353	Thin sections
270	Pebble count analyses for samples collected from 10 Ohio counties
241	Sidewall core or core plugs
199	Oil samples from Ohio's producing horizons
186	Reports detailing sand-and-gravel sample geology and quality
68	County sand-and-gravel data file inventories
37	Lake Erie bottom, shoreline, bay, or estuary vibracores
21	Folders of environmental impact reports containing boring logs or data

sample envelope (3 x 5 in [7.6 x 12.8 cm]) or coin envelope (2.5 x 4.25 in [6.4 x 10.9 cm]) that may contain only a few grams to over 100 g of sample. Each cutting suite is assigned a unique Survey sample number that is entered into the Oil and Gas Field and Wells Database and written on all the boxes storing the individual sample envelopes from a cutting suite. Cutting sample numbers begin with the number one and ascend sequentially. If a duplicate cutting suite is available, this cutting suite is identified by the original sample number and is entered in the duplicate cutting column of the Oil and Gas Field and Wells Database. The cutting sample number also is used to identify sample descriptions, laboratory analyses, strip logs, or other information gathered for an individual cutting suite.

The capture of the range data and missing intervals for well cutting collections is a time-consuming process that requires Survey staff (1) to compare the range of cutting samples recorded on the outside of the box with the range recorded on envelopes contained inside the box and with the Oil and Gas Field and Wells Database and (2) to examine the interval from which the cuttings were collected (e.g., 100–110 ft) on each individual envelope to determine if any intervals are missing. A typical box of well cuttings may range from a count of less than 20 to more than 100 envelopes, depending on the amount of cuttings samples in each envelope.

From 2010 through 2012, Chesapeake Energy Corporation donated cuttings from 392 wells, comprising 47,544 sample envelopes. These wells were located primarily in east-central Ohio (Fig. 11). So as part of this OCDO grant, the Survey inventoried these sample sets and recorded the range data and missing intervals. Some 288 of these cutting suites were new to the Survey's collection and 104 were useful duplicate cutting suites.

These 288 samples sets provided by Chesapeake contained 236 cutting suites that ranged stratigraphically from the Ordovician shale above the organic-rich Utica shale and Point Pleasant Formation, then downward in section through the oil- and gas-producing horizons of the Trenton Limestone, Black River Group, Rose Run sandstone, and upper Knox Dolomite. These cutting suites ended in the underlying Knox Dolomite or deeper units (Fig. 12). These newly donated cutting suites provide original and duplicate cuttings now available to be studied and analyzed for potential oil- and gas-producing or source rock horizons, for CO_2 sequestration targets, for brine or hazardous-waste injection well siting, and for identifying potential underground natural gas or liquid waste storage fields.

Core collection

The Survey's core collection through 2008 consisted of 845 individual cores located in Ohio, Kentucky, and West Virginia (Schumacher and others, 2008). Through 2012, the core collection has grown to 955 individual cores containing more than 300,000 ft (91,440 m) of core samples. Cores have been donated from 86 of the 88 Ohio counties and range in length from 4 in (0.1 m) to well over 1 mi (1.6 km). Core diameter ranges from 1 in (0.03 m) to 4 in (0.1 m), and the collection is stored in a wide variety of cardboard, plastic, and wood boxes. Each core or core description is identified with a unique number, beginning with the number one and ascending sequentially. In many cases, the Survey does not possess the core but rather holds a donated core description. Each core description is assigned a unique core number and entered into the Oil and Gas Field and Wells Database as a core description only.

The capture of core range data and missing cored intervals requires Survey staff members to compare the cored interval written on the outside of each box with the core present within each box. Once this information is captured it is compared with information stored in the Oil and Gas Field and Wells Database.

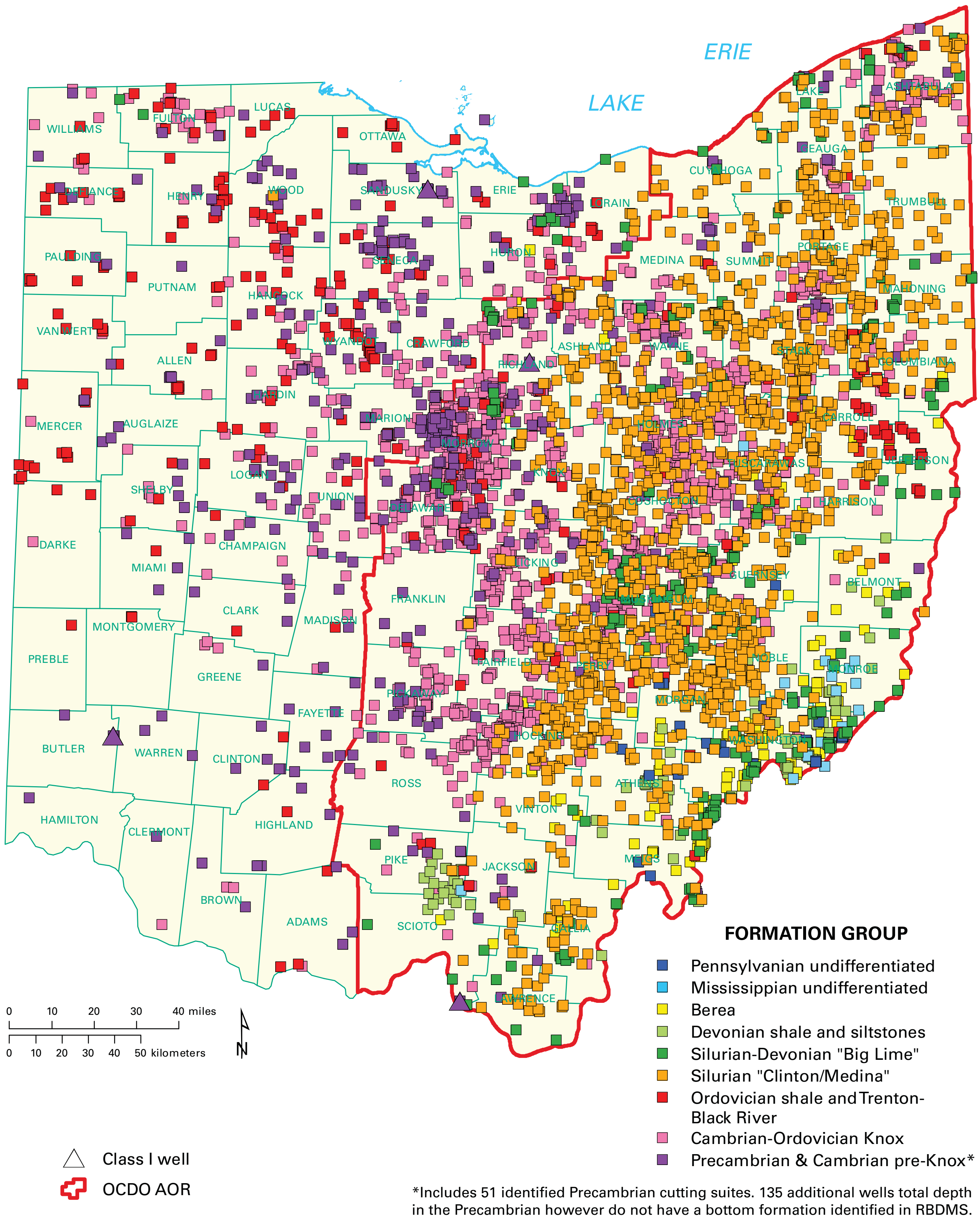

FIGURE 9.—Map showing available rock cuttings sample sets, composite. See Appendix B for a listing of the formation(s) for each OCDO group.

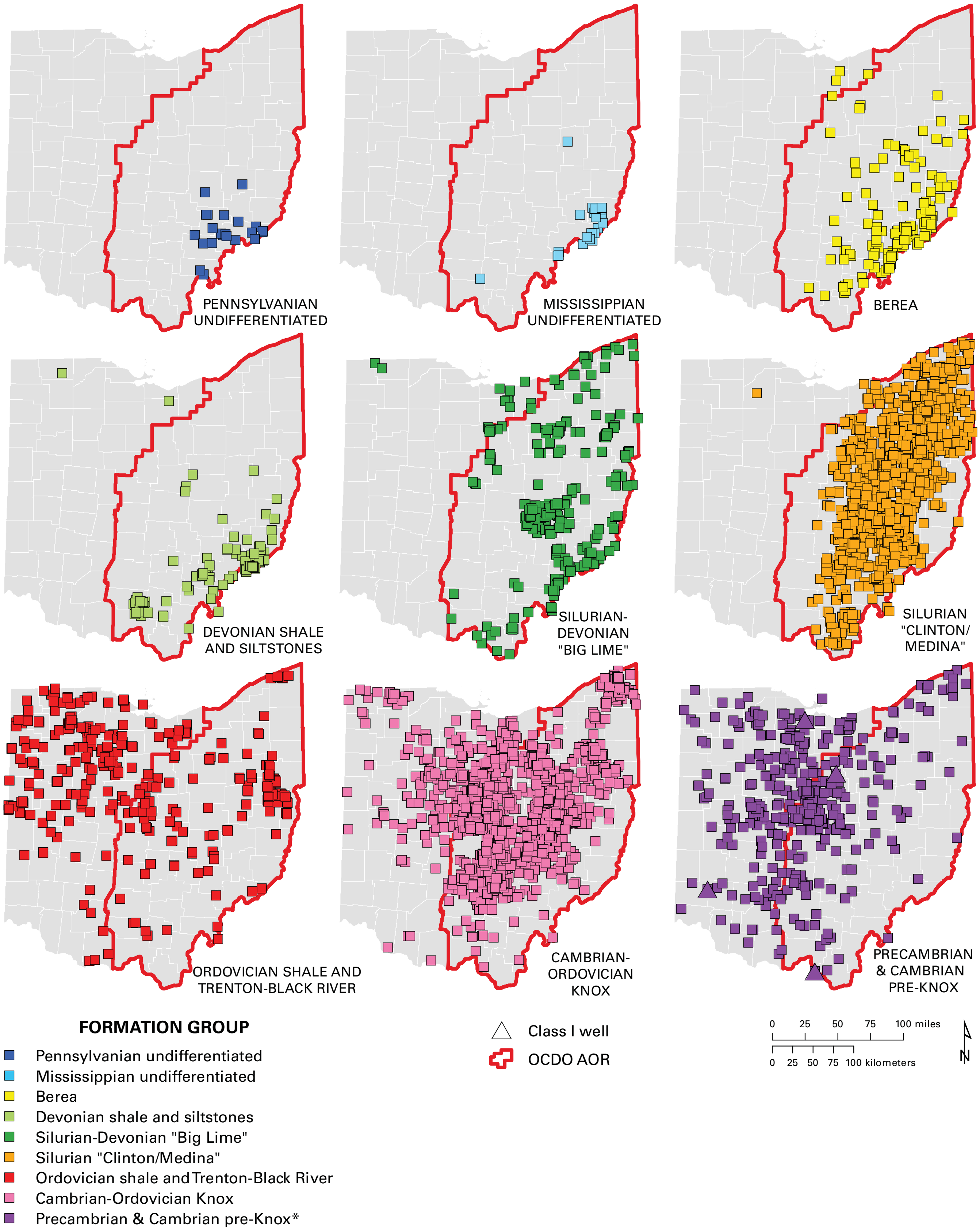

*Includes 51 identified Precambrian cutting suites. 135 additional wells total depth in the Precambrian however do not have a bottom formation identified in RBDMS.

FIGURE 10.—Maps showing available rock cuttings sample sets, by formation group. See Appendix B for a listing of the formation(s) for each OCDO group.

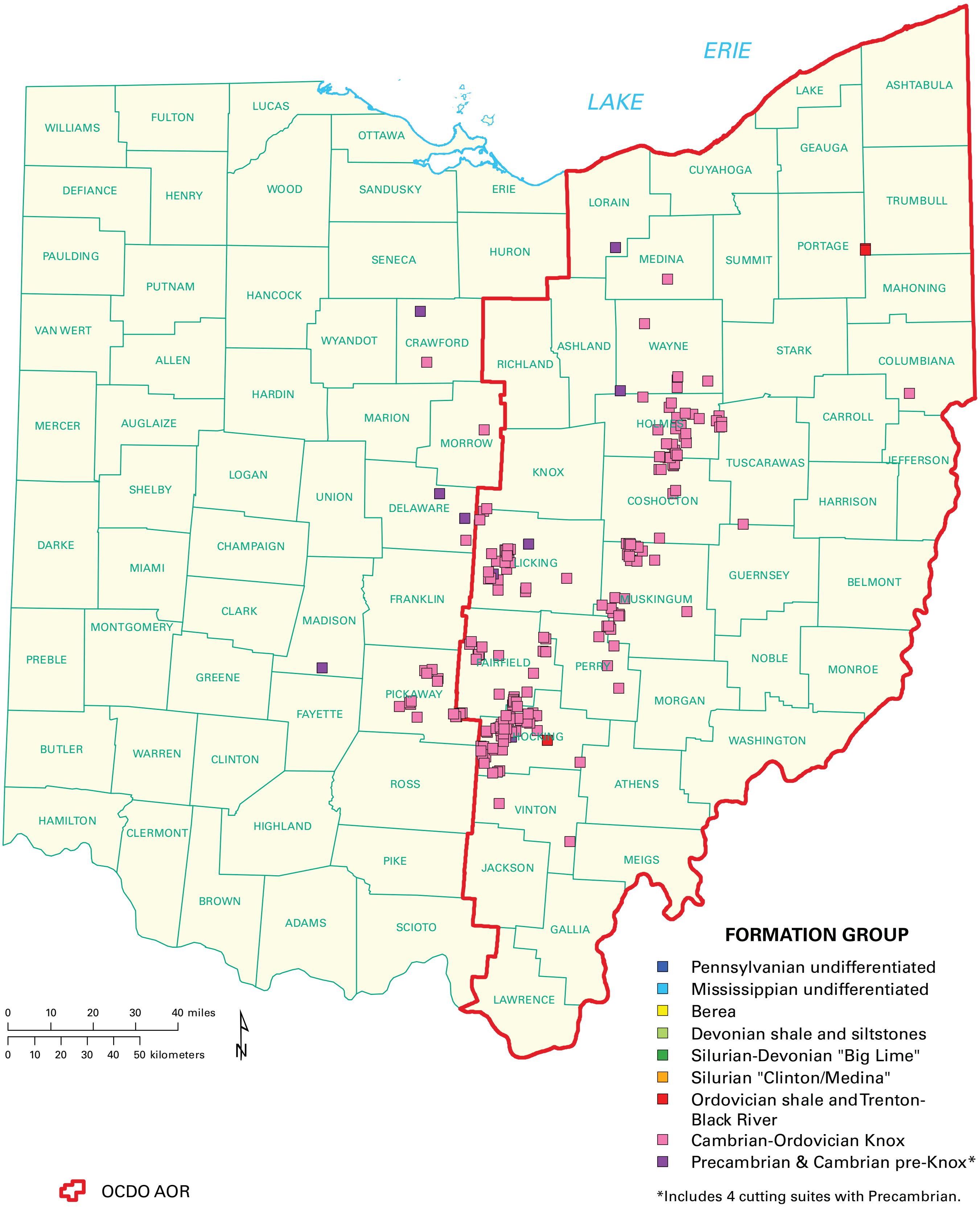

FIGURE 11.—Map showing distribution of cutting suites from eastern Ohio, donated by Chesapeake Energy Corporation. See Appendix B for a listing of the formation(s) for each OCDO group.

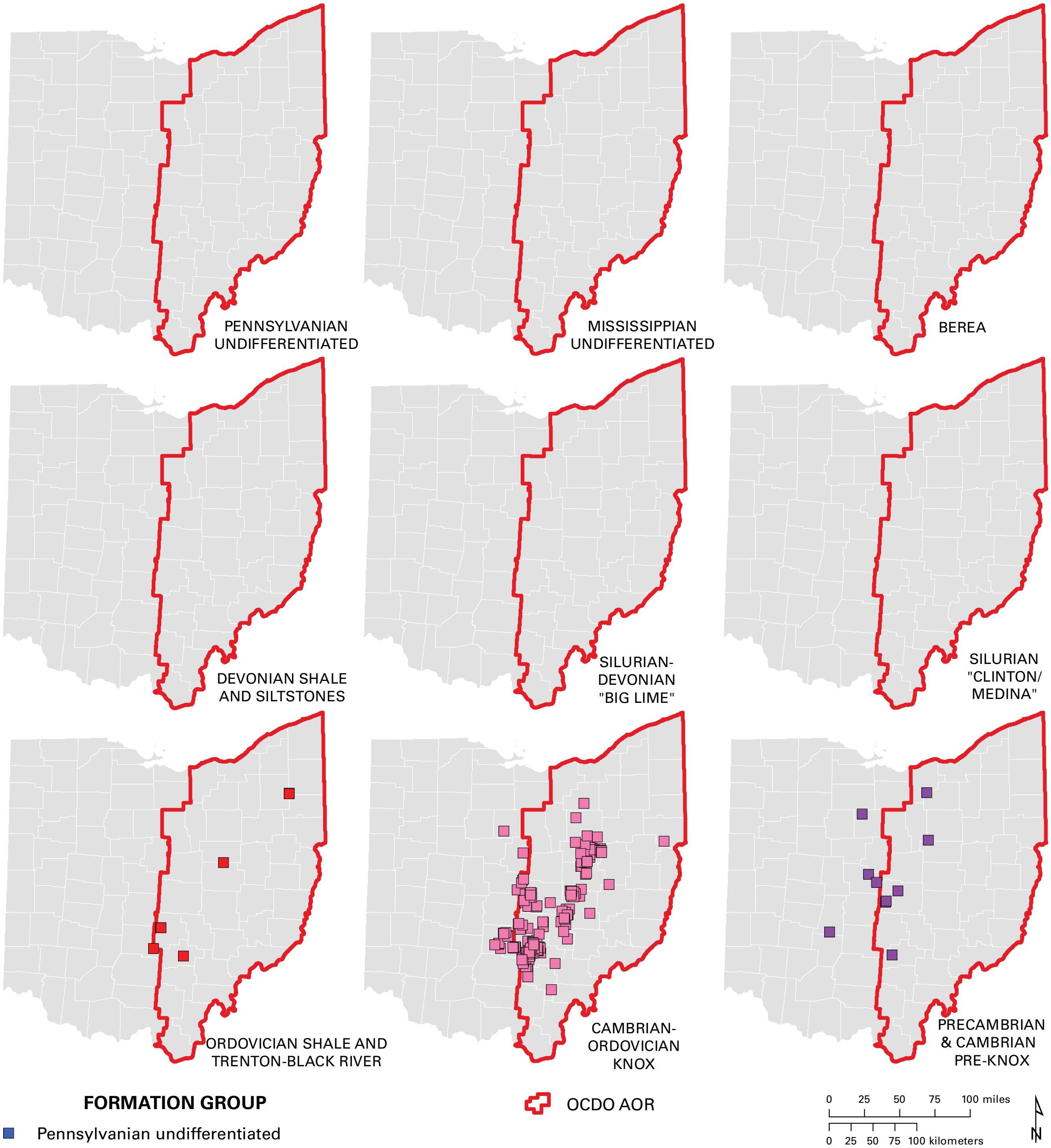

FORMATION GROUP

- Pennsylvanian undifferentiated
- Mississippian undifferentiated
- Berea
- Devonian shale and siltstones
- Silurian-Devonian "Big Lime"
- Silurian "Clinton/Medina"
- Ordovician shale and Trenton-Black River
- Cambrian-Ordovician Knox
- Precambrian & Cambrian pre-Knox*

*Includes 4 cutting suites with Precambrian.

FIGURE 12.—Maps showing distribution of cutting suites donated by Chesapeake Energy Corporation, subdivided by the basal formation or group in which each well was completed. See Appendix B for a listing of the formation(s) for each OCDO group.

Based on the comparison between database values and values written on each box, if there are missing intervals, then boxes were removed from the storage shelves and examined to determine what core is missing. This required the movement of hundreds of core boxes. Fortunately, a large percentage of the missing interval data had been collected and entered into the Oil and Gas Field and Wells Database over the years.

For this OCDO grant, the Survey initially targeted the 85 cores located in eastern Ohio that sampled geologic formations below 2,500 ft from the land surface. The cored range and missing intervals for each of these cores was checked, and range and missing intervals were captured in the Oil and Gas Field and Wells Database (Table 5). In addition, Survey staff members entered the cored range and missing interval data for all cores in the Survey core collection below 2,500 ft and the 110 new cores donated between 2008 and 2012.

TABLE 5.—*Eastern Ohio cores drilled below 2,500 ft from the land surface*†

Core Number	Top-Bottom Footage	Missing Intervals
2876	3300-3315	none
2877	4388-4500	Box 20/21: 2 ft (4492-94)
2883	2725-2747	Box 1: 2 ft (2725-37)
2884	2514-2554	Box 2: 1 ft (2517-24)
2886	2627-2651	none
2887	2558-2585	Box 1: 3 ft (2558-71) Box 2: 4 ft (2571-85)
2888	2743-2762	none
2889	2792-2815	Box 1: 3 ft (2792-2805)
2890	2715-2729	none
2891	2677-2706	Box 1: 7 ft (2677-86) Box 2: 6 ft (2686-94) Box 3 missing (2694-2702) Box 4: 2 ft (2702-06)
2903	4086-4142	none
3532	5757-5890	none
2845	2080-3198	none
2866	2488-2510	none
2871	1842-2682	Boxes 229-280 missing: 2526-2682
2904	5357-6076	Box 12 missing: 5417-6071
3414	3824-3876	none
3415	6145-6250	Box 4: 2 ft (6172-6184)
3416	6221-6276.5	none
3417	3730-3826	Box 1/2: 7 ft (3737-44) Box 8 missing: 3784-92 Box 9: 2 ft (3792-3802)
3418	3480-3587	Box 4: 1 ft (3503-12)
3419	3642-3713	Box 3: 1 ft (3656-65) Box 4 missing: 3665-74 Box 5: 3 ft (3674-85) Box 6: 1 ft (3685-94) Box 8: 1 ft (3702-11)
3543	5736-5485	5379-5412 missing, 5415-29 missing, Box 3-1/2: 2 ft (5440-45) 5447-54 missing, Box 3-10/11/12: 5 ft (5467-75)
3583	3860-4177	Box 3/4: 3872-4100 Box 11: 11 ft (4127-42) Box 12: 6 ft (4142-52) Box 17: 5 ft (4168-77)
3640	5947-6017	none
3003	5630-5660	Box 1/2: 1 ft (5639-40)
3006	6736-6795.7	none
3382	8097-8295	Box 2: 1 ft (8103-10) Box 5/6: 123 ft (8126-8249) Box 6: 2 ft (8255-63)
3383	4255-4300	none
3385	5967-5986	Box 2: 5 ft (5973-84)
3389	3853-3967.5	none
3390	5280-5426	Box 1/2: 5 ft (5283-88) Box 3: 2 ft (5295-5305) Box 18: 1 ft (5412-22)
3410	5042-5169	Box 4: 9 ft (5051-63) Box 10: 3 ft (5076-82) Box 12: 2 ft (5084-89), Box 17: 2 ft (5101-06) Box 21: 3 ft (5113-19) Box 28: 5 ft (5134-42)
3424	2682-2712	Box 3: 1 ft (2688-92) Box 4: 1 ft (2692-96) Box 6/7: 3 ft (2702-05)
3427	4775-4860	Box 6: 3 ft (4786-92)
3477	4882-4998	Box 2-1 missing (4916-20), Box 2-6 missing (4391-33), Boxes 2-10/11/12 missing (4941-48), 4954-58 missing 4963-66 missing, Box 4-10: 1 ft (4989-93)
3488	3664-4309	Box 1: 7 ft (3664-80) Box 2: 7 ft (3680-96) Box 3: 6 ft (3696-3711), jump from 3711-4264, Box 5: 6 ft (4283-98) Box 6: 2 ft (4298-4309)
3492	3875-3993	Box 1: 1 ft (3875-85) Box 2: 3 ft (3886-98_ Box 2/3: 5 ft (3898-3903) Box 3/4: 14 ft (3909-23) Box 4/5: 17 ft (3936-53) Box 6/7: 10 ft (3969-79) Box 7/8: 5 ft (3982-87
3501	720-2680	Box 3: 1 ft (726-30) Box 18/19: 3 ft (773-76), jump from 783-1069, Box 49/50: 4 ft (1746-50), jump from 1835-2301
3503	3692-3816	Box 2: 2 ft (3694-99) Box 3: 1 ft (3699-3703) Box 4: 2 ft (3703-08) Box 11: 2 ft (3725-30) Box 12: 1 ft (3730-34) Box 13: 1 ft (3734-38)
3542	4765-4832	Box 2-6 missing (4796-98) Box 2-13 missing (4815-18)
510	12 to 2810	Box 5: 2 ft (52-64) Box 17: 2 ft (172-84) Box 20: 5 ft (204-19) Box 22: 1 ft (229-40) Box 28: 9 ft (290-309) Box 38: 9 ft (399-418) Box 41: 3 ft (438-51) Box 49: 2 ft (519-31) Box 52: 1 ft (551-62) Box 54: 2 ft (572-80) Box 59: 1 ft (622-33) Box 60: 3 ft (633-46) Box 61: 3 ft (646-59) Box 82: 2 ft (859-71) Box 124: 1 ft (1281-92) Box 136: 1 ft (1400-11) Box 168: 6 ft (1720-36) Box 172: 3 ft (1766-79) Box 176: 7 ft (1809-26) Box 181: 1 ft (1866-77) Box 186: 1 ft (1917-28) Box 191: 1 ft (1968-79) Box 199: 1 ft (2049-60) Box 201: 2 ft (2070-82) Box 206/207: 3 ft (2132-35) Box 210: 1 ft (2165-76) Box 217: 2 ft (2236-48) Box 220: 3 ft (2318-31) Box 224: 4 ft (2361-75) Box 227: 4 ft (2395-2409) Box 234: 20 ft (2469-99)

		Box 237: 1 ft (2519-30) Box 261: 16 ft (2759-85) Box 263: 4 ft (2795-2809)
520	3510-3627.7	Box 16: 1 ft (3567-72) Box 17: 1 ft (3572-77) Box 20: 2 ft (3585-91)
569	2548-3306	none
988	3601-3677	Box 13/14: 2 ft (3624-26) Box 20/21: 2 ft (3640-42) Box 25/26: 2 ft (3651-53)
990	3900-3925	Box 1: 1 ft (3900-03)
991	802-3573	Box 61/62: 3 ft (3565-68) Box 64/65: 1 ft (3574-75)
2713	6801-6928	Box 4: 0.5 ft (6818.5-25) Box 6: 2.5 ft (no 6832-34.5) Box 9: 2 ft (6850-58) Box 15: 1 ft (6884-91)
2835	4169-4217	Box 1: 3 ft (4169-74) Box 2: 3 ft (4174-79) Box 3/4: 2.5 ft (4181-83.5) Box 8: 0.5 ft (4190.5-93)
2914	3324-3339	none
2921	2914-3370	Box 124: 2 ft (3283-88) Box 126: 1 ft (3290-94) Box 150: 5 ft (3358-64)
2922	3360-3684	none
2936	1750-4151	none
2937	4690-4748	none
2939	4344-4360	none
2941	3096-3120	Box 2: 2 ft (3105-16)
2942	3211-3237	Box 2: 3 ft (3220-32)
2943	2900-2922	Box 1: 2 ft (2900-11) Box 2: 1 ft (2911-21)
2948	3692-3817	Box 1: 5 ft (3692-3737) Box 2: 30 ft (3737-77) Box 3: 30 ft (3777-3817)
2951	3976-4062	Box 12: 2 ft (3995-99)
2952	3900-4000	Box 1: 28 ft (3900-38) Box 2: 27 ft (3938-75) Box 3: 15 ft (3975-4000)
2961	4410-4567	Box 1: 1 ft (4453-56) 1 ft (4456-59) 1 ft (4467-70)
		Box 2: 6 ft (4506-14) 5.5 ft (4516-23.5) 1 ft (4526-29) 1.5 ft (4529-32.5) 5 ft (4560-67)
2962	1500-2710	none
2963	7646-7688	none
2964	960-4216	jump from 998-4080
2965	3133-3185	Box 10: 1 ft (3151-54) Box 13: 1 ft (3158-61) Box 18: 1 ft (3169-22) Box 20: 1 ft (3174-77)
2966	3490-3713.5	Box 1-21: 1 ft (3544-48) Box 2-7: 1 ft (3563-67) Box 3-12: 1 ft (3637-41) Box 3-13: 1 ft (3641-45)
		Box 3-14: 5 ft (3645-53) Box 4-4: 1 ft (3661-65) Box 4-11 missing (3682-84) Box 4-20: 1 ft (3707-11)
2967	2462.5-?	none
2979	4993-5037	none
2980	2820-2839	Box 2: 2 ft (2828-38)
2989	6570-6652	Box 1: 17 ft (6570-93) Box 2: 2 ft (6593-6601) Box 3: 19 ft (6601-26) Box 4: 3 ft (6626-35) Box 5: 11 ft (6635-52)

†Cored interval and missing intervals provided.

Cutting and paper strip log collection

The Survey collection of cutting and paper strip logs consists of over 3,500 strip logs. These logs record many geologists' observations on the lithology, mineral content, fossils, and other geologic information for cores, oil and gas cutting samples, and measured sections from Ohio. The Survey's collection contains cutting strip logs from 676 wells. A cutting strip log consists of a small sample of cuttings that are glued to cardboard logs, measuring 4 x 28 in (10 x 71 cm). The cuttings removed from each envelope are glued to the corresponding footage range recorded on the envelope. For example, if an envelope of cuttings was collected between 100 and 110 ft, then a small amount would be glued on the log between 100 and 110 ft. Individual strip logs can be joined together to form a single strip log displaying all the cuttings recovered from a particular well. These logs are very useful to quickly review all the cuttings from a well and to focus on the cuttings from the interval or intervals of interest.

Paper strip logs are produced by geologists to summarize their descriptions, observations, and interpretations of the well cuttings, core, or stratigraphic sections studied from Ohio. Paper strip logs come in a variety of sizes. The Survey uses a standard paper strip log measuring 3.25 x 14 in (8.25 x 35.5 cm) with an adhesive strip that can be used to connect one log to another. Each paper strip log is labeled with the Survey cutting sample, core, or measured section number for easy identification.

A portion of the cutting and paper strip log collection was inventoried as part of the work completed for the NGGDPP grant funded between 2006 and 2007. In 2008–2009, two large collections of cuttings and paper strip logs were donated to the Survey, consisting of cutting strip logs from 99 wells and paper strip logs from 1,819 wells. For the OCDO grant, each of these strip logs were examined to determine the range and the missing intervals displayed on each. The information gathered then was captured in the Oil and Gas Field and Wells Database.

Data Mining Results

The goal of the data mining effort for the OCDO grant was to capture range data and missing intervals from the Survey's cutting, core, and strip log collections. These data were captured and entered into the Survey's Oil and Gas Field and Wells Database. The work completed to mine and catalogue cuttings, strip logs, and core is summarized in the following paragraphs.

The Survey the checked Oil and Gas Field and Wells Database for range data and missing intervals for all cores and cutting suites in the Survey collections; captured range data and missing intervals for those cores and cuttings suites that did not have this information; and examined over 5,800 records and then checked the cutting suite and core collections to capture missing data.

The Survey updated the Oil and Gas Field and Wells Database by entering the necessary data for cores and cuttings suites acquired since 2008 and also corrected erroneous data present in the database. Survey staff entered over 600 new cuttings suites and cores in this effort.

Finally, the Survey completed review and revision of its strip log collection. The Oil and Gas Field and Wells Database was updated to separate the cutting strip logs from the collection of paper strip logs. Data captured included missing intervals, cutting suite range data, and the top and bottom geologic formation sampled. Over 1,900 records were checked and revised, as necessary, and new strip logs were entered.

Oil & Gas Geophysical Logs (TIFF and LAS Locations)

The Survey has collected and archived some 74,400 suites of borehole geophysical logs in hardcopy form, provided by various members of the oil-and-gas industry as they explore for and develop oil and gas reserves. Maps were generated showing the locations and geographic coverage of wells drilled and logged to certain formation groups or intervals of interest (Table 3). (See Figs. 13 and 14 for logged locations within the state.)

As Survey geologists engage in various research projects involving log correlation and petrophysical analysis on either a local or regional scale (e.g., reservoir characterization of the East Canton oil field or deep regional geologic mapping for Class I permit evaluations), there is a need to create composite Log ASCII Standard (LAS) files of various logs either from the hardcopy archive or from Tagged Image File Format (TIFF) images. Simply put, LAS files are digital versions of scanned geophysical (TIFF) logs. These files are collected, created, and managed by the Survey through the digital archiving process. These LAS files are beneficial because they can be built to combine multiple paper logs from an individual well into one comprehensive file. As unique files are created, they are merged together until the log suite is completed; they are then added to the archives. The added value of LAS files for research projects across the state is incalculable. Having the digital geophysical information allows geologists to easily calculate new geophysical parameters to help define and determine rock properties for individual units that can be correlated regionally. To date, using a table top-digitization process and NeuraLog software, the Survey has created over 600 LAS log files. Due to the complexity and diversity of these files, they can only be mapped based on location, as a composite. (See Fig. 15 for locations of all the final LAS files created or compiled by the Survey.)

For this grant, a significant number of LAS files were created and used by the Survey and also provided to Battelle to enable development of geologic interpretations. The Survey also has created LAS log files to map the thickness of organic-rich shale in the Marcellus and the Utica-Point Pleasant interval and to support mapping of key source rock geochemical parameters of Utica/Point Pleasant interval. The Survey also has used LAS files in conjunction with the GeoGraphix software module PRIZM to perform petrophysical analyses of complex mineral relationships present in sub-Knox clastic rocks, such as the Mt. Simon Sandstone, Conasauga Formation, and the Cambrian basal sand. Such work has been performed, in part, to account for the fact that some minerals (e.g., glauconite) elicit a positive gamma-ray response on basic wireline logs that implies the presence of clay-rich shale when actual lithology is less clay-rich and more permeable than implied by the basic gamma log.

Porosity and Permeability Data

Porosity and permeability are hydraulic properties for which data is collected from specific formations at specific locations. These data can be used to address a wide variety of objectives surrounding fluid flow characteristics through a rock matrix. Ohio's porosity and permeability data set is managed by the Survey and is stored in RBDMS. The majority of the data collected derives from analysis of core samples as well as Class I and ClassII injection wells. These data can identify favorable formation or reservoir fluid flow and storage potential and also hydraulically conductive zones. Using these data in conjunction with other data types (e.g., geophysical logs) enables characterization and mapping of formations across broader regions.

Porosity and permeability data were compiled by querying the database as well as going through individual wells files. Once all the data was gathered and associated to specific formations, they were mapped in composite (Fig. 16) and by formation groups (Fig. 17). These data were mapped based on the same formation groups discussed in Table 3. The relatively limited dataset demonstrates the need of additional data in order to perform regional reservoir analysis.

Formation and Well Pressure Data

Formation pressure and formation pressure gradient are key reservoir characteristics for storage potential. The pressure database is obtained from well completion reports and is managed by DOGRM in the RBDMS. The dataset includes minimum, maximum, and average pressures of the following data types: bottom hole pressure (BHP), breakdown pressure, treating pressure, instantaneous shut-in pressure (ISIP), and five-minute ISIP. Each of these types of pressure data is collected during a specific time within the well completion process and the pressure gradient is calculated using the measured pressure divided by depth. The pressure gradient equalizes the pressures to depth, which indicate if a reservoir is over, normal, or under pressured. The BHP is measured in pounds per square inch (psi), collected at the bottom of the borehole.

It is important to know the BHP while circulating drilling fluids, keeping it above the formation pressure or pressure gradient in order to prevent an excessive influx of formation fluids into the borehole. Equally important is sustaining a BHP below the formation breakdown pressure. This helps to maintain wellbore integrity in weak formations, preventing them from breaking down, which results in a loss of borehole fluids.

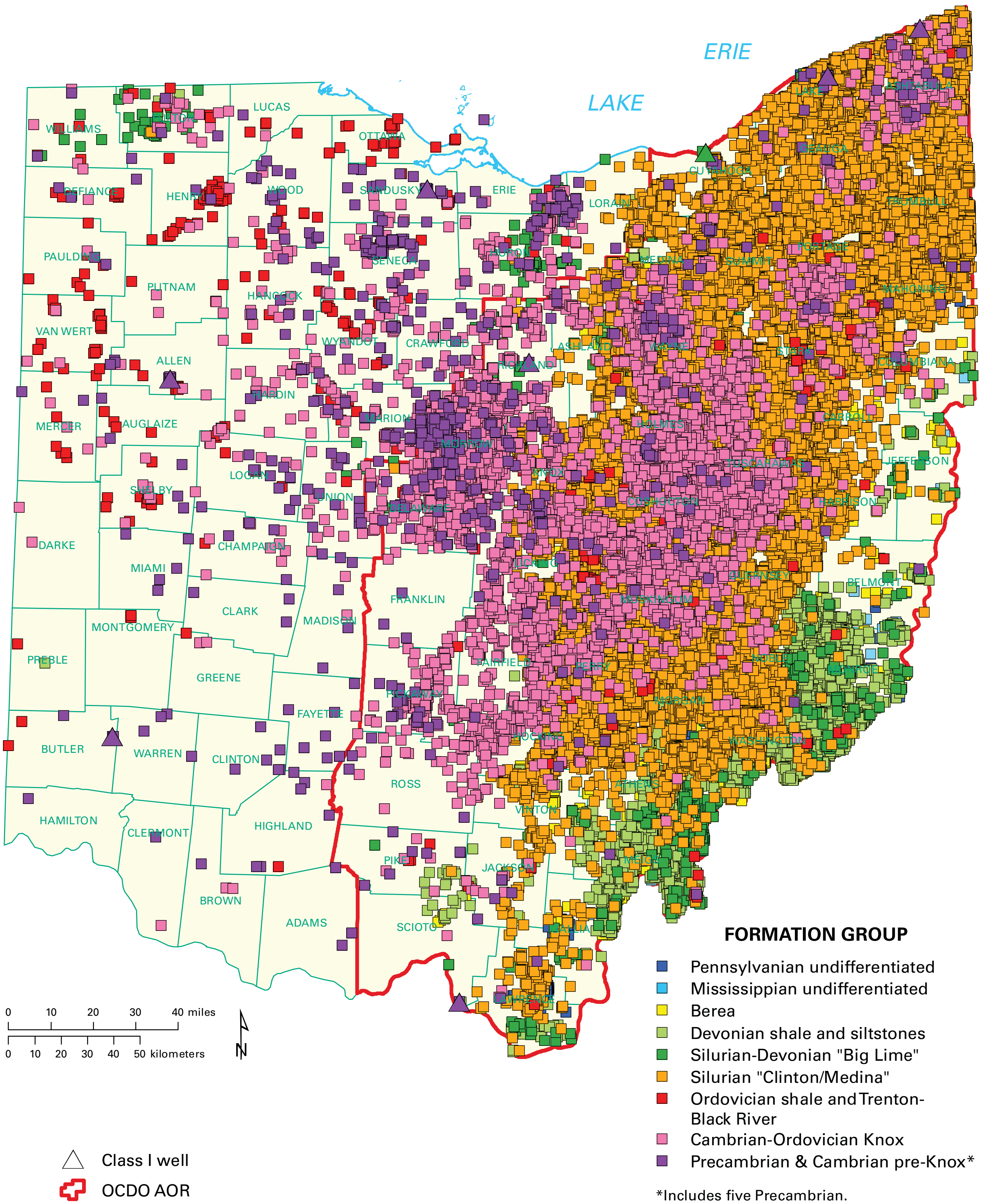

FIGURE 13.—Map showing geophysical log locations, composite. See Appendix B for a listing of the formation(s) for each OCDO group.

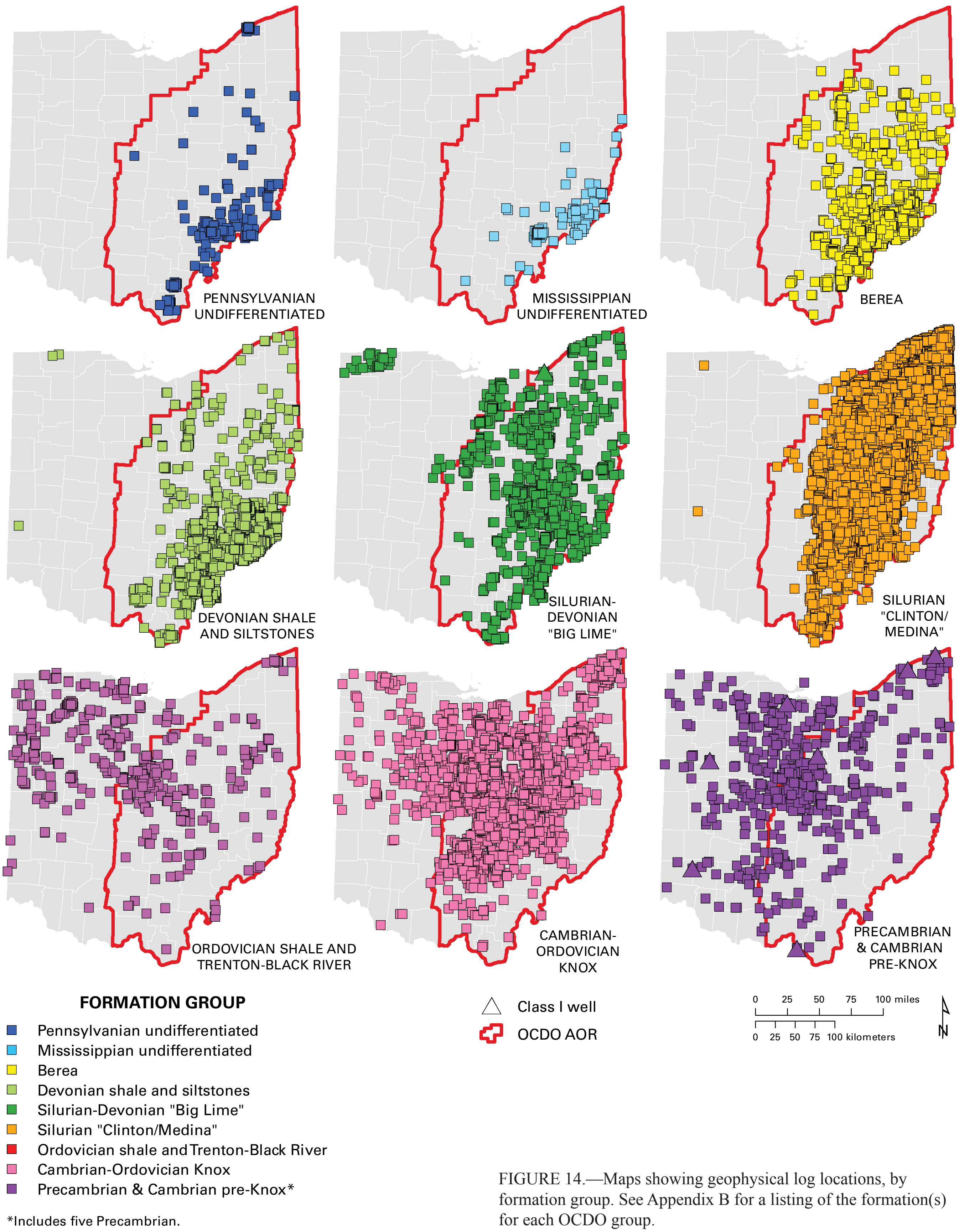

FIGURE 14.—Maps showing geophysical log locations, by formation group. See Appendix B for a listing of the formation(s) for each OCDO group.

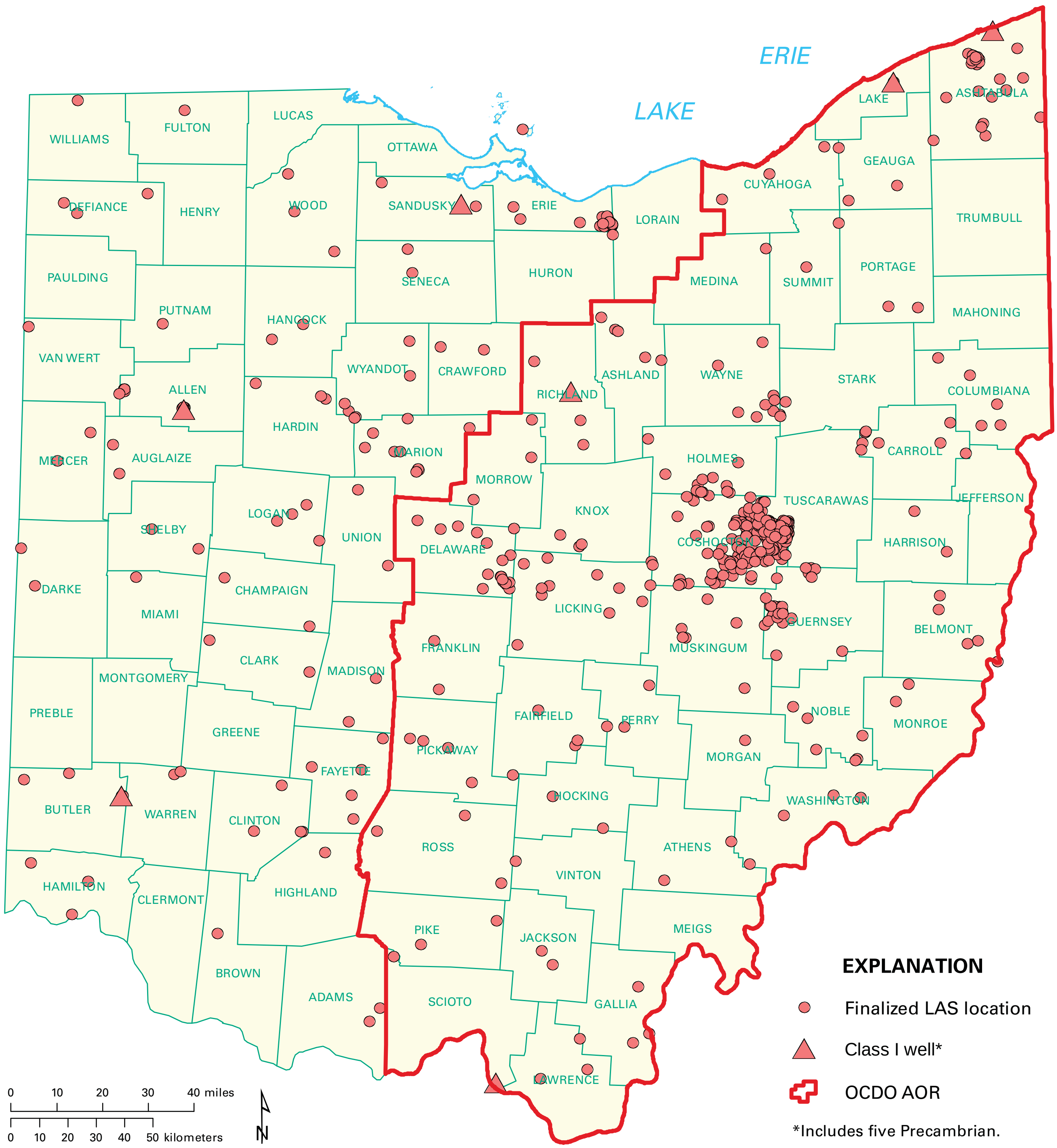

FIGURE 15.—Map showing finalized LAS locations. See Appendix B for a listing of the formation(s) for each OCDO group.

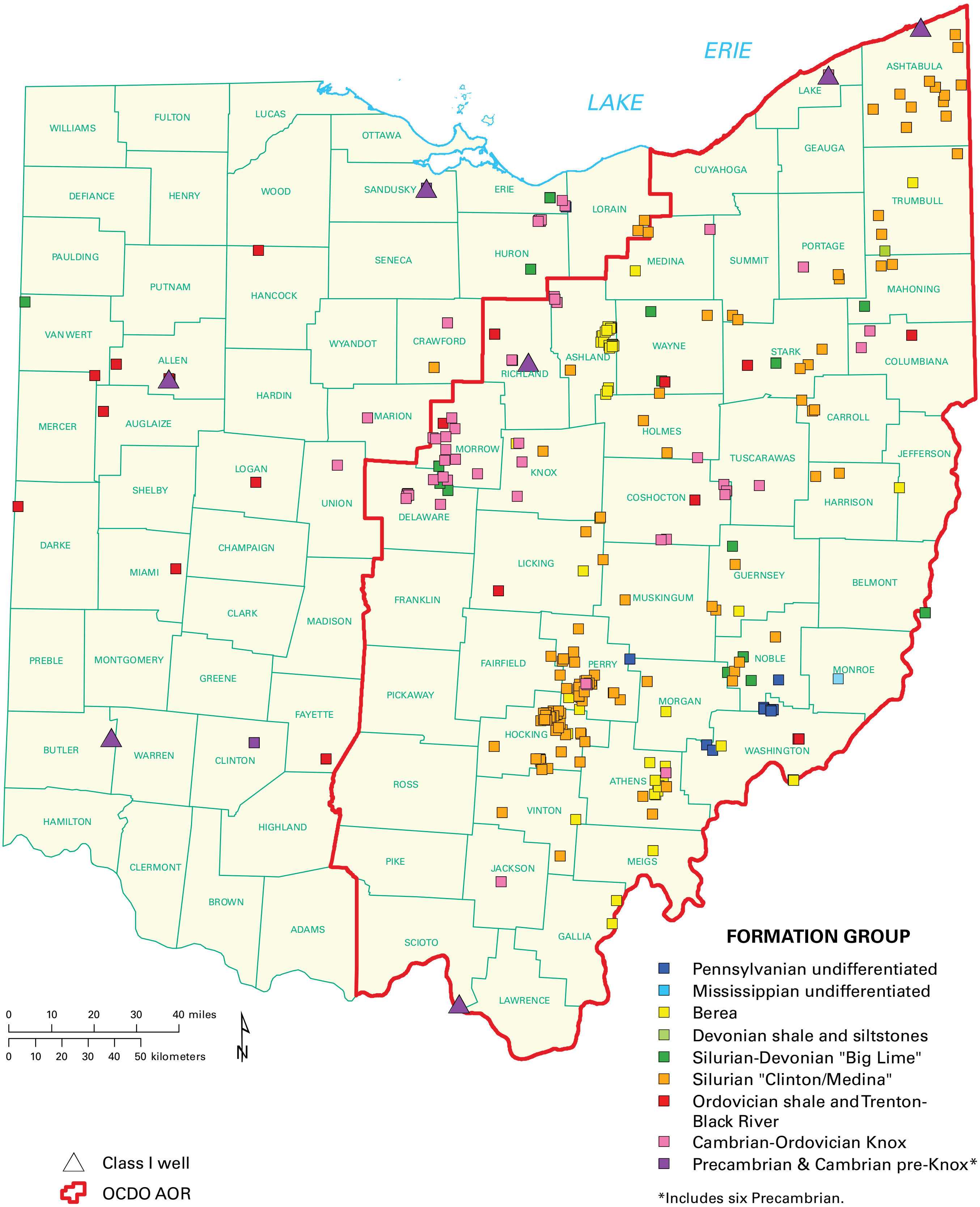

FIGURE 16.—Map showing available porosity and permeability data from rock cores and well testing, composite. See Appendix B for a listing of the formation(s) for each OCDO group.

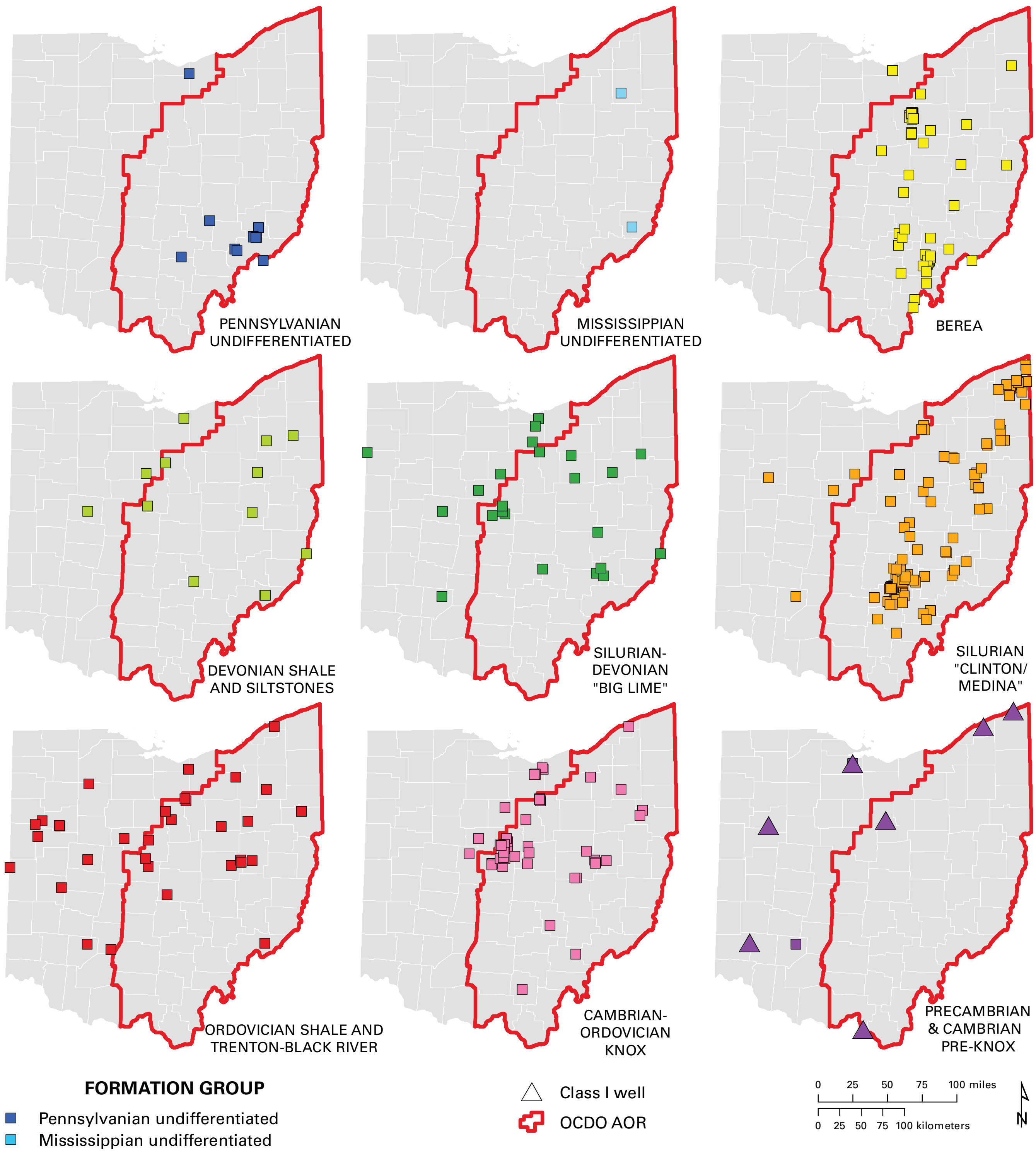

FORMATION GROUP

- Pennsylvanian undifferentiated
- Mississippian undifferentiated
- Berea
- Devonian shale and siltstones
- Silurian-Devonian "Big Lime"
- Silurian "Clinton/Medina"
- Ordovician shale and Trenton-Black River
- Cambrian-Ordovician Knox
- Precambrian & Cambrian pre-Knox*

*Includes six Precambrian.

FIGURE 17.—Maps showing available porosity and permeability data from rock cores and well testing, by formation group. See Appendix B for a listing of the formation(s) for each OCDO group.

The breakdown pressure, measured in psi, is the pressure at which the rock matrix begins to fracture, allowing fluids to invade the exposed formations. This parameter is important in many drilling processes. For instance, the process of hydraulic fracturing requires that the fracture pressure exceed the formation breakdown pressure, thus allowing the fracture fluids to induce and propagate new rock fracturing.

Other types of well stimulation and treatment must be done at pressures that avoid hydraulic fracturing but yet are high enough to allow treatment fluids to enter the formation. These types of activities are done at pressures well below the breakdown pressure. Treating pressure, measured in psi, allows fluids to infiltrate the formation while maintaining hole integrity by not creating new fracture systems.

The ISIP, measured in psi, is the pressure measured immediately after injection/treatment stops. The ISIP provides a measure of the pressure in the fractures at the wellbore by removing contributions from the fluid friction.

Lastly, the five-minute ISIP is the pressure measured five minutes after injection/treatment stops. This parameter can be used alongside other parameters to better evaluate and understand the success of an applied completion process. Figure 18 shows a hypothetical graph of pressure versus time during the formation treatment and/or the hydraulic fracturing process; the captions identify pressure data collected during the process.

Combining the pressure datasets described above and looking at individual formations across a geographic area and the pressures needed to complete drilling and treating processes help us understand the characteristics and the overall nature of the subject formation. These data can be used to delineate areas that are under higher gradient pressures, which may result in better hydrocarbon production or may have poorer CO_2 injectivity for CCS or CCUS. Conversely, an area exhibiting lower pressure gradients may have less hydrocarbon production potential but, in turn, may have better CO_2 storage potential.

Available pressure data have been mapped both in a composite plot (Fig. 19) and by formation groups discussed and outlined in Table 3 (Fig. 20). These maps display well locations at which we have recovered and compiled any type of formation pressure. There are numerous errors within this dataset and it needs to be scrupulously reviewed to correct formation names, as well as transcription or transposition errors.

Injection Well Data

Well injection data is compiled by DOGRM in RBDMS. This data is very relevant to the objectives of CCS and CCUS in that these are records of injection activities alreading occuring successfully at locations across the state. Injection data is a very significant data set gathered by DOGRM and recorded in RBDMS. These data provide a general indication of the formations and locations across the state possessing favorable characteristics for injecting and storing fluids. During the data mining process, the Survey gathered data on the total volumes of injected liquid and the total days of injection for various injection wells possessing records. Useful data are derived from active and inactive Class I and Class II wells, solution-mining wells, and other injection well types. Once these data were collected, the Survey calculated injection rates based on the

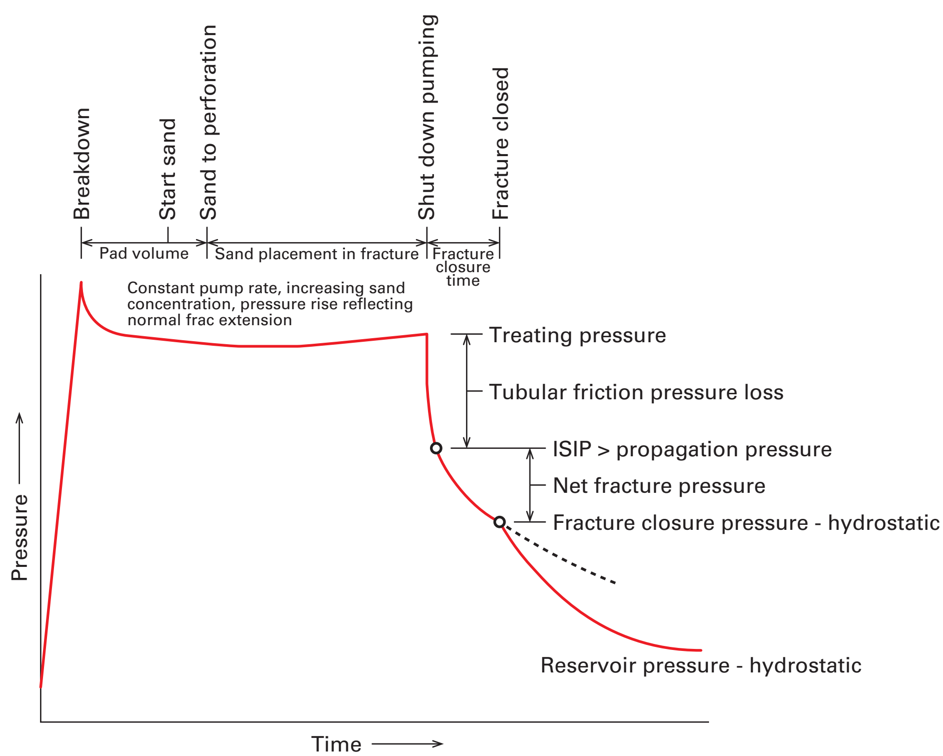

FIGURE 18.—Graph of pressure versus time during formation treatment and/or hydraulic fracturing process. Modified from U.S. Environmental Protection Agency. (2012).

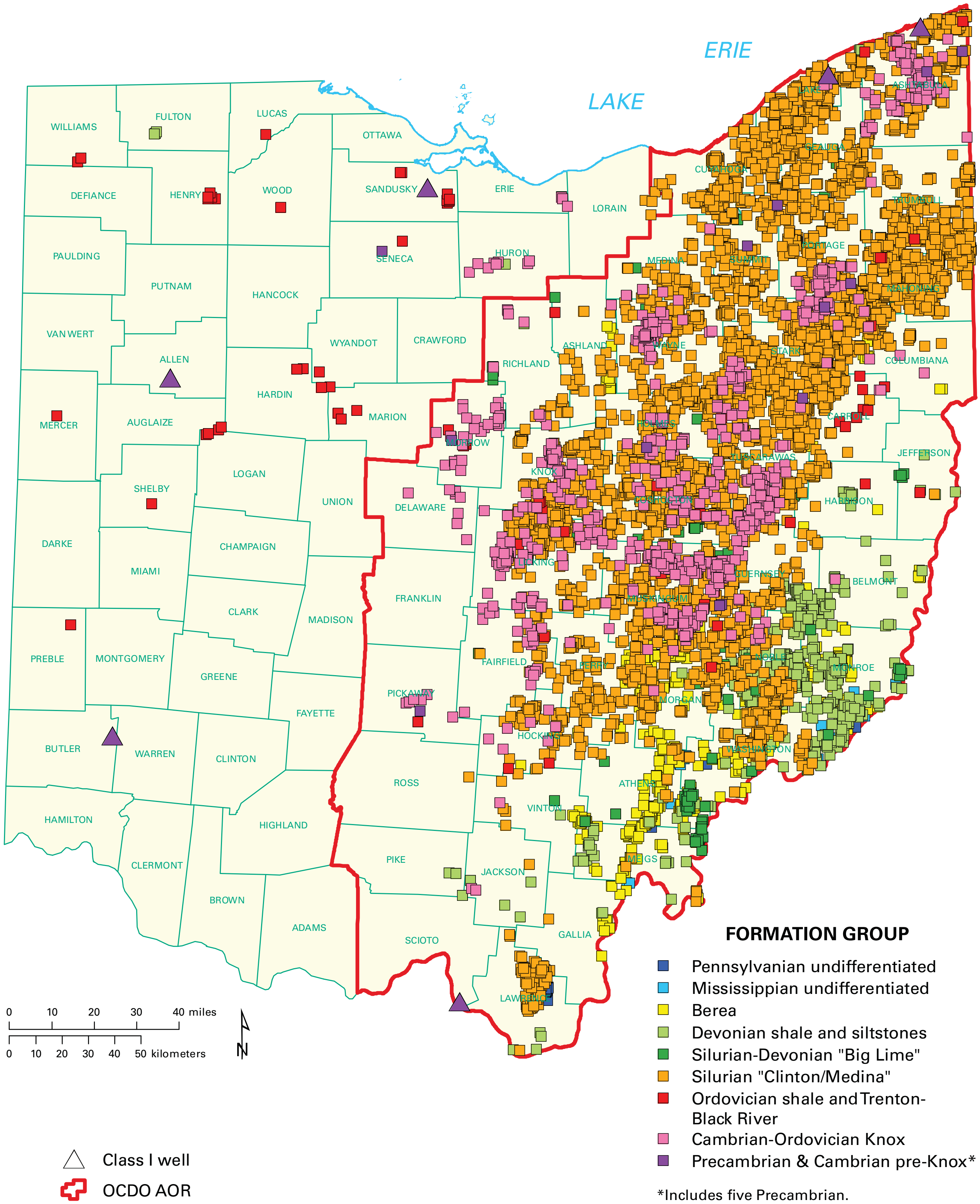

FIGURE 19.—Map showing available formation pressure data, composite. See Appendix B for a listing of the formation(s) for each OCDO group.

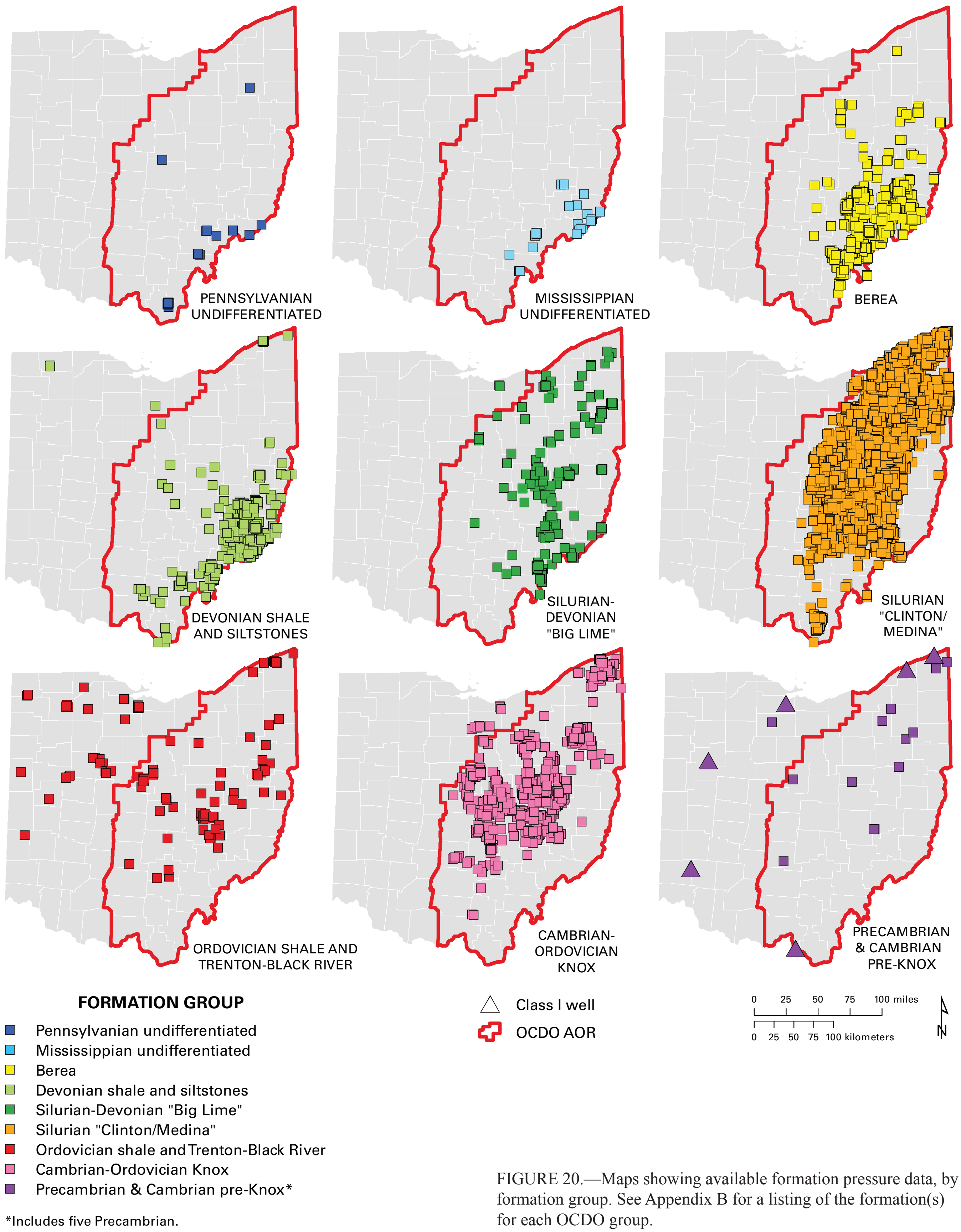

FIGURE 20.—Maps showing available formation pressure data, by formation group. See Appendix B for a listing of the formation(s) for each OCDO group.

recorded total volumes of barrels injected divided by the total number of days of injection, as shown in the following equation:

$$\text{Rate of injection} = \frac{\text{Total injection volume (bbls)}}{\text{Total days of injection}}$$

Note that the Class I data set does not contain records of the number of injection days, therefore only Class I well locations are shown in figure 21. For all other wells that the Survey plotted, the calculated injection rates were normalized to show how much fluid was stored in one injection day. For this mapping exercise, with respect to designating targeted injection intervals, the Survey correlated and mapped each well based on the uppermost unit open in the well, according to the delineated formation groups (see Table 3). Figure 21 is the composite map of brine injection wells across Ohio; figure 22 locates these injection wells according to targeted formation group. As explained in the key on each map, for each well, the well symbol was sized based on its normalized injection rate.

It is worth noting that there are inherent limitations to this dataset. One of the biggest limitations is that injection wells are open-hole completions so that there are multiple formations open in these wells. In such cases it is impossible to know exactly into which formation the fluid is entering and being stored. Another map limitation is that not all wells are known to be injecting at maximum capacity. Many wells likely have higher injection capacities but only show the injected amount of brine supplied; so if supply is low, injection volume is shown to be low. While we have a good starting dataset, more work is needed to more thoroughly appraise and quantify injection capacity per formation across the OCDO AOR. The wells plotted on these maps point to areas and formations showing favorable performance, injectivity, and storage potential, but finding new injection areas and knowing why some areas perform better than others remains to be determined.

Reservoir Brine Geochemistry Data

There are two definitions worth citing when investigating brine data in Ohio. Ohio Revised Code 1509.01(U) defines *brine* as "all saline geological formation water resulting from, obtained from, or produced in connection with exploration, drilling, well stimulation, production of oil or gas, or plugging of a well" (ORC, 2000). The regulatory definition of brine would include stimulation fluids introduced into a formation. This broad definition of brine will not be used in this report; instead we will use the geological definition of brine as the natural pore fluids in deep sedimentary basins that consist of highly saline waters containing calcium, sodium, potassium, chlorine, and minor amounts of other elements (Jackson, 1997).

The chemistry of waters in a storage reservoir will be one of the main influences on solubility and mineral trapping once carbon dioxide has been injected into the subsurface (Parris and others, 2010). Successful geologic sequestration of carbon in deep saline aquifers requires accurate predictive models of rock-brine-CO_2 interaction. Often overlooked in siliciclastic-hosted saline reservoirs is the carbonate buffering of the formation water (Newell and others, 2008). The Ohio Brine Geochemistry Database is an important tool to help determine areas most favorable for carbon sequestration.

The Ohio Brine Geochemistry Database, which is maintained in Microsoft Access, currently consists of 569 formation water analyses. The Survey contributed geochemical analyses of 201 brine samples (Orton, 1888; Root, 1888; Bownocker, 1906; Conrey, 1921; Stout and Lamborn, 1924; Stout and others, 1932; Lamborn, 1952; Clifford, 1975; Stith and others, 1979; Stith and Knapp, 1989) collected primarily from producing oil and gas wells located in eastern Ohio. In addition, 260 geochemical or log analyses of subsurface brines were added from various published sources and unpublished Master of Science theses (Ransome, 1913; Mills and Wells, 1919; Thompson, 1973; Ohio River Valley Water Sanitation Commission, 1976; Shindel and others, 1983; Breen and others, 1985; Lowry, 1986; Sanders, 1986; Wilk, 1987; Leahy, 1996; Barton and others, 1998; A.H. Lawhead, unpub. data, n.d.). Resistivity (Rw) values and limited geochemical and geologic information was obtained from the Ohio Chapter of the Society of Professional Well Log Analysts for 108 locations.

The majority of the brine analyzed came from the Lower Silurian "Clinton/Medina" sandstone (267); the Cambrian-Ordovician Knox Dolomite, which includes the Copper Ridge dolomite, Rose Run sandstone, and Beekmantown dolomite (129); and the Silurian Lockport Dolomite (88). Depths to the intervals sampled ranged from 220 ft to 9,080 ft, with 329 formation brine analyses from hydrocarbon-producing zones greater than 2,500 ft in depth. There are approximately 324 formation water analyses from greater than 2,500 ft within the OCDO AOR.

The brine geochemistry data in the OCDO AOR is not distributed uniformly, either by geographic location across the state or by producing zone or formation (Figs. 23 and 24; Perry and others, 2012). The Ohio counties in the study area that produce the largest amount of carbon dioxide from large-point sources, such as coal-fired electric generating stations (Gallia, Jefferson, Lorain, and Washington Counties), have little to no brine geochemistry data from depths greater than 2,500 ft. The lone exception to this is Coshocton County where 22 geochemical and 14 R_w analyses are available; however, the data is concentrated in the Rose Run sandstone and/or Beekmantown dolomite and the "Clinton" sandstone. If brine data availability in surrounding counties is considered, the situation improves in Jefferson, Washington, and Lorain Counties where additional brine geochemistry or R_w information can be accessed for 9, 19, and 32 locations, respectively. Gallia County produces the largest amount of carbon dioxide from a large-point source in Ohio and is the fourth largest carbon dioxide emitter by county in the United States. However there is no brine geochemistry data in Gallia County and limited brine data available in the four surrounding counties.

Total dissolved solids (TDS) was plotted versus depth for 84 wells for which brine data ia available within the OCDO AOR (Fig. 25). The TDS varied from approximately 35,000 ppm to approximately 390,000 ppm. The TDS was plotted versus depth for 31 wells completed in the Knox Dolomite to illustrate typical TDS values encountered in a major potential injection zone (Fig. 26). Data plotting outside of the margin of error may result from improper sampling procedures, sample contamination, and/or laboratory error.

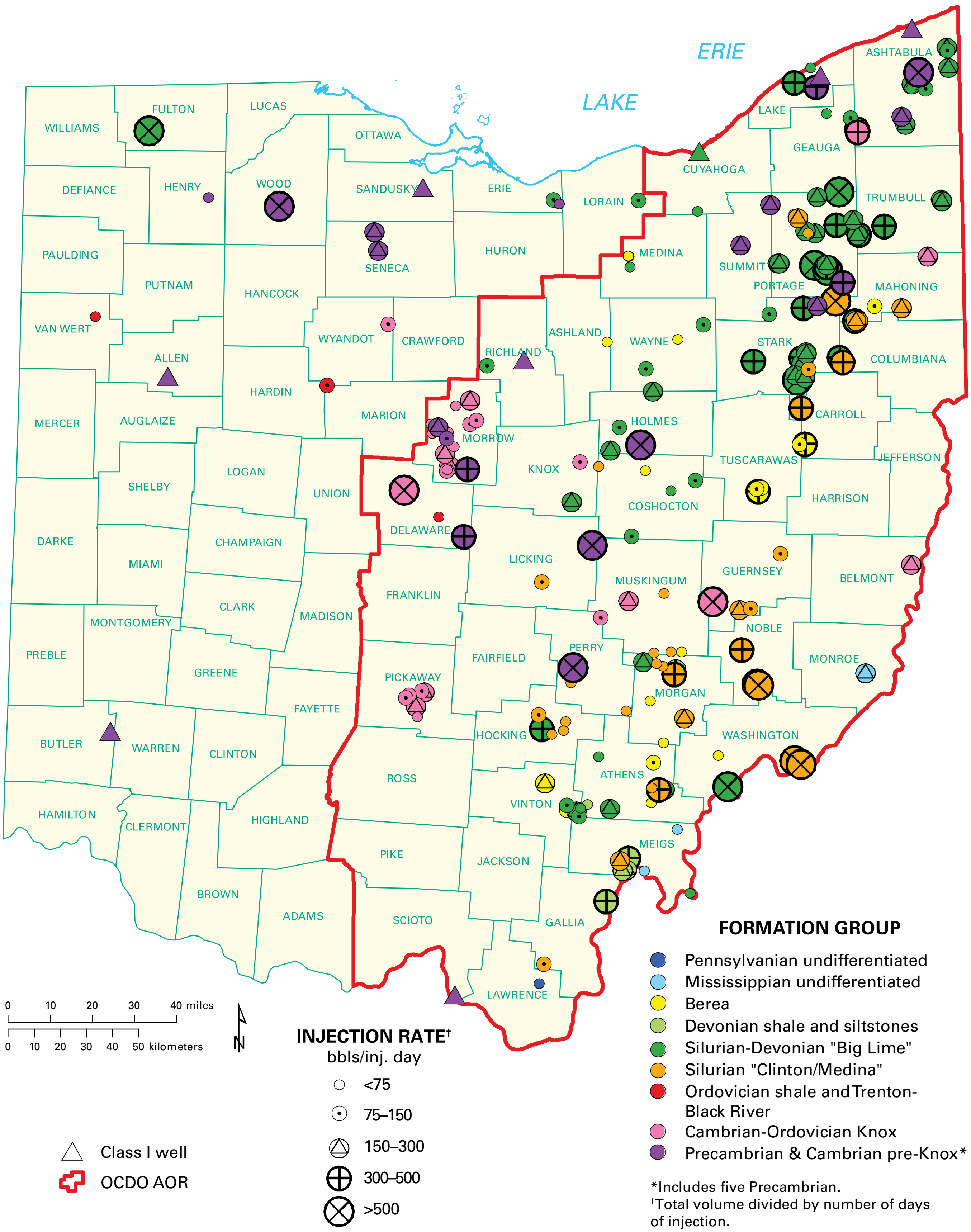

FIGURE 21.—Map showing brine disposal well injection rates, composite. See Appendix B for a listing of the formation(s) for each OCDO group.

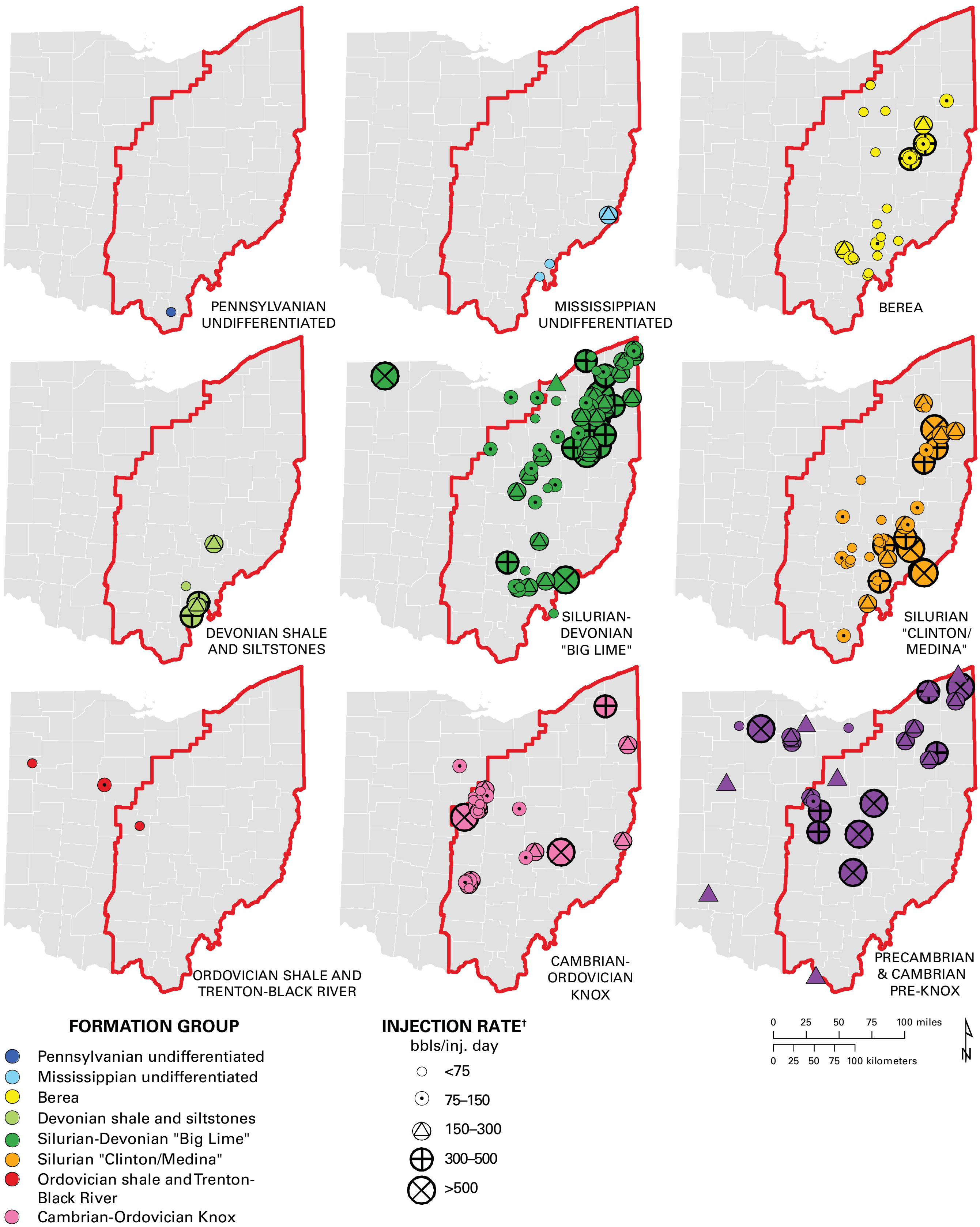

FIGURE 22.—Maps showing brine disposal well injection rates, by formation group. See Appendix B for a listing of the formation(s) for each OCDO group.

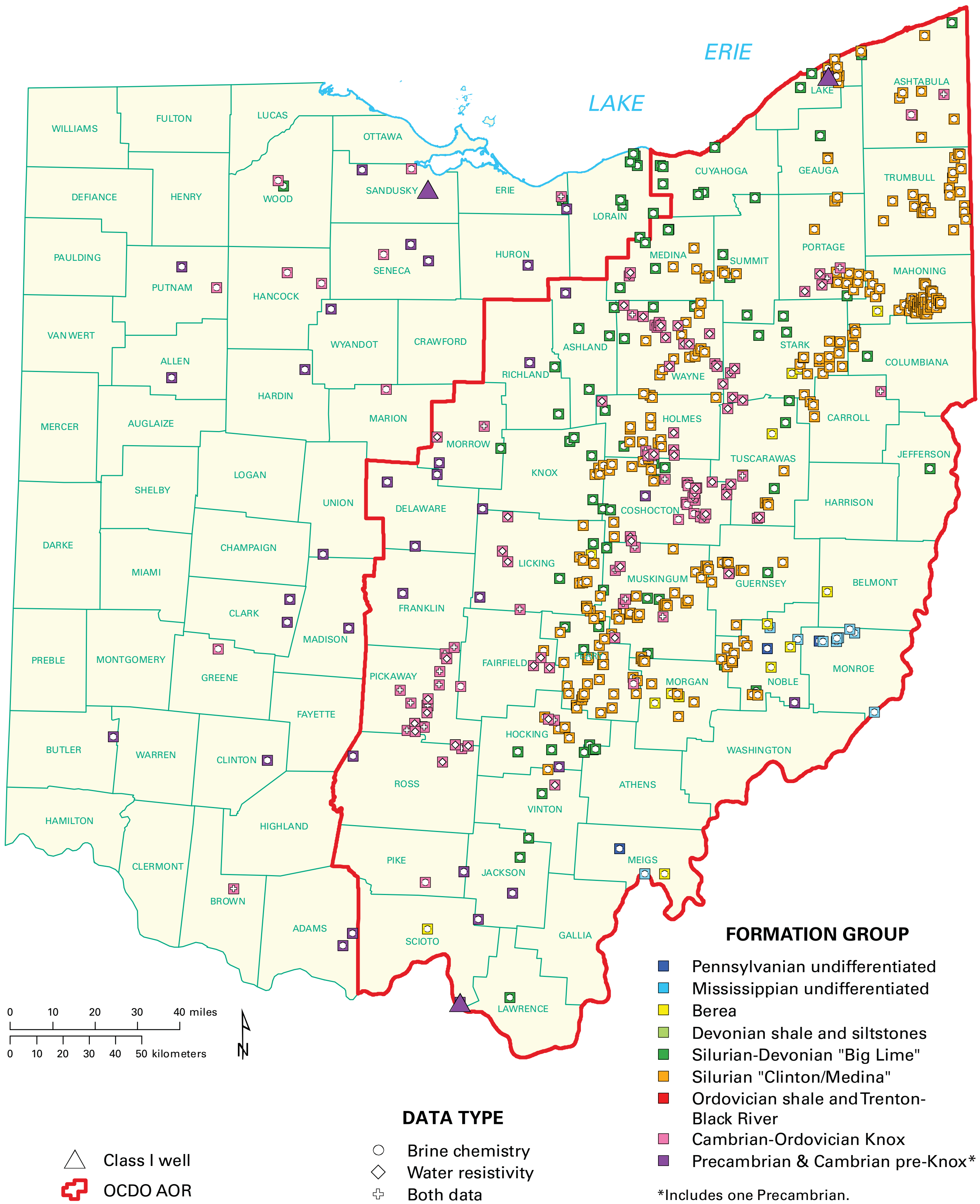

FIGURE 23.—Map showing available brine chemical composition data, composite. See Appendix B for a listing of the formation(s) for each OCDO group.

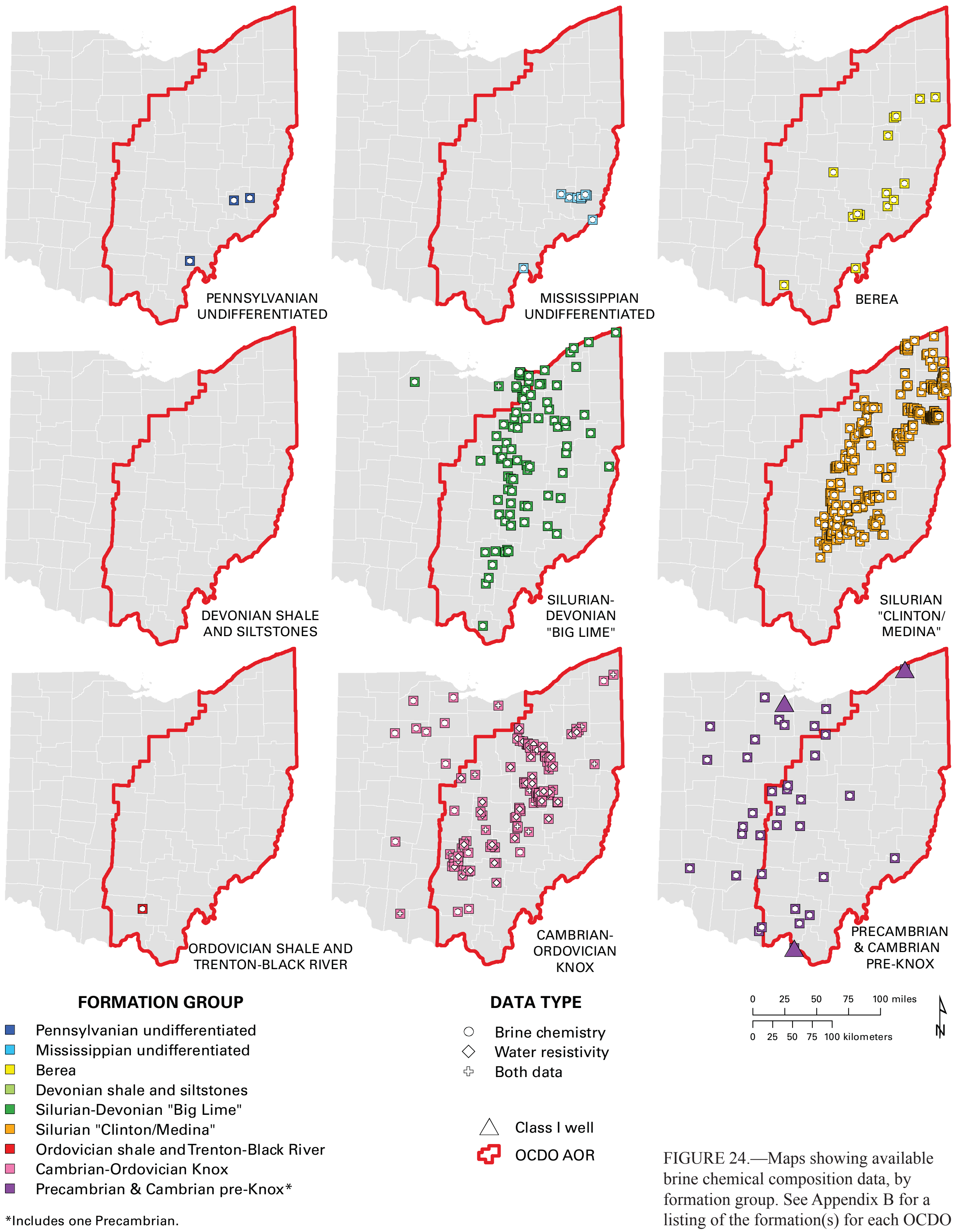

FIGURE 24.—Maps showing available brine chemical composition data, by formation group. See Appendix B for a listing of the formation(s) for each OCDO group.

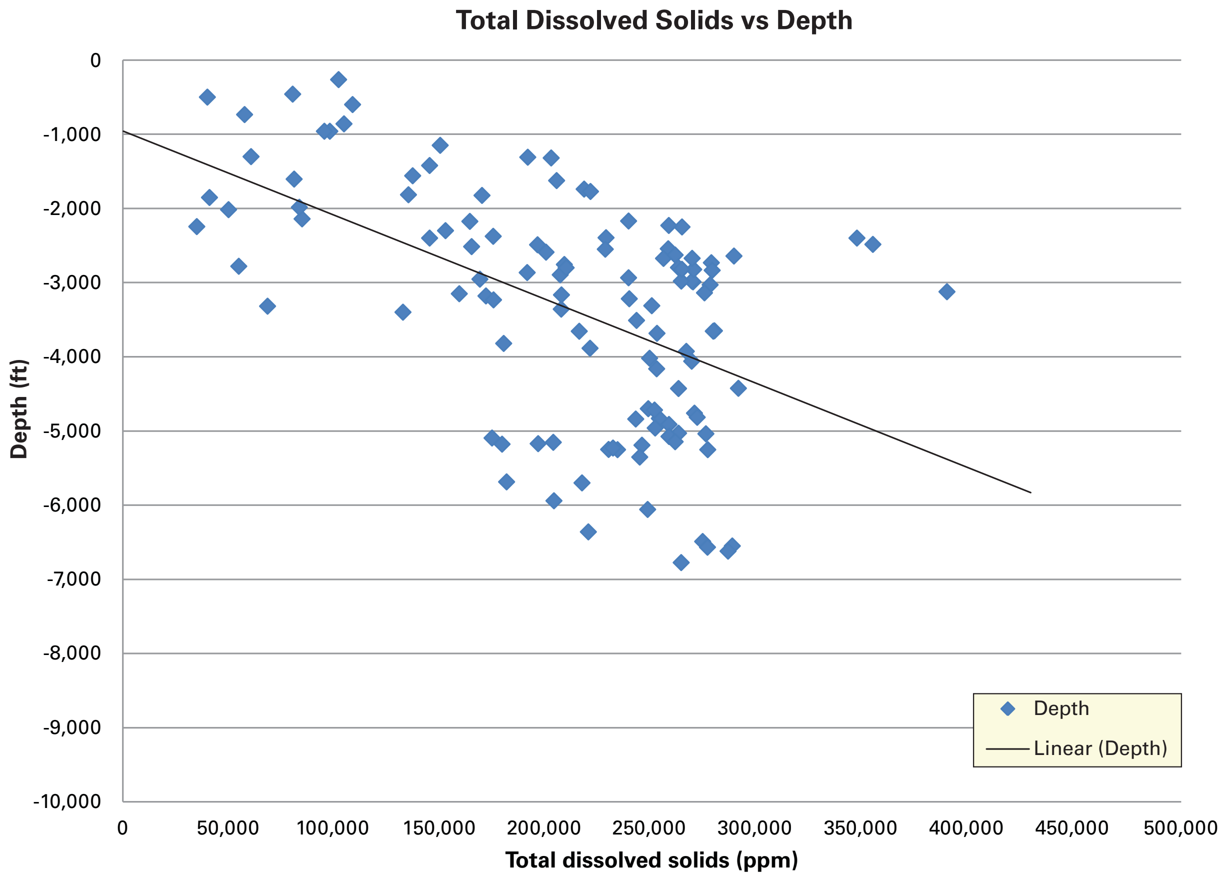

FIGURE 25.—Graph of total dissolved solids (ppm) versus depth for 84 wells within the AOR.

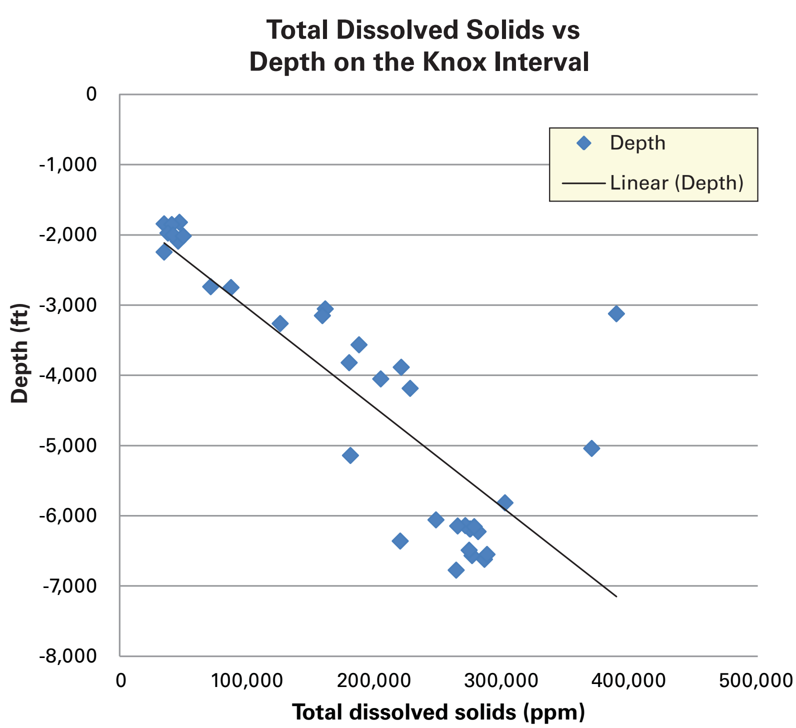

FIGURE 26.—Graph of total dissolved solids (ppm) versus depth for wells in the Knox interval.

Lineament Studies

Understanding the distribution and locations of fracture systems is a critical issue in applying risk assessment to predict the long-term fate of CO_2 within storage reservoirs. Analysis of the orientation and density of surface lineaments has been a useful tool for identifying fracture systems and also has been used to better understand the migration and trapping of hydrocarbons in the subsurface. Published studies of lineaments in eastern Ohio include work performed during the Eastern Gas Shales Project (EGSP) by Gray and others (1982), during the Gas Research Institute (GRI) Devonian Shale project by Baranoski and Riley (1987), and as part of a hydrocarbon migration study in eastern Ohio by Mason (1999).

Remote-sensing techniques using aerial photographs and satellite imagery was used in the EGSP study to identify lineaments and possible fracture trends in the Devonian shale interval in eastern Ohio (Fig. 27). The lineament mapping was done using 1:250,000-scale LANDSAT imagery and 1:80,000-scale aerial photos. Satellite imagery has been available since 1972 when the Earth Resources Technology Satellite (ERTS-1) was launched. Various authors have reported on the use of satellite imagery for identifying lineaments and associated fracture systems (Collins and others, 1974; Drahovzal and others, 1974; and Jacobi, 2000). The relationship between fractures and fracture traces identified from aerial photos also has been recognized by previous workers (Trainer, 1967; Komar and others, 1971; and Alpay, 1973). The primary objectives of the EGSP fracture study were to locate and map local and regional lineaments using aerial photos and satellite imagery showing their lengths and orientations. From this they developed trend-surface and residual-height maps that identify areas in eastern Ohio where fracture density exceeds the norm. Another objective was to see if surface lineaments are reflected in the subsurface and relate to Devonian Shale production with the goal of using surface lineaments as a tool for hydrocarbon exploration.

Remote sensing data using synthetic aperture radar (SAR) at a scale of 1:250,000 was analyzed and interpreted for eastern Meigs County and Lawrence County (Fig. 27) in a GRI-funded Devonian shale project (Baranoski and Riley, 1987). Four dominant regional trends were interpreted: (1) northwest–southeast, (2) northeast–southwest, (3) west/northwest–east/southeast, and (4) north/northeast–south/southwest. The lineaments were proximal to and parallel with a number of structures and faults mapped on the Berea and Huron structure maps. The most notable of these trends were northwest–southeast-trending faults and northwest–southeast-plunging structural noses. Some lineaments were coincident with higher Devonian shale gas production.

Mason (1999) did an investigation of surface topography and lineaments, correlated them to subsurface features, and interpreted possible hydrocarbon migration routes in eastern Ohio. Surface lineaments were mapped using 1:250,000 Digital Elevation Model (DEM) files (Fig. 28). Topographic linear trends are interpreted to have developed along zones of weakness along joints, faults, and fractures. He postulated that surface topography can often correlate to basement structure. Mason (1999) interpreted that these lineaments or zones of weakness and fracture zones can be correlated to productive Cambrian-Ordovician oil and gas fields in eastern Ohio and are interpreted as major hydrocarbon migration pathways. He interpreted two dominant lineament orientations from surface topography—northwest–southeast and northeast–southwest.

Gravity, Magnetic, and Geothermal Data and Surveys

Geopotential field anomalies arise from the contrasts in physical properties of rocks within Earth and thus are important constraints on the lithology and structure of the subsurface (e.g., von Frese and Hinze, 1993). Gravity and magnetic anomalies arise from contrasts in density and magnetization, respectively. The juxtaposition of rocks of different densities due to faulting, for example, produce an anomalous gravity signature over the structure (e.g., Nettleton, 1971; Blakely, 1996). Likewise, contrasts of materials of differing magnetization from intrusions of igneous rock, faults, or other geologic features produce an anomalous magnetic signature over the structure. Like gravity and magnetic anomalies, steady state heat flow also is a potential field that reflects crustal structure (e.g., Kellog, 1953). Gravity, magnetic, and thermal anomalies thus yield powerful constraints on the subsurface geology and may provide a much more comprehensive view of trends not available in individual data sets or widely separated areas of outcrop or boreholes.

The crustal geology of Ohio is dominated by Precambrian igneous and metamorphic rocks that are still poorly understood due to the 0.6–2.9 mi (1–4 km) of overlying Paleozoic sedimentary rocks (e.g., von Frese and others, 1997; Baranoski, 2002). Direct sampling of the Precambrian basement is limited because only 207 wells have been drilled into these lithic arenites, deep metamorphic and igneous complexes of Ohio (Baranoski, 2002). Nevertheless, Ohio's relict Precambrian structural features and lithologic contrasts are reflected in gravity and magnetic datasets. Hence, magnetic and gravity anomalies provide critical information on the subsurface Precambrian faults and lithologic boundaries and their possible continuations into the overlying Phanerozoic sedimentary units that are the potential targets for carbon sequestration in eastern Ohio.

Geothermal data provide additional geologic information for assessing CO_2 sequestration potential. Heat is continually flowing from the hot interior to the cooler exterior of Earth and subsurface temperatures increase with depth (e.g., Carslaw and Jaeger, 1959; Bullard, 1965). Geothermal anomalies arise because of contrasts in thermal conductivity, including variations in the thermal conductivity contrasting terrain surface; contrasts in heat production primarily from the radioactive decay of uranium, thorium, and potassium isotopes; and convection of fluids at depth (e.g., Beardsmore and Cull, 2001). The physical state (gas-liquid) of CO_2 placed underground is dependent on the temperature and pressure where CO_2 in the liquid state is termed "supercritical" (e.g., Yam and Schmitt, 2011). The density of supercritical CO_2 is about ten times that of its gaseous form, so sequestration of CO_2 in its liquid state may be preferred. Geothermal data sets and derivative maps that yield information about subsurface

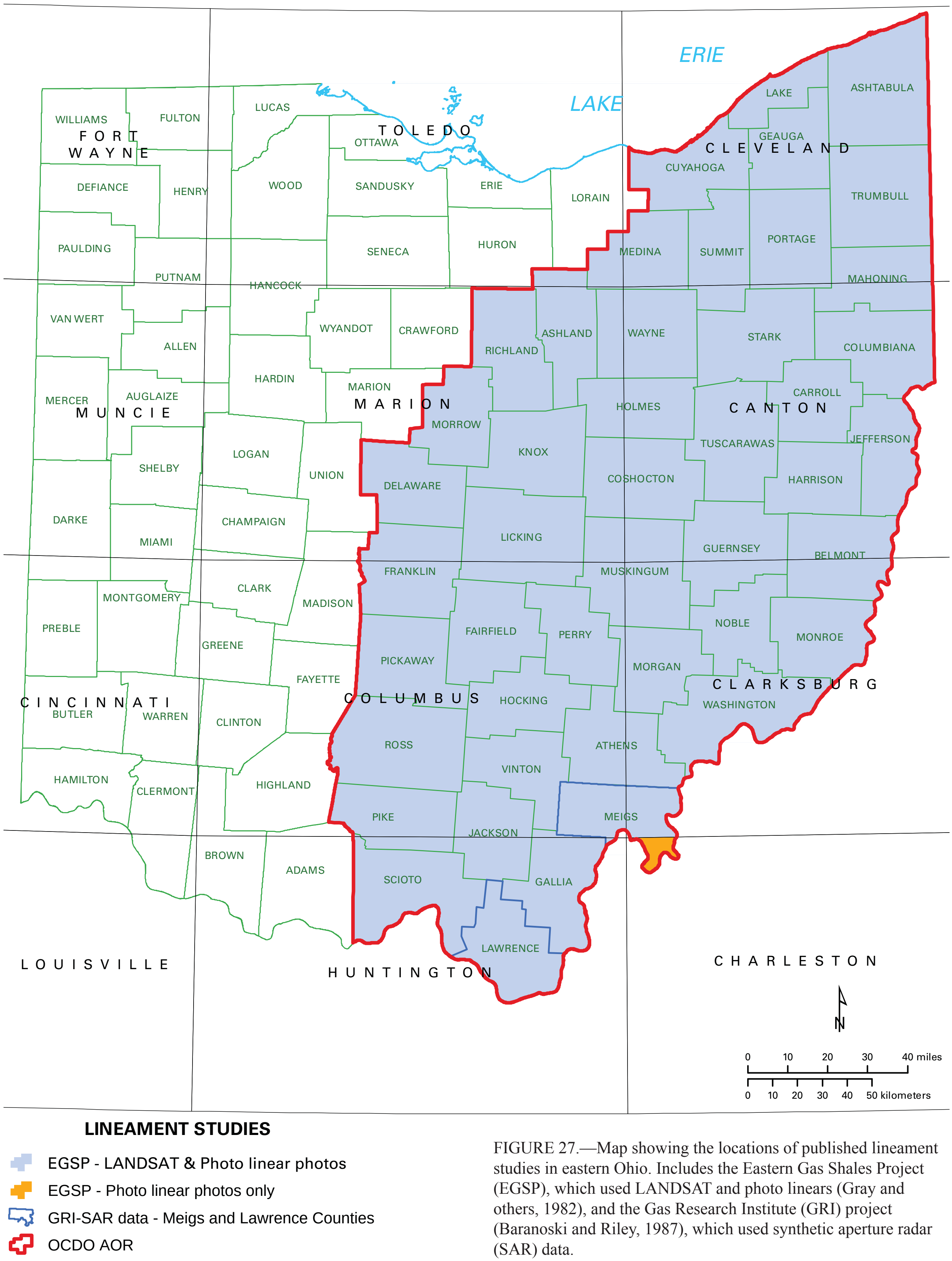

FIGURE 27.—Map showing the locations of published lineament studies in eastern Ohio. Includes the Eastern Gas Shales Project (EGSP), which used LANDSAT and photo linears (Gray and others, 1982), and the Gas Research Institute (GRI) project (Baranoski and Riley, 1987), which used synthetic aperture radar (SAR) data.

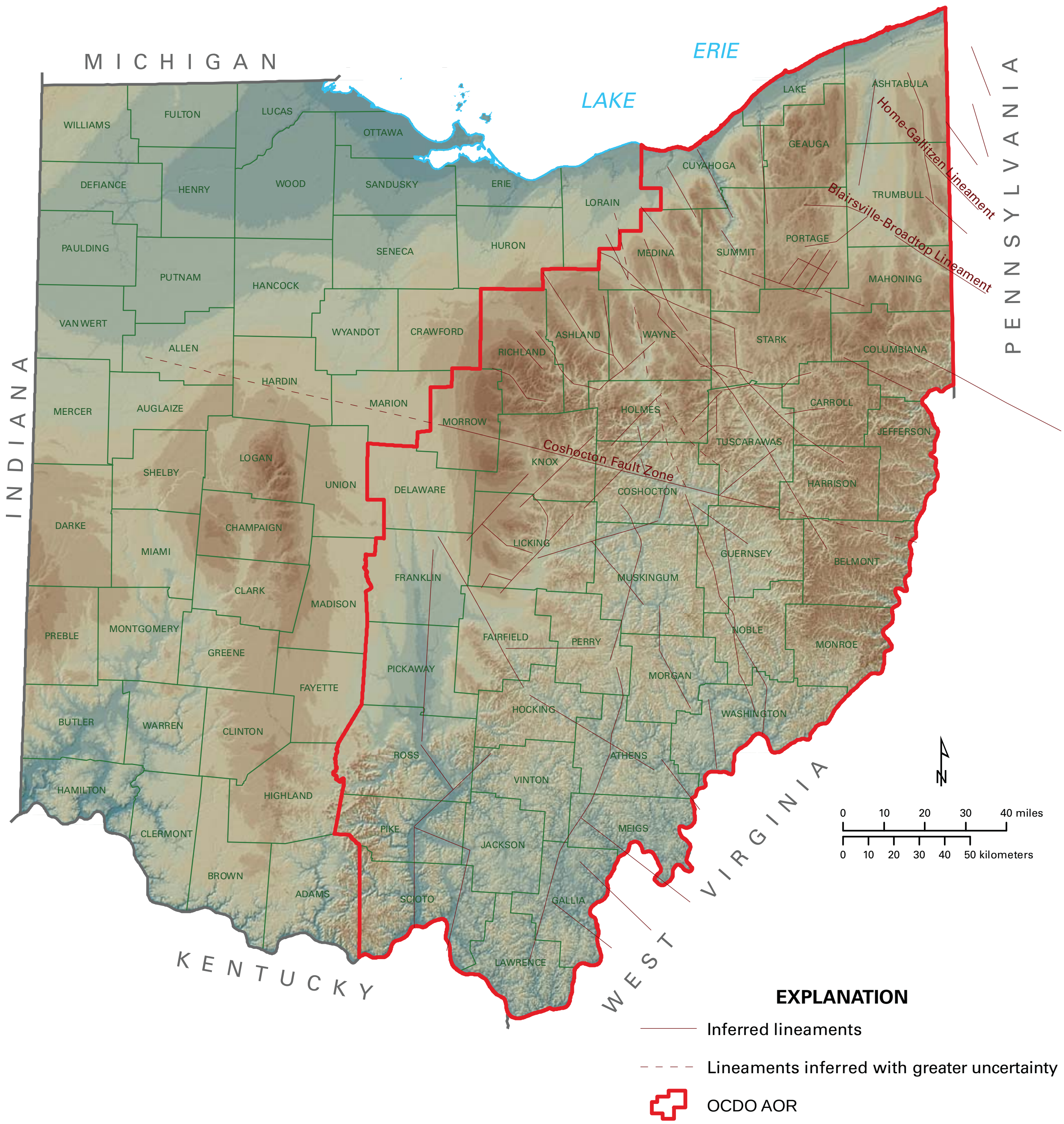

FIGURE 28.—Lineament map of eastern Ohio using Digital Elevation Model data files. Modified from Mason (1999).

temperatures may therefore be of potential interest for the study of carbon sequestration targets.

In this report we present a limited set of potential field data including the regional complete Bouguer gravity anomalies (CBA), total intensity magnetic anomalies (TF), and bottom-hole temperature (BHT) and geothermal gradient datasets. A map of Ohio earthquakes also is given to complement the discussion of the potential-field data. These data sets are described in more detail in Appendix C.

Seismic Reflection and Synthetic Seismogram Data

Seismic reflection data can be very useful for estimating formation depth and thickness, provided that raw field data acquisition and computer processing are commensurate with experience and knowledge of local geologic conditions and that adequate lithologic contrasts are present in the subsurface. This data is collected in the field via ground-based electrical devices called *geophones*, which have had their physical locations surveyed. Typical seismic surveys are acquired along roadways and termed *two-dimensional* (2D), whereas more advanced three-dimensional (3D) seismic surveys are laid out in plan view in a grid pattern.

During the acquisition phase of a seismic survey, sound energy sourced at Earth's surface (usually via large truck-mounted hydraulic vibrators or small charges of dynamite in shallow drill holes) is propagated deep into the earth. The energy reverberates through the subsurface rock layers and returns to Earth's surface as valuable energy data. This energy data is picked up by the geophones along a surveyed line and recorded by a sophisticated computer system located in a separate dedicated data acquisition vehicle.

The recorded reflection data is next taken to a processing center for additional mathematical analyses. A series of outputs typically are created and presented for interpretation on large paper plots. These paper outputs represent different depictions of the actual subsurface stratigraphic and structural conditions. Properly processed seismic reflection data can help delineate (1) stratigraphy and structural trends, (2) relative chronology of structural development, (3) faulting, and (4) variations in depositional thickness, to name a few. Advanced seismic data processing is performed to create complex mathematical data attributes used to develop geologic models, which in turn can be used to enhance and/or predict subsurface geologic relationships (e.g., paleotopography). Advanced seismic processing also is used in reservoir characterization.

Wireline electrical logging tools commonly are used to collect geologic data from deep open-hole wells. Complex electrical instrumentation contained within a long, narrow cylindrical sonde or tool is lowered into an open borehole via a cable. The instrumentation and data acquisition system has been designed to detect and collect various types of geologic data related to the physical properties of the rocks encountered along the length of the logged open borehole. This information is very useful in geologic characterization and in some cases for seismic interpretation.

In general, sonic and density electric logs measure acoustic properties and density, respectively, and are used to estimate porosity. The *sonic log* is a type of porosity log that records the time required for a compressional sound wave to travel in the rock formation in the well bore. The interval transit time (Δt) is the reciprocal of the velocity of the compressional sound wave and is dependent on the lithology and porosity of the formation (Schlumberger, 1972). The sonic and density electric logs also can be used to mathematically model seismic reflection data, creating a synthetic seismogram. This information can be used to correlate geologic well data to seismic reflection profiles. Advanced drill hole modeling data also includes acquisition and processing of a vertical seismic profile (VSP). The VSP also is used for geologic correlation to seismic reflection profiles. Detailed, rigorous interpretation of seismic reflection data is beyond the scope of this report. Instead, this document focuses on identifying and presenting an inventory of publicly available and selected proprietary 2D data for Ohio. For further reading about general log interpretation and seismic reflection, see Schlumberger (1972), Asquith (1982), Sherrif (1982), and Riley and others (1993).

Public Domain Seismic Reflection Data

The Survey has public domain seismic reflection data from four sources: Consortium for Continental Reflection Profiling (COCORP), Ohio Environmental Protection Agency (OEPA), U.S. Department of Energy (US DOE) and the Survey (see Appendix D). These sources represent approximately 555 line-miles of public domain data acquired dominantly in Ohio (including approximately 75 line-miles of US DOE and OEPA data in adjacent Indiana, Kentucky, and West Virginia). Appendix D contains a spreadsheet listing the seismic lines and acquisition parameters. Approximately 519 line-miles of COCORP, OEPA, and Survey data are available in paper output and digital SEG-Y formats. Approximately 253 line-miles of COCORP data were acquired by Cornell University (New York). The Ohio COCORP data set was part of a continent-wide study of deep crustal features. Although the data was acquired with relatively coarse parameters, when compared to more-shallow industry seismic, it was useful when reprocessed. The OEPA requires all Class I waste injection sites in Ohio to acquire and process industry standard seismic data. The 278 line-miles of OEPA data have been used to demonstrate structural integrity and absence of significant faulting at six Class I facilities throughout the state. Only three Class I facilities are currently in operation in western Ohio. The remaining three Class I facilities are located in eastern Ohio in the Appalachian Basin and waste injection operations are permanently shut down (see Fig. 21).

The 519 line-miles of seismic data were used along with deep well data to interpret subsea elevations of structural contours for the top of the Precambrian unconformity surface (Baranoski, 2002). Approximately 25 line-miles of US DOE data are available in paper output format. This US DOE data was used in various reports on carbon sequestration (e.g., Battelle, 2011). The Survey was part of a consortium that acquired approximately eight line-miles of data in Warren County, Ohio (Shrake and others, 1990). Synthetic seismograms are available for 42 wells in Ohio (see Appendix E). One VSP is available for the Coshocton County Reiss No. 3-A well (see Appendix F).

The OCDO AOR is bounded on the west by the approximate western limit of the Appalachian Basin, which occurs in west-central Ohio; Lake Erie to the north; and the state line to the south and east (Fig. 2). Approximately 286 line-miles of public domain seismic reflection data are available within the OCDO AOR and adjacent Kentucky and West Virginia. The vintage COCORP OH-1 and OH-2 deep crustal study lines cover approximately 150 line-miles in the study area. Approximately 114 line-miles of OEPA seismic data are available from three Class 1 waste injection sites in the Appalachian Basin of Ohio and adjacent Kentucky as previously described. Battelle (2008) utilized approximately 11 line-miles of seismic data to characterize and evaluate potential carbon sequestration reservoirs at the AEP power plant site in Mason County, West Virginia, and adjacent Meigs County, Ohio. Battelle (2011) also utilized approximately 11 line-miles of seismic data to characterize and evaluate potential carbon sequestration reservoirs at the R. E. Burger power plant site in Belmont County, Ohio, and adjacent Marshall County, West Virginia.

Proprietary Data

An Internet search was conducted to identify seismic brokerage firms possessing proprietary Ohio seismic reflection data that may be applied to geologic characterization. Two firms were found to maintain an inventory of available Ohio data for purchase: (1) Evans Geophysical of Suttons Bay, Michigan, and (2) Seismic Exchange, Inc., of Houston, Texas. Seismic survey location maps from these firms were perused for potentially usable seismic lines that are at least 10 mi in length. Appendix G contains a base map showing locations of proprietary seismic lines brokered by Evans Geophysical that would be applicable to CCS objectives in eastern Ohio.

SITE SPECIFIC INVESTIGATIONS

In order to evaluate CCS and CCUS options in Ohio, site specific investigations have been conducted to better characterize both saline formations and oil-and-gas reservoirs. These investigations include the stratigraphic test drilled to the Precambrian in Tuscarawas County (Ohio Geological Survey CO_2 No. 1 well, APINO 3415725334) and the cyclic-CO_2 test drilled in the East Canton oil field in Stark County (Sickafoose-Morris No. 1 well, APINO 3415122018). These projects provided new geologic data and interpretations for evaluating sequestration opportunities in Cambrian through Devonian saline formations and sequestration potential through CO_2-EOR in the Silurian “Clinton” sandstone.

Geologic Assessment of the Ohio Geological Survey CO_2 No. 1 Well for Potential Injection of Carbon Dioxide

This project was conducted in cooperation with Battelle Memorial Institute and was funded by the Ohio general revenue fund, the OCDO, and US DOE. The Ohio Geological Survey CO_2 No. 1 well was a Precambrian stratigraphic test conducted to evaluate the CO_2 injectivity and storage capacity of potential reservoirs and the effectiveness of potential confining units in eastern Ohio. Figure 29 shows the location of the well and of all other Precambrian well tests in Ohio. Wells penetrating the Precambrian that can evaluate the entire Paleozoic section of sedimentary rocks in eastern Ohio are relatively rare. Ohio has had more than 250,000 wells drilled, yet less than 250 have penetrated the Precambrian basement. Most of these Precambrian penetrations are located in western Ohio, where the depth through the sedimentary rocks is considerably less than in eastern Ohio. Many of these deep tests are older wells for which the state does not have geophysical logs and/or rock samples. Thus in eastern Ohio, where there are few or no deep wells, the presence and geographic extents of and reservoir properties for many deep sequestration targets are not well understood. The lack of sufficient data to thoroughly evaluate much of eastern Ohio for CO_2 sequestration was the impetus for drilling this deep stratigraphic test well in Tuscarawas County. This stratigraphic test provided valuable data and analyses from a full suite of modern geophysical logs, sidewall cores, and injectivity tests in an area of eastern Ohio where there is limited deep well data. Wickstrom and others (2011) provide a comprehensive report that summarizes the data and interpretations for the CO_2 No.1 well and surrounding vicinity.

Drilling, Completion, and Testing of the CO_2 No. 1 Well

Drilling of the Ohio Geological Survey CO_2 No. 1 well began May 10, 2007, and reached total depth of 8,695 ft in the Precambrian crystalline rocks on June 9, 2007 (Fig. 30). Logging and coring operations were completed on June 10, 2007. Subsequent injection testing in the Cambrian basal sandstone and the Rose Run sandstone was completed August 6, 2007. Following completion of injection testing, the well was turned over to Artex Oil Company and Northwood Energy Corporation, the operators who own the oil and gas mineral rights to the site. Wireline logging was performed by Schlumberger, Inc., and included Gamma Ray, Neutron, and Density (GR/N/D); Laterolog (LL); Combinable Magnetic Resonance (CMR); Formation Microscanner Image (FMI); and Sonic (S) tool measurements. Perforation (Perf) and Cement Bond (CB) logs were run to identify correct injection zones and confirm the integrity of the cement behind the casing. The Schlumberger PressureXpress also was run to provide high-quality pressure and fluid mobility measurements in potential CO_2 sequestration zones of interest. In addition, 82 sidewall cores were taken in selected reservoirs and confining units to assist in the evaluation of CO_2 sequestration potential (Fig. 30). Sidewall cores were sent to Weatherford Labs (formerly OMNI Labs) to obtain quantitative measurements of porosity and permeability, total organic content (TOC), thermal maturity, and rock mechanics. Weatherford Labs also examined reservoir quality of selected cores with thin section petrography, Scanning Electron Microscopy (SEM), and x-ray diffraction techniques.

Discussion of Potential Saline Injection Zones

Stratigraphic analysis of geologic units deeper than 2,500 ft in the AOR indicate nine deep saline formations that have potential as injection zones (Fig. 30). In ascending order these

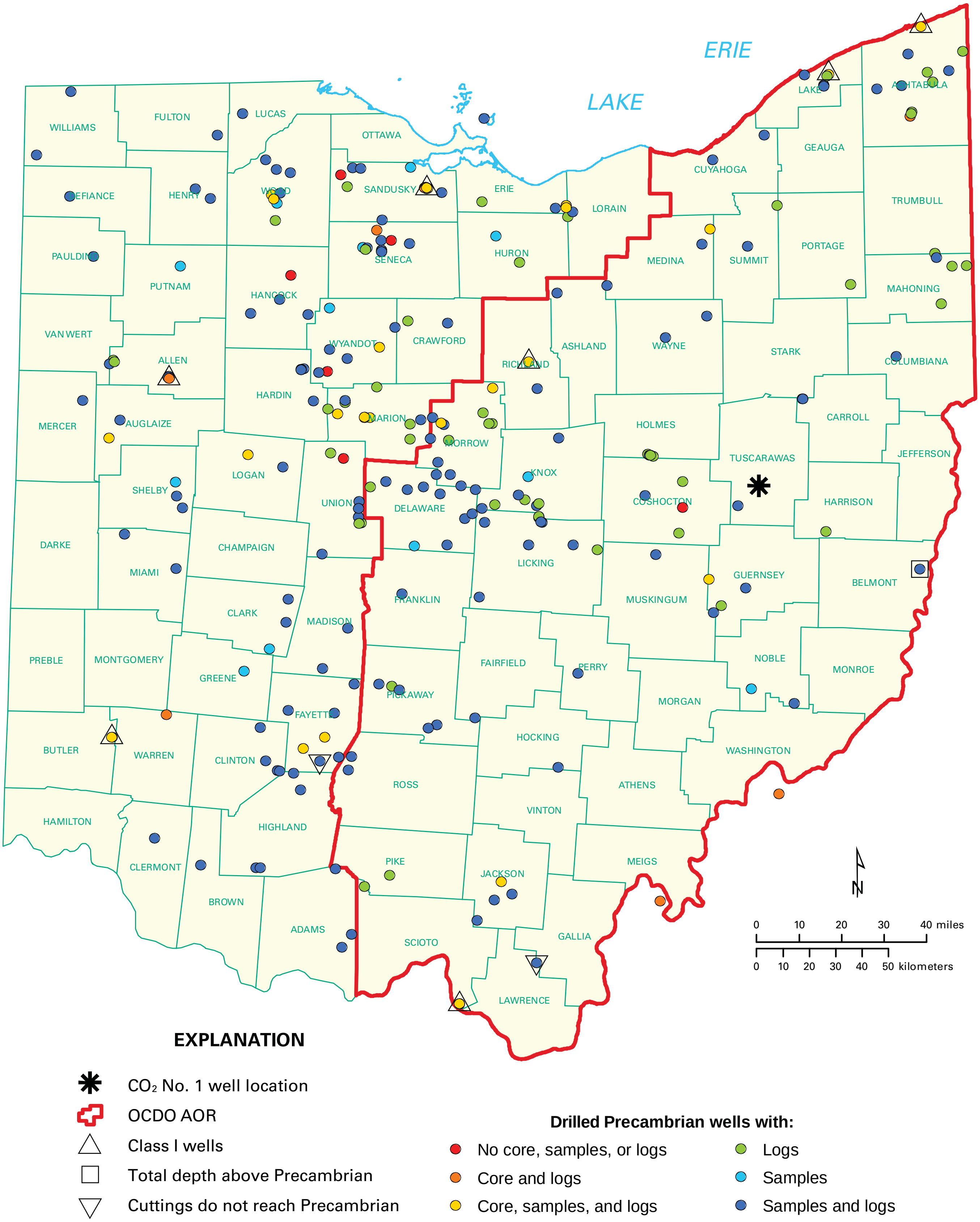

FIGURE 29.—Map showing the location of the Ohio Geological Survey CO_2 No. 1 well and all Precambrian penetrations in eastern Ohio. From Wickstrom and others (2011).

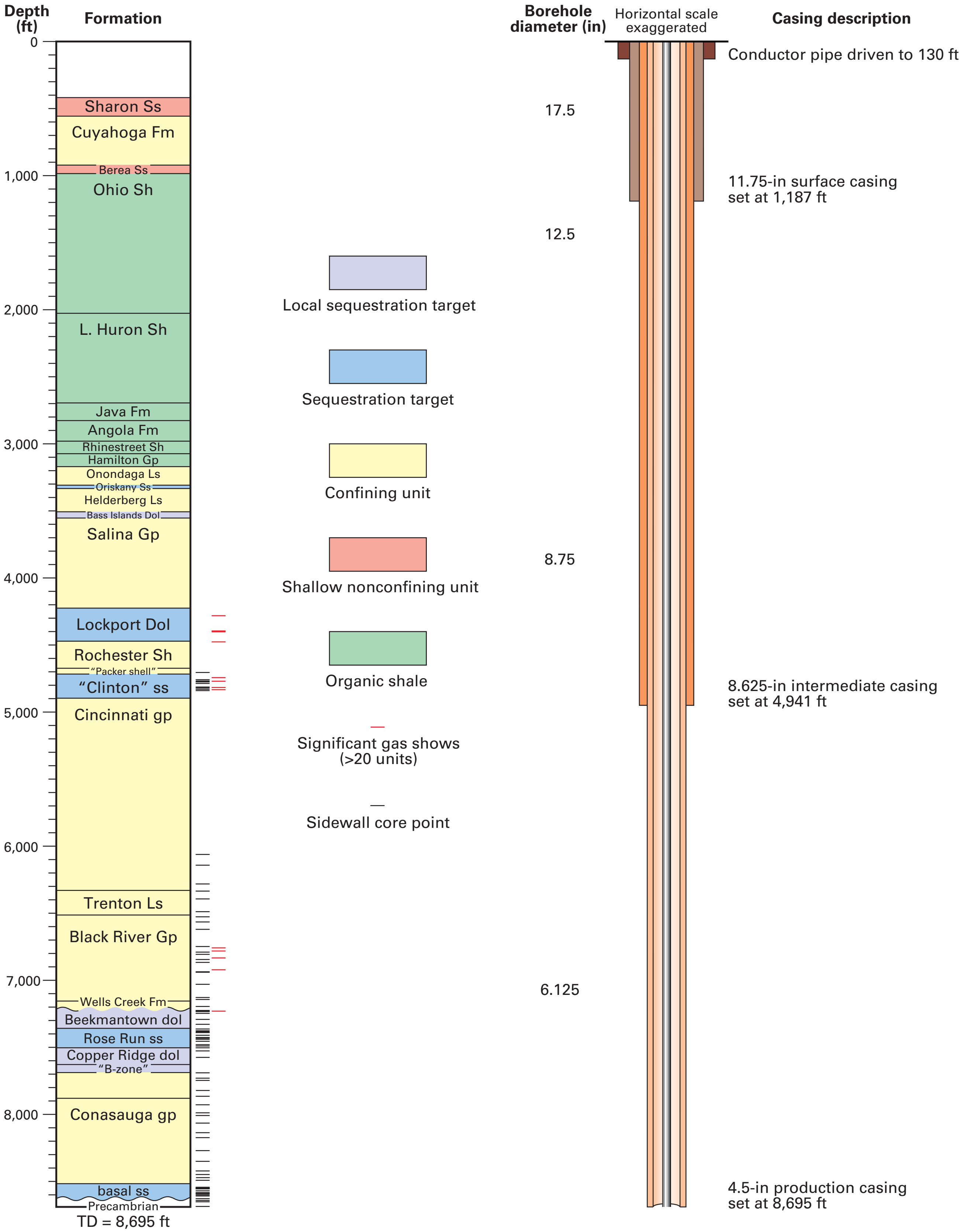

FIGURE 30.—Diagram of well construction of the CO_2 No. 1 well and the primary stratigraphic units and depths encountered. Also shown are the sidewall core points and significant gas shows. Modified from Wickstrom and others (2011).

include: the Cambrian basal sandstone; the Copper Ridge dolomite, which contains both vuggy carbonate zones and the “B-zone” clastic; the Rose Run sandstone; the Ordovician Beekmantown dolomite; the Silurian Cataract Group (“Clinton” sandstone), the Lockport Dolomite, the Bass Islands Dolomite, and the Devonian Oriskany Sandstone.

Cambrian basal sandstone

From geophysical log interpretation, the CO_2 No. 1 well contains approximately 110 ft (gross thickness) of the Cambrian basal sandstone, ranging in depth from 8,524 to 8,634 ft (Fig. 31). Within this interval, there are approximately 56 ft of net sandstone with greater than 6 percent porosity. Maximum log-derived porosity is 15 percent and averages 10 percent. From 12 sidewall cores selected in this interval, the porosities range from 2.8 to 10.7 percent. Permeabilities from core analyses reach a maximum value of 1.06 md in one sample with the remainder being less than 0.18 md. Thin section petrography indicates this unit consists of an arkose with interbedded dolomite (Fig. 32A, B). The arkose is comprised dominantly of monocrystalline and polycrystalline quartz (51 percent) and feldspar (21 percent). Lithic fragments occupy 1 percent or less of the framework. The dominant cements include quartz and feldspar overgrowths and pore-lining clay. Pore types include intergranular and secondary dissolution between detrital sand grains. Reservoir quality has been reduced by low permeabilities from the presence of numerous thin shale laminations, pore-lining clays, and cementation from quartz and feldspar overgrowths.

The quartz sandstone content and porosity (net porosity thickness) of the lower Conasauga group cannot be reliably mapped in eastern Ohio because of a paucity of wells drilled through this interval. However, based on available geophysical logs, the closest Precambrian penetrations to the CO_2 No. 1 well indicate appreciable amounts of porous sandstone in the Cambrian basal sandstone (Fig. 33).

Cambrian Copper Ridge dolomite

The Copper Ridge interval is 390 ft thick in the CO_2 No. 1 well, ranging from a driller’s depth of 7,508 to 7,898 ft. Interpretation of geophysical logs and sidewall cores from the CO_2 No. 1 well indicate no appreciable amount of rock with good reservoir quality in the Copper Ridge interval. The only noticeable porosity is a thin zone (less than 2 ft) of enhanced porosity that is present at a depth of 7,729–7,731 ft. This zone is 40 ft below the base of the “B-zone” and correlates to the approximate stratigraphic position of the injection zone in the AEP No. 1 well (APINO 4705300423). A discussion of this porosity zone in the AEP No. 1 well from interpretation of well logs and core is discussed in Battelle’s complementary OCDO report. Thin section petrography in this zone of the CO_2 No. 1 well indicates enhanced porosity at the microscopic scale. However, sidewall core analyses had a measured permeability of 0.0001 md and porosity of 1.3 percent. Core analyses from seven selected intervals throughout the Copper Ridge indicate porosities ranging from 1.0 to 3.8 percent, and permeabilities less than 0.03 md.

Cambrian Rose Run sandstone

The CO_2 No. 1 well is located approximately 10 mi downdip and east of the Rose Run subcrop (Fig. 34). Thus it is situated in an area with a complete Rose Run interval underlying the Beekmantown dolomite. Subsea elevations at the top of the Rose Run sandstone in Ohio dip to the east and southeast and range from –1,750 ft within the subcrop to –11,750 ft below sea level in extreme southeastern Ohio (Fig. 34).

From geophysical logs of the CO_2 No. 1 well, the Rose Run had a gross interval thickness of 146 ft, between depths of 7,362 and 7,508 ft (Fig. 35). There is approximately 24 ft of net sandstone (greater than 6 percent porosity). Eleven sidewall cores were taken in the Rose Run interval. The porosity ranges from 6 to 13.5 percent, with an average of 8 percent. Permeability measurements from selected core range from 0.001 to 31.6 md. There were three Rose Run cores that contained permeabilities greater than 1.0 md. These occurred at depths of 7,392; 7,434; and 7,506 ft and correlate with the zones of highest porosity indicated on the GR/N/D wireline log curves (Fig. 35). Based on x-ray diffraction and thin section petrography, the Rose Run is a subarkose composed dominantly of monocrystalline quartz and k-feldspar (Fig. 36A, B). Polycrystalline quartz, plagioclase feldspar, lithic fragments, and muscovite also are present. Pore types include intergranular, grain-moldic, and intragranular (leached feldspar). Cementation from quartz and feldspar overgrowths reduces the effective porosity (Fig. 36A, B).

Ordovician Beekmantown dolomite

In the CO_2 No. 1 well, the total thickness of the Beekmantown dolomite ranges from drill depths of 7,226 to 7,374 ft. From GR-N/D log interpretation, the CO_2 No.1 well has approximately 6 ft of net porosity thickness (4 percent or greater) in the Beekmantown dolomite (Fig. 37). Porosity development is largely related to subaerial exposure and paleokarst development on the Knox unconformity. In this well the Beekmantown porosity development is located within 12 ft of the top of the Knox unconformity (Figs. 37 and 38). The FMI log and the sidewall cores correlate with the GR/N/D logs and indicate well-developed pinpoint and vuggy porosity in the upper Beekmantown. Breccia and angular rip-up clasts up to 1 ft across are observed at the top of the Knox unconformity on the FMI (Fig. 38). From seven sidewall cores in the Beekmantown, porosity measurements range from 1.5 to 9.4 percent and permeabilities range from 0.0009 to 0.941 md. It should be noted that these are taken from selective intervals and thus measured porosities and permeabilities may be substantially lower than what is actually present throughout the entire interval. Thin section petrography indicates the Beekmantown to be a fine- to medium-crystalline dolomite that contains secondary intergranular and vuggy porosity. Saddle dolomites (large infilling crystals from secondary dolomitization) and minor amounts (1 percent or less) of pore-lining clays are present that reduce the porosity. Porosity on GR/N/D logs for the entire Beekmantown interval ranges

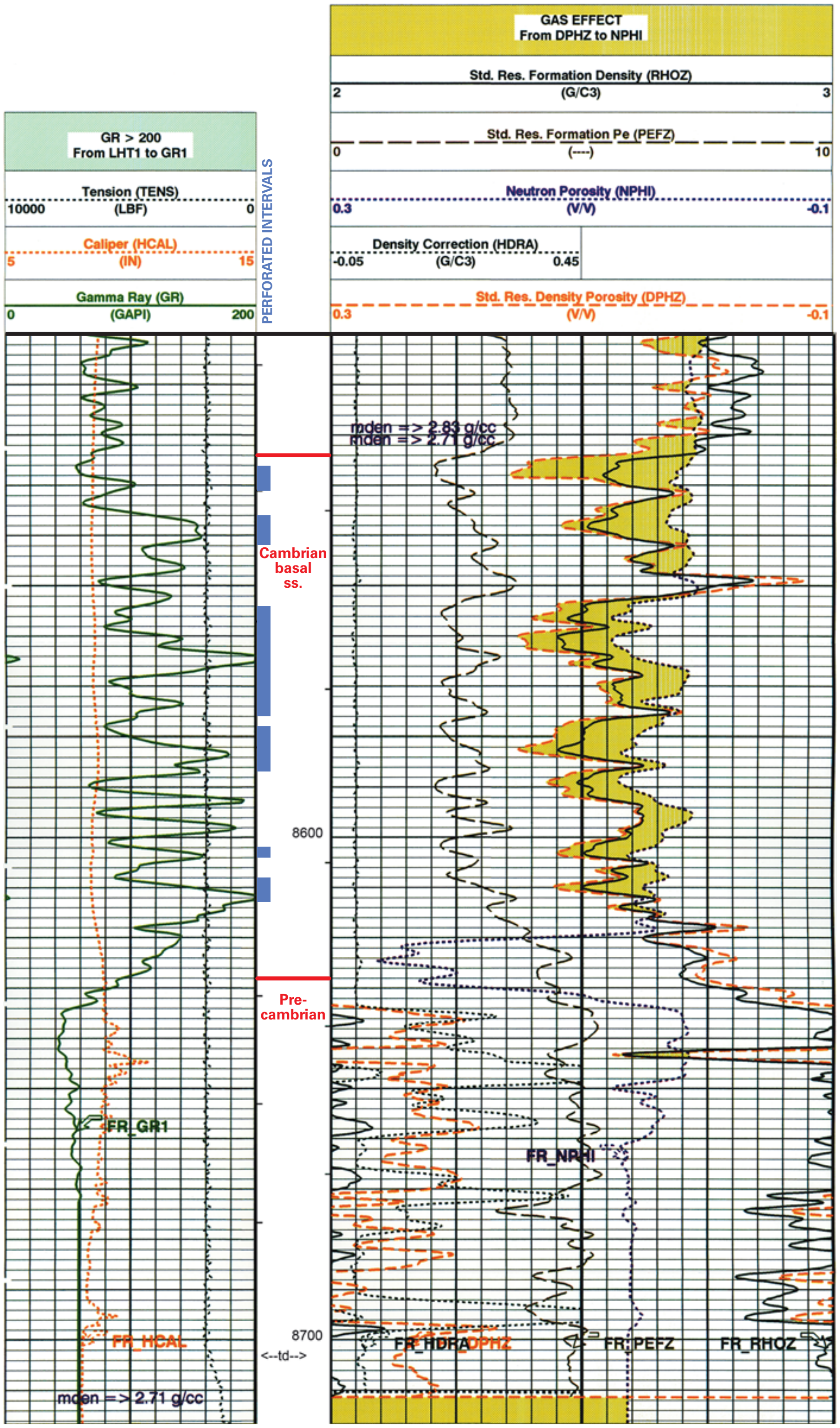

FIGURE 31.—Geophysical log of the Precambrian and Cambrian basal sandstone intervals in the CO_2 No. 1 well. Also shown are the perforated intervals used for the brine injection zones. From Wickstrom and others (2011).

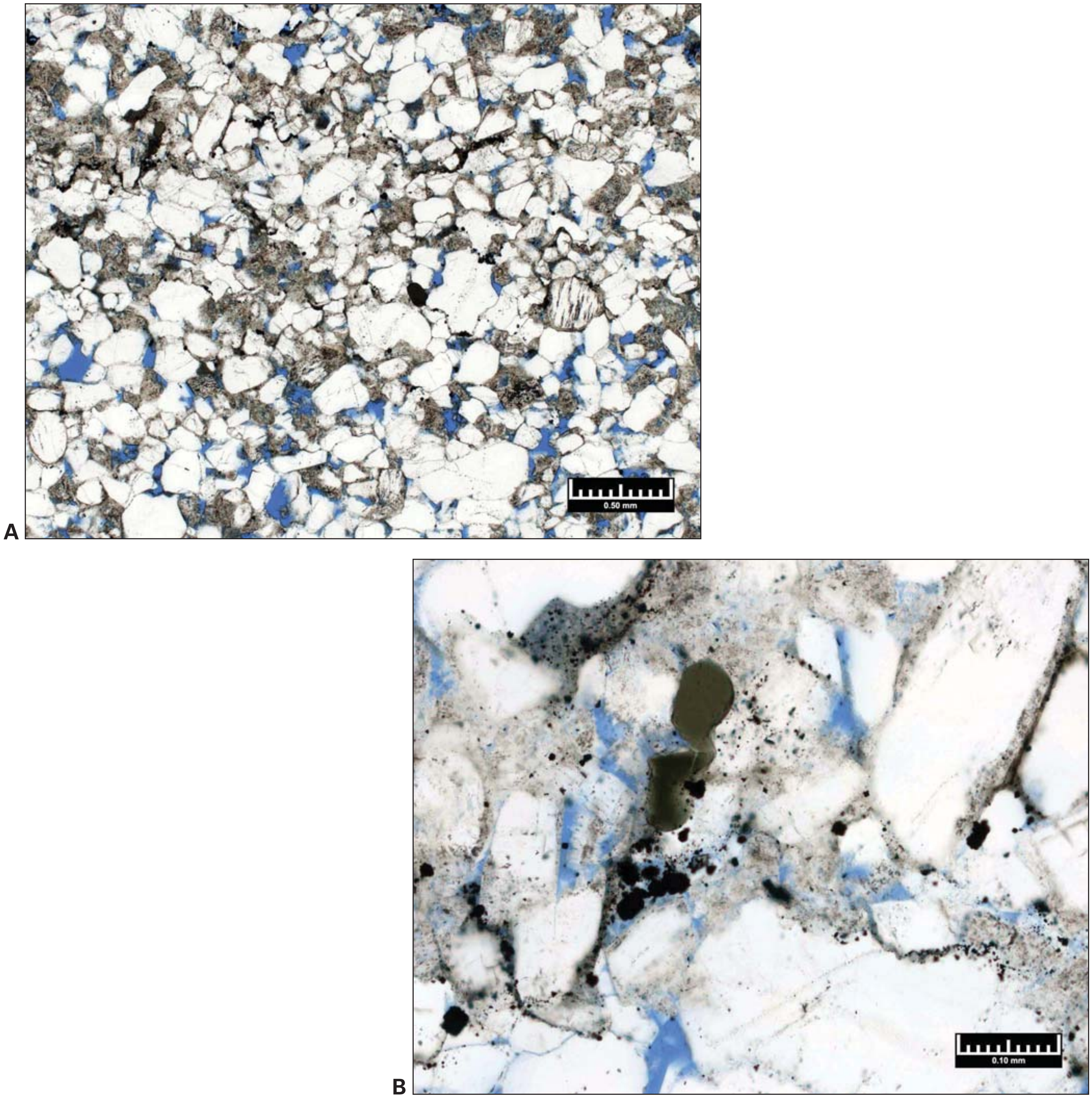

FIGURE 32.—Thin section photomicrographs of the Cambrian basal sandstone at a depth of 8,561 ft. (**A**) Magnification of 40x; (**B**) magnification of 200x. From Wickstrom and others (2011).

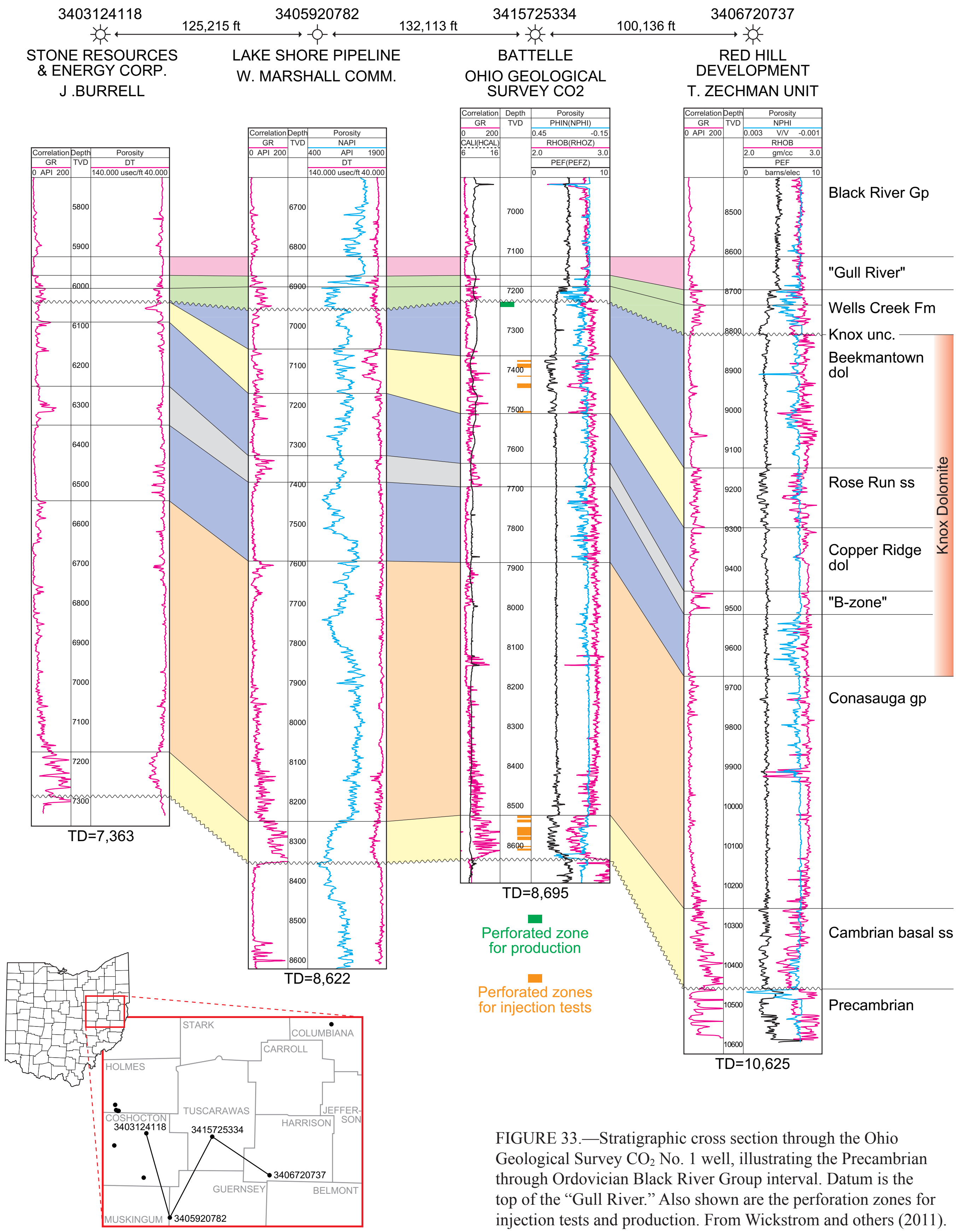

FIGURE 33.—Stratigraphic cross section through the Ohio Geological Survey CO_2 No. 1 well, illustrating the Precambrian through Ordovician Black River Group interval. Datum is the top of the "Gull River." Also shown are the perforation zones for injection tests and production. From Wickstrom and others (2011).

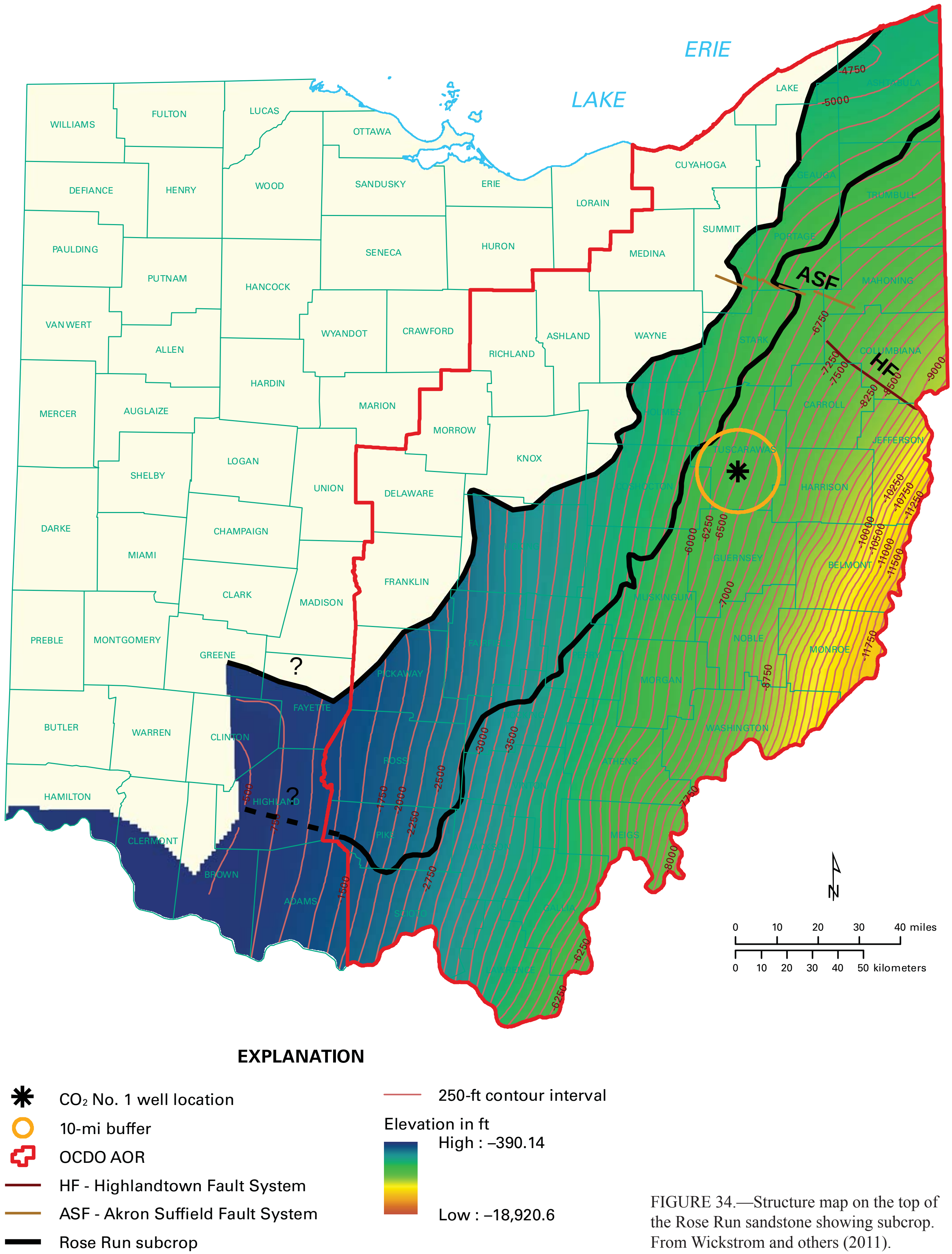

FIGURE 34.—Structure map on the top of the Rose Run sandstone showing subcrop. From Wickstrom and others (2011).

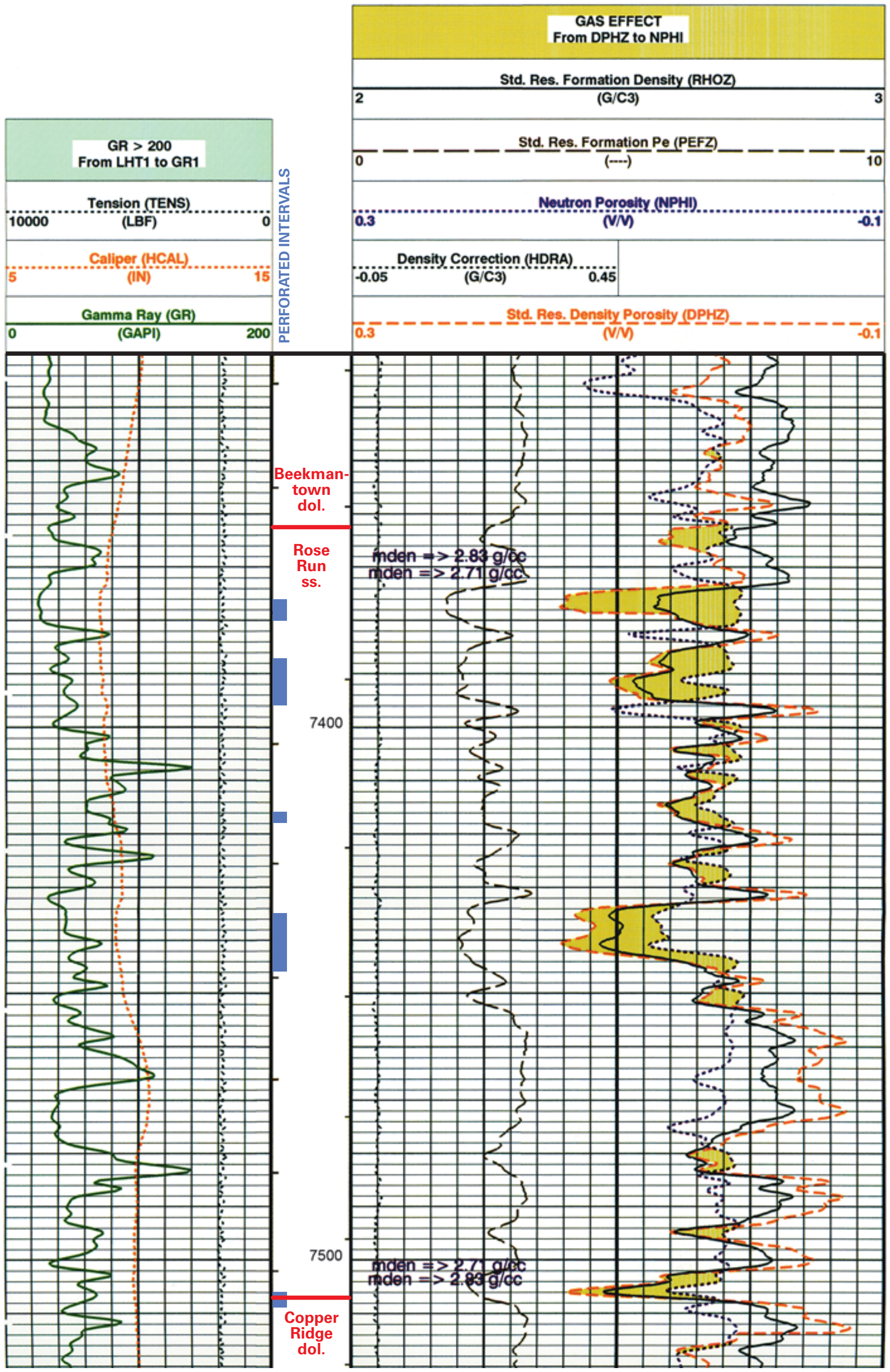

FIGURE 35.—Geophysical log of the Rose Run sandstone interval in the CO_2 No. 1 well. Also shown are the perforated intervals used for brine injection zones. From Wickstrom and others (2011).

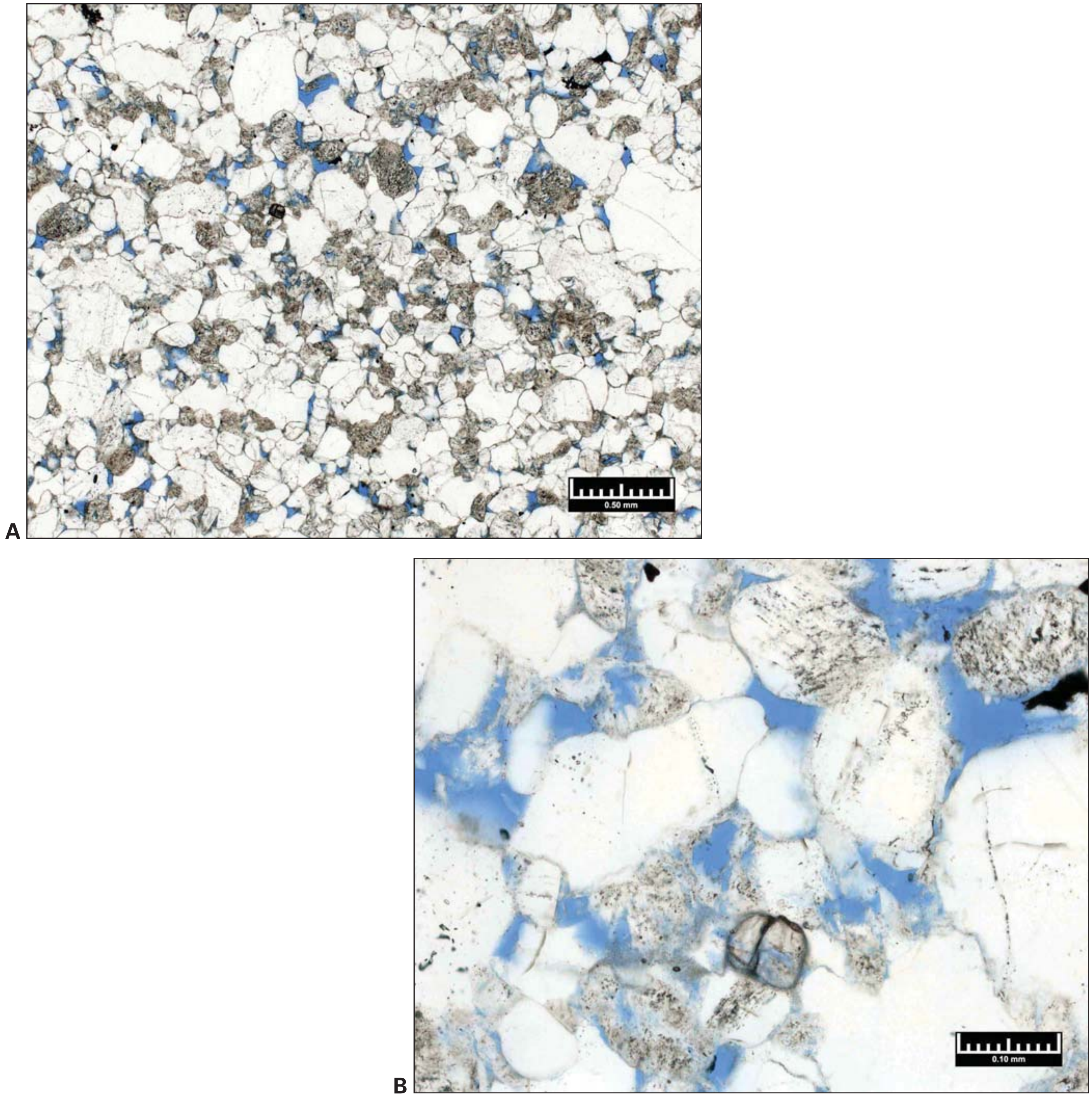

FIGURE 36.—Thin section photomicrographs of the Rose Run sandstone at a depth of 7,441 ft. (**A**) Magnification 40x, subarkose composed dominantly of quartz and feldspar; (**B**) magnification 200x, pore types include intergranular and intragranular (leached feldspar). From Wickstrom and others (2011).

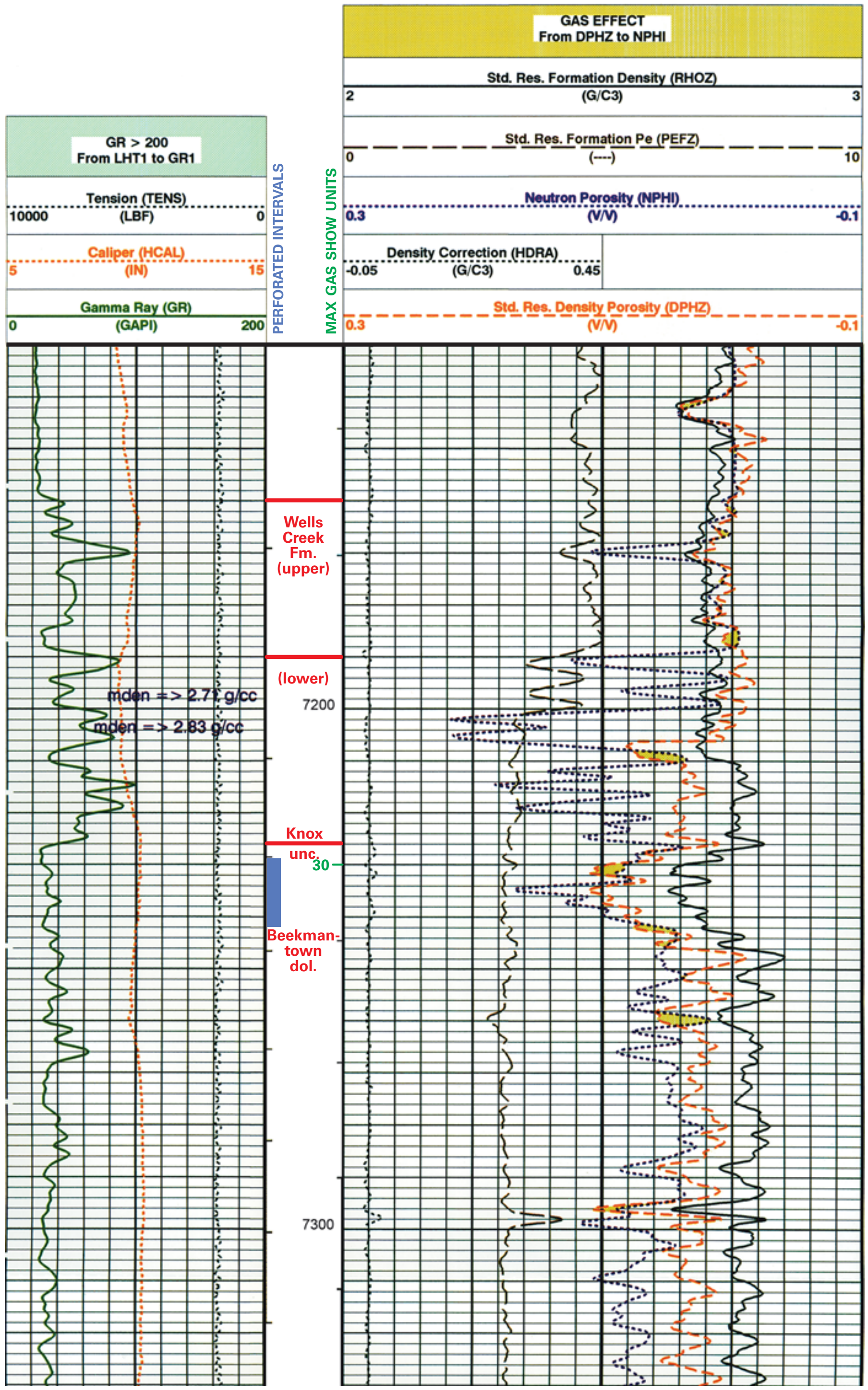

FIGURE 37.—Geophysical log of the upper Beekmantown dolomite and overlying Wells Creek Formation intervals in the CO_2 No. 1 well. Also shown are the perforated intervals for the producing zone. Gas show is also noted. From Wickstrom and others (2011).

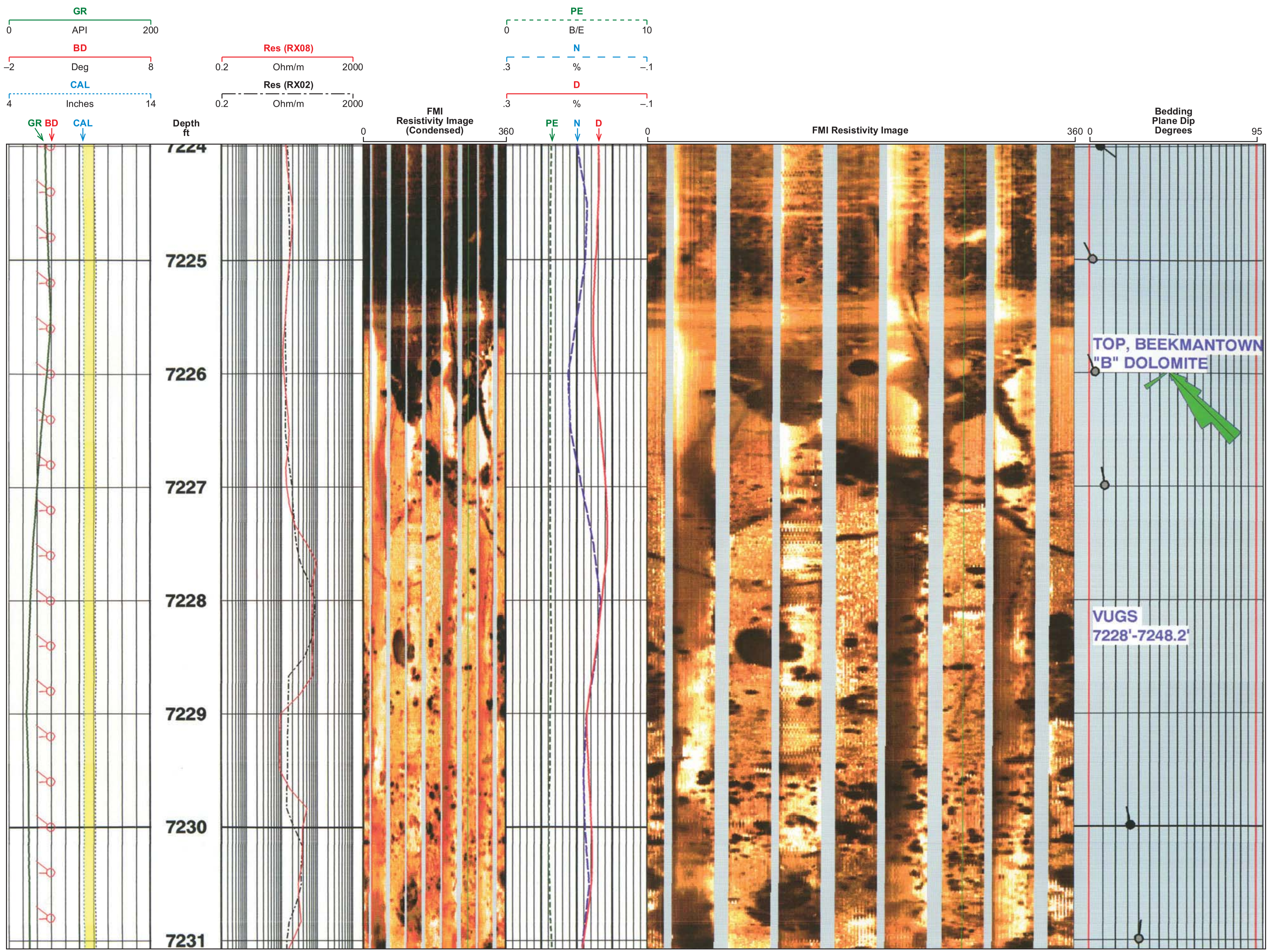

FIGURE 38.—Formation Microscanner Image of the Knox unconformity, displaying the Beekmantown dolomite and overlying Wells Creek Formation. Note brecciated zone with clasts up to 1 ft across. Well-developed pinpoint and vuggy porosity is present. From Wickstrom and others (2011).

from less than one percent to a maximum of 4 percent. Natural fractures are interpreted on the FMI in four Beekmantown intervals at depths of 7,284; 7,294; 7,322; and 7,360 ft.

Silurian Cataract Group ("Clinton" sandstone)

The CO_2 No. 1 well contains approximately 24 ft of net sandstone (greater than 50 percent shale free) based on log interpretation. The gross thickness of the "Clinton" interval is 96 ft, ranging from drillers' depths of 4,746 to 4,842 ft. The "Clinton" and overlying Rochester Shale were the uppermost stratigraphic units in which sidewall cores were taken. Porosities ranged from 3.6 to 8.6 percent and permeabilities were very low with all measured values of 0.01 md or less. Thin section petrography indicates the "Clinton" sandstone interval is a quartz arenite to subarkose. The primary framework grains consist dominantly of monocrystalline quartz (48–63 percent), feldspar (1–3 percent), lithic fragments (1–4 percent), and carbonaceous shale (2–3 percent). Cements comprise 15 to 18 percent of the rock and consist primarily of quartz overgrowths and pore-lining clay.

Silurian Lockport Dolomite and Bass Islands Dolomite

Both the Lockport Dolomite and Bass Islands Dolomite are considered as secondary injection horizons because of their regional variability in terms of reservoir quality. In the CO_2 No. 1 well, the Lockport interval is 248 ft thick, ranging from a depth of 4,228 ft to 4,476 ft below ground level. There were no significant zones of porosity development noted on logs within the Lockport in the CO_2 No. 1 well. Regionally, average log-derived porosities for gas productive intervals in the Lockport Dolomite are typically 8–10 percent, with values as high as 14 percent (Noger and others, 1996).

The Bass Islands Dolomite is 124 ft thick in the CO_2 No. 1 well, ranging from a depth of 3,430 ft to 3,554 ft below ground level. There were no zones with significant reservoir quality (greater than 4 percent porosity) noted in samples or logs within this well. However in many wells of eastern Ohio, this interval is a locally brecciated carbonate zone, perhaps associated with the Wallbridge unconformity found at the base of the Oriskany Sandstone. These brecciated zones often have very high porosities and permeabilities. Some of the state's highest volume Class II brine-injection wells utilize this zone.

Devonian Oriskany Sandstone

The Oriskany Sandstone also is considered to be a potential secondary injection horizon in this region. In the CO_2 No. 1 well, the Oriskany Sandstone is 23 ft thick, ranging from a depth of 3,313 ft to 3,336 ft below ground level. Based on well cuttings and geophysical logs, the Oriskany reservoir quality at this site is poor with no significant porosity development greater than 4 percent.

Detailed Hydrologic Characterization Tests

Battelle conducted detailed hydrologic tests on selected perforated test intervals of the Ohio Geological Survey CO_2 No. 1 well. The objectives of the hydrologic test program were to provide detailed hydraulic and storage property information for the Cambrian basal sandstone and Rose Run sandstone, which are primary-candidate, deep injection reservoirs for carbon sequestration in eastern Ohio. The principal hydraulic/storage parameters characterized during testing include transmissivity (T), hydraulic conductivity (K), intrinsic permeability (k), and storativity (S). The field-test characterization was completed using a hydrologic test sequence approach that included short-duration, slug-injection/drill-stem (DST) recovery tests used in conjunction with longer duration injection tests and test recoveries. Specific intervals tested are shown in Table 6.

TABLE 6.—*Stratigraphic intervals and footage perforated and hydrologically tested in the CO_2 No. 1 well*

Test Unit	Stratigraphic Position	Test Depth, ft below ground surface
Cambrian basal sandstone	Total	8,526–8,613
Rose Run #1	Bottom	7,506–7,509
Rose Run #2	Middle	7,416–7,446
Rose Run #3	Upper	7,377–7,396
Composite Rose Run	Total	7,377–7,509

Following completion of the logging and sidewall coring operations, a 4.5-in outside diameter casing was cemented in place from ground surface to the total depth (Fig. 30). Intervals within the Cambrian basal sandstone and overlying Rose Run sandstone were then perforated, acidized, and tested for detailed hydraulic-property characterization.

An entire set of six discrete, perforated depth intervals within the Cambrian basal sandstone (8,526–8,531 ft; 8,536–8,542 ft; 8,554–8,576 ft; 8,578–8,587 ft; 8,602–8,604 ft; and 8,608–8,613 ft) were brine injected tested collectively. The perforated depth intervals occur within the upper 87 ft of this stratigraphic unit. Collectively, the basal sandstone perforated intervals exhibited relatively low hydraulic properties: $T = 0.073$ ft^2/day, $K = 0.0015$ ft/day, and $k = 0.5$ md. Low permeabilities from these injection tests corresponded with low permeabilities (generally less than 0.18 md) measured in sidewall cores for this interval.

Following the injection testing of the basal sandstone, a bridge plug packer was set above the basal sandstone at a depth of 7,530 ft and the Rose Run sandstone was perforated. Working upward, three Rose Run intervals were perforated at depths of 7,506–7396 ft (Table 6). Test results indicate that approximately 95 percent of the composite transmissivity is contained within the middle Rose Run test interval (Rose Run #2). The composite summation transmissivity value for all perforated Rose Run test intervals is 0.93 ft^2/day. This is slightly higher than the Rose Run transmissivity estimate of 0.79 ft^2/day for the Mountaineer AEP No. 1 well (APINO 4705300423) located approximately 100 mi south of the CO_2 No. 1 well (Spane and others, 2006). These results are consistent with previous work showing that siliciclastic deposition and reservoir quality in the Rose Run decreases to the south and southeast away from the subcrop (Riley and others, 1993). The CO_2 No. 1 and the AEP No. 1 wells are shown later in this report in cross section profiles in the section entitled “Regional Cross Sections and Structure Maps” (p. 63).

While injection tests were disappointing, uncertainty exists in the injection test procedures. It is questionable if the perforations were completely open from acidization, whether the injection pressures used were adequate for the depths being tested, and if the duration of the testing was long enough to be sure it had reached back into the formations. Comparison of injectivity to existing Class II brine-injection wells calls these results into question. It was recommended that open-hole testing be considered for future injection testing. The problems with perforations and acidizing cited above can be eliminated by performing the injection testing in an open-hole environment rather than through casing and cement (Wickstrom and others, 2011).

Silurian “Clinton” Sandstone Reservoir Characterization for Evaluation of CO_2-EOR Potential and Sequestration in the East Canton Oil Field

The purpose of this investigation was to evaluate the efficacy of using CO_2 for sequestration and enhanced oil recovery (EOR) in the East Canton oil field (Fig. 39). The primary goal was to conduct a practical study for potential geologic CO_2 sequestration and demonstration of CO_2 injection at a geological site, which in this case is a nearly depleted but economically promising oil reservoir.

Since its discovery in 1947, the East Canton oil field in northeastern Ohio has produced approximately 95 million barrels (MMbbl) of oil from the Silurian “Clinton” sandstone. Production has been solely from primary recovery under 40-acre state spacing requirements. Encompassing 175,000 reservoir acres with more than 3,100 current or historical producing wells, this is the most significant, actively producing oil field in Ohio. The original oil-in-place (OOIP) for this field is estimated to be approximately 1.5 billion bbl of oil. Using an average primary recovery factor of 7 percent, the estimated original oil reserves are 105 MMbbl. Thus an estimated 10 MMbbl of remaining oil reserves could be produced through primary recovery alone. In this study it was estimated by modeling known reservoir parameters that between 76 and 279 MMbbl of additional oil could be produced through secondary recovery in this field, depending on the fluid and formation response to CO_2 injection.

Stratigraphic Nomenclature

A basin-wide correlation chart illustrates the varied nomenclature used for equivalent units in the “Clinton” interval in Ohio and the surrounding Appalachian Basin states (Fig. 40). In Ohio, the Lower Silurian “Clinton” sandstone is an informal drillers’ term applied to units within the Cataract Group. The Cataract Group is bounded at both the top and base by unconformities. A regionally widespread unconformity is recognized at the top of the Upper Ordovician Queenston Shale and has been named the Cherokee unconformity by Dennison and Head (1975) and Brett and others (1990); the basal unconformity, Castle (1998); and unconformity 1 by Hettinger (2001) and Ryder (2000, 2004). The base of the Dayton Formation (“Packer Shell”) marks the upper unconformity (Brett and others, 1990).

These units do not outcrop in Ohio. The stratigraphic relationships in the study area are determined by interpretation of subsurface wireline logs and cores. The “Clinton” interval is stratigraphically equivalent to the Lower Silurian Grimsby Formation, which outcrops in northwestern New York and in Ontario at the Niagara escarpment. In eastern Ohio, various authors have applied informal drillers’ terminology to subdivide and correlate “Clinton” units into the “Stray,” “Red,” and “White” (Pepper and others, 1953; Knight, 1969). For this study, the “Clinton” interval was subdivided into five sandstone units, informally named the “CLNN1” through “CLNN5.” The Sickafoose-Morris No. 1 well (APINO 3415122018) log was used as a type log to illustrate the mapped units; the log also shows the relationship to drillers’ units of the “Stray,” “Red,” and “White” (Fig. 41).

Sickafoose-Morris No. 1 Cyclic-CO_2 Test (“Huff-n-Puff”)

A CO_2-cyclic test (“Huff-n-Puff”) was conducted on the Sickafoose-Morris No. 1 well (APINO 3415122018) in Stark County during August 2008 (Fig. 42). The well was drilled and completed in 1969 to a total depth of 5,010 ft with the “Clinton” at depths between 4,812 ft and 4,900 ft below ground surface. The initial production was 115 bopd and a total cumulative production over 50,000 bbl of oil and 47 MMCF of gas. The well was hydraulically fractured with 5,010 bbl of water using 75,000 lbs of sand proppant. Modeling of the hydraulic fracture by Halliburton Energy Services estimated the breakdown pressure of 3,300 psi with a fracture half-length of 513 ft and height of 358 ft. The subsurface working volume at the time the well was treated was estimated at 24,500 ft^3.

The CO_2-cyclic process involves the injection of CO_2 into a single wellbore (the “huff”), followed by a “soak” period during which time the CO_2 contacts matrix oil. It then diffuses into the oil adding solution gas drive to the system upon returning the well to production status (the “puff”). In a successful test, CO_2 moves into solution in the oil and swells the oil in the pore space, reducing its viscosity and decreasing interfacial tensions of the oil with the rock. This allows freer movement of the oil by enhancing the reservoir’s permeability relative to water and gas.

This test was designed to evaluate and assess the injectivity in a “Clinton”-producing oil well in the East Canton oil field and to better understand the dispersion or potential breakthrough of the CO_2 to surrounding wells. For this cyclic-CO_2 test, production casing was set at a depth of 5,001 ft and a packer was set at 4,796 ft (Fig. 42). Perforations were made between 4,830 ft and 4,890 ft, and eighty tons of CO_2 (1.39 MMCF) were injected over a 20-hr period. The well was then shut in for a 32-day “soak” period before production was resumed. Results demonstrated injection rates of 1.67 MMCF of CO_2 per day, which was much higher than anticipated. It is presumed that the injected CO_2 stayed within an area close to the wellbore as no CO_2 was detected in gas samples taken from eight immediately offsetting observation wells. There also was no pressure increase detected at any of the offset wells during and after the injection test. Furthermore,

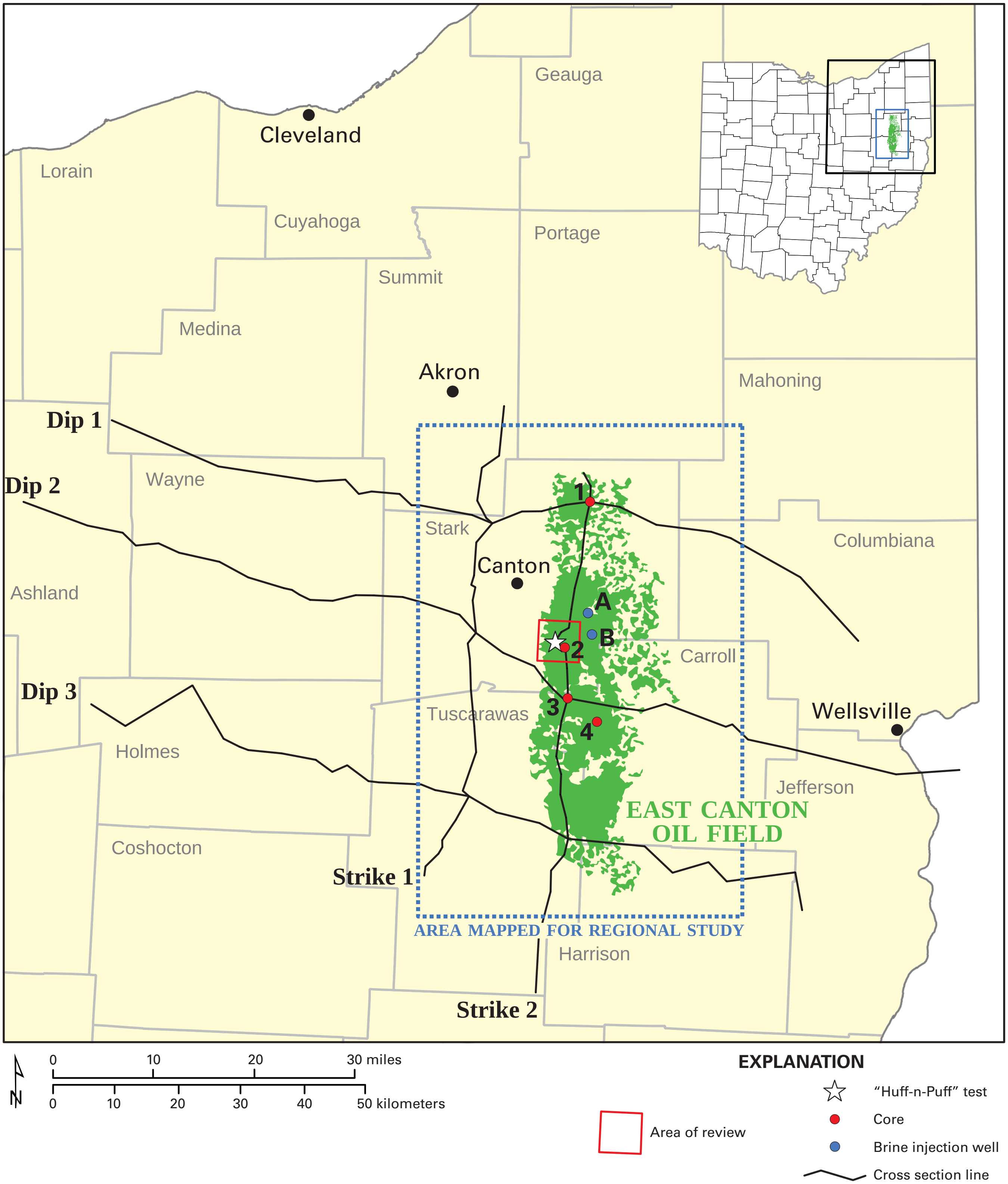

FIGURE 39.—Location map showing the East Canton oil field, regional mapped area of net sandstone, regional cross section lines, area of review, and "Clinton" cores and injection wells used in the Ohio Division of Geological Survey CO_2-EOR Study. From Riley and others (2011).

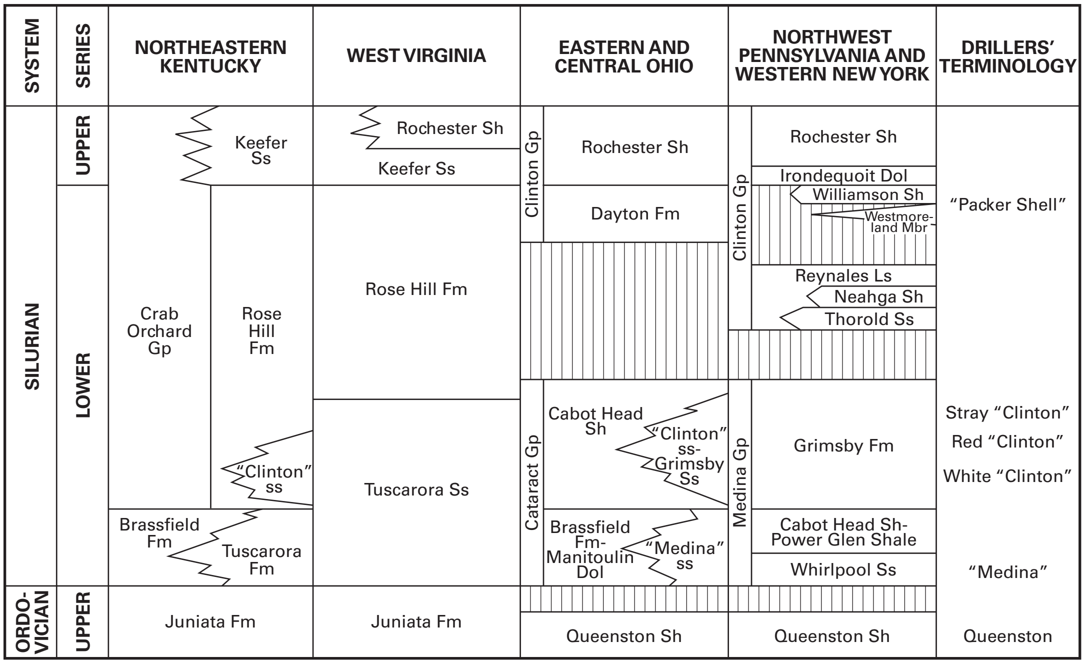

FIGURE 40.—Stratigraphic correlation chart of the Upper Ordovician through Upper Silurian units in Ohio and adjacent states. From Riley and others (2011).

a large quantity of CO_2 was gradually recovered during the production monitoring period, indicating there was no rapid CO_2 migration into fracture systems.

Results strongly suggest that the majority of the injected CO_2 entered the matrix porosity of the reservoir pay zones, where it diffused into the oil. Evidence includes:

(1) The volume of injected CO_2 was over 50 times greater than the estimated capacity of the hydraulic fracture and natural fractures.
(2) There was a gradual injection and pressure rate build-up during the test.
(3) There was a subsequent, gradual flashout of the CO_2 within the reservoir during the ensuing, monitored production period.
(4) A large amount of CO_2 continually off-gassed from wellhead oil samples collected as late as 3½ months after injection.

After the test well was returned to production, it produced 174 bbl of oil during a 60-day period (September 22–November 21, 2008), which represents an estimated 58 percent increase in incremental oil production over pre-injection estimates of production under normal, unstimulated conditions. The cyclic-CO_2 test had a CO_2 utilization factor (ratio of CO_2 injected to additional oil recovered) of 8 MSCF/STBO (thousand standard cubic ft/stock tank barrel of oil), assuming all oil production is attributed to CO_2 injection over the two-month monitoring period. The CO_2 utilization factor was 21 MSCF/STBO, if only the estimated additional incremental oil production is attributed to CO_2 injection.

Reservoir Characterization and Geologic Model

A regional study of the East Canton oil field and surrounding area was conducted to establish a consistent geologic framework and to better understand the depositional systems specific to this field. Regionally, the "Clinton" interval has an average gross thickness of 110 ft. The regional net sandstone map (Fig. 43) and published core studies (Overbey and Henniger, 1971; Castle and Byrnes, 2005) suggest a fluvial-deltaic and offshore marine depositional environment. The clastic source is from the east and is dominantly controlled by three deltaic lobes oriented east–west and southeast–northwest. Net sand thickness ranges from less than 10 ft in the offshore marine environment and interchannel areas to over 60 ft in the thicker, deltaic/tidal channel sands (Fig. 43). The western boundary of the East Canton oil field is parallel to the north–south-trending shoreline.

The "Clinton" sandstone interval is a progradational episode that followed the "Medina" flooding of the upper Ordovician unconformity (Fig. 44). Three to four marine incursions and one sea-level downshift occurred during "Clinton" deposition. The objective for subdividing the interval into five sandstone units was to develop a geologic model to better understand and delineate the porosity and permeability distribution and compartmentalization, as these affect fluid flow within the reservoir. Mapped units were based on identification

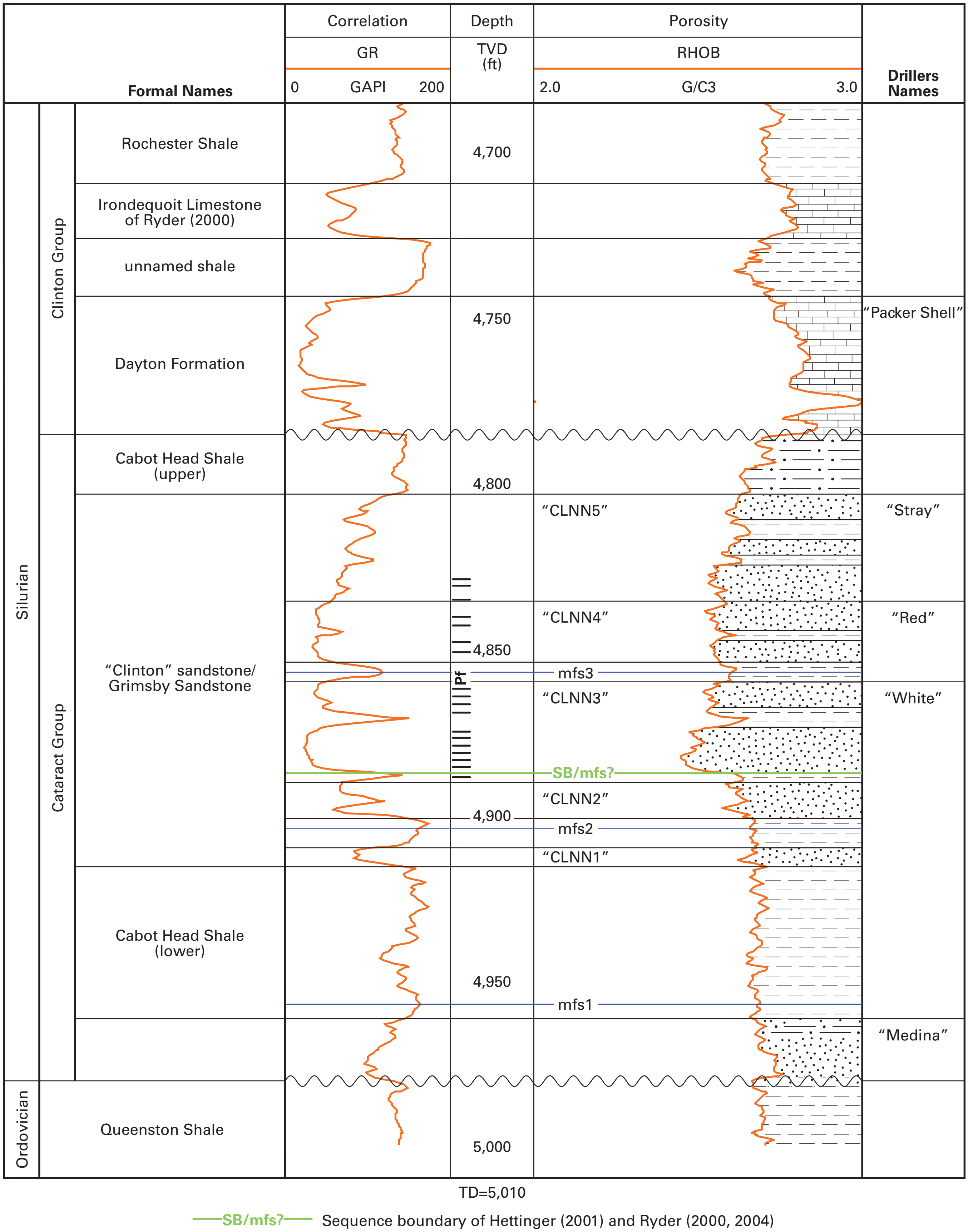

FIGURE 41.—The Sickafoose-Morris No. 1 well (APINO 3415122018) type log and the mapped units for the 2007 East Canton oil field study. Also shown are the formal names and corresponding drillers' names. The proposed sequence boundary (SB) is uncertain according to the authors of this report and may be a maximum flood surface (mfs). From Riley and others (2011).

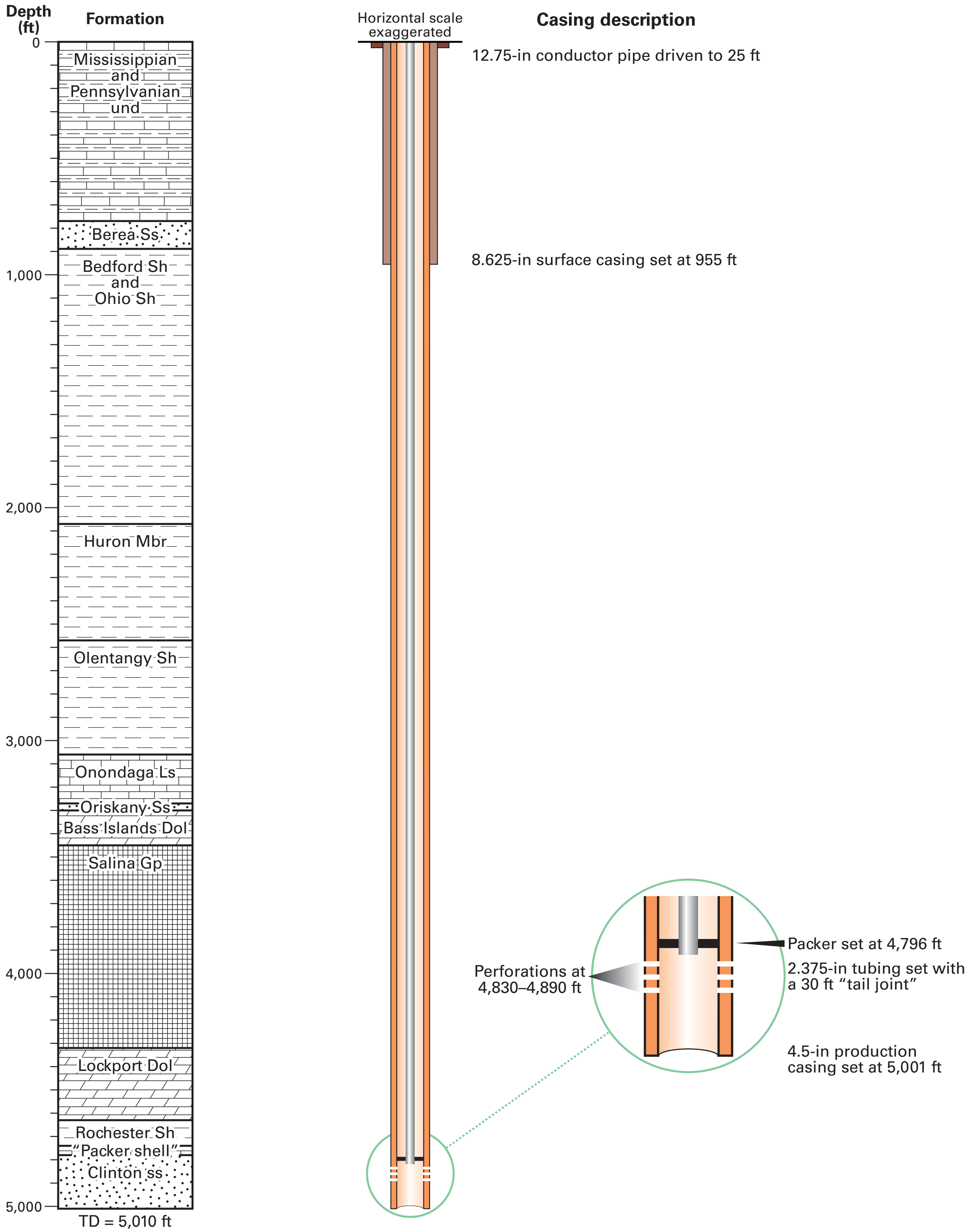

FIGURE 42.—Sickafoose-Morris No. 1 well completion diagram with perforations and test set-up. Modified from Wicks and others (2009).

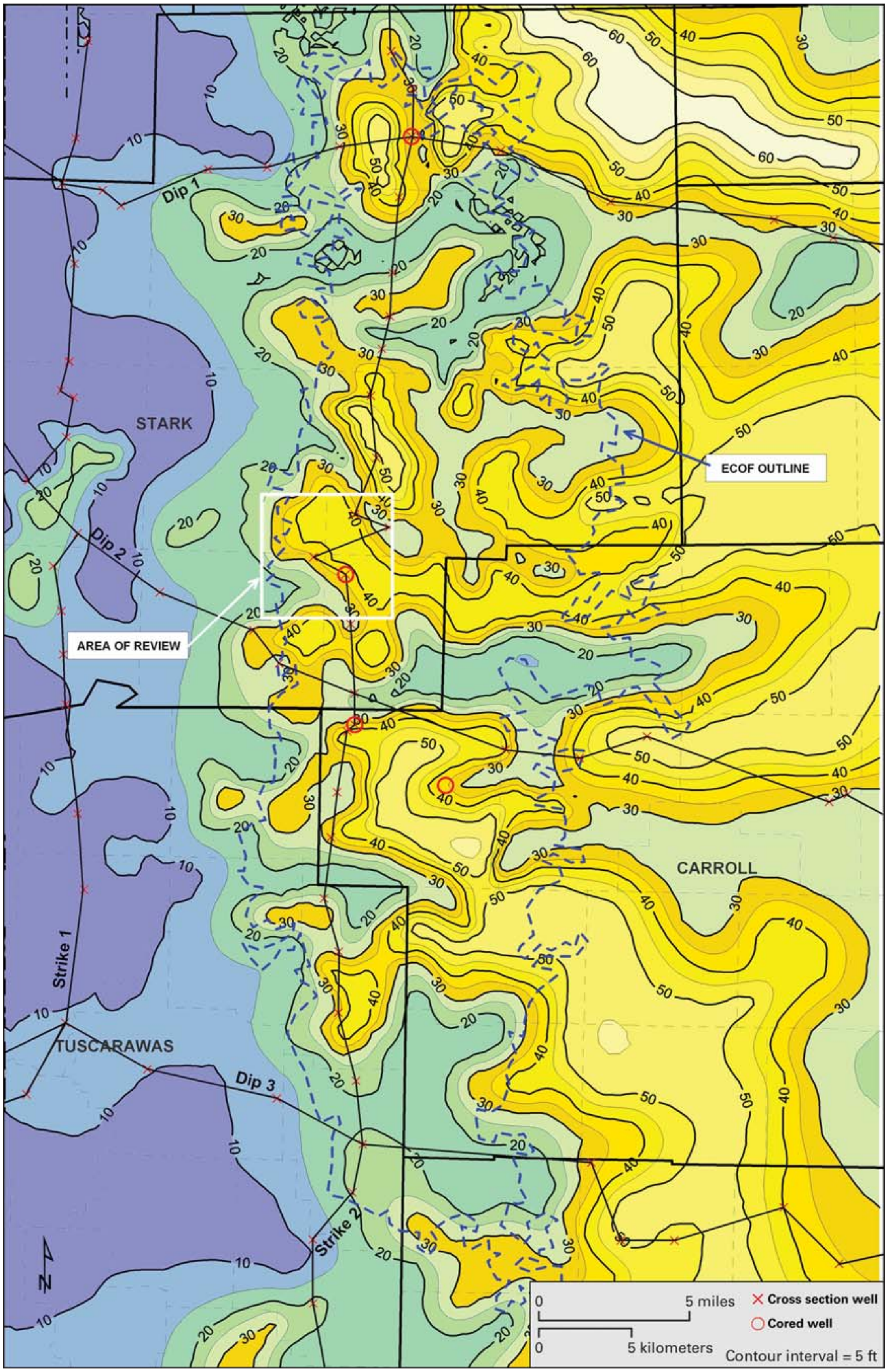

FIGURE 43.—Net sandstone map for the "Clinton" sandstone interval in the 2007 East Canton oil field study area of review. Regional cross section lines are shown along with cored wells. From Riley and others (2011).

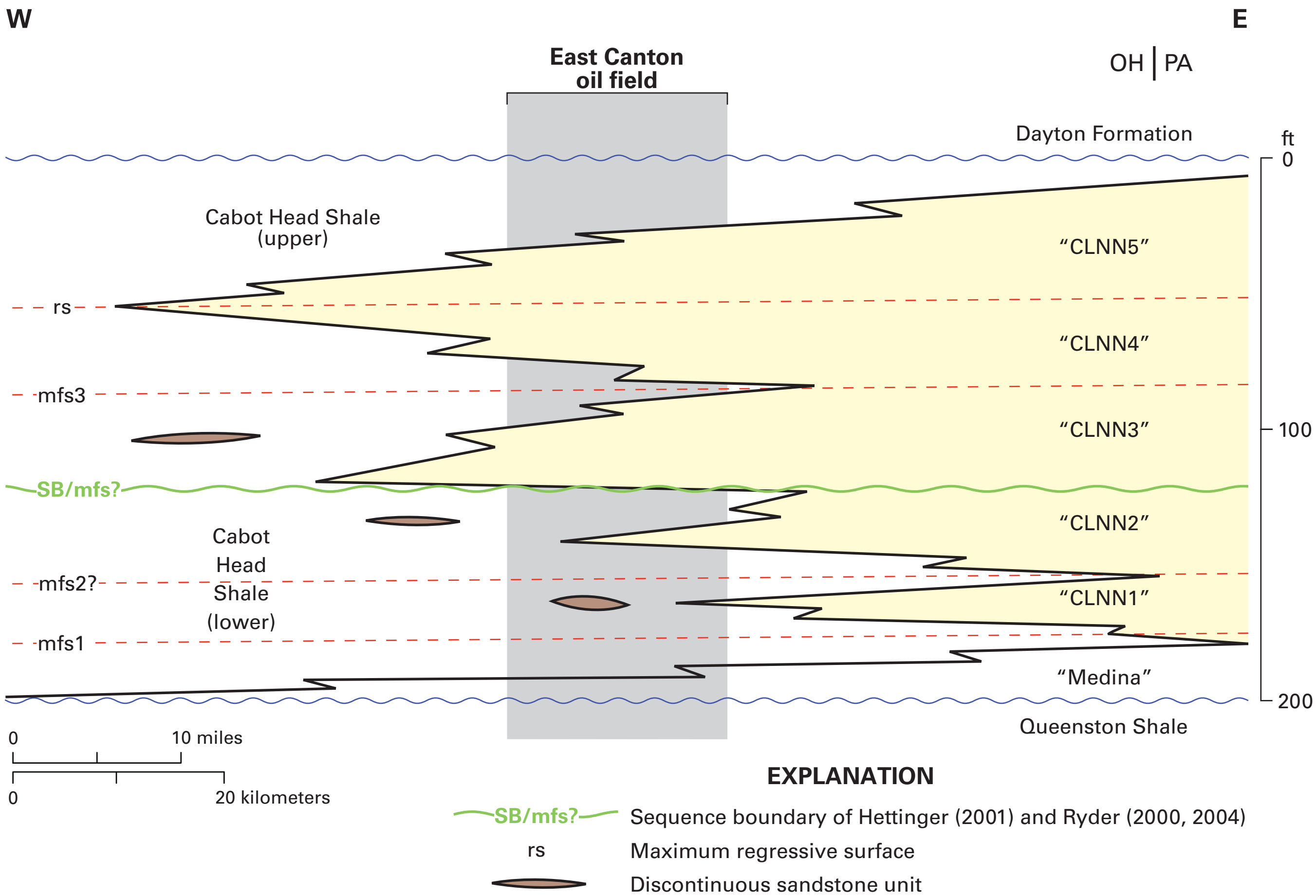

FIGURE 44.—Diagrammatical illustration through the East Canton oil field and surrounding area of review for the 2007 study, illustrating the major depositional units of the "Clinton" interval ("CLNN1" through "CLNN5") and maximum flood surfaces (mfs1 through mfs3) as interpreted for this study. From Riley and others (2011).

of four parasequences separated by three to four maximum flood surfaces (mfs1, mfs2, and mfs3) and/or one possible sequence boundary. These sequences were interpreted from wireline logs by the coarsening upward (prograding) or fining upward (retrograding) character of the gamma ray curve and the continuity of bounding shales. The prograding/retrograding cycles are named the "CLNN1" through "CLNN4" and the final fining upward cycle is named the "CLNN5" (Fig. 44).

The regional study was followed by detailed geologic mapping and reservoir characterization of a 4 × 4-mi (10,240-acre) AOR in Stark County (Fig. 45). A grid of 32 stratigraphic cross sections using digitized well logs was constructed across the 10,240-acre AOR. Compartmentalization due to shale baffles between individual sandstone units is evident between wells. The "CLNN3" and "CLNN4," as interpreted on gamma-ray and density logs, represent the bulk of the "Clinton" reservoir with a combined net sand thickness up to 57 ft. The average values for water saturation (Sw) range from 13 to 42 percent in the "CLNN3" and from 13 to 34 percent in the "CLNN4." Matrix permeability for this study was estimated based on core data from three wells in the East Canton oil field. In the AOR, average maximum matrix permeability (Kmax) from core is 0.69 md. Where log porosity average is greater than 8 percent, the permeability averages 1.05 md.

A 700-acre model area was selected from within the AOR for simulation work that was performed by Fekete Associates, Inc. This model area was selected based upon the availability of well log and production data and also due to its impressive production history. A geologic model was developed based on maps for each "Clinton" unit ("CLNN1"–"CLNN5") of structure, gross thickness, net ft of sandstone, average porosity, average Sw, and estimated permeability. Within the model area there are 23 wells with reported production data, and they have produced a combined total of 866,000 bbl of oil and 2.5 BCF of gas. The Sickafoose-Morris No. 1 well, subject of the cyclic-CO_2 test, has produced 60,654 bbl of oil and 133 MMCF of gas since 1969.

For this study, 16 wells in the model area were used to plot oil production versus porosity-ft. The plot showed little to no correlation, which suggests other factors, such as fractures or completion practices, are contributing to the oil production yield. From published reports, the hydraulic fracture direction in the "Clinton" is N. 63º E.; a recent proprietary microseismic test in the East Canton oil field showed a preferential direction

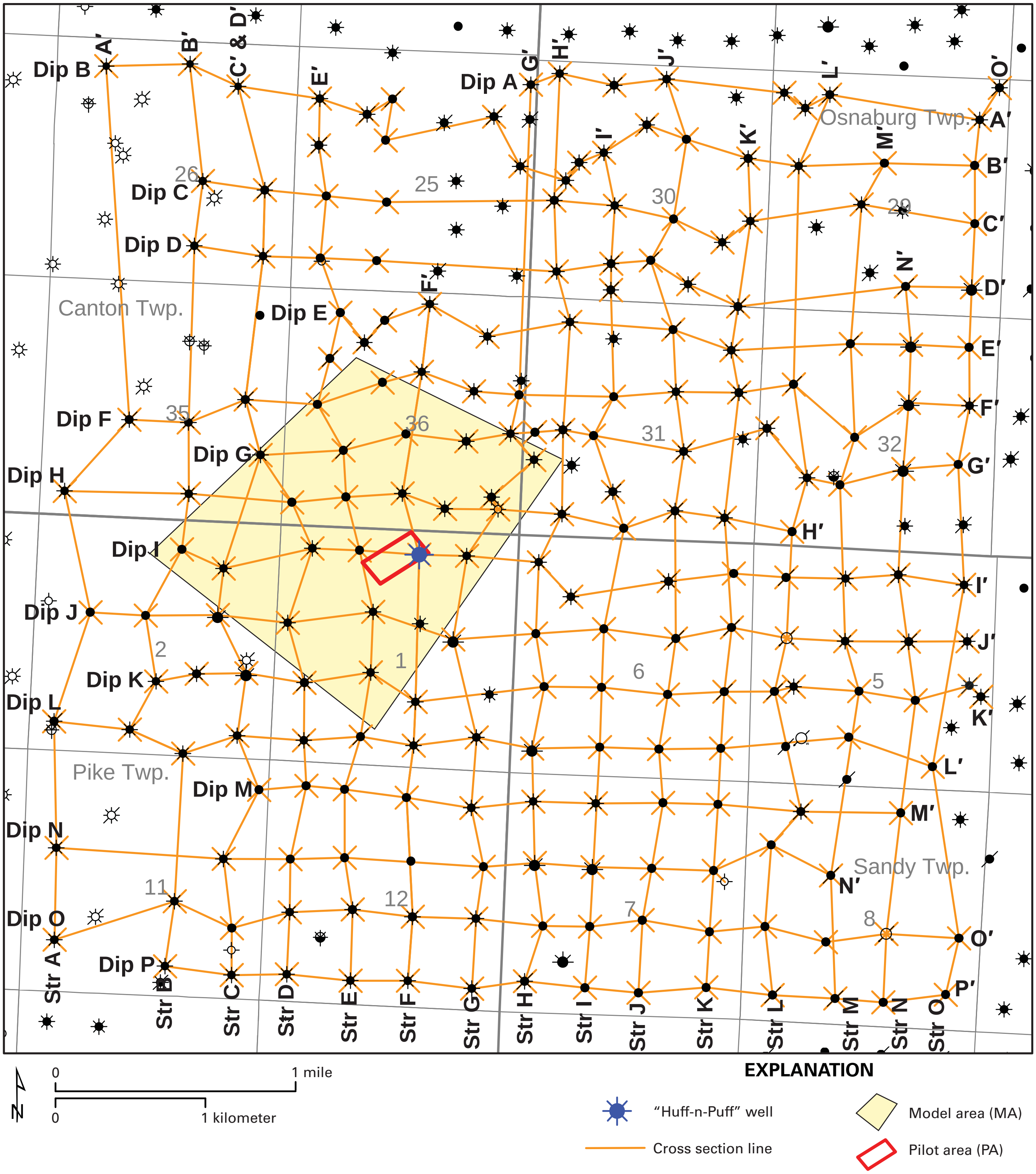

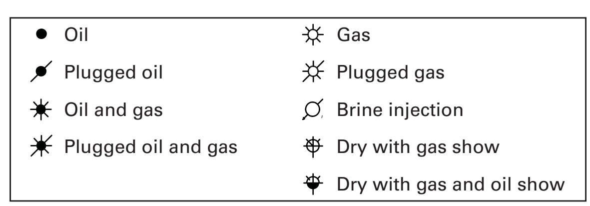

FIGURE 45.—Map showing the East Canton oil field 2007 study area of review (AOR), model area, and pilot area. Also shown are the detailed stratigraphic cross section lines in the AOR. From Riley and others (2011).

of N. 55° E. Anecdotal evidence from other hydraulic fracture treatments in the East Canton oil field confirms the general direction between N. 55° E. and N. 63° E. from limited observed communication between wells.

The extent to which natural fractures affect production within the "Clinton" sandstone reservoir in the East Canton oil field remains unclear. The best evidence for fluid communication between wells is from artificially induced hydraulic fractures, which trend in the direction parallel to the northeast–southwest contemporary stress field. Core measurements and basin tectonic features suggest a northwest–southeast trend for the natural fractures. However, based upon the aforementioned observations and the opinions of oil and gas operators in the ECOF, a natural fracture network was incorporated in the modeling and simulation in a direction parallel to the hydraulic fractures.

Reservoir Modeling and Simulation

Using the Survey's geologic model, Fekete Associates, Inc., conducted a reservoir simulation for the 700-acre model area and designed a pilot to test the model. Within the model area the OOIP is estimated at nearly 13 MMSTBO, 90 percent of which is in the "CLNN3" and "CLNN4" units. Recovery to date has been 866 MSTBO or 6.7 percent of the OOIP. A dual-porosity (matrix and fracture) model was used; the pilot design included four CO_2 injection wells and one central producer drilled on a 12-acre pattern elongated in the assumed direction of fracture orientation.

Fekete concluded that injection wells could enhance oil production and lead to an additional 20 percent recovery in the pilot area over a five-year period. The base case estimated that by injecting 500 MCF per day of CO_2 into each of the four corner wells, 26,000 STBO would be produced by the central producer over the five-year period. This would compare to 3,000 STBO if a new well were drilled without the benefit of CO_2 injection. During simulation, peak rate of 32 bopd was attained within the first seven months. As a result of fractures in the simulation model, CO_2 breakthrough to the central producer first occurred within weeks and increased over the five-year simulation period to 1.4 MMCF/d of CO_2 or 70 percent of the injected volumes. During the same period the oil production rate steadily decreased to an estimated 10 bopd baseline. Average pressure in the pilot area increases to 1,000 psi in less than one year, with a very gradual rise to 1,200 psi in year five. This is 250 psi less than the measured minimum miscibility pressure of 1,450 psi, the pressure needed to attain the most effective CO_2 sweep and oil production response.

Considerable uncertainty exists in the model due to our limited knowledge of fluid properties and fracture distribution and connectivity. Sensitivity studies were conducted during simulation by varying different properties within the pilot area. Results showed CO_2-enhanced peak production rates ranged from 14 bopd to 43 bopd, depending on the assumed values for fluid properties, matrix permeability, and fracture anisotropy (Fig. 46). By altering the values, cumulative production for the central producer in the pattern would vary from 12,000 to 42,000 bbl of oil over the five-year simulation period.

Recommendations

Core, petrophysical, and fracture analyses and detailed mapping are critical to assess the "Clinton" reservoir and provide necessary information for planning proper well spacing and design of future pilot floods in secondary recovery efforts. Additional oriented cores, fracture data, and fluid analyses are needed to high-grade the next stage of modeling and simulation work. Such additional modeling and simulation will enable future efforts to more definitively evaluate CO_2-EOR potential in the East Canton oil field and to finalize pilot design configuration. After collection of this data and refinement of the model and simulation, it is recommended that a larger-scale (10,000–20,000 t) cyclic-CO_2 injection test be conducted to better determine the efficacy of CO_2-EOR in the "Clinton" reservoir in the East Canton oil field.

REGIONAL CROSS SECTIONS AND KEY MAPPED UNITS

Regional Cross Sections and Structure Maps

Cross section profiles are used to illustrate subsurface stratigraphic and structural geologic conditions and relationships (e.g., Ryder, 1991; Greb and others, 2012). Cross section data includes drilling depths to well-known geologic formation units (geologic "tops") based on well drilling records. Well locations along the cross section profile can be spaced equally apart, projected onto an arbitrary line segment, or set to a relative horizontal scale. Specific data types used to construct cross sections include descriptive logs of core and samples, wire-line electrical logs, and reported unit names from open-file records and reports. These types of information are all very useful in geologic characterization, which includes but is not limited to:

(1) Defining the thicknesses and extents of geologic units.
(2) Identifying stratigraphic facies and facies variations.
(3) Calculating relative porosity.
(4) Evaluating lithologic characteristics that impact porosity.
(5) Determining relative structural position.
(6) Contour mapping thicknesses of reservoir, cap rocks, and other relevant geologic facies.

For the regional cross section presented in this report, only geologic wire-line electrical log tops were utilized, obtained from both existing reports and from unpublished studies. The digitized electric logs are not displayed on the cross sections. Company- or operator-reported geologic tops were not applied as these data can be unreliable and inconsistent. For further reading about wire-line electrical log interpretations see Asquith (1982) and Schlumberger (1972).

The Survey has public domain wire-line electrical logs for approximately 74,800 wells in its ever growing archives. From this log set, only wells drilled deeper than the Knox Dolomite were used to construct "stick" cross sections created for this report. To simplify the graphics, "stick"cross sections omit display of the geophysical log curves upon which the

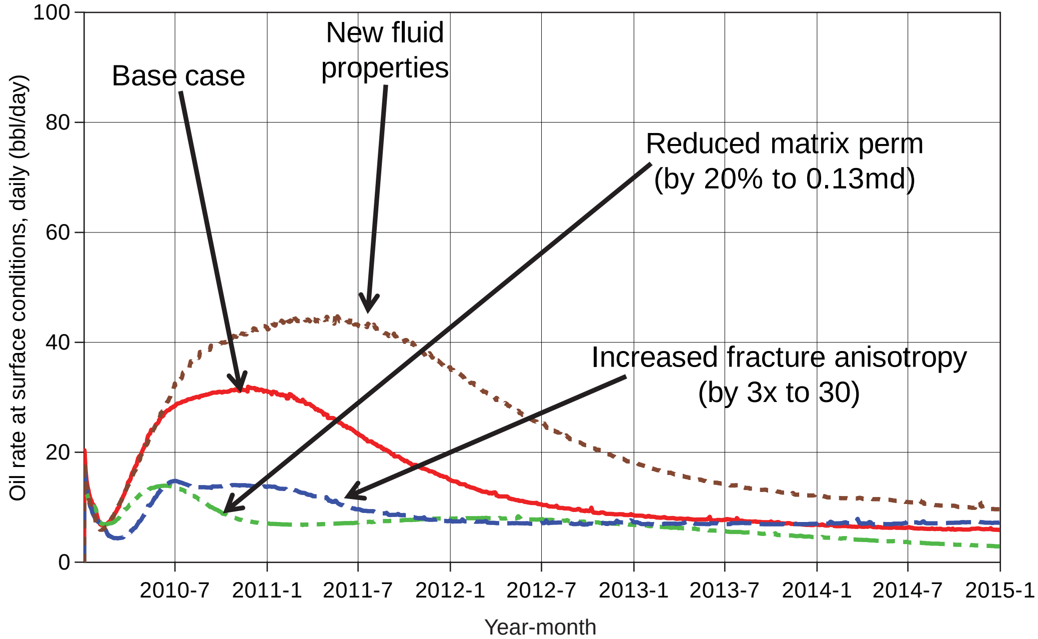

FIGURE 46.—Forecast of oil production rate for the East Canton oil field pilot-area central producer for the five-year simulation period, showing the Base Case and three sensitivity study cases. From Riley and others (2011).

interpretations are primarily based. These cross sections depict the stratigraphic interval spanning from the Ordovician Utica-Point Pleasant interval downward in section to the top of the Precambrian basement. Regional unconformities are identified at the top of the Knox Dolomite and at the top of the Precambrian surface. The Wells Creek Formation was used as datum. Where practical, relatively recent deep wells or piggyback wells receiving public research funding were utilized in the cross sections because the suite of logs run in these wells are more advanced, providing data of higher quality and greater reliability. More information on these piggyback wells is presented in Battelle's OCDO report that complements this study and in well reports created by Battelle for work performed and data collected at each of these wells. Battelle's work and reports on these topics were completed under Grant Agreement No. CDO/D-10-7a.

For this report, the Survey has created four regional cross sections using existing well data and GeoGraphix® Geographic Information System (GIS). The locations of these cross sections are presented in Figure 47. These four cross sections (A–A′ through D–D′) are shown as Figures 48 through 51, respectively. Strike cross section A–A′ follows roughly the depositional strike of formations lying on the western flank of the Appalachian Basin. Dip cross sections B–B′, C–C′ and D–D′ are roughly normal to the strike cross section A–A′, dipping from central Ohio eastward into the Appalachian Basin. To the west, the three dip cross sections extend over Owens hinge line and the Findlay Arch into the Illinois and Michigan Basins.

Precambrian Surface

The Survey has published a structure map of the Precambrian basement surface (Baranoski, 2002; Fig. 52 is a page-sized version of this structure map).

Cambrian Pre-Knox Interval

The Cambrian Pre-Knox interval lies unconformably on the Precambrian basement surface. This interval consists, in ascending order, of the basal sandstone of the Conasauga group in eastern Ohio, Maryville Formation, and Nolichuky Formation. In central Ohio, the Mount Simon Sandstone becomes the lowermost unit, which is overlain by basal sandstone equivalents and the Eau Claire Formation in western Ohio. The Mount Simon Sandstone and basal sandstone of the Conasauga group have served as waste and brine disposal reservoirs since the late 1960s. Given their proven ability to accept and store liquid wastes, they are also considered favorable CO_2 sequestration targets in eastern Ohio. Thickness of the Pre-Knox interval ranges from approximately 350 ft in northeastern Ohio to 800 ft in southwestern Ohio.

Cambrian to Ordovician Knox Interval

The Cambrian-Ordovician Knox interval lies conformably on the Cambrian Pre-Knox interval. This interval is generally termed the Knox Dolomite or "Trempealeau" by drillers. The interval consists, in ascending order, of the Copper Ridge dolomite, Rose Run sandstone, and Beekmantown dolomite. The top of the interval is marked by the regional angular Knox unconformity. Notable on the dip cross sections is the absence of the Rose Run sandstone and Beekmantown dolomite in central Ohio due to the angular unconformity (see Riley and others, 1993). The Beekmantown, Rose Run, and Copper Ridge have produced hydrocarbons in Ohio since the early 1900s and have also served as waste and brine disposal reservoirs

FIGURE 47.—Map showing cross sections and wells drilled to the Precambrian in Ohio and adjacent states.

TABLE 7.—*API numbers corresponding to wells in cross sections (Figs. 48–51)*

Cross section ID	API number	Cross section ID	API number
A-1	3414520212	B-9	3415320907
A-2	3407920078	B-10	3413322860
A-3	3407920102	B-11	3409923127
A-4	3407321222	B-12	3409923171
A-5	3412726595	B-13	3708520036
A-6	3405924067		
A-7	3405924202	C-1	3400363691
A-8	3415725334	C-2	3410120174
A-9	3401922045	C-3	3411724190
A-10	3413322860	C-4	3408321413
A-11	3400722038	C-5	3407525231
A-12	3400721847	C-6	3403124118
A-13	3400760010	C-7	3415725334
		C-8	3406720737
B-1	3417120046	C-9	3401320611
B-2	3405120049		
B-3	3409520060	D-1	3416560005
B-4	3417320239	D-2	3402720010
B-5	3414320147	D-3	3404720010
B-6	3414320235	D-4	3414120021
B-7	3404320011	D-5	3407920102
B-8	3410321143	D-6	4705300423

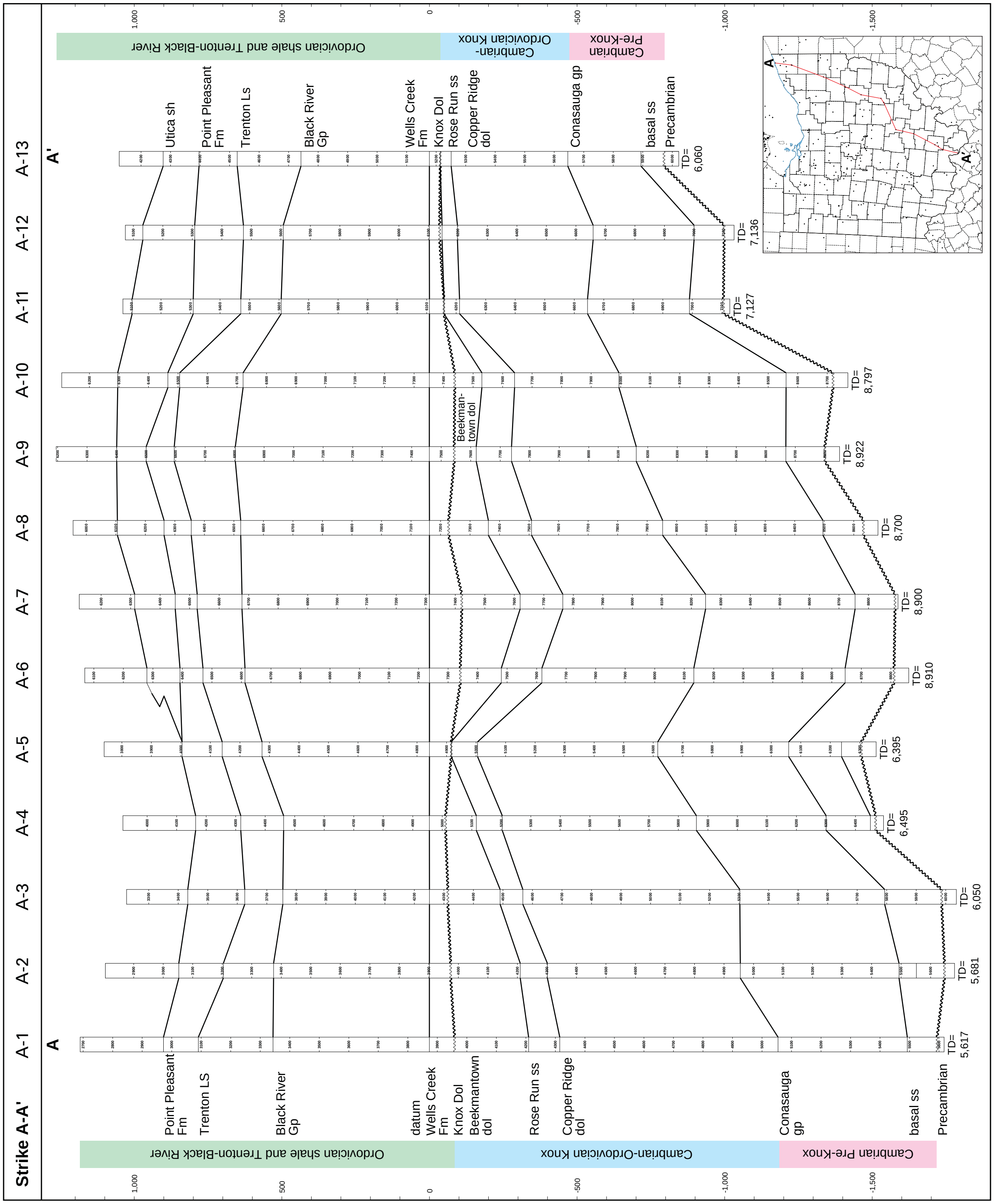

FIGURE 48.—Strike cross section A–A′, as shown in Figure 47.

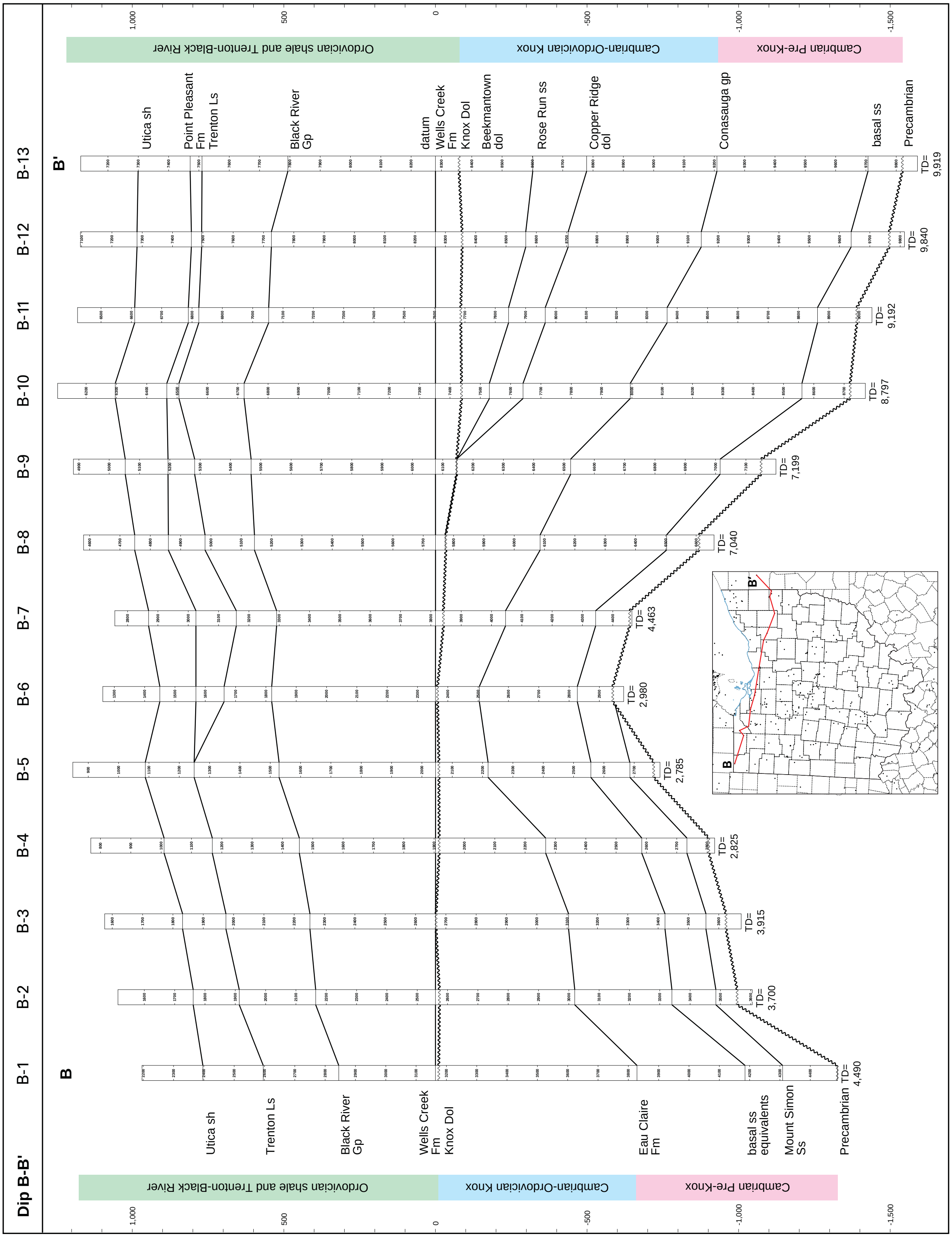

FIGURE 49.—Dip cross section B–B′, as shown in Figure 47.

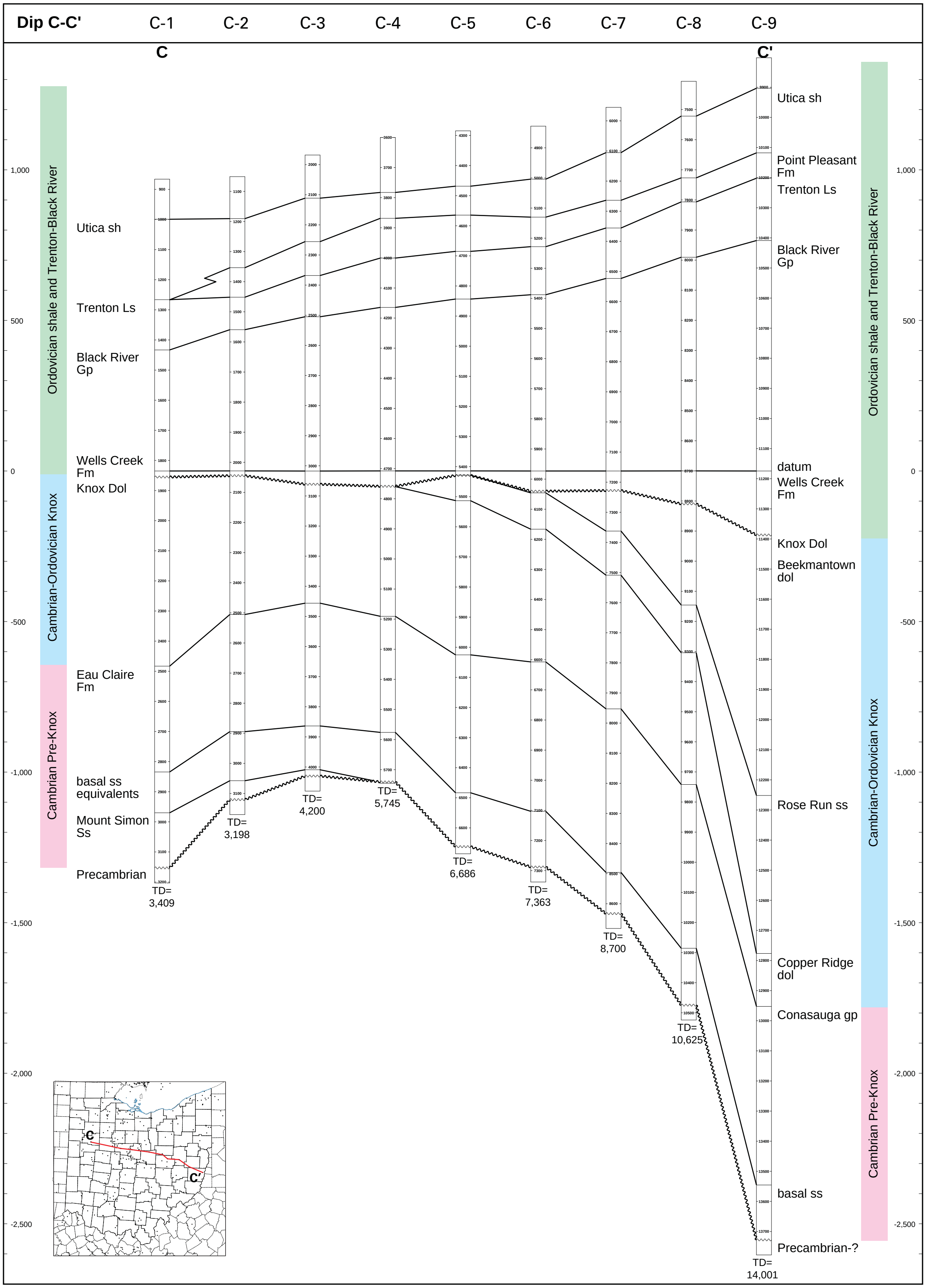

FIGURE 50.—Dip cross section C–C′, as shown in Figure 47.

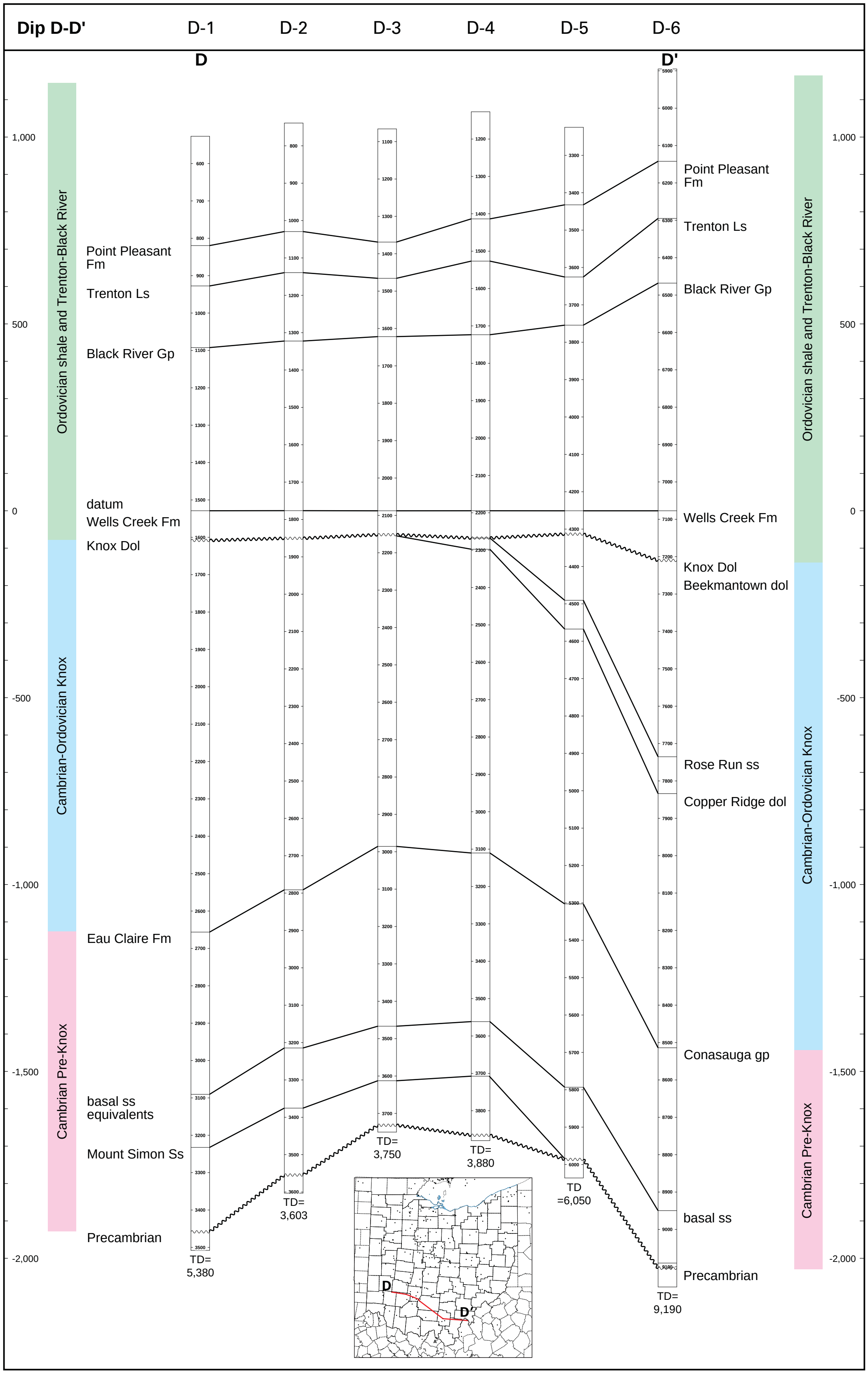

FIGURE 51.—Dip cross section D–D′, as shown in Figure 47.

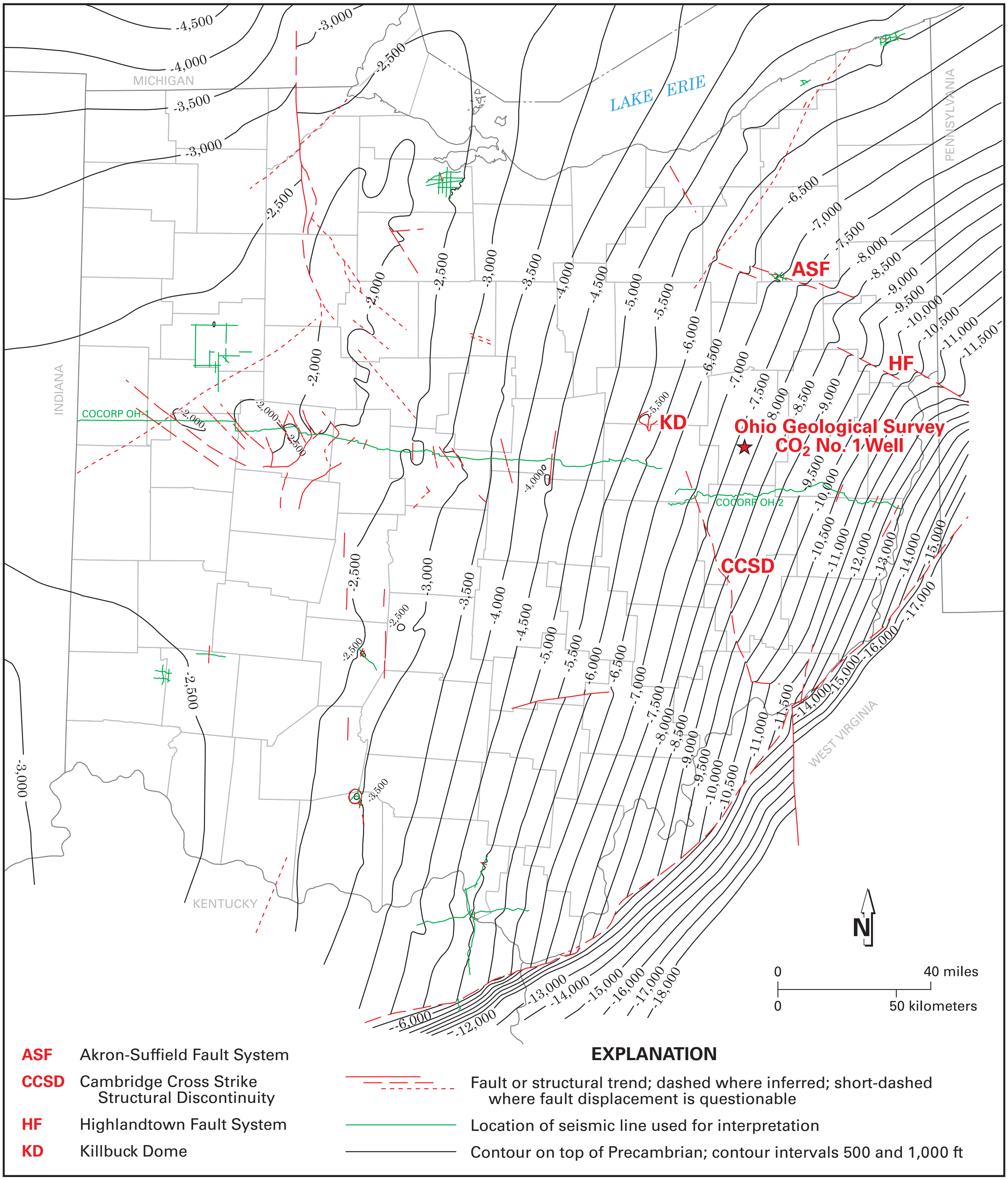

FIGURE 52.—Structure contours drawn on the Precambrian unconformity surface in Ohio. Major structural trends and faults and locations of COCORP seismic profiles shown (from Baranoski, 2002).

since the late 1960s. Thickness of the Knox interval ranges from approximately 450 ft in northeastern Ohio to 1,500 ft in eastern Ohio. As discussed in previous sections (p.4–9) of this report and in Battelle's complimentary report, these units are thought to be favorable CO_2 sequestration targets in eastern Ohio.

Ordovician Shale and Trenton-Black River Interval

The Ordovician shale and Trenton-Black River interval lies unconformably on the Cambrian-Ordovician Knox interval. The interval consists, in ascending order, of the Wells Creek Formation, Black River Group, Trenton Limestone, Point Pleasant Formation, Utica shale, and Ordovician shale undifferentiated. Notable on the cross sections is the often variable thickness of the Wells Creek Formation; this variation in thickness is due to localized paleotopography on the Knox unconformity. Hydrocarbon production from this interval is spotty throughout Ohio, except for the Lima Field in northwestern Ohio, where significant hydrocarbon production from this interval has occurred since the late 1800s. Recently, there is great interest and increasing activity focused on horizontal drilling and hydraulically fracturing the Point Pleasant and Utica shale in much of eastern Ohio. Thickness of the Ordovician shale and Trenton-Black River interval ranges from approximately 800 ft in western Ohio to 1,300 ft in eastern Ohio.

Structure Maps for Key Shallow Horizons

In addition to the Precambrian unconformity structure map presented in the previous section (Fig. 52), efforts to investigate CO_2-CCS options in eastern Ohio include evaluating and creating structure maps of other key, shallower geologic formations, including the Silurian Dayton Formation ("Packer Shell"), the Middle Devonian Onondaga Limestone ("Big Lime"), and the Upper Devonian Berea Sandstone. Though this project is focusing on sub-Knox saline reservoirs for CCS targets, in addition to the Silurian "Clinton" oil and gas fields for CCUS or CO_2-EOR, structural mapping of the Dayton, the Onondaga, and the Berea have been performed. These tops were chosen for mapping because these units have been penetrated by a large number of oil and gas wells and these formation tops are easy to identify by drillers. Since they have been extensively drilled, there are large data sets available containing formation tops, useful for detailed mapping applications. As detailed in "Formation Groups" section (p. 14–15), much of the tops data are derived from drillers' completion cards. Figure 53 highlights these three formations in the Silurian–Devonian stratigraphic column for Ohio.

Very few localized structural trends are identifiable on a wide variety of previously created maps for any or all of Ohio. The added data density provided by drillers' tops for these three formations provide sufficient detail to discern what may be significant structural features. Mapping to date indicates that at least some of these structural features project downward across at least portions of the Paleozoic rock column and are founded in the Precambrian. Previously, Mason (1999) mapped the Onondaga Limestone using GeoGraphix® and high well density. In his work, Mason (1999) was able to detect and delineate several lineaments during mapping. However, he was unable to demonstrate if these lineaments had significant vertical extents (i.e., if they carried downward in section as subsurface vertical or near vertical planes).

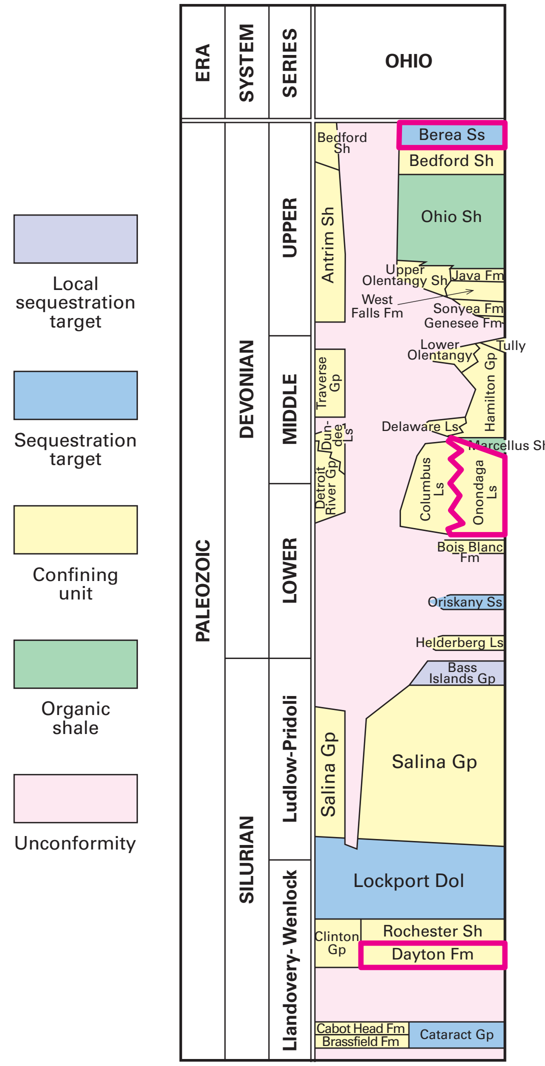

FIGURE 53.—Formation structure maps kriged for this study include: the Dayton Formation, Onondaga Limestone, and Berea Sandstone (outlined in red).

In an effort to better identify localized trends and develop a more 3D structural framework for Ohio, all available drillers' and geologists' tops were used to contour these subsurface horizons for this project. The surfaces that were contoured were selected based on data density provided by more than 50,000 wells per map. Figure 54 is the structure map of the Silurian Dayton Formation ("Packer Shell") created during this effort. Figure 55 shows the Middle Devonian Onondaga Limestone ("Big Lime") structure map. Figure 56 shows the Upper Devonian Berea Sandstone structure map. Appendix H provides a comprehensive summary of the work performed and interpretations based on these mapped results, however summary results are presented here.

Dayton Formation

The Dayton Formation structure map (Fig. 54) shows several continuous northwest–southeast sub-parallel trends. Smaller east–west trends also are evident (Tuscarawas County and south). Several of the identified trends closely approximate faults mapped by Baranoski (2002), such as the Starr Fault System, Cambridge Cross Strike Structural Discontinuity, Highlandtown Fault, Akron-Suffield Fault System, and Middleburg Fault, suggesting these basement faults may prorogate upward well into the Paleozoic section. A large structural low in east-central Mahoning County is defined by one well.

Onondaga Limestone

The Onondaga Limestone has approximately the same data density as the Dayton Formation, but a better distribution of data (Fig. H-2). The resulting surface (Fig. 55) shows many trends coincident with basement faults as with the Dayton Formation (Figs. 52 and 54). Furthermore, many of the new proposed trends identified on the Dayton Formation surface are evident on the Onondaga Limestone surface. The proposed trends may project vertically approximately 1,600 ft through the Paleozoic section, suggesting that near-vertical planes project through the stratigraphic section between the Dayton and the Onondaga.

Berea Sandstone

The Berea Sandstone had the best data density and distribution of the three mapped formations (Fig. H-3). Trends evident on the Dayton Limestone and Onondaga Limestone are also visible on the surface of the Berea Sandstone (Fig. 56). These trends are located coincidently on each respective structure map implying that vertical plains or features may project through approximately 7,000 ft of Paleozoic section.

Results

The proposed trends or lineaments for each of the produced maps are not structurally diagnostic by themselves. However, many of the proposed trends are coincident to these three horizons, indicating that these proposed trends describe transecting near-vertical planes in the subsurface. At this time, the precise nature and location of each trend is unknown. The preliminary trends identified (Fig. 57) serve as areas meriting further investigation.

SUMMARY OF PROJECT RESULTS

As part of a collaborative effort between the ODNR Division of Geological Survey and Battelle, this report summarizes geologic research conducted during the first step of a three-step program to better define sequestration options in eastern Ohio and the UORV. The ultimate goal of the program is to explore for, identify, and characterize appropriate geologic settings, locales, and formation targets for CCS and CCUS. To that end, this initial step focused on identifying, reviewing, organizing, and mapping all available geologic data pertinent to the overall effort.

Significant results of this project include:

(1) Generation of an extensive amount of geologic data retrieval, review, and organization, much of which was poorly indexed and catalogued and previously inaccessible to the public.
(2) Addition of new geologic data from four piggyback wells drilled during this project and a previous stratigraphic test penetrating deep Cambrian sequestration targets.
(3) Acquisition of 280 mi of regional 2D seismic reflection data.
(4) Creation of three new detailed regional structure maps and four cross sections.
(5) Evaluation of CO_2-EOR potential in the East Canton oil field.
(6) Preliminary identification of six potential CO_2 reservoirs, three locally potential CO_2 reservoirs, thirteen confining units and three major intervals of organic shale.

A comprehensive digital database and location maps were generated from a thorough inventory of all pertinent geologic information, which included data for over 250,000 oil and gas wells; cuttings from 5,066 wells; 74,400 suites of borehole geophysical logs; 845 cores; 203 Class I and Class II injection wells; 569 brine geochemistry data points; bottom-hole temperature datasets from 488 wells; and 555 mi of public domain seismic data. These datasets and accompanying maps are necessary to evaluate sequestration potential and also to identify geographic areas where additional geologic data is needed. Piggyback wells drilled during this project, in collaboration with Battelle, provided new data from advanced wireline logging suites, flow meter tests, pressure falloff tests, and brine injection tests that were incorporated into this and the complementary Battelle reports. The Ohio Geological Survey CO_2 No. 1 well stratigraphic test, drilled to the Precambrian in Tuscarawas County, also provided valuable data used in maps and cross sections generated in these reports. Preliminary interpretations of newly acquired seismic reflection data has greatly assisted in developing the regional geologic framework. New regional structure maps, which used over 50,000 well control points, were created on the top of the Berea Sandstone, top of the Onondaga Limestone, and top of the Dayton Formation. These detailed maps identified trends that are coincident on all three mapped layers and will be used in developing a 3D structural model of the subsurface. The 80-ton cyclic-CO_2 test in Stark County was the first in the state and demonstrated that the “Clinton” sandstone would accept significant volumes of CO_2 and subsequently mobilize and produce additional oil through secondary recovery. This successful test has sequestration and secondary oil recovery implications for not only the entire East Canton oil field but for other “Clinton” fields and reservoirs throughout eastern Ohio and the UORV.

The data collected during this study and summarized in this report—coupled with previous and forthcoming piggyback, seismic, and other new data gained during step 2 of this three-step program—will lead to updated interpretations that will supersede the maps and cross sections presented herein and

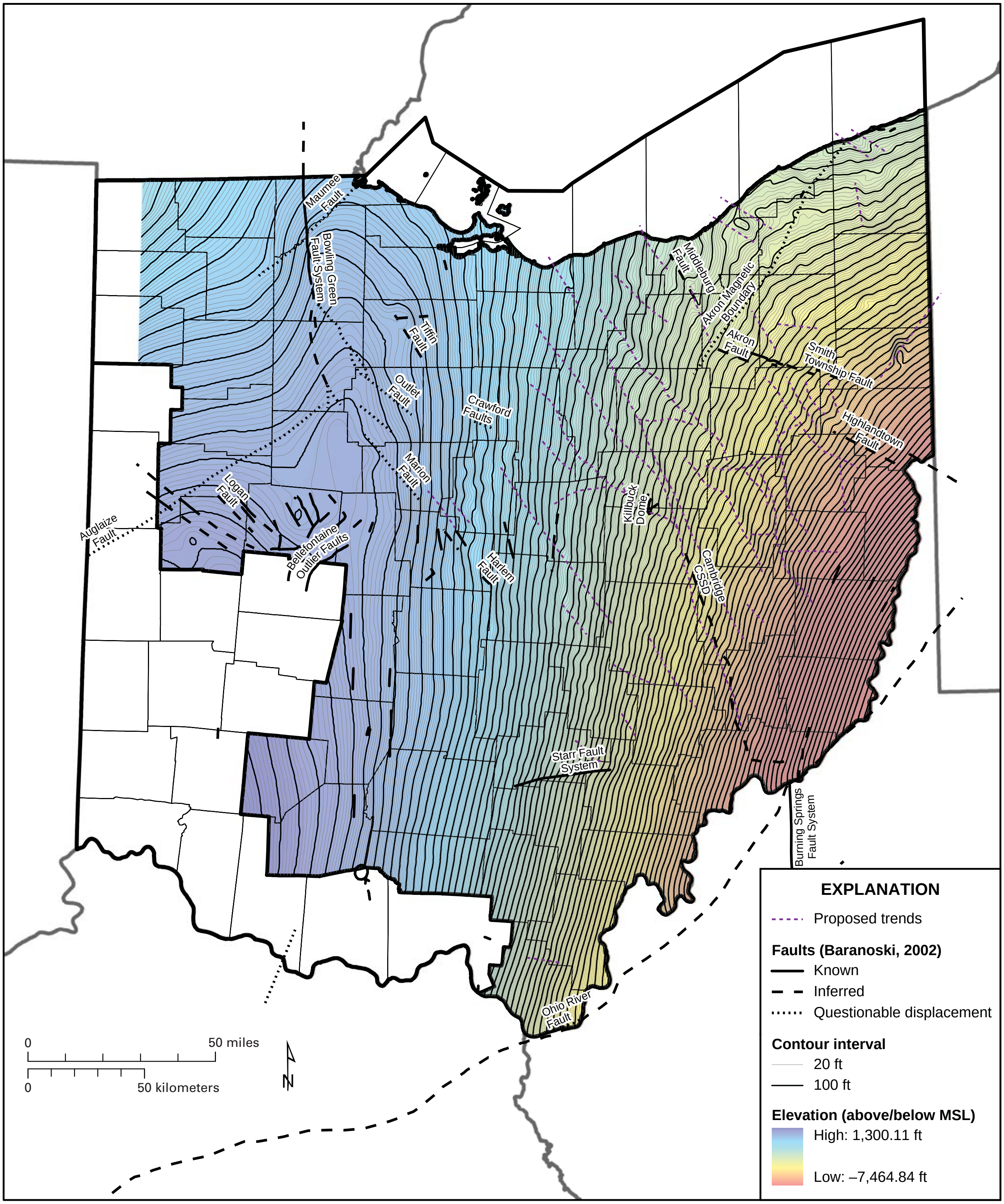

FIGURE 54.—Composite surface of the Dayton Formation. Proposed trends are delineated by consistent deflections of strike along the Dayton surface.

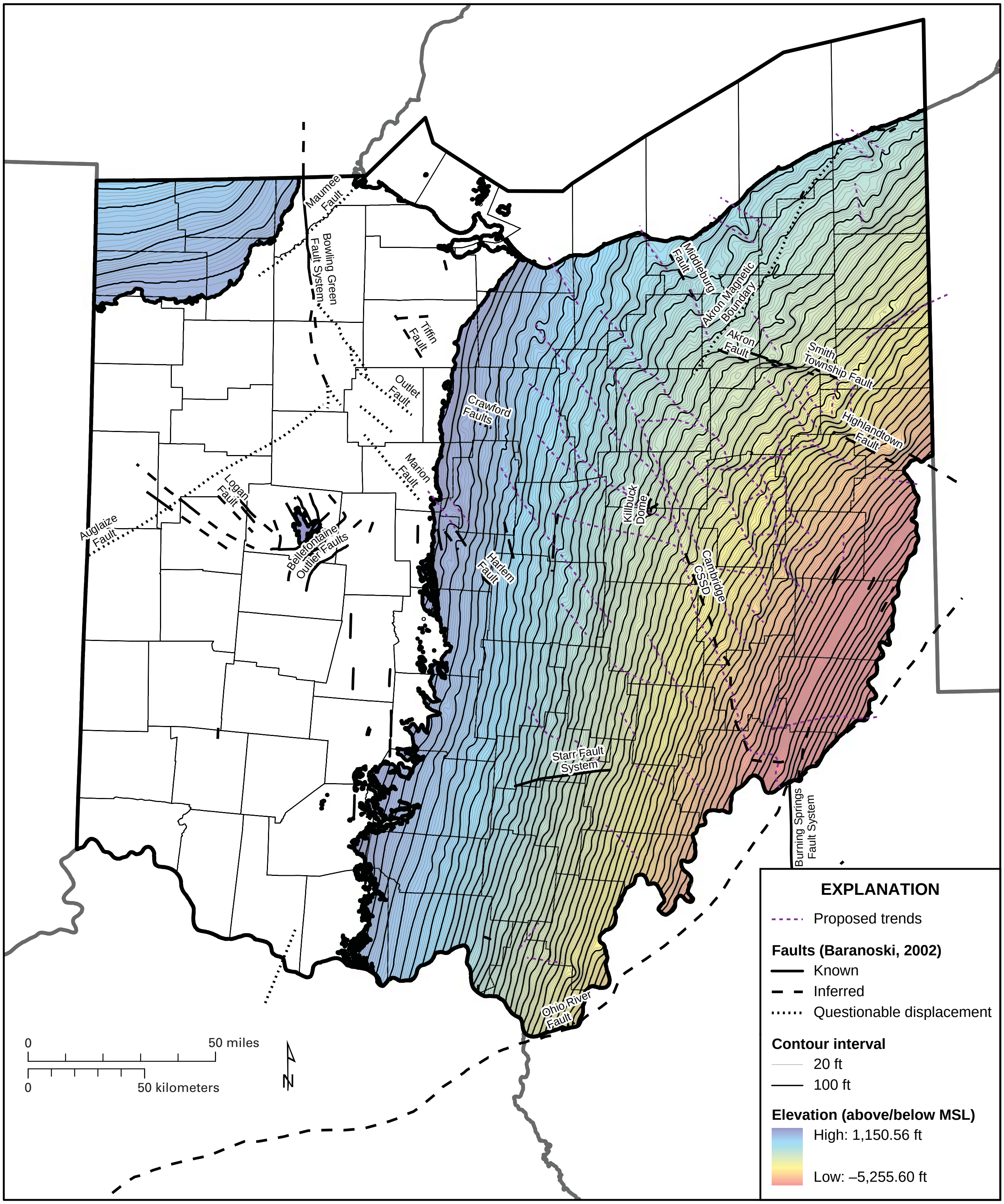

FIGURE 55.—Final hand-edited surface of the Onondaga Limestone. Proposed trends are delineated by consistent deflections of strike along the Onondaga Limestone. Many of the proposed trends evident on the Onondaga surface are evident on the Dayton surface as well.

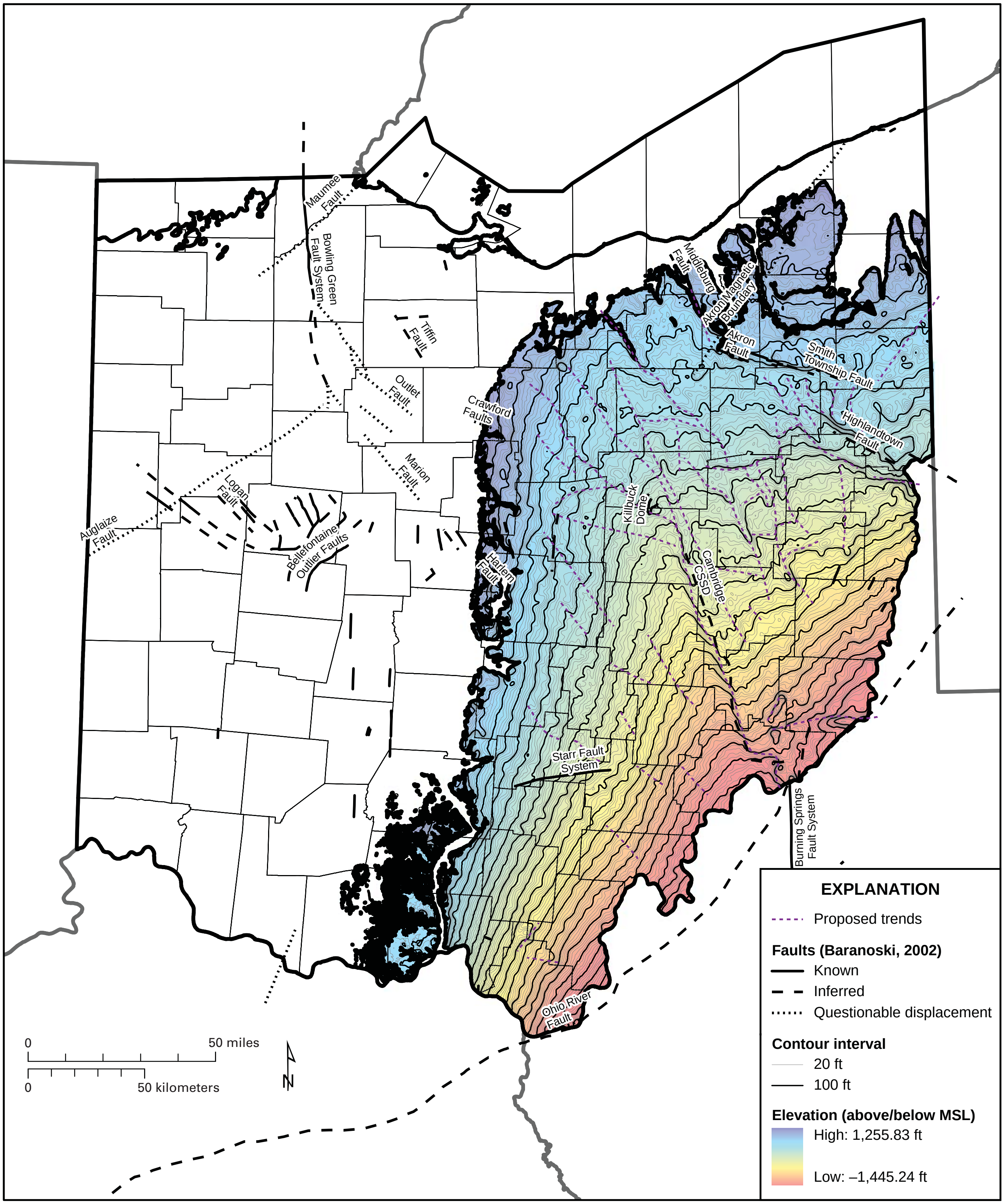

FIGURE 56.—Final surface of the Berea Sandstone. Proposed trends are delineated by consistent deflections of strike along the Berea Sandstone. Many of the proposed trends evident on the Berea surface are evident on the Onondaga and Dayton surfaces as well, suggesting the trends are continuous.

FIGURE 57.—Line map of all trends evident on the surfaces of the Dayton Formation, Onondaga Limestone, and Berea Sandstone; coincident lineaments on multiple surfaces imply a structural plane.

in Battelle's complementary report. Interpretations in both reports represent existing knowledge and identify promising locations and geologic formations thought to be most suitable to implement CCS and CO_2-EOR initiatives. More information can be gleaned from existing data combined with new data and testing as we work to characterize eastern Ohio geology to effectively sequester CO_2, enhance the value of our coal reserves, and enhance oil and gas production within the state.

REFERENCES CITED

Alpay, A.O., 1973, Application of aerial photographic interpretation to the study of reservoir natural fracture systems: Journal of Petroleum Technology, p. 37–45.

Ammerman, M.L., and Keller, G.R., 1979, Delineation of the Rome trough in eastern Kentucky by gravity and deep drilling data: Tulsa, Okla., AAPG Bulletin, v. 63, no. 3, p. 341–353.

Asquith, G.B., 1982, Basic well log analysis for geologists: American Association of Petroleum Geologists, Methods in Exploration Series, 216 p.

Babcock, L.E., 1994, Biostratigraphic significance and paleogeographic implications of Cambrian fossils from a deep core, Warren County, Ohio: Journal of Paleontology, v. 68, p. 24–30.

Bachu, S., and Adams, J.J., 2003, Sequestration of CO_2 in geological media in response to climate change: capacity of deep saline aquifers to sequester CO_2 in solution: Energy Conversion and Management, v. 44, p. 3,151–3,175.

Baranoski, M.T., 2002, Structure contour map on the Precambrian unconformity surface in Ohio and related basement features: Columbus, Ohio Department of Natural Resources, Division of Geological Survey Map PG-23, scale 1:500,000, 18 p. text.

Baranoski, M.T., and Riley, R.A., 1987, Analysis of stratigraphic and production relationships of Devonian shale gas reservoirs in Ohio: Columbus, Ohio Department of Natural Resources, Division of Geological Survey annual report for Gas Research Institute, 58 p.

Barton, G.J., Burruss, R.C., and Ryder, R.T., 1998, Water quality in the vicinity of Mosquito Creek Lake, Trumbull County, Ohio, in relation to the chemistry of locally occurring oil, natural gas, and brine: U.S. Geological Survey Water-Resources Investigation Report 98-4180, 46 p.

Battelle, 2008, The Ohio River Valley CO_2 storage project, AEP Mountaineer Plant, West Virginia numerical simulation and risk assessment report, final topical report prepared for U.S. Department of Energy, National Energy Technology Laboratory Cooperative Agreement DE-AC26-98FT40418: Columbus, Battelle, 105 p.

Battelle, 2011, Appalachian Basin—R.E. Burger Plant geologic CO_2 sequestration field test, final report prepared for the U.S. Department of Energy, National Energy Technology Laboratory Cooperative Agreement DE-FC26-05NT42589: Columbus, Battelle, 302 p., last accessed at <http://www.netl.doe.gov/technologies/carbon_seq/infrastructure/rcsp/mrcsp/appbasinsitereport_final_10411.pdf>.

Beardsley, R.W., and Cable, M.S., 1983, Overview of the evolution of the Appalachian Basin: Northeastern Geology, v. 5, nos. 3 and 4, p. 137–145.

Beardsmore, G.R., and Cull, J.P., 2001, Crustal heat flow—A guide to measurement and modeling: Cambridge University Press, 324 p.

Bentham, M., and Kirby, G., 2005, CO_2 Storage in Saline Aquifers: Oil & Gas Science and Technology – Rev. IFP, v. 60, no. 3, p. 559–567.

Blakely, R.J., 1996, Potential theory in gravity and magnetic applications: Cambridge University Press, 441 p.

Bownocker, J.A., 1906, Salt deposits and the salt industry in Ohio: Columbus, Ohio Geological Survey, Fourth Series, Bulletin 8, 42 p.

Breen, K.J., Angelo, C.G., Masters, R.W., and Sedam, A.C., 1985, Chemical and isotopic characteristics of brines from three oil- and gas-producing sandstones in eastern Ohio, with applications to the geochemical tracing of brine sources: U.S. Geological Survey Water-Resources Investigations Report 84-4314, 58 p.

Brett, C.E., Goodman, W.M., and LoDuca, S.T., 1990, Sequence stratigraphy of the type Niagaran Series (Silurian) of western New York and Ontario, *in* Lash, G.G., ed., Annual Meeting of the New York State Geological Association, 62nd, Fredonia, N.Y., 1990: New York State Geological Association, Guidebook 62, p. C1–71.

Bullard, E.W., 1965, Historical introduction to terrestrial heat flow, *in* Lee, W.H.K., ed., Terrestrial heat flow: Washington, D.C., American Geophysical Union Geophysical Monograph Series, v. 8, p. 1–6.

Carslaw, H.S., and Jaeger, J.C., 1959, Conduction of heat in solids: London, Oxford University Press, 510 p.

Castle, J.W., 1998, Regional Sedimentology and stratal surfaces of a Lower Silurian clastic wedge in the Appalachian foreland basin: Journal of Sedimentary Research, v. 68, no. 6, p. 1201–1211.

Castle, J.W., and Byrnes, A.P., 2005, Petrophysics of Lower Silurian sandstones and integration with the tectonic-stratigraphic framework, Appalachian basin, United States: Tulsa, Okla., AAPG Bulletin, v. 89, no. 1, p. 41–60.

Clifford, M.J., 1975, Subsurface liquid-waste injection in Ohio: Columbus, Ohio Department of Natural Resources, Division of Geological Survey Information Circular 43, 27 p.

Collins, R.J., and others, 1974, An evaluation of the suitability of ERTS data for the purpose of petroleum exploration, *in* Freden, S.C., Mercanti, E.P., and Becker, M.A., eds., Third Earth Resources Technology Satellite-1 Symposium, Volume I: Technical Presentations, Section A, December 10–14, 1973, Washington, D.C., [Proceedings]: Washington, D.C., National Aeronautics and Space Administration, Scientific and Technical Information Office, NASA SP-351, p. 809–822.

Conrey, G.W., 1921, The geology of Wayne County: Columbus, Ohio Geological Survey, Fourth Series, Bulletin 24, 155 p.

Culshaw, N., and Dostal, J., 2002, Amphibolites of the Shawanaga domain, Central Gneiss Belt, Grenville Province, Ontario—Tectonic setting and implications for relations between the Central Gneiss Belt and Midcontinental USA: Precambrian Research, v. 113, p. 65–85.

Dennison, J.M., and Head, J.W., 1975, Sea level variations interpreted from the Appalachian basin Silurian and Devonian: American Journal of Science, v. 275, p. 1089–1120.

Drahovzal, J., and others, 1974, Significance of selected lineaments in Alabama, *in* Freden, S.C., Mercanti, E.P., and Becker, M.A., eds., Third Earth Resources Technology Satellite-1 Symposium, Volume I: Technical Presentations, Section A, December 10–14, 1973, Washington, D.C., [Proceedings]: Washington, D.C., National Aeronautics and Space Administration, Scientific and Technical Information Office, NASA SP-351, p. 897–910.

Eble, C.F., Nuttall, B.C., Greb, S.F., and Bustin, R.M., 2010, Petrography and geochemistry of the Devonian Ohio Shale from a drill core in eastern Kentucky—Implications for potential CO_2 sequestration and enhanced methane production [abs.], *in* GSA Annual Meeting, Oct. 31–Nov. 4, 2010, Denver, Colo. [Proceedings]: Geological Society of America, <https://gsa.confex.com/gsa/2010AM/finalprogram/abstract_181399.htm>.

Energy Information Administration (EIA), 2012, Coal production and coalbed thickness by major coalbeds and mine types, 2003: Washington, D.C., U.S. Department of Energy, 2003 Annual Report, <www.eia.gov/cneaf/coal/page/acr/tabl5.html>.

Erenpreiss, M.S., Wickstrom, L.H., Perry, C.J., Riley, R.A., Martin, D.R., and others, 2011, Regional organic-thickness map of the Marcellus Shale with additional organic-rich shale beds in the Hamilton Group included for New York, Pennsylvania, and West Virginia: Columbus, Ohio Department of Natural Resources, Division of Geological Survey, scale 1 inch equals 52 mi.

Gale, J., and Freund, P., 2001, Coal-bed methane enhancement with CO_2 sequestration worldwide potential: Environmental Geosciences, v. 8, no. 3, p. 210–217.

Gao, D., Shumaker, R.C., and Wilson, T.H., 2000, Along-axis segmentation and growth history of the Rome Trough in the Central Appalachian Basin: Tulsa, Okla., AAPG Bulletin, v. 84, no. 1, p. 75–99.

Gray, J.D., Struble, R.A., Carlton, R.W., Hodges, D.A., Honeycutt, F.M., Kingsbury, R.H., Knapp, N.F., Majchszak, F.L., and Stith, D.A., 1982, An integrated study of the Devonian-age black shales in eastern Ohio—Ohio Geological Survey final report for U.S. Department of Energy Eastern Gas Shales Project: U.S. Department of Energy, Technical Information Center Report No. DOE/ET/12131-1399, 257 p., accessible at <http://www.osti.gov/bridge/purl.cover.jsp?purl=/5841004>.

Greb, S.F., Eble, C.F., Slucher, E.R., Carter, K.M., and Avary, K.L., 2010, Storing and using CO_2 for enhanced coalbed methane recovery in unmineable coal beds of the northern Appalachian Basin and parts of the central Appalachian Basin—MRCSP phase II topical report for DOE cooperative agreement No. DE-FC26-05NT42589: Battelle/Midwest Regional Carbon Sequestration Partnership, 41 p., accessible at <http://216.109.210.162/userdata/phase_II_reports/topical_5_coalbed_methane.pdf>.

Greb, S.F., Sparks, T., Barnes, D., Harrison, W., III, Medina, C., Rupp, J., Baranoski, M., Riley, R., Solis, M., Perry, C., Lewis, E., Carter, K., and Harper, J., 2012, MRCSP regional geologic cross section and correlation chart: Columbus, Ohio Department of Natural Resources, Division of Geological Survey, poster (1 sheet), accessible at <http://www.dnr.state.oh.us/portals/10/pdf/Posters/NETL2012_Greb.pdf>.

Harris, L.D., 1978, The eastern interior aulacogen and its relation to Devonian shale gas production, *in* Preprints for Second Eastern Gas Shales Symposium: U.S. Department of Energy, Morgantown Energy Technology Center, METC/SP-78/6, v. 1, p. 55–72.

Hettinger, R.D., 2001, Subsurface correlations and sequence stratigraphic interpretations of Lower Silurian strata in the Appalachian Basin of northeast Ohio, southwest New York, and northwest Pennsylvania: U.S. Geological Survey Geologic Investigations Series I-274, 22 p., 1 pl.

Humphreys, M., and Watson, A., 1996, Play Osp—Middle Ordovician St. Peter Sandstone, *in* Roen, J.B. and Walker, B.J., eds., The atlas of major Appalachian gas plays: West Virginia Geological and Economic Survey Publication V-25, p. 177–180.

Jacobi, R.D., Loewenstein, S., Martin, J., and Smith, G., 2000, Magnetic, gravity, and LANDSAT lineaments in the Appalachian Basin, New York State: Groundtruth, faults, and traps, [abs.]: American Association of Petroleum Geologists Search and Discovery Article #90907, accessed at <http://www.searchanddiscovery.com/abstracts/html/2000/eastern/abstracts/029.htm?q=%2BtitleStrip%3Alineaments#hit0#hit0>.

Jackson, J.A., ed., 1997, Glossary of geology (4th ed.): Alexandria, Va., American Geological Institute, p. 83.

Janssens, A., 1973, Stratigraphy of the Cambrian and Lower Ordovician rocks in Ohio: Columbus, Ohio Department of Natural Resources, Division of Geological Survey Bulletin 64, 197 p.

Kellog, O.D., 1953, Foundations of potential theory: New York, Dover Publications, 384 p.

King, E.R., and Zietz, I., 1978, The New York-Alabama Lineament—Geophysical evidence for a major crustal break in the basement beneath the Appalachian basin: Geology, v. 6, no. 5, p. 312–318.

Knight, W.V., 1969, Historical and economic geology of Lower Silurian Clinton Sandstone of northeastern Ohio: American Association of Petroleum Geologists Bulletin, v. 53, no. 7, p. 1421–1452.

Komar, C.A., Overbey, W.K., Jr., Rough, R.L., and Lambert, W.G., 1971, Factors that predict fracture-orientation in a gas storage reservoir: Journal of Petroleum Technology, v. 23, no. 5, p. 37–45.

Koottungal, L., 2012, Survey: Miscible CO_2 now eclipses steam in U.S. EOR production: Oil and Gas Journal, April 2, 2012, p. 56–69.

Lamborn, R.E., 1952, Additional analyses of brines from Ohio: Columbus, Ohio Department of Natural Resources, Division of Geological Survey Report of Investigations 11, 56 p.

Law, D.H-S., and Bachu, S., 1996, Hydrogeological and numerical analysis of CO_2 disposal in deep aquifers in the Alberta sedimentary basin: Energy Conversion and Management, v. 37, p. 1,167–1,174.

Leahy, J.N., 1996, Abandoned Alpha Portland Cement Company mine facility site, Ironton, Ohio—A groundwater flow and brine migration analysis: Cincinnati, Ohio, University of Cincinnati, M.S. Thesis, 246 p.

Lowry, R.M., 1986, Origin and evolution of brines from the “Clinton” sandstone, eastern Ohio: Columbus, Ohio State University, M.S. Thesis, 149 p.

Mason, G., 1999, Structurally related migration of hydrocarbons in the central Appalachian Basin of eastern Ohio, *in* Into the new millennium: The changing face of exploration in the Knox play, Proceedings from the Sixth Annual Fall Symposium, October 1999, Akron, Ohio: Columbus, Ohio Geological Society, p. 20–33.

McGuire, W.H., and Howell, P., 1963, Oil and gas possibilities of the Cambrian and Lower Ordovician in Kentucky: Lexington, Ky., Spindletop Research Center, 216 p.

Mills, R.V.A., and Wells, R.C., 1919, The evaporation and concentration of waters associated with petroleum and natural gas: U.S. Geological Survey Bulletin 693, 104 p.

Nettleton, L.L., 1971, Elementary gravity and magnetics for geologists and seismologists: Society of Exploration Geologists, Monograph Series, v. 1, 121 p.

Newell, D.L., Kaszuba J.P., Viswanathan, H.S., Pawar, R.J., and Carpenter, Thomas, 2008, Significance of carbonate buffers in natural waters reacting with supercritical CO_2—Implications for monitoring, measuring and verification (MMV) of geologic carbon sequestration: Geophysical Research Letters, v. 35, L23403, 5 p.

Noger, M.C., Meglen, J.F., Humphreys, M., and Baranoski, M.T., 1996, Upper Silurian Lockport Dolomite–Keefer (Big Six) sandstone, *in* Roen, J.B., and Walker, B.J., eds., The atlas of major Appalachian gas plays: West Virginia Geological and Economic Survey publication V-25, p. 145–150.

Nuttall, B.C., Drahovzal, J.A., Eble, C.F., and Bustin, R.M., 2005, Analysis of the Devonian black shale in Kentucky for potential carbon dioxide sequestration and enhanced natural gas production, quarterly report: Kentucky Geological Survey, report of research in progress, 83 p. <http://www.uky.edu/KGS/emsweb/devsh/quarterly.pdf>.

Ohio Division of Geological Survey, 1990 (rev. 2000, 2004), Generalized column of bedrock units in Ohio: Ohio Department of Natural Resources, Division of Geological Survey, 1 p.

Ohio Revised Code (ORC), 2000, 1509.01 Division of Oil and Gas Resources Management - oil and gas definitions, *in* Title [15] XV Conservation of Natural Resources: State of Ohio Legislature, Ohio Revised Code, accessed at <http://codes.ohio.gov/orc/1509.01>.

Ohio River Valley Water Sanitation Commission, 1976, Evaluation of the Ohio Valley Region basal sandstone as a wastewater injection interval: Ohio River Valley Water Sanitation Commission, 30 p.

Orton, Edward, 1888, The Trenton Limestone as a source of oil and gas in Ohio, chap. 3 *of* Report of the Geological Survey of Ohio, v. 6—Economic geology: Columbus, [State of Ohio Legislature], vol. 6, p. 101–310.

Overbey, W.K., Jr., and Henniger, B.R., 1971, History, development, and geology of oil fields in Hocking and Perry Counties, Ohio: American Association of Petroleum Geologists Bulletin, v. 55, no. 2, p. 183–203.

Parris, T.M., Webb, D.J., Takacs, K.G., and Fedorchuk, N., 2010, Geochemical characterization of formation waters in Kentucky and implication for geologic carbon storage, *in* Parris, T.M., Greb, S.F., and Nuttall, B.C., eds., Evaluation of geologic CO_2 sequestration potential and CO_2 enhanced oil recovery in Kentucky: Kentucky Geological Survey Report of Investigation 21, p. 37–55.

Pashin, J.C., Carroll, R.E., Groshong Jr., R.H., Raymond, D.E., McIntyre, M.R., and Payton, W.J., 2003, Geologic screening criteria for sequestration of CO_2 in coal: quantifying potential of the Black Warrior coalbed methane fairway, Alabama: Annual Technical Progress Report, U.S. Department of Energy, National Energy Technology Laboratory, contract DE-FC-00NT40927, 190 p.

Patchen, D.G., Hickman, J.B., Harris, D.C., Drahovzal, J.A., Lake, P.D., Smith, L.B., Nyahay, R., Schulze, R., Riley, R.A., Baranoski, M.T., Wickstrom, L.H., Laughrey, C.D., Kostelnik, J., Harper, J.A., Avary, K.L., Bocan, J., Hohn, M.E., and McDowell, R., 2006, A geologic play book for Trenton-Black River Appalachian Basin exploration: Morgantown, W. Va., U.S. Department of Energy Report, DOE Award Number DE-FC26-03NT41856, 601p., accessible at <http://www.wvgs.wvnet.edu/www/tbr/project_reports.asp>.

Pepper, J.F., de Witt, Wallace, Jr., and Everhart, G.M., 1953, The "Clinton" sands of Early Silurian age in Canton, Dover, Massillon, and Navarre quadrangles: U.S. Geological Survey Bulletin 1003-A, 13 p.

Perry, C.J., Erenpreiss, M.S., Riley, R.R., Wickstrom, L.H., 2012, Geologic data mining, analysis, and mapping to identify prospective disposal zones in eastern Ohio [abs]: AAPG Eastern Section Meeting, September 22–26, 2012, Cleveland, Ohio, Abstracts with Program, p. 52.

Ransome, F.L., 1913, Contributions to economic geology, 1911, Part I, Metals and nonmetals except fuels—Copper; Lead and Zinc: U.S. Geological Survey Bulletin 530-B, 400 p.

Reichle, D., and 19 others, 1999, Carbon Sequestration Research and Development: Washington, D.C., U.S. Department of Energy, Offices of Science and Fossil Energy, 1999, 289 p. <http://www.osti.gov/energycitations/servlets/purl/810722-9s7bTP/native/810722.PDF>

Reznik, A., Singh, P.K., and Foley, W.L., 1982, An analysis of the effect of carbon dioxide injection on the recovery of in-situ methane from bituminous coal: An experimental simulation: Society of Petroleum Engineers/U.S. Department of Energy 10822.

Riley, R.A., Harper, J.A., Baranoski, M.T., Laughrey, C.D., and Carlton, R.W., 1993, Measuring and predicting reservoir heterogeneity in complex deposystems—The Late Cambrian Rose Run sandstone of eastern Ohio and western Pennsylvania: Morgantown, W. Va., National Research Center for Coal and Energy, Appalachian Oil and Natural Gas Research Consortium report for the U.S. Department of Energy, Contract No. DE-AC22-90BC14657, 257 p.

Riley, R.A., Baranoski, M.T., and Wickstrom, L.H., 2004, Oil and gas fields map of Ohio: Columbus, Ohio Department of Natural Resources, Division of Geological Survey Map PG-1, scale 1:500,000.

Riley, R.A., Wicks, J.L., and Perry, C.J., 2011, Silurian "Clinton" sandstone reservoir characterization for evaluation of CO_2-EOR potential in the East Canton oil field, Ohio: Columbus, Ohio Department of Natural Resources, Division of Geological Survey Open-File Report 2011-2, 31 p., 4 appendices.

Rogers, J.D., 2012, CO2 applications: Journal of Petroleum Technology, v. 64, no. 7, p. 1,635.

Root, W.J., 1888, The manufacture of salt and bromine, chap. 12 *of* Report of the Geological Survey of Ohio, v. 6—Economic geology: Columbus, [State of Ohio Legislature], vol. 6, p. 653–670.

Ryder, R.T., 1991, Stratigraphic framework of Cambrian and Ordovician rocks in the Central Appalachian basin from Richland County, Ohio, to Rockingham County, Virginia: U.S. Geological Survey Miscellaneous Investigations Series Map I-2264.

Ryder, R.T., 1992, Stratigraphic framework of Cambrian and Ordovician rocks in the Central Appalachian basin from Morrow County, Ohio, to Pendleton County, West Virginia: U.S. Geological Survey Bulletin 1839-G, 25 p., 1 pl.

Ryder, R.T., 2000, Stratigraphic framework and depositional sequences in the lower Silurian regional oil and gas accumulation, Appalachian Basin: from Jackson County, Ohio, through northwestern Pennsylvania, to Orleans County, New York: U.S. Geological Survey Geologic Investigations Series Map I-2726 (2 sheets), 8 p.

Ryder, R.T., 2004, Stratigraphic framework and depositional sequences in the lower Silurian regional oil and gas accumulation, Appalachian Basin—from Ashland County, Ohio, through southwestern Pennsylvania, to Preston County, West Virginia: U.S. Geological Survey Geologic Investigations Series Map I-2810 (2 sheets), 11 p.

Ryder, R.T., Burruss, R.C., and Hatch, J.R., 1998, Black shale source rocks and oil generation in the Cambrian and Ordovician of the central Appalachian Basin, USA: Tulsa, Okla., AAPG Bulletin, v. 82, no. 3, p. 412–441.

Ryder, R.T., Repetski, J.E., and Harris, A.G., 1996, Stratigraphic framework of Cambrian and Ordovician rocks in the central Appalachian Basin from Fayette County, Ohio, to Botetourt County, Virginia: U.S. Geological Survey Map Series I-2495, accessed at <http://pubs.usgs.gov/imap/i-2495/>.

Sanders, L.L., 1986, Geochemistry and paleotemperature of formation waters from the Lower Silurian "Clinton" formation, Eastern Ohio: Kent, Ohio, Kent State University, Ph.D. Dissertation, 141 p.

Schlumberger, 1972, Log interpretation, vol. 1—Principles: New York, Schlumberger Limited, 112 p.

Schroeder, K., Ozdemir, E., and Morsi, B.I., 2002, Sequestration of carbon dioxide in coal seams: Journal of Energy and Environmental Research, v. 2, no. 1, p. 54–63. [From U.S. Department of Energy, National Energy Technology Laboratory, First National Conference on Carbon Sequestration, 2001.]

Schumacher, G.A., Goodman, M.H., and Harrison, J.M., with GIS database administration by Wells, J.G., and GIS and cartography by Vogt, K.L., 2008, Core locations in Ohio and adjacent states: Columbus, Ohio Department of Natural Resources, Division of Geological Survey Map MG-4 [version 2.0], scale 1:500,000.

Scotese, C.R., and McKerrow, W.S., 1991, Ordovician plate tectonic reconstructions, *in* Barnes, C.R., and Williams, S.H., eds., Advances in Ordovician geology: Geological Survey of Canada Paper 90-9, p. 271–282.

Sherrif, R.E., 1982, Encyclopedic dictionary of exploration geophysics: Society of Exploration Geophysics, 266 p.

Shindel, H.S., Stewart, L.J., and Kolva, J.R., 1983, Water resources data, Ohio water year 1982—vol. 2, St. Lawrence River Basin statewide project data: U.S. Geological Survey Water-Data Report OH-82-2, p. 277–286.

Shrake, D.L., Wolfe, P.J., Richard, B.H., Swinford, E.M., Wickstrom, L.H., Potter, P.E., and Sitler, G.W., 1990, Lithologic and geophysical description of a continuously cored hole in Warren County, Ohio, including description of the Middle Run Formation (Precambrian?) and a seismic profile across the core site: Columbus, Ohio Department of Natural Resources, Division of Geological Survey Information Circular 56, 11 p.

Slucher, E.R., Swinford, E.M., Larsen, G.E., Schumacher, G.A., Shrake, D.L., Rice, C.L., Caudill, M.R., and Rea, R.G., 2006, Bedrock geologic map of Ohio: Columbus, Ohio Department of Natural Resources, Division of Geological Survey Map BG-1, scale 1:500,000.

Spane, F.A., Thorne, P.D., Gupta, N., Jagucki, P., Ramakrishnan, T.S., and Mueller, N., 2006, Results obtained from reconnaissance-level and detailed reservoir characterization methods utilized for determining hydraulic property distribution characteristics at Mountaineer AEP #1, *in* International Symposium on Site Characterization for CO_2 Geological Storage (CO2SC 2006), March 20–22, 2006, Berkeley, Calif. [Proceedings]: Lawrence Berkeley National Laboratory, p. 149–153, accessed at <http://esd.lbl.gov/CO2SC>.

Stith, D.A., and Knapp, N.F., 1989, Characterization of trace metals in Ohio brines, final report: Columbus, Ohio Department of Natural Resources, Division of Geological Survey Open-File Report 89-1, unpaginated.

Stith, D.A., Morth, A.H., and Hatch, J.R., 1979, Brine analyses, 1972–1974: Columbus, Ohio Department of Natural Resources, Division of Geological Survey Open-File Report 79-1, unpaginated.

Stout, W., and Lamborn, R.E., 1924, The geology of Columbiana County: Columbus, Ohio Geological Survey, Fourth Series, Bulletin 28, 408 p.

Stout, W., Lamborn, R.E., and Schaaf, Downs, 1932, Brines of Ohio: Columbus, Ohio Geological Survey, Fourth Series, Bulletin 37, 123 p.

Thompson, W.E., 1973, The concentration of selected elements in brines of Perry County, Ohio: Columbus, Ohio State University, M.S. Thesis, 62 p.

Trainer, F.W., 1967, Measurement of the abundance of fracture traces on aerial photographs: U.S. Geological Survey Professional Paper 575-C, p. C184–C188.

U.S. Department of Energy (US DOE), 1999, Carbon sequestration research and development: Washington, D.C., U.S. Department of Energy, Office of Fossil Energy/Office of Science, 195 p.

U.S. Department of Energy (US DOE), 2004, Carbon sequestration technology roadmap and program plan: Washington, D.C., U.S. Department of Energy, National Energy Technology Laboratory, 24 p. <www.fe.doe.gov/programs/sequestration/publications/programplans/2004/SequestrationRoadmap4-29-04.pdf>

U.S. Department of Energy (US DOE), 2005, Carbon sequestration, technology roadmap and program plan 2005: Washington, D.C., U.S. Department of Energy, National Energy Technology Laboratory, 26 p., accessed at <http://www.fe.doe.gov/programs/sequestration/publications/programplans/2005/sequestration_roadmap_2005.pdf>.

U.S. Environmental Protection Agency, 2012, Determination of Maximum Injection Pressure for Class 1 Wells, Region 5 Underground Injection control section regional guidance #7, http://www.epa.gov/region5/water/uic/r5guid/r5_07.htm

U.S. Environmental Protection Agency (USEPA), 2012, Executive Summary of Inventory of U.S. Greenhouse Gas Emissions and Sinks, 1990–2010: U.S. Environmental Protection Agency, EPA 430-R-12-001, p. ES-4, table ES-2, accessed at <http://www.epa.gov/climatechange/Downloads/ghgemissions/US-GHG-Inventory-2012-ES.pdf>.

von Frese, R.R.B., and Hinze, W.J., 1993, Geophysics, in Trigg, G.L., ed., Encyclopedia of Applied Physics, American Institute of Physics: VCH Publishers, v. 7, p. 149–195.

von Frese, R.R.B, Jones, M.B., Kim, J.W., Li, W.S., 1997, Spectral correlation of magnetic and gravity anomalies of Ohio: Geophysics, v. 62, p. 365–380.

Wagner, W.R., 1976, Growth faults in Cambrian and Lower Ordovician rocks of western Pennsylvania: Tulsa, Okla., AAPG Bulletin, v. 60, no. 3, p. 414–427.

Westrich, H., and 12 others, 2002, Sequestration of CO_2 in a depleted oil reservoir: an overview: Journal of Energy and Environmental Research, v. 2, no. 1. p. 64–74. [From U.S. Department of Energy, National Energy Technology Laboratory, First National Conference on Carbon Sequestration, 2001.]

Wicks, J.L., Riley, R.A., Melzer, S., and Perry, C.J., 2009, Results of the Sickafoose-Morris cyclic CO_2 test, East Canton Oil Field, Ohio—Final report prepared for U.S. DOE Cooperative Agreement No. DE-NT0005115: Columbus, Ohio Department of Natural Resources, Division of Geological Survey, 16 p., 8 appendices.

Wickstrom, L.H., and 28 others, 2005, Characterization of geologic sequestration opportunities in the MRCSP region: prepared for DOE cooperative agreement No. DE-PS26-05NT42255, 152 p., 1 appendix.

Wickstrom, L.H., Riley, R.A., Spane, F.A., McDonald, James, Slucher, E.R., Zody, S.P., Wells, J.G., and Howat, E., 2011, Geologic assessment of the Ohio Geological Survey CO_2 No. 1 well in Tuscarawas County and surrounding vicinity: Columbus, Ohio Department of Natural Resources, Division of Geological Survey Open-File Report 2011-3, 82 p., 5 appendices.

Wilk, G.B., 1987, Interpretation and geochemical analysis of "Clinton" brines from Mahoning County, Ohio: Akron, Ohio, University of Akron, M.S. Thesis, 73 p.

Woodward, H.P., 1961, Preliminary subsurface study of southeastern Appalachian interior plateau: Tulsa, Okla., AAPG Bulletin, v. 45, no. 10, p. 1634–1655.

Yam, H., and Schmitt, D.R., CO_2 rock physics—A Laboratory Study [abs], in Road to Recovery—2011 CSPG CSEG CWLS Conference [proceedings]: Canadian Society of Petroleum Geologists, 7 p., accessible at <http://www.cspg.org/documents/Conventions/Archives/Annual/2011/050-CO_2_Rock_Physics.pdf>.

APPENDIX A

List of Class I (hazardous and industrial-waste injection) wells and Class II (oil-and-gas brine or enhanced recovery injection) wells with injection formations

Ron Riley—Ohio Geological Survey, Columbus, Ohio

Includes formal, informal, drillers, and obsolete terms from RBDMS

API_WELLNO	Class	Injection FM_Top	Injection FM_Base	Informal Formation Grouping
34003636910000	Class I	ECLR	MDLR	Precambrian/Cambrian preKnox
34007600100000	Class I	KNOX	PCMB	Precambrian/Cambrian preKnox
34017200040000	Class I	ECLR	MDLR	Precambrian/Cambrian preKnox
34085201420000	Class I	CNSG	PCMB	Precambrian/Cambrian preKnox
34035207440000	Class I	ORSK	ORSK	Silurian-Devonian “Big Lime”
34139204480000	Class I	CNSG	PCMB	Precambrian/Cambrian preKnox
34143202100000	Class I	KNOX	PCMB	Precambrian/Cambrian preKnox
34145202120000	Class I	CNSG	PCMB	Precambrian/Cambrian preKnox
34005211550000	Class II	BERE	BERE	Berea
34007200950000	Class II	NWBG	CLNN	Silurian-Devonian “Big Lime”
34007203570000	Class II	NWBG	CLNN	Silurian-Devonian “Big Lime”
34007203600000	Class II	NWBG	NWBG	Silurian-Devonian “Big Lime”
34007208660000	Class II	BILDF	BILDF	Silurian-Devonian “Big Lime”
34007209190000	Class II	NWBG	CLNN	Silurian-Devonian “Big Lime”
34007212930000	Class II	NWBG	NWBG	Silurian-Devonian “Big Lime”
34007216730000	Class II	LCKP	LCKP	Silurian-Devonian “Big Lime”
34007220380000	Class II	RSRN	RSRN	Cambrian-Ordovician Knox
34007230970000	Class II	NWBG	NWBG	Silurian-Devonian “Big Lime”
34007231920000	Class II	MNSM	MNSM	Precambrian/Cambrian preKnox
34007232620000	Class II	NWBG	NWBG	Silurian-Devonian “Big Lime”
34007236920000	Class II	NWBG	NWBG	Silurian-Devonian “Big Lime”
34007243550000	Class II	NWBG	RSRN	Silurian-Devonian “Big Lime”
34009218920000	Class II	MDIN	MDIN	Silurian “Clinton/Medina”
34009218990000	Class II	OHIO	NWBG	Devonian shale and siltstones
34009223210000	Class II	BERE2	BERE2	Berea
34009224020000	Class II	BERE	BERE	Berea
34009227040000	Class II	ORSK	ORSK	Silurian-Devonian “Big Lime”
34009229330000	Class II	CLNN	CLNN	Silurian “Clinton/Medina”
34009230360000	Class II	NWBG	NWBG	Silurian-Devonian “Big Lime”
34009234800000	Class II	OHIO	OHIO	Devonian shale and siltstones
34013206110000	Class II	BKMN	MNSM	Cambrian-Ordovician Knox
34019203260000	Class II	CLNN	CLNN	Silurian “Clinton/Medina”
34019207900000	Class II	BERE	BERE	Berea
34029208720000	Class II	CLNN	CLNN	Silurian “Clinton/Medina”
34031216650000	Class II	BERE	BERE	Berea
34031220410000	Class II	NWBG	NWBG	Silurian-Devonian “Big Lime”
34031232770000	Class II	NWBG	NWBG	Silurian-Devonian “Big Lime”
34031233530000	Class II	CLNN	CLNN	Silurian “Clinton/Medina”
34031241780000	Class II	NWBG	NWBG	Silurian-Devonian “Big Lime”
34035203310000	Class II	NWBG	NWBG	Silurian-Devonian “Big Lime”
34041201600000	Class II	GLRV	GLRV	Ordovician shale and Trenton-Black River
34041202750000	Class II	TMPL	TMPL	Cambrian-Ordovician Knox
34041203390000	Class II	MNSM	MNSM	Precambrian/Cambrian preKnox
34043200430000	Class II	BBLC	BBLC	Silurian-Devonian “Big Lime”
34043200790000	Class II	KRSK	KRSK	Precambrian/Cambrian preKnox
34051200920000	Class II	NGRN	NGRN	Silurian-Devonian “Big Lime”
34053209680000	Class II	OHIO	OHIO	Devonian shale and siltstones
34053209740000	Class II	CLNN	CLNN	Silurian “Clinton/Medina”
34055207730000	Class II	NWBG	NWBG	Silurian-Devonian “Big Lime”
34055210590000	Class II	NWBG	NWBG	Silurian-Devonian “Big Lime”
34059209650000	Class II	CLNN	CLNN	Silurian “Clinton/Medina”
34059222920000	Class II	CLNN	CLNN	Silurian “Clinton/Medina”
34059226880000	Class II	CLNN	CLNN	Silurian “Clinton/Medina”
34059240670000	Class II	RSRN	MNSM	Cambrian-Ordovician Knox
34069201390000	Class II	MNSM	MNSM	Precambrian/Cambrian preKnox
34073209150000	Class II	CLNN	CLNN	Silurian “Clinton/Medina”
34073215430000	Class II	NWBG	NWBG	Silurian-Devonian “Big Lime”

API_WELLNO	Class	Injection FM_Top	Injection FM_Base	Informal Formation Grouping
34073219490000	Class II	CLNN	CLNN	Silurian “Clinton/Medina”
34073221610000	Class II	CLNN	CLNN	Silurian “Clinton/Medina”
34073222110000	Class II	CLNN	CLNN	Silurian “Clinton/Medina”
34075227320000	Class II	NWBG	NWBG	Silurian-Devonian “Big Lime”
34075243750000	Class II	LCKP	LCKP	Silurian-Devonian “Big Lime”
34075245270000	Class II	MNSM	MNSM	Precambrian/Cambrian preKnox
34083241950000	Class II	TMPL	TMPL	Cambrian-Ordovician Knox
34083244120000	Class II	NWBG	NWBG	Silurian-Devonian “Big Lime”
34085201860000	Class II	NWBG	NWBG	Silurian-Devonian “Big Lime”
34085202660000	Class II	ORSK	ORSK	Silurian-Devonian “Big Lime”
34085210940000	Class II	RSRN	MNSM	Cambrian-Ordovician Knox
34087204000000	Class II	CWRN	CWRN	Pennsylvanian undifferentiated
34089234060000	Class II	CLNN	CLNN	Silurian “Clinton/Medina”
34089247920000	Class II	MNSM	MNSM	Precambrian/Cambrian preKnox
34093212360000	Class II	NWBG	NWBG	Silurian-Devonian “Big Lime”
34099209030000	Class II	CLNN	CLNN	Silurian “Clinton/Medina”
34099209720000	Class II	CLNN	CLNN	Silurian “Clinton/Medina”
34099209740000	Class II	CLNN	CLNN	Silurian “Clinton/Medina”
34099212610000	Class II	BERE	BERE	Berea
34099219560000	Class II	NWBG	NWBG	Silurian-Devonian “Big Lime”
34099231270000	Class II	KNOX	MNSM	Cambrian-Ordovician Knox
34103221680000	Class II	BERE	BERE	Berea
34103221700000	Class II	BERE	BERE	Berea
34103245150000	Class II	NWBG	NWBG	Silurian-Devonian “Big Lime”
34103246470000	Class II	BERE	BERE	Berea
34103246480000	Class II	BERE	BERE	Berea
34105219950000	Class II	BERE	BERE	Berea
34105222960000	Class II	BERE	BERE	Berea
34105224610000	Class II	BGIJ	BGIJ	Mississippian undifferentiated
34105227380000	Class II	CLNN	CLNN	Silurian “Clinton/Medina”
34105227390000	Class II	MRCL	MRCL	Devonian shale and siltstones
34105233190000	Class II	OHIO	CLNN	Devonian shale and siltstones
34105234330000	Class II	OHIO	CLNN	Devonian shale and siltstones
34105234730000	Class II	BGIJ	BGIJ	Mississippian undifferentiated
34105236190000	Class II	NWBG	NWBG	Silurian-Devonian “Big Lime”
34111215590000	Class II	BGIJ	BGIJ	Mississippian undifferentiated
34115204320000	Class II	NWBG	NWBG	Silurian-Devonian “Big Lime”
34115218960000	Class II	MDIN	MDIN	Silurian “Clinton/Medina”
34115221500000	Class II	CLNN	CLNN	Silurian “Clinton/Medina”
34115225270000	Class II	CLNN	CLNN	Silurian “Clinton/Medina”
34115226170000	Class II	BERE	BERE	Berea
34115227960000	Class II	OHIO	OHIO	Devonian shale and siltstones
34115229810000	Class II	BERE	BERE	Berea
34115238740000	Class II	MDIN	MDIN	Silurian “Clinton/Medina”
34117214440000	Class II	TMPL	TMPL	Cambrian-Ordovician Knox
34117219010000	Class II	TMPL	TMPL	Cambrian-Ordovician Knox
34117222600000	Class II	TMPL	TMPL	Cambrian-Ordovician Knox
34117223420000	Class II	TMPL	TMPL	Cambrian-Ordovician Knox
34117228290000	Class II	TMPL	TMPL	Cambrian-Ordovician Knox
34117228840000	Class II	TMPL	TMPL	Cambrian-Ordovician Knox
34117230200000	Class II	TMPL	TMPL	Cambrian-Ordovician Knox
34117231220000	Class II	TMPL	TMPL	Cambrian-Ordovician Knox
34117233880000	Class II	TMPL	TMPL	Precambrian/Cambrian preKnox
34117234020000	Class II	FRCO	FRCO	Precambrian/Cambrian preKnox
34117234140000	Class II	FRCO	FRCO	Precambrian/Cambrian preKnox
34117234700000	Class II	TMPL	TMPL	Cambrian-Ordovician Knox
34117235270000	Class II	TMPL	TMPL	Cambrian-Ordovician Knox
34117237810000	Class II	TMPL	TMPL	Cambrian-Ordovician Knox
34117240800000	Class II	TMPL	TMPL	Cambrian-Ordovician Knox
34119230930000	Class II	CLNN	CLNN	Silurian “Clinton/Medina”
34119244390000	Class II	BERE	BERE	Berea
34119247580000	Class II	CLNN	CLNN	Silurian “Clinton/Medina”
34119262260000	Class II	CLNN	CLNN	Silurian “Clinton/Medina”
34119273500000	Class II	RSRN	RSRN	Cambrian-Ordovician Knox
34121233900000	Class II	MDIN	MDIN	Silurian “Clinton/Medina”
34121239950000	Class II	MDIN	MDIN	Silurian “Clinton/Medina”
34121240860000	Class II	MDIN	CLNN	Silurian “Clinton/Medina”

API_WELLNO	Class	Injection FM_Top	Injection FM_Base	Informal Formation Grouping
34127226160000	Class II	CLNN	CLNN	Silurian “Clinton/Medina”
34127242600000	Class II	CLNN	CLNN	Silurian “Clinton/Medina”
34127265950000	Class II	MNSM	MNSM	Precambrian/Cambrian preKnox
34127271150000	Class II	RSRN	RSRN	Cambrian-Ordovician Knox
34129200590000	Class II	RSRN	RSRN	Cambrian-Ordovician Knox
34129200880000	Class II	RSRN	MNSM	Cambrian-Ordovician Knox
34129200950000	Class II	RSRN	RSRN	Cambrian-Ordovician Knox
34129201050000	Class II	RSRN	RSRN	Cambrian-Ordovician Knox
34129201250000	Class II	TMPL	TMPL	Cambrian-Ordovician Knox
34129201940000	Class II	TMPL	TMPL	Cambrian-Ordovician Knox
34133201140000	Class II	NWBG	NWBG	Silurian-Devonian “Big Lime”
34133205250000	Class II	NWBG	NWBG	Silurian-Devonian “Big Lime”
34133207470000	Class II	NWBG	NWBG	Silurian-Devonian “Big Lime”
34133210760000	Class II	NWBG	NWBG	Silurian-Devonian “Big Lime”
34133214360000	Class II	NWBG	NWBG	Silurian-Devonian “Big Lime”
34133214390000	Class II	CLNN	CLNN	Silurian “Clinton/Medina”
34133214590000	Class II	CLNN	CLNN	Silurian “Clinton/Medina”
34133214730000	Class II	NWBG	NWBG	Silurian-Devonian “Big Lime”
34133222830000	Class II	NWBG	CLNN	Silurian-Devonian “Big Lime”
34133225230000	Class II	NWBG	NWBG	Silurian-Devonian “Big Lime”
34133226600000	Class II	NWBG	NWBG	Silurian-Devonian “Big Lime”
34133227360000	Class II	NWBG	NWBG	Silurian-Devonian “Big Lime”
34133228600000	Class II	ROME	ROME	Precambrian/Cambrian preKnox
34133233430000	Class II	NWBG	NWBG	Silurian-Devonian “Big Lime”
34133235420000	Class II	NWBG	NWBG	Silurian-Devonian “Big Lime”
34133236140000	Class II	NWBG	NWBG	Silurian-Devonian “Big Lime”
34139206460000	Class II	LCKP	LCKP	Silurian-Devonian “Big Lime”
34147202440000	Class II	MNSM	MNSM	Precambrian/Cambrian preKnox
34147203480000	Class II	KRBL	KRBL	Precambrian/Cambrian preKnox
34151211790000	Class II	NWBG	NWBG	Silurian-Devonian “Big Lime”
34151211980000	Class II	NWBG	NWBG	Silurian-Devonian “Big Lime”
34151213370000	Class II	ORSK	NWBG	Silurian-Devonian “Big Lime”
34151213510000	Class II	NWBG	NWBG	Silurian-Devonian “Big Lime”
34151218860000	Class II	NWBG	NWBG	Silurian-Devonian “Big Lime”
34151219200000	Class II	NWBG	NWBG	Silurian-Devonian “Big Lime”
34151220880000	Class II	CLNN	CLNN	Silurian “Clinton/Medina”
34151220890000	Class II	NWBG	NWBG	Silurian-Devonian “Big Lime”
34151224590000	Class II	NWBG	CLNN	Silurian-Devonian “Big Lime”
34151227830000	Class II	NWBG	NWBG	Silurian-Devonian “Big Lime”
34151228490000	Class II	CLNN	CLNN	Silurian-Devonian “Big Lime”
34151234200000	Class II	NWBG	NWBG	Silurian-Devonian “Big Lime”
34151238520000	Class II	BERE	BERE	Berea
34151238770000	Class II	NWBG	NWBG	Silurian-Devonian “Big Lime”
34151243520000	Class II	CLNN	CLNN	Silurian “Clinton/Medina”
34151252370000	Class II	MNSM	MNSM	Precambrian/Cambrian preKnox
34153209070000	Class II	MNSM	MNSM	Precambrian/Cambrian preKnox
34153215910000	Class II	MNSM	MNSM	Precambrian/Cambrian preKnox
34155206820000	Class II	NWBG	NWBG	Silurian-Devonian “Big Lime”
34155218930000	Class II	CLNN	CLNN	Silurian-Devonian “Big Lime”
34155218940000	Class II	NWBG	NWBG	Silurian-Devonian “Big Lime”
34155224030000	Class II	NWBG	NWBG	Silurian-Devonian “Big Lime”
34155232030000	Class II	NWBG	NWBG	Silurian-Devonian “Big Lime”
34155235840000	Class II	NWBG	NWBG	Silurian-Devonian “Big Lime”
34155237950000	Class II	NWBG	NWBG	Silurian-Devonian “Big Lime”
34157205420000	Class II	BERE	BERE	Berea
34157205750000	Class II	BERE	BERE	Berea
34157236900000	Class II	BERE	BERE	Berea
34157243110000	Class II	BERE	BERE	Berea
34161201300000	Class II	TRNN	TRNN	Ordovician shale and Trenton-Black River
34163203180000	Class II	BERE	BERE	Berea
34163205410000	Class II	BERE	BERE	Berea
34163207050000	Class II	ONDG	ONDG	Silurian-Devonian “Big Lime”
34163207560000	Class II	ONDG	ONDG	Silurian-Devonian “Big Lime”
34163207570000	Class II	BERE	BERE	Berea
34163208160000	Class II	BERE	BERE	Berea
34163208430000	Class II	BERE	BERE	Berea
34163208830000	Class II	ORSK	ORSK	Silurian-Devonian “Big Lime”

API_WELLNO	Class	Injection FM_Top	Injection FM_Base	Informal Formation Grouping
34163208850000	Class II	ONDG	ONDG	Silurian-Devonian “Big Lime”
34167279580000	Class II	BERE	BERE	Berea
34167284620000	Class II	ORSK	ORSK	Silurian-Devonian “Big Lime”
34167293950000	Class II	CLNN	MDIN	Silurian “Clinton/Medina”
34167296580000	Class II	CLNN	MDIN	Silurian “Clinton/Medina”
34169201490000	Class II	BERE	BERE	Berea
34169207750000	Class II	NWBG	NWBG	Silurian-Devonian “Big Lime”
34169217670000	Class II	BILDF	BILDF	Silurian-Devonian “Big Lime”
34169221980000	Class II	BILDF	BILDF	Silurian-Devonian “Big Lime”
34173212150000	Class II	KRBL	ROME	Precambrian/Cambrian preKnox
34175202670000	Class II	TMPL	TMPL	Cambrian-Ordovician Knox
34175203410000	Class II	BKRV	BKRV	Ordovician shale and Trenton-Black River

APPENDIX B

Geologic Formation Names and Corresponding OCDO Formation Groups

Matthew Erenpreiss—Ohio Geological Survey, Columbus, Ohio

Includes formal, informal, drillers, and obsolete terms from RBDMS

Formation Name	OCDO Formation Group
glacial deposits	n/a
limestone	n/a
sandstone	n/a
shale	n/a
shale	n/a
slate	n/a
Paleozoic undifferentiated	n/a
Unknown	n/a
Pennsylvanian	Pennsylvanian undifferentiated
Pittsburgh coal	Pennsylvanian undifferentiated
Conemaugh Gp	Pennsylvanian undifferentiated
Mitchell sand	Pennsylvanian undifferentiated
Glenshaw	Pennsylvanian undifferentiated
Peeker sand	Pennsylvanian undifferentiated
Cow Run	Pennsylvanian undifferentiated
Buell Run	Pennsylvanian undifferentiated
Macksburg	Pennsylvanian undifferentiated
Macksburg 300	Pennsylvanian undifferentiated
Coal	Pennsylvanian undifferentiated
Allegheny	Pennsylvanian undifferentiated
Cow Run 2	Pennsylvanian undifferentiated
Dorr Run marine zone	Pennsylvanian undifferentiated
Washingtonville marine zone	Pennsylvanian undifferentiated
Macksburg 500	Pennsylvanian undifferentiated
Macksburg 700	Pennsylvanian undifferentiated
Germantown sandstone	Pennsylvanian undifferentiated
Pottsville Group	Pennsylvanian undifferentiated
Pottsville	Pennsylvanian undifferentiated
Quakertown Coal	Pennsylvanian undifferentiated
Number 2 Coal	Pennsylvanian undifferentiated
Brill Sand	Pennsylvanian undifferentiated
Sharon	Pennsylvanian undifferentiated
Maxton	Pennsylvanian undifferentiated
Second Salt sand	Pennsylvanian undifferentiated
Salt sand	Pennsylvanian undifferentiated
Mitchell	Pennsylvanian undifferentiated
Mississippian Undifferentiated	Mississippian undifferentiated
Upper Mississippian undifferentiated	Mississippian undifferentiated
Maxville	Mississippian undifferentiated
Logan	Mississippian undifferentiated
Keener	Mississippian undifferentiated
Big Injun	Mississippian undifferentiated
Squaw	Mississippian undifferentiated
Weir	Mississippian undifferentiated
Hamden	Mississippian undifferentiated
Henley Shale Member	Mississippian undifferentiated
Coffee Shale	Mississippian undifferentiated
Cussewago Sandstone	Mississippian undifferentiated
Sunbury	Berea
Berea	Berea
Berea 2	Berea
Bedford	Berea
Gantz	Berea
Thirty Foot	Berea
Gordon	Berea
Fifth Sand	Berea
Cuyahoga	Devonian shale and siltstones
Devonian	Devonian shale and siltstones

Formation Name	OCDO Formation Group
Ohio	Devonian shale and siltstones
Cleveland Shale Member	Devonian shale and siltstones
Little Cinnamon	Devonian shale and siltstones
Chagrin Shale Member	Devonian shale and siltstones
Warren 1st	Devonian shale and siltstones
Speechley Sand	Devonian shale and siltstones
Balltown Sand	Devonian shale and siltstones
Huron	Devonian shale and siltstones
Big Cinnamon	Devonian shale and siltstones
Lower Huron	Devonian shale and siltstones
Antrim	Devonian shale and siltstones
Olentangy	Devonian shale and siltstones
Rhinestreet Shale Member	Devonian shale and siltstones
Sonyea Formation	Devonian shale and siltstones
Marcellus	Devonian shale and siltstones
Gordon Stray	Silurian - Devonian “Big Lime”
Traverse	Silurian - Devonian “Big Lime”
Delaware	Silurian - Devonian “Big Lime”
Onondaga	Silurian - Devonian “Big Lime”
Columbus	Silurian - Devonian “Big Lime”
Big Lime	Silurian - Devonian “Big Lime”
Detroit Group	Silurian - Devonian “Big Lime”
Sylvania	Silurian - Devonian “Big Lime”
Bois Blanc	Silurian - Devonian “Big Lime”
Oriskany	Silurian - Devonian “Big Lime”
Helderberg Group	Silurian - Devonian “Big Lime”
Helderburg	Silurian - Devonian “Big Lime”
Silurian	Silurian - Devonian “Big Lime”
Bass Island	Silurian - Devonian “Big Lime”
Bass Island Group	Silurian - Devonian “Big Lime”
Salina	Silurian - Devonian “Big Lime”
Salina G	Silurian - Devonian “Big Lime”
Salina F	Silurian - Devonian “Big Lime”
Salina E	Silurian - Devonian “Big Lime”
Salina B	Silurian - Devonian “Big Lime”
Salina A	Silurian - Devonian “Big Lime”
Salina undifferentiated	Silurian - Devonian “Big Lime”
Undifferentiated Salina Dolomite	Silurian - Devonian “Big Lime”
Tymochtee	Silurian - Devonian “Big Lime”
Greenfield	Silurian - Devonian “Big Lime”
Salina Dolomite	Silurian - Devonian “Big Lime”
Williamsport Sandstone	Silurian - Devonian “Big Lime”
Lockport	Silurian - Devonian “Big Lime”
Newburg	Silurian - Devonian “Big Lime”
First Water	Silurian - Devonian “Big Lime”
Lockport Group	Silurian - Devonian “Big Lime”
Guelph Dolomite	Silurian - Devonian “Big Lime”
Gasport	Silurian - Devonian “Big Lime”
Rochester Formation	Silurian - Devonian “Big Lime”
Niagaran	Silurian - Devonian “Big Lime”
Neahga Shale	Silurian - Devonian “Big Lime”
Laurel	Silurian - Devonian “Big Lime”
Dayton Formation	Silurian “Clinton/Medina”
Dayton Limestone Member	Silurian “Clinton/Medina”
Packer Shell	Silurian “Clinton/Medina”
Little Shell	Silurian “Clinton/Medina”
Cabot Head	Silurian “Clinton/Medina”
Clinton	Silurian “Clinton/Medina”
Stray Clinton	Silurian “Clinton/Medina”
Red Clinton	Silurian “Clinton/Medina”
White Clinton	Silurian “Clinton/Medina”
Manitoulin Dolomite	Silurian “Clinton/Medina”
Medina	Silurian “Clinton/Medina”
Brassfield	Silurian “Clinton/Medina”
Brassfield	Silurian “Clinton/Medina”
Queenston	Silurian “Clinton/Medina”
Red Medina	Silurian “Clinton/Medina”

Formation Name	OCDO Formation Group
Ordovician undifferentiated	Ordovician shale and Trenton-Black River
Ordovician undivided	Ordovician shale and Trenton-Black River
Upper Ordovician undifferentiated	Ordovician shale and Trenton-Black River
Cincinnatian	Ordovician shale and Trenton-Black River
Drakes	Ordovician shale and Trenton-Black River
Waynesville Formation and Arnheim Formations	Ordovician shale and Trenton-Black River
Richmond Group	Ordovician shale and Trenton-Black River
Miamitown Shale	Ordovician shale and Trenton-Black River
Fairview	Ordovician shale and Trenton-Black River
Kope	Ordovician shale and Trenton-Black River
Eden Formation	Ordovician shale and Trenton-Black River
Utica	Ordovician shale and Trenton-Black River
Point Pleasant	Ordovician shale and Trenton-Black River
Trenton	Ordovician shale and Trenton-Black River
Lexington	Ordovician shale and Trenton-Black River
Logana	Ordovician shale and Trenton-Black River
Black River	Ordovician shale and Trenton-Black River
Upper Chazy	Ordovician shale and Trenton-Black River
Gull River	Ordovician shale and Trenton-Black River
Middle Chazy	Ordovician shale and Trenton-Black River
Lower Chazy	Ordovician shale and Trenton-Black River
Lower Argillaceous Unit of Wells Creek	Ordovician shale and Trenton-Black River
Wells Creek	Ordovician shale and Trenton-Black River
Glenwood	Ordovician shale and Trenton-Black River
St Peter	Ordovician shale and Trenton-Black River
Knox Unconformity Surface	Cambro-Ordovician Knox
Beekmantown	Cambro-Ordovician Knox
Rose Run	Cambro-Ordovician Knox
Prairie Du Chien Group	Cambro-Ordovician Knox
Knox	Cambro-Ordovician Knox
Lower Knox	Cambro-Ordovician Knox
Copper Ridge	Cambro-Ordovician Knox
Trempealeau	Cambro-Ordovician Knox
Knox B	Cambro-Ordovician Knox
Cambrian undifferentiated	Precambrian - Cambrian Pre-Knox
Krysik Sand	Precambrian - Cambrian Pre-Knox
Kerbel	Precambrian - Cambrian Pre-Knox
Maynardville	Precambrian - Cambrian Pre-Knox
Franconian	Precambrian - Cambrian Pre-Knox
Conasauga	Precambrian - Cambrian Pre-Knox
Rome	Precambrian - Cambrian Pre-Knox
Eau Claire	Precambrian - Cambrian Pre-Knox
Shady Formation	Precambrian - Cambrian Pre-Knox
Middle Cambrian undifferentiated	Precambrian - Cambrian Pre-Knox
Mount Simon	Precambrian - Cambrian Pre-Knox
basal sand	Precambrian - Cambrian Pre-Knox
Precambrian	Precambrian - Cambrian Pre-Knox
Precambrian crystalline basement	Precambrian - Cambrian Pre-Knox
Middle Run	Precambrian - Cambrian Pre-Knox
Granite	Precambrian - Cambrian Pre-Knox
Granite Wash	Precambrian - Cambrian Pre-Knox
Grenville Orogenic Belt	Precambrian - Cambrian Pre-Knox

APPENDIX C

Geopotential Gravity, Magnetic, and Geothermal Surveys

by Timothy Leftwich, Ohio Geological Survey, Columbus, Ohio

Gravity Surveys and Data

The gravity field measured near the surface of Earth reflects the mass of Earth and any local gravity effects due to elevation, terrain, motions of the Sun and Moon, movement of the measuring platform, and local variations in density (i.e., geology; e.g., Nettleton, 1971; von Frese and Hinze, 1993; Blakely, 1996). The largest density contrasts evident in the gravity field observations are those of the terrain and the crust-mantle interface or "Moho." A number of gravity data products, including the free-air gravity anomalies (FAGA), complete Bouguer gravity anomalies (CBA) and isostatic residual gravity (IRG) anomalies are available from the U.S. Geological Survey (USGS). In addition to these products, several new gravity anomaly datasets are available from the Electric Power Research Institute (EPRI, 2012). The EPRI data sets include FAGA and CBA data (Fig. C-1) and several permutations of these data that were frequency filtered to isolate particular wavelengths of the data.

The gravity map after the application of latitude, free-air, and terrain corrections is the so called "Bouguer" map. Because the terrain gravity effects and the gravity effects of the Moho density contrast largely and cancel each other for isostatically compensated crust, removal of the terrain effects for crust that is compensated generally creates Bouguer anomalies that are small in amplitude. Because this "reduced" form of gravity data mostly reflects the density variations in Earth, this is the usual form in which gravity anomaly results are presented (Nettleton, 1971). The Bouguer gravity map reflects the reduced free-air gravity observations minus the gravity effects of the terrain. Areas with high positive topographic relief produce strong positive terrain gravity effects that result in negative Bouguer anomalies. On the other hand, where the terrain gravity effect is small relative to the gravity effects of relatively dense crust, the Bouguer anomalies are relatively more positive. Information on how gravity is measured and corrected can be found in Blakely (1996).

Herein, we show the CBA map of Ohio (Fig. C-1) using data from EPRI (2012). The EPRI gravity anomaly data sets are compiled from several public domain and unpublished sources that were used in the EPRI central and eastern United States seismic source characterization (CEUS-SSC) project. These data are given in units of milligals (mGal). The average Earth gravity acceleration is roughly 980,000 mGal. A principal survey used in the Ohio region is that of Heiskanen and Uotila (1957), wherein they report that errors in the gravity measurements are generally less than 0.1 mGal.

The gravity anomaly data are a very useful tool for further evaluation of the structure, geologic processes, and tectonic evolution of Ohio. Gravity anomalies, for example, may reflect the Appalachian Basin structure and any major structural trends in the eastern Ohio area of interest. The EPRI Ohio gravity anomaly map provides a more comprehensive gravity view of basin-scale trends not available in individual data sets and helps link widely separated areas of outcrop, seismic reflection and refraction profiles, and data from boreholes to help unify disparate geologic studies. Some excellent sources for insights into Ohio geology from gravity and magnetic anomaly data are available in Lucius and von Frese (1988), Braile (1989), von Frese and others (1997), and Kim and others (2000).

Magnetic Data

The magnetic field measured near the surface of Earth includes the magnetic field generated within Earth's core (i.e., the core field) plus the magnetic field induced by the core field in iron-bearing rocks and minerals of the crust plus any remnant magnetism locked into crustal rocks during formation (e.g., Butler, 1992). A description of induced and remnant magnetism is beyond the scope of this work, but details can be found in Butler (1992). Herein, we present the USGS regional residual total intensity anomalies (TF) of the magnetic field from Bankey and others (2002). The TF magnetic anomalies are the total magnetic value minus a geomagnetic reference field (GRF), which is a long-wavelength regional magnetic field. Hence, the TF anomalies mostly reflect the component of the magnetic field induced in the crust, which is of great interest for geologic interpretations. Whereas sedimentary rocks are essentially non-magnetic and so are "transparent" in the magnetic anomaly maps, the more iron-rich, metamorphic and igneous Precambrian basement rocks are the relatively magnetic sources for TF anomalies.

The most commonly used reference field (core field model) is developed by the International Association of Geomagnetism and Aeronomy (IAGA). The International Geomagnetic Reference Field (IGRF) is a predictive model adopted at the beginning of a model period (e.g., in 1989 for 1990–1995). After the model period, a revised definitive model is adopted—the DGRF. This is the preferred model to use for removing regional magnetic fields (e.g., Nettleton, 1971; Blakely, 1996). A general description of magnetometers and how they measure the total magnetic field can be found in Dobrin (1976).

Grid values in the TF anomalies represent the total intensity of Earth's magnetic field after removal of the IGRF. The grids represented in this report were made from numerous individual grids that were mathematically merged using standard techniques (Bankey and others, 2002). The aeromagnetic measurements were made using a variety of magnetometer systems with typical accuracies of 1 to 10 nanoTesla (nT; Ravat and others, 2009), whereas the mean field strength of Earth is about 60,000 nT. The original 0.1-by-0.1 degree grid was also resampled to a 0.01-by-0.01 degree grid size by cubic spline interpolation for the Ohio TF magnetic anomalies (Fig. C-2).

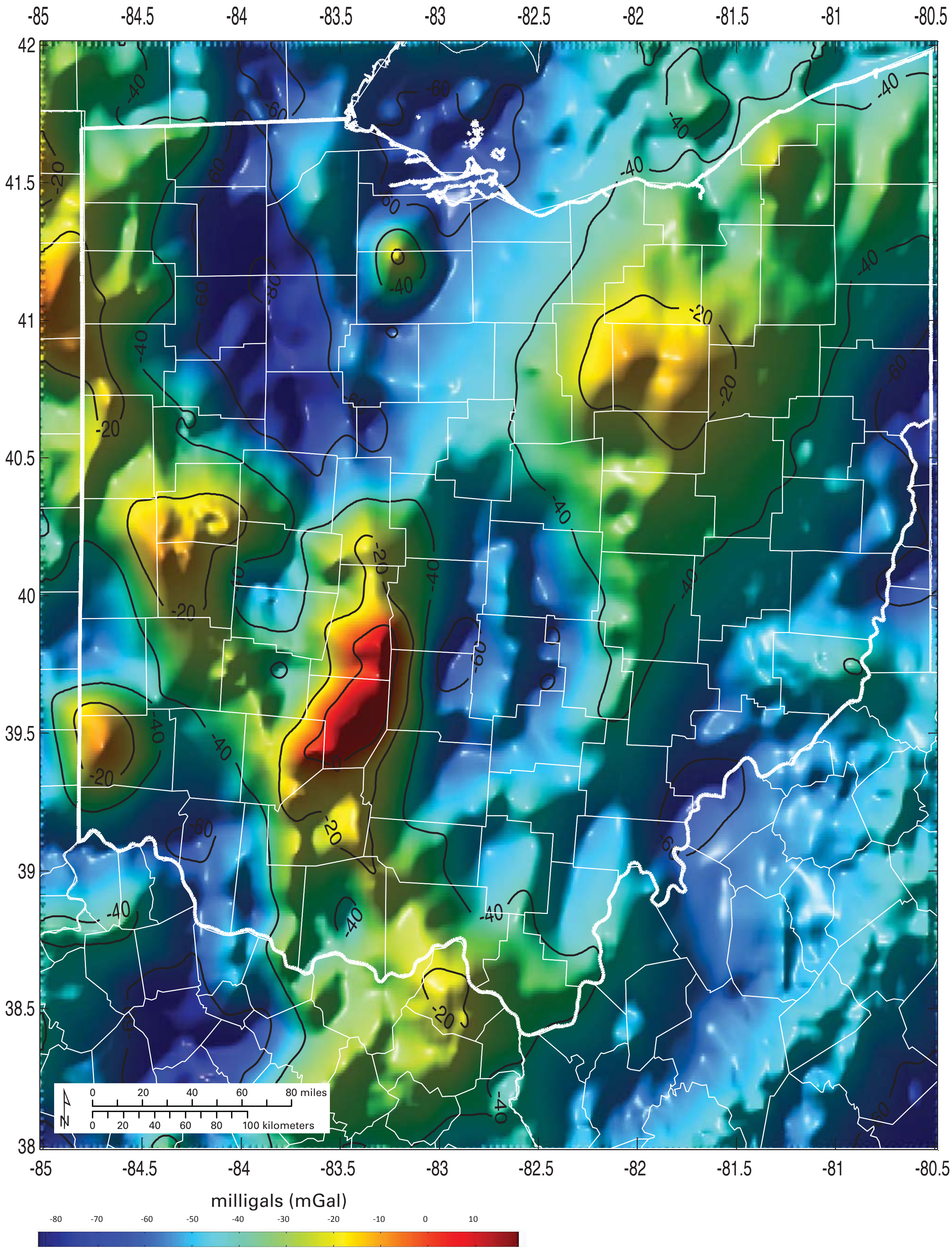

FIGURE C-1—Map of complete Bouguer gravity anomalies (CBA) for the state of Ohio using data from the Electric Power Research Institute: Central Eastern U.S. Seismic Source Characterization study (EPRI, 2012).

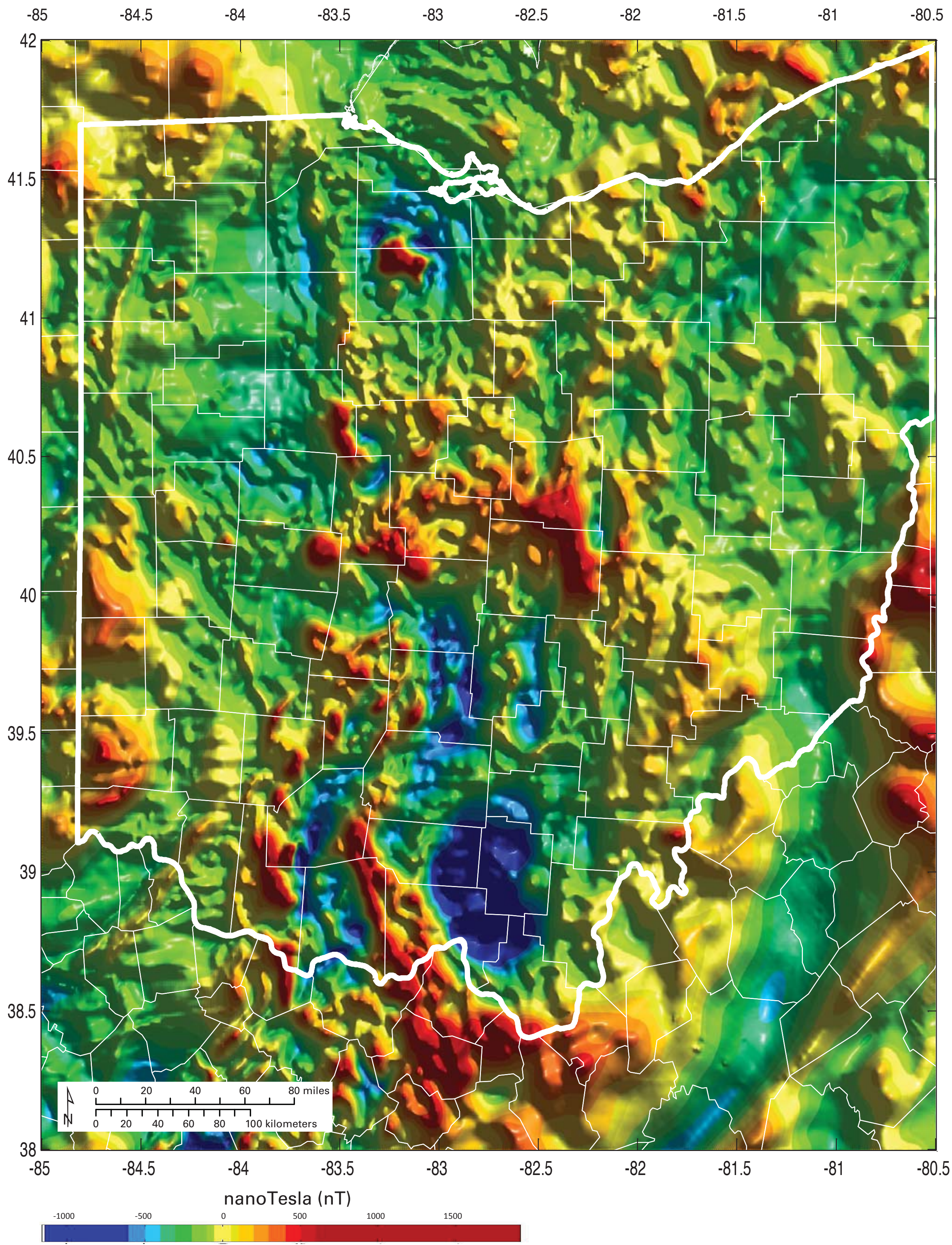

FIGURE C-2—Map of total-field magnetic anomalies for the state of Ohio using data from U.S. Geological Survey (Ravat and others, 2009).

These magnetic anomaly data are useful tools for further evaluation of the structure, geologic processes, and tectonic evolution of Ohio that may also be used to better reveal the Appalachian Basin structure and any potential faulting in the eastern Ohio area of interest. The Ohio magnetic anomaly map derived and modified from the original digital database (Ravat and others, 2009) provides a comprehensive magnetic view of basin-scale trends not available in individual data sets and helps link widely separated areas of outcrop and boreholes to unify disparate geologic studies. Other magnetic field components that may be of interest include reduced-to-pole magnetic anomalies, derivative magnetic fields, and several permutations of these data that were frequency filtered to isolate particular wavelengths of the data (e.g., Ravat and others, 2009). For more information on the uses of magnetic anomaly data for geologic mapping and interpretation, one might consult von Frese and Hinze (1993) or Finn and others (2002). Additional excellent sources for insights into Ohio geology from magnetic anomaly analysis are available in Lucius and von Frese (1988) and von Frese and others (1997).

Geothermal Data & Mapping

The Ohio Geological Survey compiled and corrected bottom-hole temperature (BHT) and geothermal gradient datasets and produced a number of maps based on the corrected temperatures of 488 wells from across the state. The State Geothermal Data project, organized by the Association of American State Geologists (AASG) with funding from the U.S. Department of Energy, is bringing data from all 50 states into the National Geothermal Data System (NGDS). The Ohio Borehole Temperatures and associated maps have been submitted to the NGDS and are available from: **http://stategeothermaldata.org**. The regional data and 144 of the Ohio BHT data are from AAPG (1994, CD-ROM), with an additional 344 Ohio BHTs obtained from Ohio Geological Survey records (Leftwich and others, 2011, 2012).

The original BHT data were converted to degrees Celsius (°C) and corrected using the methods of Harrison and others (1989) and the so-called Southern Methodist University (SMU) BHT correction (Blackwell and Richards, 2004a). The Harrison-corrected values were used for the site-specific geothermal gradients for the SMU correction. The SMU correction added or subtracted amounts form the Harrison-corrected BHT values according to each well's gradient. However, the method was modified slightly for low and moderate gradients because the resultant BHT values were too low. Hence:

- 5°C was added to BHTs with associated gradients of less than 20°C/km.
- 5°C was subtracted from BHTs with associated gradients of 20–27°C/km.
- 5°C was added for wells with gradients of 27–30°C/km.
- 11°C was added to BHTs with gradients greater than 30 °C/km.

With the addition of the SMU correction, the final calibrated temperatures have an accuracy of about 5–10 percent based on the direct comparison with equilibrium temperature logs (Blackwell and Richards, 2004a). However, these data and maps can readily be updated as new data or correction methods become available.

The BHT map (Fig. C-3; Leftwich 2011a) and derivative geothermal gradient map (Fig. C-4; Leftwich 2011b) were gridded by kriging routine. Gridding was performed using ESRI ArcMap software (ordinary kriging, variable distance with 12 points and a maximum distance of 50). This kriging method was used to show the predominant trends in the BHT and geothermal gradient data without adhering to each data point.

Heat flow estimates, *Q* (usually given in milliwatts per square meter [mW/m^2]) for eastern Ohio range from perhaps as low as 48 mW/m^2 (Leftwich, 2012) to about 57 mW/m^2 (Eckstein and others, 1982; Blackwell and Richards, 2004b). According to Fourier's equation, heat flow, *Q*, is the product of the geothermal gradient, *dT/dZ*, and the layer's thermal conductivity, *K*, (e.g., Kellog, 1953; Eckstein and others, 1982) according to:

$$Q = -\frac{dT}{dZ}K$$

For Earth's crust, where heat is flowing from the hot interior to the cool exterior, this linear relationship becomes:

$$Q = a + bA$$

where *a* is the heat flow originating from the mantle and lower crust; *A* is the radiogenic heat production of the crustal layer(s) from the decay of uranium, thorium, and potassium; and *b* is the thickness of the heat-producing layer (e.g., Lachenbruch, 1968; Eckstein and others, 1982; Beardsmore and Cull, 2001).

Geopotential Anomalies and Ohio Crustal Structure

Important crustal features for Ohio are reflected in the TF magnetic anomalies and Bouguer gravity anomalies as well in the BHT and geothermal gradient maps. Of course, many additional magnetic (e.g., reduced-to-pole) and gravity field (e.g., free-air gravity, isostatic residual gravity) data sets, derivative maps, and filtered components are not presented or discussed in this report. Also in this report we discuss only a few major crustal features associated with these data sets. However, additional references for insights into Ohio geology from geothermal, gravity, and magnetic anomaly analyses include Eckstein and others (1982), Lucius and von Frese (1988), von Frese and others (1997), and Kim and others (2000).

As shown in the basement relief map (Baranoski, 2002), Ohio has relatively elevated relief of the Precambrian basement along Owen's hinge line and the Findlay Arch, which defines the western limit of the Appalachian Basin. This major Precambrian surface also is strongly reflected in the CBA gravity map (Fig. C-1) and TF magnetic anomalies map (Fig. C-2). Coincident with the Precambrian structural features, magnetic highs trend N–S through the center of Ohio, and a

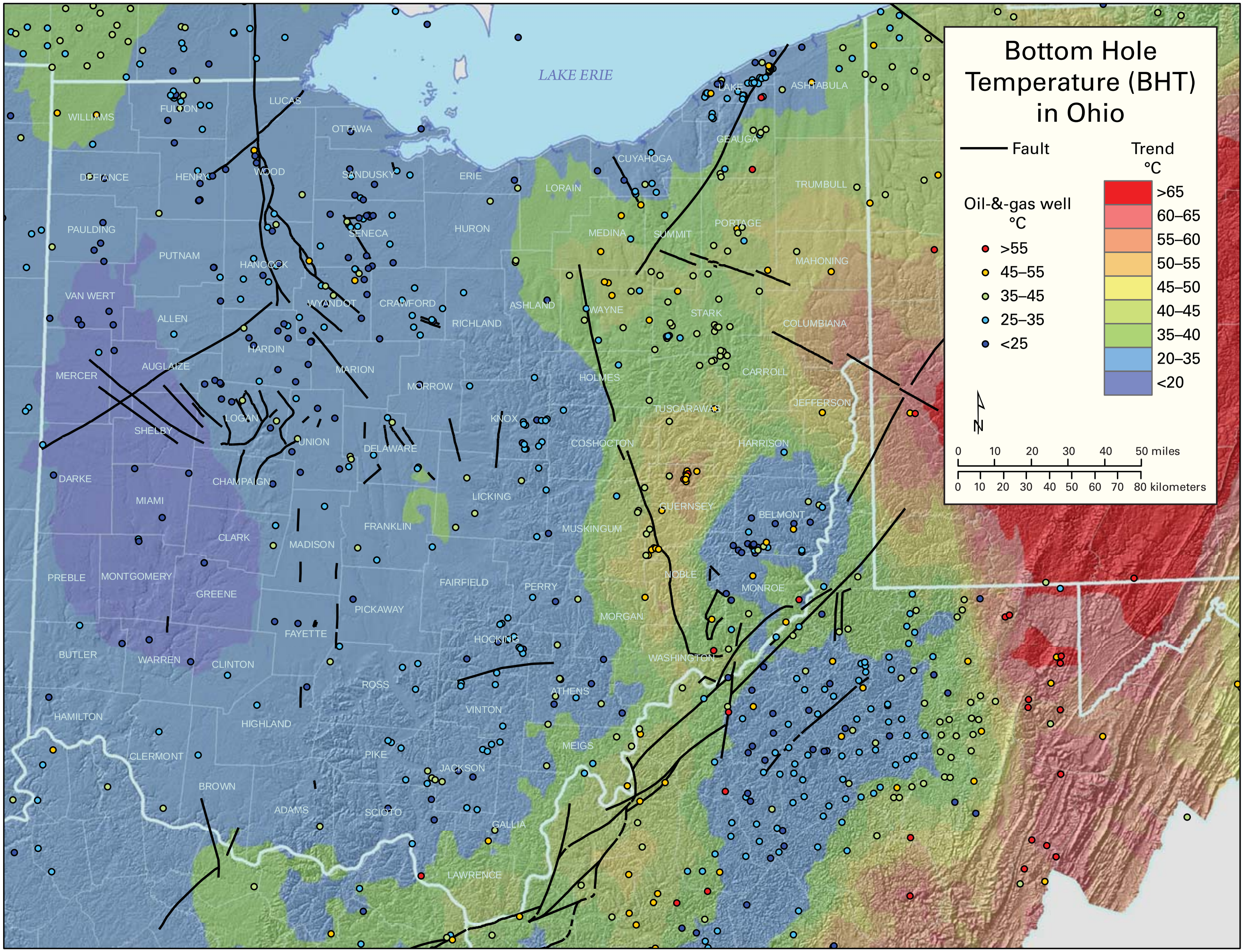

FIGURE C-3—Kriged corrected bottom-hole temperature (BHT) observations based on corrected temperatures from 488 wells across the state of Ohio (AAPG, 1994; Leftwich and others 2011a; 2012a). Ohio BHT data were converted to degrees Celcius (°C) and corrected using the methods outlined in Harrison and others (1989) and the Southern Methodist University (SMU) correction (Blackwell and others, 2004a).

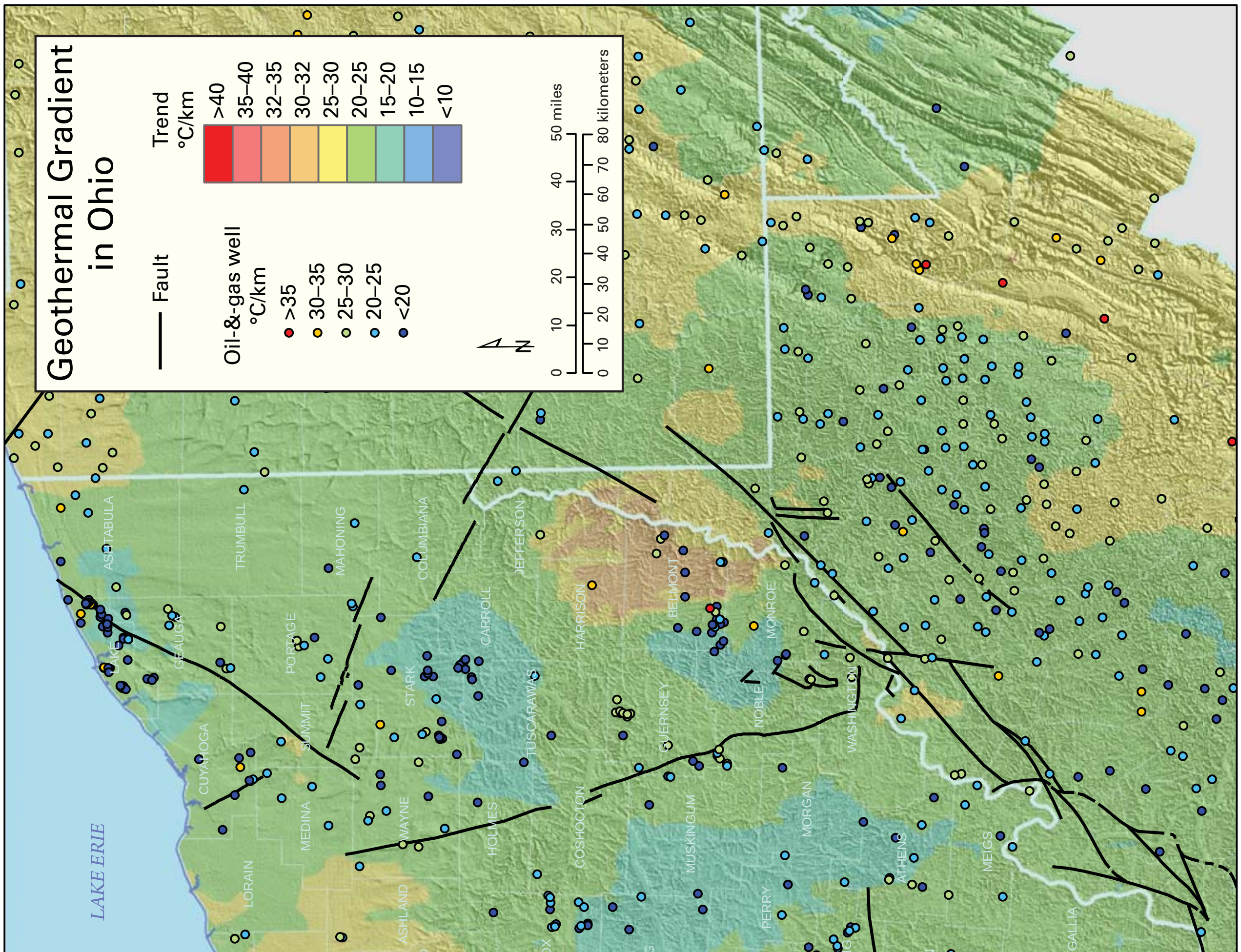

FIGURE C-4—Kriged geothermal gradient observations (*T_bottom–T_surface/total depth*) based on corrected BHT temperatures from 488 wells across the state of Ohio (AAPG, 1994; Leftwich and others 2011a; 2012a).

N–S-trending dichotomy between eastern and western Ohio also is evident in the CBA gravity anomalies. This strong N–S-trending dichotomy in both gravity and magnetism was previously interpreted as the possible western extension of Grenville tectonism (e.g., Heiskanen and Uotila, 1956; Bass, 1960; Lucius and von Frese, 1988).

Another notable geopotential anomaly trend is seen in the broad NW–SE-trending magnetic high extending from central Ohio to Washington County that is also coincident with the Cambridge monocline or cross-strike discontinuity (Baranoski, 2002). Anomalously elevated BHT and geothermal gradients along the Cambridge monocline suggest possible hydrothermal circulation may transport heat from deeper rocks along this structure. The northeastern side of the Cambridge monocline is upthrown relative to the southeast side (Ohio Division of Geological Survey, 2006). Hence, this deep Precambrian suture zone was apparently reactivated during Phanerozoic time and is expressed all the way through the overlying sedimentary units to the surface.

Using regional gravity and magnetic data, workers speculated on the presence of Precambrian rifts in western Ohio (McGuire and Howell, 1963; Lidiak and Zietz, 1976; Halls, 1978; Keller and others, 1982, 1983; Cable and Beardsley, 1984; Denison and others, 1984; Black, 1986; Hinze and others, 1987; Lucius and von Frese, 1988). Drahovzal and others (1992) used well control and geophysical data to interpret a regional Precambrian rift system in western Ohio, which they named the East Continent Rift Basin (ECRB). The ECRB rift zone is seen distinctly as a local Bouguer gravity high extending into western Ohio, which is consistent with a failed rift containing relatively dense, mafic intrusive and volcanic sequences. This CBA high is also coincident with NW–SE trending lineaments in the TF magnetic anomalies that are also consistent with fault-bounded rifting.

Whereas relatively strong, high-frequency magnetic anomalies are associated with central and western Ohio, the TF magnetic anomalies are lower in amplitude and smoother looking for eastern Ohio, West Virginia, and Pennsylvania. This “smoothing” in the magnetic anomalies reflects the deepening of the Appalachian Basin. Where the magnetic basement rocks deepen into the Appalachian Basin, they move farther away from the aircraft magnetometers, which are flown at constant elevation above the terrain. It is as if the magnetometers were higher and farther away from the crustal sources over the basins and so the magnetic signals became weaker and more integrated into broad trends. In eastern Ohio, TF magnetic and Bouguer gravity lows extend from West Virginia into eastern Washington, Nobel, Monroe, Belmont, Harrison, and Jefferson Counties, suggestive of a deep basement filled with thick and relatively low-density, sedimentary rocks.

The Rome Trough is bounded by a relative magnetic high, which is seen in Figure C-2 as sub-parallel to the Ohio River along the West Virginia line. This magnetic high is part of the New York-Alabama magnetic lineament (e.g., Hinze and others, 1988; Thomas, 2005). The Rome Trough is part of a buried rift system that deepens from about 3 km northwest of the Ohio River to up to 5 km on the West Virginia side of the Ohio River (Baranoski, 2002).

The BHT and gradient data and maps help to show the temperature environment of the boreholes and the associated rates of increase of temperature with depth for the state of Ohio and its immediate neighborhood. In general, eastern Ohio BHTs are higher owing to the increasing depth that most boreholes penetrate as the Appalachian Basin and its associated oil and gas deposits deepen eastward. Heterogeneity of geothermal gradients, on the other hand, may locally reflect additional contributions of heat from relatively radiogenic basement rocks, such as granites.

Crustal features apparent in these magnetic and gravity maps are associated with seismic activity. A map of Ohio earthquakes is given in Figure C-5. A focus of earthquake activity in western Ohio, in an area known as the Anna Seismic Zone, is coincident with the ECRB extension into western Ohio that is evident in the potential field anomalies, as noted above. Earthquakes also are much more frequent for northeastern Ohio. The northeastern Ohio earthquakes are coincident with prominent lineaments in the magnetic anomalies and in the CBA anomalies where a relative CBA high trends NE–SW along the Lake Erie shore.

References Cited

AAPG, 1994, DataRom (CSDE, COSUNA, and GSNA) 1994: Tulsa, Okla., American Association of Petroleum Geologists, CD-ROM.

Bankey, V., Cuevas, A., Daniels, D., Finn, C.A., Hernandez, I., Hill, P., Kucks, R., Miles, W., Pilkington, M., Roberts, C., Roest, W., Rystrom, V., Shearer, S., Snyder, S., Sweeney, R., Velez, J., Phillips, J.D., and Ravat, D., 2002, Digital data grids for the magnetic anomaly map of North America: U.S. Geological Survey Open-File Report 02-414, accessible at < http://pubs.usgs.gov/of/2002/ofr-02-414/>.

Baranoski, M.T., 2002, Structure contour map on the Precambrian unconformity surface in Ohio and related basement features—A description to accompany Division of Geological Survey Map PG-23: Columbus, Ohio Department of Natural Resources, Division of Geological Survey, 19 p.

Bass, M.N., 1960, Grenville boundary in Ohio: Journal of Geology, v. 68, p. 673–677.

Beardsmore, G.R., and Cull, J.P., 2001. Crustal heat flow: A guide to measurement and modeling: Cambridge University Press, 324 p.

Black, D.F.B., 1986, Basement faulting in Kentucky: Proceedings of the 6th International Conference on Basement Tectonics, p. 125–139.

Blackwell, D.D., and Richards, M.C., 2004a, Calibration of the AAPG Geothermal Survey of North America BHT Data Base [abs.]: Tulsa, Okla., AAPG Bulletin, v. 88, no. 13 (supplement).

Blackwell, D.D., and Richards, M.C., 2004b, Geothermal map of North America: AAPG Map, scale 1:6,500,000.

Blakely, R.J., 1996, Potential theory in gravity and magnetic applications: Cambridge University Press, 441 p.

Braile, L.W., 1989, Crustal structure of the continental interior, *in* Pakiser, L.C., and Mooney, W.D., eds., Geophysical framework of the continental United States: GSA Memoir 172, p. 285–315.

Butler, R.F., 1992, Paleomagnetism: Magnetic domains to geologic terrains: Cambridge, Mass., Blackwell Scientific, 237 p.

Cable, M.S., and Beardsley, R.W., 1984, Structural controls on Late Cambrian and Early Ordovician carbonate sedimentation in eastern Kentucky: American Journal of Science, v. 284, p. 797–823.

Denison, R.E., Lidiak, E.G., Bickford, M.E., and Kisvarsanyi, E.B., 1984, Geology and geochronology Precambrian rocks of the central interior region of the United States: U.S. Geological Survey Professional Paper 1241-C, 20 p.

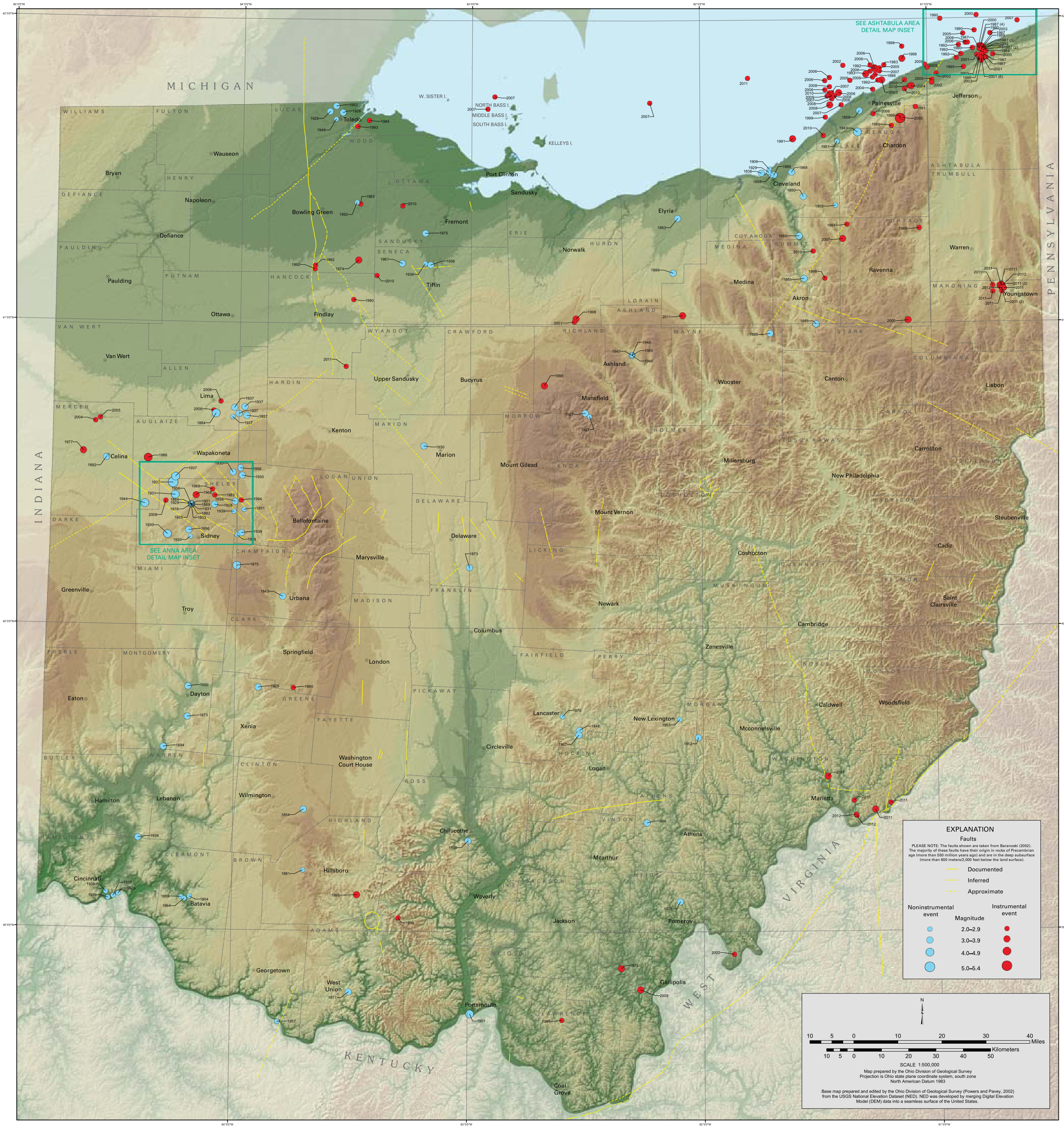

FIGURE C-5—Map depicting the approximate locations of earthquakes that either were felt in Ohio or had instrumental magnitudes of 2.0 or greater. Noninstrumental earthquake locations and magnitudes have been calculated from historical accounts. Because of the paucity of original reports for some earthquakes, noninstrumental locations and magnitudes may be very imprecise. Some border-region earthquakes are depicted on this map as well. The border region is arbitrarily defined as a grid from latitude 38.0° to 43.0°N and longitude 80.0° to 85.5°W. This grid includes most of the small-to-moderate (2.0 magnitude or greater) earthquakes that were beyond the state border but were, or may have been, felt in Ohio. Modified from Hansen (2007).

Dobrin, M.B., 1976, Introduction to geophysical prospecting: New York, McGraw Hill, 630 p.

Drahovzal, J.A., Harris, D.C., Wickstrom, L.H., Walker, D., Baranoski, M.T., Keith, B., and Furer, L.C., 1992, The East Continent Rift Basin—A new discovery: Columbus, Ohio Department of Natural Resources, Ohio Division of Geological Survey Information Circular 57, 25 p.

Eckstein, Y., Heimlich, R.A., Palmer, D.F., and Shannon, S.S., Jr., 1982, Geothermal investigations in Ohio and Pennsylvania, Los Alamos National Laboratory, LA-9223-HDR, UC-66b, 89 p.

EPRI, 2012, Central Eastern United States - Seismic Source Characterization for Nuclear Facilities: Electric Power Research Institute Report No. NUREG-2115, <http://www.ceus-ssc.com>.

Finn, C.A., Pilkington, M., Blakely, R., Johnson, S., Cannon, W., Gettings, M., and Roest, W., 2002, Examples of the utility of magnetic anomaly data for geologic mapping: U.S. Geological Survey Open-File Report OFR 02-400, 16 p.

Halls, H.C., 1978, The late Precambrian central North America rift system—A survey of recent geological and geophysical investigations, in Neuman, E.-R., and Ramberg, I.B., eds., Tectonics and geophysics of continental rifts: NATO Advanced Study Institute, Series C, Mathematical and Physical Sciences, v. 37, p. 111–123.

Harrison, W.E., Luza, K.V., Prater, M.L., and Cheung, P.K., 1989, Geothermal resource assessment in Oklahoma: Oklahoma Geological Survey Special Publication 83-1, 42 p.

Hinze, W.J., Braile, L.W., Keller, G.R., and Lidiak, E.G., 1987, An update of midcontinent tectonism: U.S. Nuclear Regulatory Commission Report, Contract No. NRC 04-81-195-01, 104 p.

Hinze, W.J., Braile, L.W., Keller, G.R., and Lidiak, E.G., 1988, Models for midcontinent tectonism—An update: Reviews of Geophysics, 26, p. 699–717.

Heiskanen, W.A., and Uotila, U.A., 1956, Gravity survey of the State of Ohio: Columbus, Ohio Department of Natural Resources, Division of Geological Survey Report of Investigations No. 30, 34 p.

Keller, G.R., Bland, A.E., and Greenberg, J.K., 1982, Evidence for a late Precambrian tectonic event (rifting) in the eastern mid-continent region, USA: Tectonophysics, v. 93, p. 213–223.

Keller, G.R., Lidiak, E.G., Hinze, W.J., and Braile, L.W., 1983, The role of rifting in the tectonic development of the mid-continent, USA: Tectonophysics, v. 94, special issue, p. 391–412.

Kellog, O.D., 1953, Foundations of potential theory: New York, Dover Publications, 384 p.

Kim, J.W., von Frese, R.R.B., and Kim, H.R., 2000, Crustal modeling from spectrally correlated free-air and terrain gravity data: Geophysics, v. 65, no. 4, p. 1,057–1,069.

Lachenbruch, A.H., 1968, Estimation of the topographic disturbance to superficial thermal gradients: Reviews of Geophysics, v. 6, no. 3, p. 365–400.

Leftwich, T.E., 2011a, Bottom-hole temperature locations and kriged BHT map for Ohio and contiguous region: Columbus, Ohio Department of Natural Resources, Division of Geological Survey, accessed at <http://stategeothermaldata.org>.

Leftwich, T.E., 2011b, Kriged geothermal gradient map for Ohio and contiguous region from BHT data: Columbus, Ohio Department of Natural Resources, Division of Geological Survey, accessed at <http://stategeothermaldata.org>.

Leftwich, T.E., 2012, Heat flow estimates for the Burger Well FEGENCO #1, Belmont County, Ohio: Columbus, Ohio Department of Natural Resources, Division of Geological Survey, accessed at <http://stategeothermaldata.org>.

Leftwich, T.E., Wolfe, M.E., and Wells, J.G., 2011, Bottom-hole temperatures for Ohio: Columbus, Ohio Department of Natural Resources, Division of Geological Survey, accessed at <http://stategeothermaldata.org>.

Leftwich, T.E., Wolfe, M.E., and Wells, J.G., 2012, Additional Ohio bottom-hole temperatures: Columbus, Ohio Department of Natural Resources, Division of Geological Survey, accessed at <http://stategeothermaldata.org>.

Lidiak, E.G., and Zietz, I., 1976, Interpretation of aeromagnetic anomalies between latitudes 37˚N and 38˚N in the eastern and central United States: Geological Society of America Special Paper 167, 37 p.

Lucius, J.E., and von Frese, R.R.B., 1988, Aeromagnetic and gravity anomaly constraints on the crustal geology of Ohio: Geological Society of America Bulletin, v. 100, no. 1, p. 104–116.

McGuire, W.H., and Howell, P., 1963, Oil and gas possibilities of the Cambrian and Lower Ordovician in Kentucky: Lexington, Ky., Spindletop Research Center, 216 p.

Nettleton, L.L., 1971, Elementary gravity and magnetics for geologists and seismologists: Society of Exploration Geologists Monograph Series, v. 1, 121 p.

Ohio Division of Geological Survey, 2006, Bedrock geologic map of Ohio: Columbus, Ohio Department of Natural Resources, Division of Geological Survey Map BG-1, generalized page-size version with text, scale 1:2,000,000, 2 p.

Ravat, D., Finn, C., Hill, P., Kucks, R., Phillips, J., Blakely, R., Bouligand, C., Sabaka, T., Elshayat, A., Aref, A., and Elawadi, E., 2009, A preliminary, full spectrum, magnetic anomaly grid of the United States with improved long wavelengths for studying continental dynamics—A website for distribution of data: U.S. Geological Survey Open-File Report 2009-1258, 2 p.

Thomas, W.A., 2005, Tectonic inheritance at a continental margin: GSA Today, v. 16.

von Frese, R.R.B., and Hinze, W.J., 1993, Geophysics, *in* Trigg, G.L., ed., Encyclopedia of Applied Physics, American Institute of Physics: VCH Publishers, v. 7, p. 149–195.

von Frese, R.R.B, Jones, M.B., Kim, J.W., and Li, W.S., 1997, Spectral correlation of magnetic and gravity anomalies of Ohio: Geophysics, v. 62, p. 365–380.

APPENDIX D

Inventory of Public Domain Seismic Data in Ohio

Ohio Geological Survey, Columbus, Ohio

County	Line No.	Source information										Recording information			Seismic Tapes			CD	Paper copies	Comments
		Operator	Acquisition Co.	Acquisition Date	Energy source	No. of shot points		Line length (mi)	Record length (s)	Sample rate (ms)	Source interval (ft)	Instruments	Group interval (ft)	Nominal fold	No. of Tapes	Observers Notes	Tape Loc.	Loc.	Loc.	
Various (see Fig. 52)	OH-1	Cornell U.	Seismograph Service	10/20/1991	Vibrator	1	2760	172.44	15.0	4	330	DFS-V	330	60					DGS	Cullotta and others (1990); Pratt and others (1989); (1992); Dean and Baranoski (2002); Baranoski and others (2009); Lauren reprocessing available for viewing only
Various (see Fig. 52)	OH-2	Cornell U.	Seismograph Service	10/20/1991	Vibrator	1	1298	81.06	15.0	4	330	DFS-V	330	60	11	N			DGS	Cullotta, and others (1990); Pratt, and others (1989); Riley and others, (p. 27, 1993); Lauren reprocessing available for viewing only
Allen	3-88	B.P. Chemicals	Paragon	11/2/1992	Wacker	102	443	3.55	1.5	2	55	DFS-V	55	30	3	N	SFS	DGS	ODNR-bld I	BP Seismic Survey, 1991 (unpub. Class 1 data)
Allen	4-88	B.P. Chemicals	Paragon	11/2/1992	Wacker	101	484	3.99	1.5	2	55	DFS-V	55	30	4	N	SFS	DGS	ODNR-bld I	BP Seismic Survey, 1991 (unpub. Class 1 data)
Allen	89-1	B.P. Chemicals																DGS	ODNR-bld I	Noise test, BP Seismic Survey, 1991 (unpub. Class 1 data)
Allen	89-2	B.P. Chemicals	Grant-Norpac	12/2/1993	Vibrator	101	1158	11.01	1.5	2	55	DFS-V	55	60	8	N	SFS	DGS	ODNR-bld I	BP Seismic Survey, 1991 (unpub. Class 1 data)
Allen	90-1	B.P. Chemicals	Grant-Norpac	11/2/1994	Vibrator	101	449	3.63	1.5	2	55	FT-1, DFS-V	55	60	21	Y	SFS	DGS	ODNR-bld I	BP Seismic Survey, 1991 (unpub. Class 1 data)
Allen	90-2	B.P. Chemicals	Grant-Norpac	11/2/1994	Vibrator	101	338	2.47	1.5	2	55	FT-1, DFS-V	55	60	10	Y	SFS	DGS	ODNR-bld I	BP Seismic Survey, 1991 (unpub. Class 1 data)
Allen	90-3	B.P. Chemicals	Grant-Norpac	12/2/1994	Vibrator	101	786	7.14	1.5	2	55	FT-1, DFS-V	55	60	33	Y	SFS	DGS	ODNR-bld I	BP Seismic Survey, 1991 (unpub. Class 1 data)
Allen	90-4	B.P. Chemicals	Grant-Norpac	11/2/1994	Vibrator	101	1173	11.17	1.5	2	55	FT-1, DFS-V	55	60	56	Y	SFS	DGS	ODNR-bld I	BP Seismic Survey, 1991 (unpub. Class 1 data)
Allen	90-5	B.P. Chemicals	Grant-Norpac	11/2/1994	Vibrator	1	1196	12.45	1.5	2	55	FT-1, DFS-V	55	60	64	Y	SFS	DGS	ODNR-bld I	BP Seismic Survey, 1991 (unpub. Class 1 data)
Allen	90-6	B.P. Chemicals	Grant-Norpac	12/2/1994	Vibrator	101	615	5.35	1.5	2	55	FT-1, DFS-V	55	60	23	Y	SFS	DGS	ODNR-bld I	BP Seismic Survey, 1991 (unpub. Class 1 data)
Allen	90-7	B.P. Chemicals	Grant-Norpac	12/2/1994	Vibrator	385	531	1.52	1.5	2	55	FT-1, DFS-V	55	60	19	Y	SFS	DGS	ODNR-bld I	BP Seismic Survey, 1991 (unpub. Class 1 data)
Allen	S-2-88	B.P. Chemicals	Paragon	9/2/1992	Wacker	101	317	2.25	1.5	2	55	DFS-V	55	30	2	N	SFS	DGS	ODNR-bld I	BP Seismic Survey, 1991 (unpub. Class 1 data)
Allen	S-5-88	B.P. Chemicals	Paragon	9/2/1992	Wacker	101	388	2.99	1.5	2	55	DFS-V	55	30	3	N	SFS	DGS	ODNR-bld I	BP Seismic Survey, 1991 (unpub. Class 1 data)
Allen	SO-1-88	B.P. Chemicals	Paragon	6/2/1992	Wacker	103	179	1.19	1.5	2	82.5	DFS-V	82.5	30	1	N	SFS	DGS	ODNR-bld I	BP Seismic Survey, 1991 (unpub. Class 1 data)
Ashtabula	ASH-V1-92	RES	Paragon	3/3/1996	Vibrator	101	222	1.72	3.0	2	75	DFS-V	75	60	3	Y	SFS	DGS	ODNR-bld I	RES Seismic Survey, 1992 (unpub. Class 1 data)
Ashtabula	ASH-V2-92	RES	Paragon	3/5/1996	Vibrator	102	510	5.80	3.0	2	75	DFS-V	75	60	8	Y	SFS	DGS	ODNR-bld I	RES Seismic Survey, 1992 (unpub. Class 1 data)
Ashtabula	ASH-V3-92	RES	Paragon	3/21/1996	Vibrator	93	432	4.82	3.0	2	75	DFS-V	75	60	6	Y	SFS	DGS	ODNR-bld I	RES Seismic Survey, 1992 (unpub. Class 1 data)

County	Line No.	Source information										Recording information			Seismic Tapes			CD	Paper copies	Comments
		Operator	Acquisition Co.	Acquisition Date	Energy source	No. of shot points		Line length (mi)	Record length (s)	Sample rate (ms)	Source interval (ft)	Instruments	Group interval (ft)	Nominal fold	No. of Tapes	Observers Notes	Tape Loc.	Loc.	Loc.	
Ashtabula	ASH-V4-92	RES	Paragon	3/31/1996	Vibrator	103	563	6.53	3.0	2	75	DFS-V	75	60	6	Y	SFS	DGS	ODNR-bld I	RES Seismic Survey, 1992 (unpub. Class 1 data)
Ashtabula	ASH-V5-92	RES	Paragon	3/25/1996	Vibrator	102	254	2.16	3.0	2	75	DFS-V	75	60	1	Y	SFS	DGS	ODNR-bld I	RES Seismic Survey, 1992 (unpub. Class 1 data)
Ashtabula	ASH-V6-92	RES	Paragon	4/17/1996	Vibrator	103	289	2.64	3.0	2	75	DFS-V	75	60	1	Y	SFS	DGS	ODNR-bld I	RES Seismic Survey, 1992 (unpub. Class 1 data)
Ashtabula	ASH-V7-92	RES	Paragon	3/26/1996	Vibrator	102	254	2.16	3.0	2	75	DFS-V	75	60	3	Y	SFS	DGS	ODNR-bld I	RES Seismic Survey, 1992 (unpub. Class 1 data)
Belmont	BURGER-V1-06	Battelle	Appalachian Geophysical	7/2/2010	Vibrator	109	365	5.33	4.0	2	110	ARAM 24-70	110	75					DGS	First Energy Burger Power Plant/ line crosses the Ohio R. into Marshall Co., WV; various DOE reports
Belmont	BURGER-V2-06	Battelle	Appalachian Geophysical	7/2/2010	Vibrator	79	327	5.17	4.0	2	110	ARAM 24-70	110	75					DGS	First Energy Burger Power Plant/ line crosses the Ohio R. into Marshall Co., WV; various DOE reports
Belmont	BURGER-V3-06	Battelle	Appalachian Geophysical	7/2/2010	Vibrator	100	149	1.02	4.0	2	110	ARAM 24-70	110	75					DGS	First Energy Burger Power Plant; various DOE reports
Butler	Noise test	Armco Steel													1	NA	SFS		ODNR-bld I	Noise test, Armco Seismic Survey, 1992
Butler	LINE A	Armco Steel	Great Lakes Geophys.	10/29/1995	Vibrator	101	453	5.50	3.0	2	82.5	DFS-V	82.5	60	6	Y	SFS	DGS	ODNR-bld I	Armco Seismic Survey, 1992 (unpub. Class 1 data)
Butler	LINE B	Armco Steel	Great Lakes Geophys.	10/29/1995	Vibrator	101	404	4.73	3.0	2	82.5	DFS-V	82.5	60	6	Y	SFS	DGS	ODNR-bld I	Armco Seismic Survey, 1992 (unpub. Class 1 data)
Butler	LINE C	Armco Steel	Great Lakes Geophys.	10/29/1995	Vibrator	102	331	3.58	3.0	2	82.5	DFS-V	82.5	60	6	Y	SFS	DGS	ODNR-bld I	Armco Seismic Survey, 1992 (unpub. Class 1 data)
Butler	LINE D	Armco Steel	Great Lakes Geophys.	10/29/1995	Vibrator	101	396	4.61	3.0	2	82.5	DFS-V	82.5	60	6	Y	SFS	DGS	ODNR-bld I	Armco Seismic Survey, 1992 (unpub. Class 1 data)
Coshocton	VSP Reiss 3-A	ODNR															DGS	DGS	DGS	Vertical seismic line; in Riley and others, 1993
Lake	ICI-88-1	ICI Americas	Grant/Norpac	11/19/1992	Viberoseis	11	95	1.75	1.5	2	110	MDS-10	110	48	3	Y	SFS	DGS	ODNR-bld I	ICI Americas Seismic Survey, 1988 (unpub. Class 1 data)
Lake	ICI-88-2	ICI Americas	Grant/Norpac	11/19/1992	Viberoseis	13	136	2.56	1.5	2	110	MDS-10	110	48	4	Y	SFS	DGS	ODNR-bld I	ICI Americas Seismic Survey, 1988 (unpub. Class 1 data)
Lake	ICI-88-3	ICI Americas	Grant/Norpac	11/20/1992	Dynamite	4	49	0.94	1.5	2	110	MDS-10	110	48	1	Y	SFS	DGS	ODNR-bld I	ICI Americas Seismic Survey, 1988 (unpub. Class 1 data)
Sandusky	CWM-89-1	CWM	Grant/Norpac	12/3/1993	Vibrator	102	386	4.03	15.0	2	75	DFS-V	75	60	5	Y	SFS	DGS	ODNR-bld I	CWM Seismic Survey, 1991 (unpub. Class 1 data)
Sandusky	CWM-89-2	CWM	Grant/Norpac	11/9/1993	Vibrator	102	655	7.86	15.0	2	75	DFS-V	75	60	11	Y	SFS	DGS	ODNR-bld I	CWM Seismic Survey, 1991 (unpub. Class 1 data)
Sandusky	CWM-89-3	CWM	Grant/Norpac	11/30/1993	Vibrator	107	618	7.26	15.0	2	75	DFS-V	75	60	10	Y	SFS	DGS	ODNR-bld I	CWM Seismic Survey, 1991 (unpub. Class 1 data)
Sandusky	CWM-89-4	CWM	Grant/Norpac	10/29/1993	Vibrator	107	392	4.05	15.0	2	75	DFS-V	75	60	6	Y	SFS	DGS	ODNR-bld I	CWM Seismic Survey, 1991 (unpub. Class 1 data)
Sandusky	CWM-89-5	CWM	Grant/Norpac	12/5/1993	Vibrator	102	492	5.54	15.0	2	75	DFS-V	75	60	7	Y	SFS	DGS	ODNR-bld I	CWM Seismic Survey, 1991 (unpub. Class 1 data)

Sandusky	CWM-89-6	CWM	Grant/Norpac	12/1/1993	Vibrator	107	362	3.62	15.0	2	75	DFS-V	75	60	5	Y	SFS	DGS	ODNR-bld I	CWM Seismic Survey, 1991 (unpub. Class 1 data)
Sandusky	CWM-89-7	CWM	Grant/Norpac	11/14/1993	Vibrator	101	805	10.00	15.0	2	75	DFS-V	75	60	13	Y	SFS	DGS	ODNR-bld I	CWM Seismic Survey, 1991 (unpub. Class 1 data)
Sandusky	CWM-89-8	CWM	Grant/Norpac	10/27/1993	Vibrator	101	805	10.00	15.0	2	75	DFS-V	75	60	8	Y	SFS	DGS	ODNR-bld I	CWM Seismic Survey, 1991 (unpub. Class 1 data)
Sandusky	CWM-89-9	CWM	Grant/Norpac	11/20/1993	Vibrator	101	800	9.93	15.0	2	75	DFS-V	75	60	13	Y	SFS	DGS	ODNR-bld I	CWM Seismic Survey, 1991 (unpub. Class 1 data)
Scioto	89-KD-5	Ken E. Davis & Assoc.	Frontier	3/20/1993	Vibrator	102	691	9.20	13.0	2	165	DFS-V	82.5	30	2	Y	SFS	DGS	ODNR-bld I	Aristech Seismic Survey, 1990 (unpub. Class 1 data) see Kentucky for other lines
Scioto	89-KD-6	Ken E. Davis & Assoc.	Frontier	4/4/1993	Vibrator	103	1233	17.66	13.0	2	165	DFS-V	82.5	30	?	Y	?		ODNR-bld I	Aristech Seismic Survey, 1990 (unpub. Class 1 data) see Kentucky for other lines; 89-KD-6 tapes missing
Warren	ODNR-1-88	Consortium	Paragon	10/12/1992	Dynamite	111	484	7.77	2.0	2	110	DFS-V	110	60				DGS	DGS	Shrake and others, 1990 (IC No. 56)
Kentucky																				
Boone	EAST BEND-V1-06	Battelle	Appalachian Geophysical	11/2/2010	Vibrator	105	450	7.19	4.0	2	110	ARAM 24-70	110	75					DGS	Duke Energy East Bend Power Plant/ line crosses the Ohio R. into Switzerland Co., IN; various DOE reports
Boone	EAST BEND-V2-06	Battelle	Appalachian Geophysical	11/2/2010	Vibrator	102	411	6.44	4.0	2	110	ARAM 24-70	110	75					DGS	Duke Energy East Bend Power Plant/ line crosses the Ohio R. into Ohio & Switzerland Cos., IN; various DOE reports
Carter	89-KD-1	Ken E. Davis & Assoc.	Frontier	4/5/1993	Vibrator	101	1145	16.31	13.0	2	165	DFS-V	82.5	30	3	Y	SFS	DGS	ODNR-bld I	Aristech Seismic Survey, 1990 (unpub. Class 1 data)
Carter	89-KD-2	Ken E. Davis & Assoc.	Frontier	4/16/1993	Dynamite/ Vibrator	125	1017	13.94	13.0	2	165	DFS-V	82.5	30	4	Y	SFS	DGS	ODNR-bld I	Aristech Seismic Survey, 1990 (unpub. Class 1 data)
Carter	89-KD-2A	Ken E. Davis & Assoc.	Frontier	4/29/1993	Dynamite/ Vibrator	103	297	3.03	13.0	2	165	DFS-V	82.5	30	1	Y	SFS	DGS	ODNR-bld I	Aristech Seismic Survey, 1990 (unpub. Class 1 data)
Carter	89-KD-3	Ken E. Davis & Assoc.	Frontier	3/15/1993	Vibrator	102	716	9.59	13.0	2	165	DFS-V	82.5	30	2	Y	SFS	DGS	ODNR-bld I	Aristech Seismic Survey, 1990 (unpub. Class 1 data)
Carter	89-KD-4	Ken E. Davis & Assoc.	Frontier	4/25/1993	Dynamite	103	358	3.98	4.0	2	165	DFS-V	82.5	30	1	Y	SFS	DGS	ODNR-bld I	Aristech Seismic Survey, 1990 (unpub. Class 1 data)
Carter	89-KD-7	Ken E. Davis & Assoc.	Frontier	4/14/1993	Vibrator	102	361	4.05	13.0	2	165	DFS-V	82.5	30	1	Y	SFS	DGS	ODNR-bld I	Aristech Seismic Survey, 1990 (unpub. Class 1 data) p. 22 in Riley and others, 1993; p. 191 in Harris and Baranoski, 1996; p.14, Harris and Baranoski,1997
West Virginia																				
Mason	MP-01-03	Battelle	Appalachian Geophysical	7/8/2007	Dynamite/ Vibrator	101	318	4.52	12.0	2	110	ARAM 24	110	60					DGS	AEP Mountaineer Power Plant; various DOE reports
Mason	MP-02-03	Battelle	Appalachian Geophysical	7/2/2007	Dynamite/ Vibrator	100	416	6.58	12.0	2	110	ARAM 24	110	60					DGS	AEP Mountaineer Power Plant; various DOE reports

References Cited

Baranoski, M.T., Dean, S.L., Wicks, J.L., and Brown, V.M., 2009, Unconformity-bounded seismic reflection sequences define Grenville-age rift system and foreland basins beneath the Phanerozoic in Ohio: Geosphere, v. 5, no. 2, p. 140–151.

Culotta, R.C., Pratt, T., and Oliver, J., 1990, A tale of two sutures: COCORP's deep seismic surveys of the Grenville province in the eastern U.S. midcontinent: Geology, v. 18, no. 7, p. 646–649.

Dean, S.L. and Baranoski, M.T., 2002, Precambrian hydrocarbon potential in Ohio: Oil & Gas Journal, v. 100, no. 29, p. 34–37 and v. 100, no. 30, p. 37–40.

Harris, D.C., and Baranoski, M.T., 1996, Play Cpk: Cambrian pre-Knox group play, *in* Roen, J.B., and Walker, B.J., eds., The atlas of major gas plays in the Appalachian Basin: Morgantown, W. Va., West Virginia Geological and Economic Survey, V-25, p. 187–192.

Harris, D.C., and Baranoski, M.T., 1997, Cambrian pre-Knox group play in the Appalachian Basin: Ohio Department of Natural Resources, Division of Geological Survey Information Circular 60, 26 p.

Pratt, T., Culotta, R., Hauser, E., Nelson, D., Brown, L., Kaufman, S., Oliver, J., and Hinze, W., 1989, Major Proterozoic basement features of the eastern midcontinent of North America revealed by recent COCORP profiling: Geology, v. 17, no. 6, p. 505–509.

Shrake, D.L., Wolfe, P.J., Richard, B.H., Swinford, E.M., Wickstrom, L.H., Potter, P.E., and Sitler, G.W., 1990, Lithologic and geophysical description of a continuously cored hole in Warren County, Ohio, including description of the Middle Run Formation (Precambrian?) and a seismic profile across the core site: Ohio Department of Natural Resources, Division of Geological Survey Information Circular 56, 11 p.

APPENDIX E

List of Synthetic Seismograms in Ohio

Ohio Geological Survey, Columbus, Ohio

APINO	LONG	LAT	TWP	LOCATION	LEASE	OPERATOR	COMP DATE	LTD	DEEPFM	DISPLAY SCALE	COMMENTS
1611318114	-84.575	37.811			SHERRER	TEXACO INC.		5800	PCMB	7.5 in./sec.	
1611320747	-84.509	37.819			WOLFINGBARGER	TEXACO INC.		6072	PCMB	7.5 in./sec.	
3400120011	-83.365	39.049	FRANKLIN	VMS 7372	RUSSELL & TENER	OXFORD	7/7/1979	3886	PCMB	7.5 in./sec.	
3400363691	-84.130	40.712	SHAWNEE	SEC 2	STANDARD OIL CO	VISTRON CORP	6/27/1968	3118	MDLR	10 in./sec.	
3400720191	-80.937	41.699	TRUMBULL	LOT 30N	A RHOA	HORIZON OIL INC	8/12/1965	3523	PCMB	10 in./sec.	
3400722038	-80.788	41.604	NEW LYME	LOT 8	PAROBEK	POI ENERGY,INC.	7/29/1982	7118	PCMB	10, 15, 20 in./sec.	
3401120071	-84.394	40.504	ST MARYS	SEC 22	D & B HOELSCHER	WEST OHIO GAS CO	12/5/1970	3068	PCMB	7.5 in./sec.	

3402320002	-83.585	39.966	PLEASANT	VMS 4673	R V & E M BROWN	N V EDMUND OIL AND GAS EXPLORATION	3/29/1962	3647	PCMB	7.5, 10 in./sec.	
3402720005	-83.623	39.382	WAYNE	LOT 1065	VAN PELT	KEWANEE OIL CO	10/12/1959	3263	PCMB	15 in./sec.	
3402720010	-83.702	39.527	WILSON	VMS 743	COY	STOCKER & SITLER INC	01/18/83	3601	PCMB	10, 15 in./sec.	AC lab?
3403122053	-82.002	40.323	JEFFERSON	4TH QTR	E L LEE	BOB TATUM	6/16/1971	6957	PCMB	7.5 in./sec.	
3403124118	-81.833	40.369	KEENE	SEC 2	J BURRELL	POMSTONE CORP	05/28/81	7347	PCMB	15 in./sec.	
3403126379	-81.644	40.325	ADAMS	SEC 12	L REISS	NGO DEVELOPMENT CORP	1/18/1992	7165	KNOX	15, “75” in./sec.	DDF-7 VSP
3403520821	-81.686	41.465	CITY OF CLEVELAND	LOT 85	JONES & LAUGHLIN STEEL CORP	JONES & LAUGHLIN STEEL CORP	6/1/1974	5801	MNSM	10 in./sec.	
3404120009	-82.933	40.395	OXFORD	LOT 5	L & K SPRAIN	KARL WEHMEYER & CO	5/11/1962	3100	PCMB	15 in./sec.	
3404120014	-83.165	40.393	RADNOR	LOT 7, VMS 6138	HUMPHREYS	JOHN ADAMS	5/18/1963	2329	KNOX		
3404120322	-83.226	40.351	THOMPSON	LOT 7, VMS 6138	JOLLIFF	FUNK EXPLORATION INC	1/19/1985	3380	PCMB	7.5 in./sec.	
3404120329	-83.060	40.343	TROY	LOT 36, 1ST QTR	CASE	FUNK EXPLORATION INC	2/18/1985	3567	PCMB	15 in./sec.	
3404120354	-82.770	40.262	TRENTON	SEC 10	COCKRELL-GODSHALL UNIT	POLING R C CO INC	1/22/1991	4766	PCMB	15 in./sec.	
3404720011	-83.376	39.580	MARION	VMS 8493	DUFF UNIT	STOCKER & SITLER INC.	01/27/83	3352	PCMB	10, 15 in./sec.	AC lab?
3405920782	-81.720	40.037	ADAMS	SEC 15	W MARSHALL COMM	LAKE SHORE PIPELINE CO.	5/31/1961	4791	PCMB	15 in./sec.	
3406720103	-80.966	40.262	GREEN		ROY BIRNEY	SANFORD MCCORMICK	1/6/1969	10177	RSRN	15 in./sec.	
3406720737	-81.197	40.195	MOOREFIELD	SEC 29	T ZECHMAN	RED HILL DEVELOPMEMT	1/15/1986	10623	PCMB	15 in./sec.	
3407525253	-81.862	40.457	BERLIN	SEC 4	HERSHBERGER UNIT	NEWSTAR ENERGY USA INC	4/6/1997	6756	KNOX	11.5 in./sec.	AC lab?
3407524922	-81.766	40.579	MECHANIC	SEC 12	HERSHBERGER UNIT	COLUMBIA NATURAL RESOURCES	7/13/1990	6289	KNOX	11.5 in./sec.	

APINO	LONG	LAT	TWP	LOCATION	LEASE	OPERATOR	COMP DATE	LTD	DEEPFM	DISPLAY SCALE	COMMENTS
3407920102	-82.638	39.009	FRANKLIN	SEC 8, LOT 42	F & C TREPANIER	NUCORP ENERGY CORP	6/2/1977	6043	PCMB	15 in./sec.	
3408520280	-81.162	41.746	PERRY	LOT 37	CALHIO CHEM.,INC.	CALHIO CHEM.,INC.	3/25/1980	6100	PCMB	7.5 in./sec.	
3408925446	-82.402	39.964	LICKING	L 25	CHURCH	OXFORD OIL CO	01/18/92	5285	CNSG	15 in./sec.	
3409120096	-83.616	40.416	RUSH CREEK	VMS 3472	R PRINKEY UNIT	ASHTOLA EXPLORATION CO INC	11/5/1991	3254	PCMB	15 in./sec.	
3410321201	-81.739	41.177	GRANGER	LOT 42, REMSEN TR	M WARNER	WISER OIL CO.	8/25/1959	6731	PCMB	10 in./sec.	
3411720033	-82.924	40.437	WESTFIELD	SEC 21	J HENRY	K WEHMEYER	1/8/1962	4044	PCMB	15 in./sec.	
3411721388	-82.822	40.357	BENNINGTON	LOT 13	J & B MCBEE	ROBERT WRAY	4/11/1964	4412	MNSM	15 in./sec.	
3412121278	-81.347	39.611	ELK	SEC 31	R ULLMAN	AMOCO	2/1/1967	11442	PCMB	7.5 in./sec.	
3412920029	-82.880	39.690	WALNUT	SEC 22	WRIGHT J & NOECKER HELEN	WEST BAY EXPLORATION CO.	9/12/1991	3224	KNOX	13.5 in./sec.	
3413323809	-81.335	41.038	SUFFIELD	LOT 17	KLINE	EXCALIBUR EXPLORATION INC	11/24/90	7260	CNSG?	15 in./sec.	
3413323873	-81.279	41.011	RANDOLPH	LOT 28	GEIGER	EXCALIBUR EXPLOR INC	09/21/91	7492	CNSG?	10 in./sec.	
3414120005	-83.265	39.368	BUCKSKIN	VMS 2309	J H FULLER	RELIANCE OIL	6/25/1963	2566	KNOX	10 in./sec.	
3414320077	-82.913	41.354	TOWNSEND	SEC 33	V & I HAFF	EAST OHIO GAS CO.	11/17/1960	3123	PCMB	10 in./sec.	
3414520257	-83.238	38.989	RARDEN	LOT 103	H SMITH	ADOBE OIL & GAS CORP	11/1/1979	4432	PCMB	10 in./sec.	
3414560033	-82.821	38.592	GREEN	GERVAIS TR	ARISTECH CHEMICAL CORP #3	ARISTECH CHEMICAL CORP		6109	PCMB	7.5 in./sec.	sidetracked
3416560005	-84.116	39.566	WAYNE	SEC 14	AMERICAL AGGREGATES	OHIO DIVISION OF GEOLOGICAL SURVEY	5/1/1989	2690	MDLR	.65 IN./SEC.	
4705300423	-81.938	38.976	MASON		AEP	AEP		9190	PCMB	10 in./sec.	

APPENDIX F

Information on Reiss No. 3-A Vertical Seismic Profile (VSP)

Ohio Geological Survey, Columbus, Ohio

The #3-A Reiss Well (APINO 3403126379) was drilled in 1992 by NGO Development in Adams Township, Coshocton County, Ohio. The well reached total depth of 7,166 ft in the Copper Ridge dolomite. Open-hole data was collected from this well as part of a case study for the U.S. Department of Energy on the Cambrian Rose Run sandstone (Riley and others, 1993 [see below]). The data was integrated into the report to gain a better understanding of the stratigraphy and geophysical properties of Ordovician and Cambrian rock units in the vicinity of the Bakersville field. The files contained on this DVD include data and scanned reports on a vertical seismic profile (VSP), sidewall core analyses, an LAS file, and TIF format geophysical logs. The original 9-track VSP data was copied into two SEG-Y files (IVSP.sgy and OVSP.sgy). Files IVSP.doc and OVSP.doc provide header information. Specialized seismic processing software is required to read the SEG-Y files. The file **BoreholeSeismicReportForTheReiss3-AInCoshoctonCountyOhio.pdf** includes processing results, modeling, and interpretation. The file **ReissNo3-A_VSPFieldComputationReport.pdf** includes field data and computations. The field reports in the file **ReissNo3-A_VSPFieldComputationReport.pdf** are the best available copies. The reader is referred to Riley and others, (1993) for addition information.

Riley, R.A., Harper, J.A., Baranoski, M.T., Laughrey, C.D., and Carlton, R.W., 1993, Measuring and predicting reservoir heterogeneity in complex deposystems—The late Cambrian Rose Run sandstone of eastern Ohio and western Pennsylvania: U.S. Department of Energy, contract no. DE-AC22-90BC14657, 257 p.

Index of files on the DVD

ReissNo3-A readme.doc
BasicRockProperties—No.3-A_ReissWell—RoseRunSandstone.pdf
BoreholeSeismicReportForTheReiss3-AInCoshoctonCountyOhio.pdf
ReissNo3-A_VSPFieldComputationReport.pdf
RotarySidewallCores—No.3-A_ReissWell.pdf
REISS_3A_VSP FIELD DATA
VSP.doc
IVSP.sgy
OVSP.doc
OVSP.doc
GEOPHYSICAL LOGS
README DOCS
    Abbreviations for Geophysical Logging Companies.doc
    Abbreviations for Geophysical Logs.doc
    Disclaimer_nondistribution.doc
    Explanation of scanning procedure.doc
    34031263790000.las
34031263790000_CORE_SCH_3953_7130_Y_126.tif
34031263790000_CP-FMS_SCH_3590_7095_Y.tif
34031263790000_CP-FMS_SCH_3950_7020_Y_TH85.tif
34031263790000_CP-LI-SYM-DM_SCH_5900_7100_N_TH85.tif
34031263790000_CP-LI_SCH_5930_7110_N_126.tif
34031263790000_CP-LI_SCH_5930_7110_N_126_TH85.tif
34031263790000_CP-LI_SCH_5930_7114_N_TH85.tif
34031263790000_CP-MP_SCH_5890_7150_N.tif
34031263790000_CP-MP_SCH_5890_7150_N_TH85.tif
34031263790000_DM_SCH_3900_7020_Y_TH85.tif
34031263790000_DM_SCH_3950_7020_Y.tif
34031263790000_EMT_SCH_5876_7145_N_126.tif
34031263790000_EMT_SCH_5876_7145_N_126_TH100.tif
34031263790000_FMS_SCH_3900_7020_Y_126_TH95.tif
34031263790000_FMS_SCH_3950_7020_Y_126.tif
34031263790000_GR-CBL-AVD_AT_3650_7095_Y.tif
34031263790000_GR-CBL-AVD_AT_3650_7095_Y_TH90.tif
34031263790000_GR-LL-MLL_SCH_970_7166_N_126.tif
34031263790000_GR-LL-MLL_SCH_970_7166_N_126_TH95.tif
34031263790000_GR-N-D-PE-LI_SCH_50_7154_N_125_TH90.tif
34031263790000_GR-N-D-PE-LI_SCH_50_7154_N_126.tif
34031263790000_GR-S_SCH_970_7158_N_126.tif
34031263790000_GR-S_SCH_970_7158_N_126_TH90.tif
34031263790000_MUD_STG_2840_7164_N.tif
34031263790000_MUD_STG_850_7165_Y_TH85.tif
34031263790000_NGT_SCH_5876_7118_N_126_TH95.tif
34031263790000_NGT_SCH_5926_7118_N_126.tif
34031263790000_VSP-INCIDENT_SCH_970_7134_N_126_TH85.tif
34031263790000_VSP-OFFSET_SCH_970_7134_Y_126_TH85.tif

Recommended bibliographic citation for DDF-7

Ohio Division of Geological Survey, 2012, Compilation of miscellaneous reports and data for NGO Development #3-A Reiss well in Adams Township, Coshocton County, Ohio: Columbus, Ohio Department of Natural Resources, Division of Geological Survey Digital Data File 7.

APPENDIX G

Map of Major Proprietary Seismic Lines in Ohio

Ohio Geological Survey, Columbus, Ohio

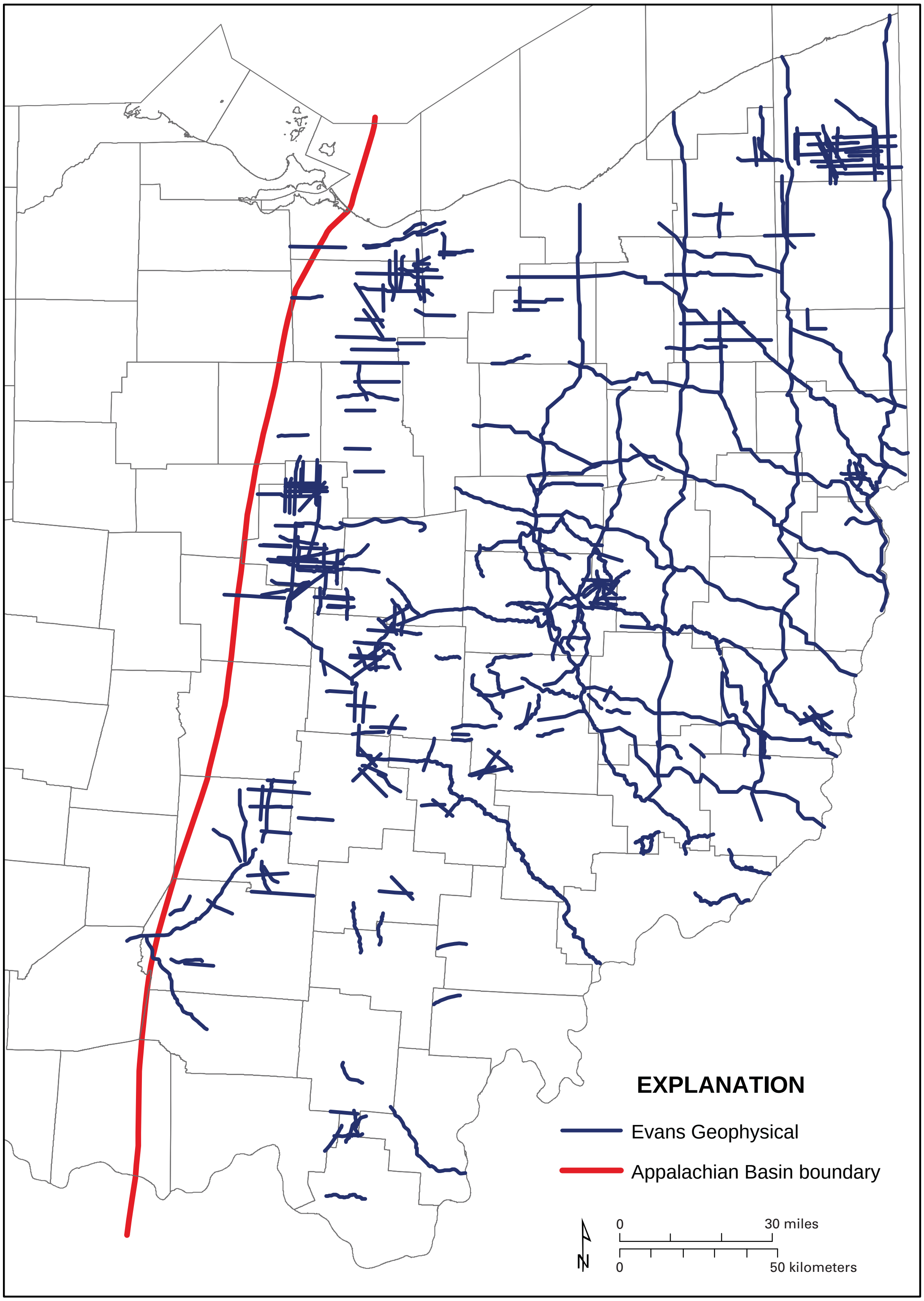

FIGURE G-1.—Map of major proprietary seismic lines in Ohio.

APPENDIX H

Delineating Subsurface Structural Trends by Applying Geostatistics to Dense Elevation Data Sets

Michael Solis—Ohio Geological Survey, Columbus, Ohio

Introduction

Completion Cards

Driller reported tops included with well completion cards are often an overlooked resource available to efficiently map a large number of data points. Currently, the Ohio department of Natural Resources, Division of Mineral Resources Management (DMRM) is tasked with recording all well information, including drillers' tops, as it is submitted into the Ground Water Protection Council's Risk Based Data Management System (RBDMS) database (McDonald and others, 2005). Many drillers have worked in Ohio for years and have a strong understanding of subsurface stratigraphy; however, not all reported tops are accurate. Geostatistical methods can be used to sort through and discard a large number of poorly identified tops in a relatively expeditious way.

Background

Several subsurface formation tops have been geostatistically mapped for Ohio (Wickstrom and others, 2005; Greb and others, 2009; Carter and others, 2010). Generally, these data sets were heavily dependent on geologists' picked tops from several projects (Gray and others, 1982; Baranoski and others, 1988; Riley, 2001; Ohio Division of Geological Survey, 2003; Patchen and others, 2006; Carter and others, 2010; M. T. Baranoski, table of formation tops, written commun., 2011).

With the previous mapping, geologists' picks were contoured to show regional trends and variations for each unit. When drillers' tops were used to augment geologists' picks, the drillers' tops were selected to have an even distribution and contoured to show regional structural trends along the horizon surface. Very few localized structural trends were consistently identifiable; from horizon to horizon, on these previously created maps. Mason (1999) mapped a series of surface lineaments (see Fig. 28) and demonstrated that the lineaments corresponded to structural trends evident on a detailed Onondaga Limestone surface, suggesting that the trends mapped on the Onondaga surface may be continuous to the surface. Mason did not demonstrate that these trends extended deeper. In an effort to better identify localized trends and develop a structural framework for Ohio, all available drillers' and geologists' tops were used to contour subsurface horizons. The surfaces that were contoured were selected based on data density (greater than 50,000 wells) and include the Wenlockian (Silurian) Dayton Formation ("Packer Shell"), the Middle Devonian Onondaga Limestone ("Big Lime"), and the Upper Devonian Berea Sandstone (see Figs. 53-56).

Methodology

Data Gathering and Initial Evaluation

After querying the Division of Geological Survey RBDMS interface, the Integrated Geologic Data System (IGDS), by formation top, the exported spreadsheet is converted to a point shapefile. This shapefile is separated by method obtained (geologists' tops versus drillers' tops). The shapefile with the drillers' tops is sorted for duplicate tops by building small, 5-ft buffers around each well location. The buffers are then intersected leaving behind only the buffered locations where more than one well is located. The well buffers are used to select from the geologists' well-location shapefile and duplicate wells are deleted. The duplicates are discarded based on the most recent geologists' tops; the most recent pick is kept. This process is repeated until there are no more intersection buffers created by duplicate well locations. The final set of geologists' well locations are then buffered and used to remove driller-recorded tops in the same location. Once all the duplicate tops are removed, the two well location shapefiles are combined.

Once the driller/geologist tops point file is complete, subsea elevation is calculated from measured depth using ground elevation. If the ground elevation is unavailable, then the raster elevation is used. If there is no elevation data, then the well is dropped. Some older wells have no location data associated with them and are deleted. The final well location shapefile consists of wells with locations and subsurface elevations as well as other well header information.

Neighborhood Statistics

Kriging using ESRI ArcMap 9.3.1 Geostatistical Analyst creates a rough surface to view the veracity of the initial dataset. Using ordinary kriging to create a prediction map, the data is detrended using polynomial (power 2) to remove the regional dip; anisotrophy is not used. Lag size is determined by Average Nearest Neighbor calculation for each formation top dataset. Neighborhood type is eighths, and neighborhood ellipse axes are determined by the distance between wells where data is sparse. After the surface is created, a grid is exported with a 1,500-ft cell size. The grid is then contoured with a 20-ft contour interval.

Cluster analysis was completed by using ESRI's Voronoi Map to calculate neighborhood statistics. Selecting points where the cluster number for a cell is *–1* often corresponds to the initial contoured bullseyes. Wells are then selected using the *–1* cluster numbered and deleted. The data is gridded again, using the same parameters (calculating a new lag size each time wells are deleted). This process is repeated until there are no longer cluster numbers of *–1* in high data density areas. The final point data is used to calculate another grid, which is used to verify the point data. The calculated error greater than 100 ft or less than –100 ft is used to select problem wells. When data density is low, error greater than 100 ft and less than –100 ft is acceptable. This point data set is then re-gridded and the point set is compared to the surface to verify that there are no residuals greater than 100 ft or less than –100 ft.

After as many as eighteen iterations of the process, approximately one-third of the data set is removed. From the final point data set, as many as three grids are created to describe the surface—one surface to describe the areas with high data density and two surfaces to describe low data density areas. The final contours generated from these surfaces are either: left unedited (Berea Sandstone), hand-edited (Onondaga Limestone), or stitched together (Dayton Formation). To create a seamless contour map, the edited contours are then used to create a raster using topo-to-raster. The resulting raster is multiplied by a unique boundary raster and then contoured (Table H-1).

Results

The initial results suggest the computed surfaces closely approximate the large number of tops for each model. Root mean square (RMS) errors are 26 ft (average), 19 ft, and 17 ft for the Dayton Formation, Onondaga Limestone, and Berea Sandstone, respectively (Table H-1). Because of the varying data distribution for each formation, the final surface grids were produced using different techniques.

Dayton Formation

The central zone of the Dayton Formation has high data density (Fig. H-1A) and an average nearest neighbor of 1,439-ft (Table H-1). The central zone was kriged with all well locations. Once the preliminary surface is created, a grid with a cell size of 1,500 ft is created. Twenty foot interval contours were generated from the initial grid, and the central zone contours were clipped out. Using the same values entered into Geospatial Analyst, a standard error prediction map was produced to check the fit of the grid (Fig. H-1B). Where well density is high, the standard error is low, and where density is low, the error is higher.

The western and eastern zones shared a similar average nearest neighbor of 3,648 ft (Table H-1and Fig. H-1). Because of their similarity, and to avoid edge-matching issues, the western and eastern zones were kriged simultaneously (along with the central zone). Contours were generated at a 20-ft interval. The central zone was removed. The finished contours were edited together.

The resulting surface (see Fig. 54) shows several continuous northwest–southeast sub-parallel trends. Smaller east–west trends are also evident (Tuscarawas County and south). Several of the identified trends closely approximate faults mapped by Baranoski (2002), such as the Star Fault System, Cambridge Cross Strike Structural Discontinuity, Highlandtown Fault, Akron Fault Suffield Fault, and Middleburg Fault, suggesting these basement faults may

TABLE H-1.—*Summary of kriging results for Dayton Formation, Onondaga Limestone, and Berea Sandstone*

Formation	$n_{initial}$	n_{final}	Kriging Type	Trend Removal	Lag (ft)	Model	Anisotrophy	Neighborhood	Axis (ft)	RMS Error (ft)	Regression Function
Berea Sandstone	Geo = 17,856	Geo = 16,741	Ordinary	Second Order	1,061	Stable	FALSE	Standard	50,000	17.44	0.999039455454221 * x + -0.0567237008665345
	Drill = 111,761	Drill = 78,885									
	bt24k = 13,524	bt24k = 13,524									
	Tot = 143,141	Tot = 109,150									
Onondaga Limestone ("Big Lime")	Geo = 16,001	Geo = 15,357	Ordinary	Second Order	1,414	Stable	FALSE	Standard	50,000	18.59	0.999810247426246 * x + -0.301320980876199
	Drill = 56,081	Drill = 52,288									
	Tot = 72,082	Tot = 67,645									
Dayton Limestone ("Packer Shell") (central)	Geo = 10,109	Geo = 9,663	Ordinary	Second Order	1,439	Stable	FALSE	Standard	50,000	29.17	0.999551876295574 * x + -1.25178635477005
	Drill = 56,107	Drill = 52,125									
	Tot = 66,216	Tot = 61,788									
Dayton Limestone ("Packer Shell") (east/west)	Geo = 10,109	Geo = 9,663	Ordinary	Second Order	3,648	Stable	FALSE	Standard	100,000	22.78	0.999649622227872 * x + -0.968977815089602
	Drill = 56,107	Drill = 52,125									
	Tot = 66,216	Tot = 61,788									

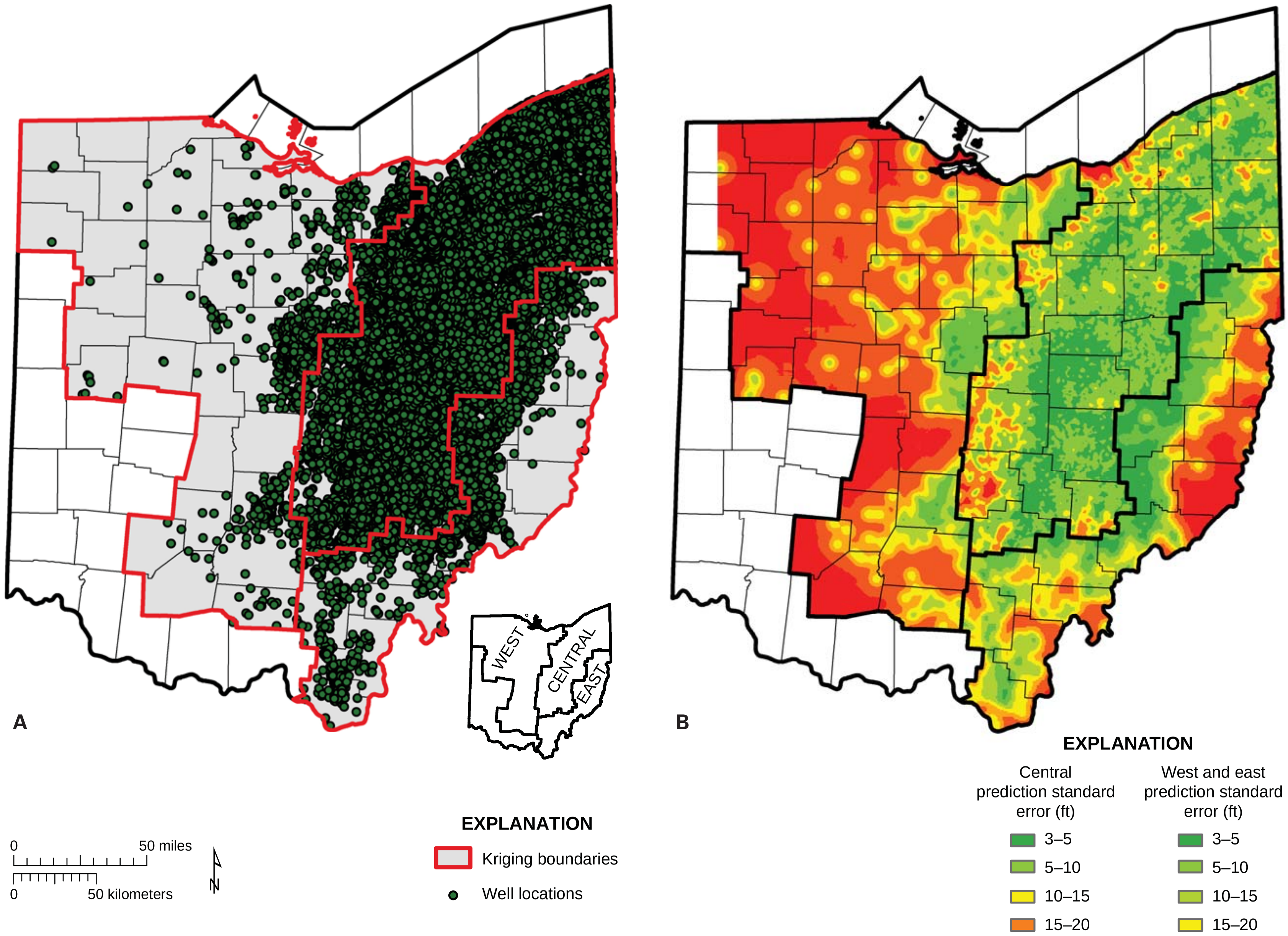

Figure H–1.—(**A**) Distribution of Dayton Formation well locations and western, central, and eastern boundaries used for kriging. (**B**) Standard error map for Dayton Formation western, central, and eastern kriging results prior to splicing contours together. Less error results where data density is high.

prorogate well into the Paleozoic section. A large structural low in Mahoning County is defined by one well (API No. 34099224950000). The drillers' top is within the fitted surface error tolerance. Repeating this method on a preliminary Queenston Shale (see Fig. 52) surface resulted with the same structural low in Mahoning County. Preliminary cross sections through the low suggest a north-striking, east-dipping reverse fault is penetrated by well 34099224950000. The lack of well control does not allow for proper automated drawing of the surface in the vicinity of the low. Further work needs to continue in northeast Ohio to resolve structural anomalies.

Onondaga Limestone

The Onondaga Limestone has approximately the same data density as the Dayton Formation, but it features a better distribution of data (Fig. H-2A). An average nearest neighbor of 1,414 ft was used for the lag size (Table H-1). The standard error prediction map displays the error as minimized in the areas with the densest data (Fig. H-2B). The preliminary surface was exported to grid and then contoured at a 20-ft interval. In the areas where data density is low, contours were hand edited to remove jagged contour lines.

The resulting surface (see Fig. 55) shows many trends consistent with basement faults as with the Dayton Formation (Baranoski, 2002; Fig. 54). Furthermore; many of the new proposed trends identified on the Dayton Formation surface are evident on the Onondaga Limestone surface. The proposed trends project approximately 1,600 ft through the Paleozoic section, suggesting that these proposed trends are near-vertical plane intersections between the Dayton and the Onondaga.

Berea Sandstone

The Berea Sandstone had the highest data density and the best data distribution of the three mapped formations (Table H-1; Fig. H-3A). Because the Berea outcrops, the Berea contact (Slucher and others, 2006) was converted to points every 1,500 ft. Elevations were assigned to outcrop points from a bedrock topography grid (Brockman and others, 2003). A total of 109,150 well and outcrop points were used, with an average of 1,061 ft apart (prior to the addition of the bedrock topography points). After generating contours, no editing was required.

Again, trends evident on the Dayton and the Onondaga are visible on the surface of the Berea Sandstone (see Fig. 56). These trends consistently are in the same locations through approximately 7,000 ft of the Paleozoic section. Furthermore, in Washington County structural features mapped using geostatistics were previously identified by Baranoski (M. T. Baranoski, structure contour map of the Berea Sandstone, unpub. data, 2012).

Discussion

The proposed trends/lineaments for each map produced are not structurally diagnostic by themselves. However, many of the proposed trends are incident to multiple horizons, indicating that these proposed trends do describe near-vertical planes in the subsurface. At this time, the precise nature and location of the trends is unknown. The preliminary trends marked on the maps (see Fig. 57) serve as areas to investigate further.

In order to verify the locations and nature of these trends, cross sections through structural features need to be drafted, and evaluation of the recently acquired seismic lines from Evans Geophysical (see Appendix G) needs to be completed. Once the structural framework of Ohio is better defined, more predictive facies models can be developed. These facies models could be used to help understand porosity trends in the subsurface.

References Cited

Baranoski, M.T., 2002, Structure contour map on the Precambrian unconformity surface in Ohio and related basement features: Columbus, Ohio Department of Natural Resources, Division of Geological Survey Map PG-23, scale 1:500,000, 18 p. text.

Baranoski, M.T., Riley, R.A., Wickstrom, L.W., and Stith, D.A., 1988, Analysis of stratigraphic and production relationships of Devonian Shale gas reservoirs in Ohio: Columbus, Ohio Department of Natural Resources, Division of Geological Survey final report for Gas Research Institute, GRI contract no. 5085-213-1154, 49 p., 15 plates.

Brockman, C.S., Larsen, G.E., Pavey, R.R., Schumacher, G.A., Shrake, D.L., Slucher, E.R., Swinford, E.M., and Vorbau, K.E, 2003, Shaded bedrock-topography map of Ohio: Columbus, Ohio Department of Natural Resources, Division of Geological Survey Map BG-3, scale 1:500,000.

Carter, K.M., Kostelnik, J.J., Laughrey, C.D., Harper, J.A., Barnes, D.A., Harrison, W.B., III, Venteris, E.R., McDonald, James, Wells, J.G., Wickstrom, L.H., Perry, C.J., Avary, K.L., Lewis, J.E., Hohn, M.E., Stolorow, A., Slater, B.E., and Greb, S.F., 2010, Characterization of geologic sequestration opportunities in the MRCSP region, Middle Devonian–Middle Silurian formations—MRCSP phase II topical report, October 2005–October 2010: Midwest Regional Carbon Sequestration Partnership report submitted to Battelle Memorial Institute and U.S. Department of Energy, Cooperative Agreement No. DE-FC26-05NT42589, 150 p.

Gray, J.D., Struble, R.A., Carlton, R.W., Hodges, D.A., Honeycutt, F.M., Kingsbury, R.H., Knapp, N.F., Majchszak, F.L., and Stith, D.A., 1982, An integrated study of the Devonian-age black shales in eastern Ohio—Ohio Department of Natural Resources, Division of Geological Survey final report for U.S. Department of Energy Eastern Gas Shales Project: U.S. Department of Energy Report No. DOE/ET/12131-1399, 169 p.

Greb, S.F., Harris, D.C., Solis, M.P., Anderson, W.H., Drahovzal, J.A., Nuttall, B.C., Riley R.A., Solano-Acosta, W., Rupp, J.A., and Gupta, N., 2009, Cambro-Ordovician Knox carbonates as seal and potential targets for carbon sequestration in the eastern Midcontinent U.S.A., *in* Grobe, M., Pashin, J.C., and Dodge, R.L., eds., Carbon dioxide sequestration in geological media—State of the science: American Association of Petroleum Geologists Studies in Geology 59, p. 241–259.

Mason, G., 1999, Structurally related migration of hydrocarbons in the central Appalachian basin of eastern Ohio, *in* Into the new millennium—The changing face of exploration in the Knox play: Ohio Geological Society, Sixth Annual Fall Symposium, Akron, Ohio, Oct. 20, 1999 [Proceedings], p. 20–33.

McDonald, J., Wickstrom, L.H., Steck, C.D., and Wells, J.D., 2005, Conversion of the Ohio oil- and gas-well township-location maps to a geographic information system: history and methodology: Columbus, Ohio Department of Natural Resources, Division of Geological Survey Information Circular No. 61, 32 p.

Ohio Division of Geological Survey, 2003, DDF-2 [Well information and records from the Risk-Based Data Management System (RB-

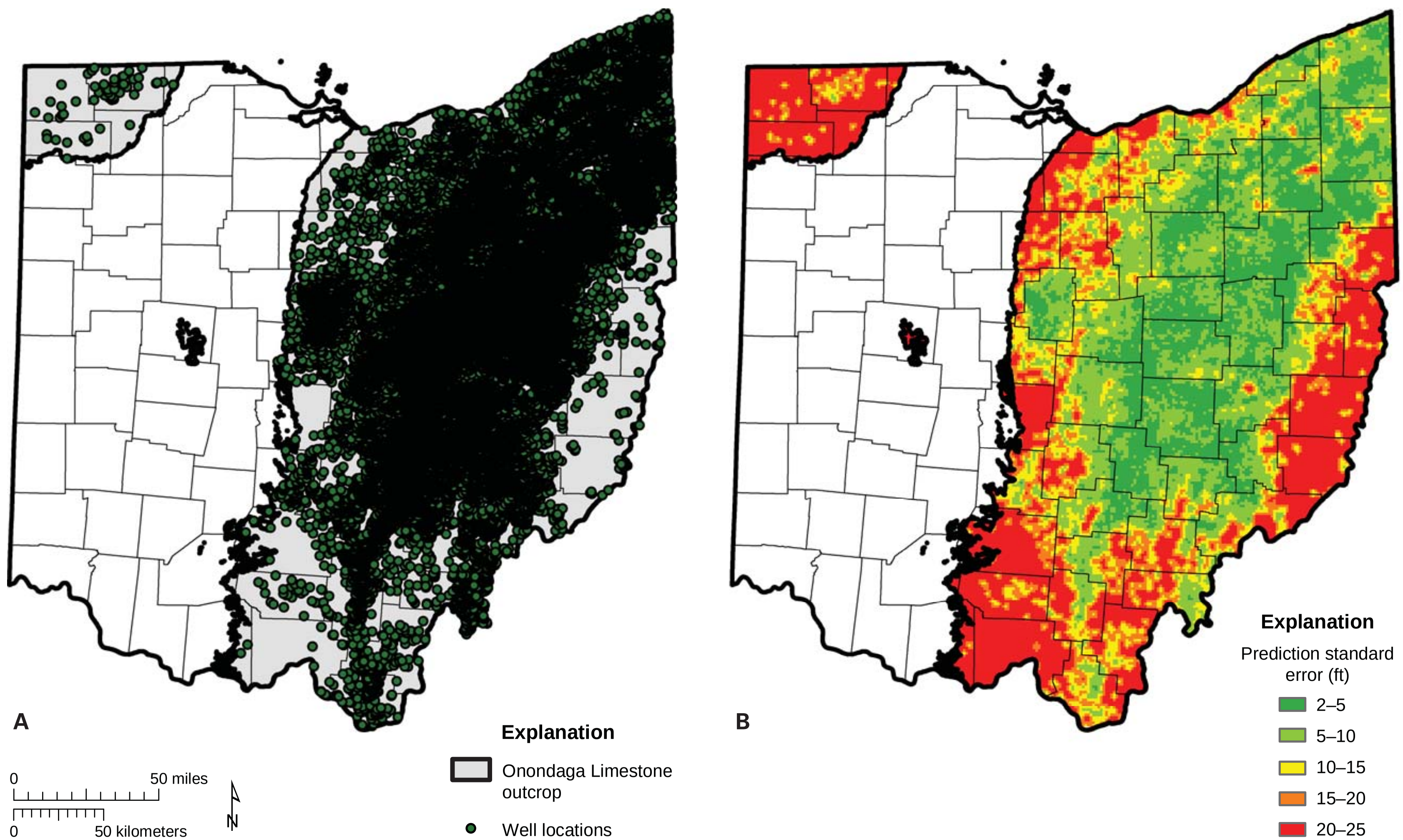

Figure H–2.—(**A**) Distribution of Onondaga Limestone well locations used for kriging. (**B**) Standard error map for Onondaga Limestone kriging results prior to hand editing.

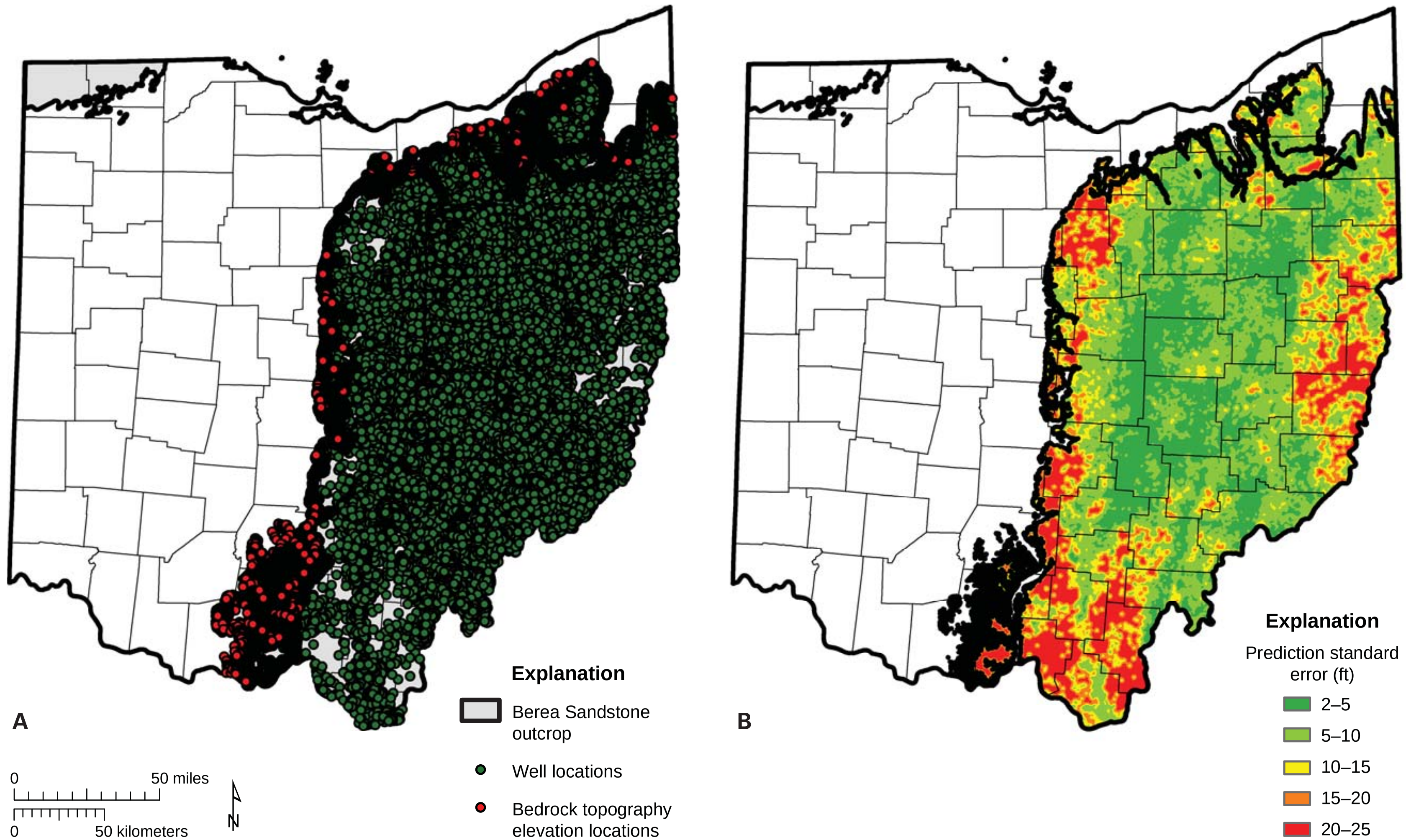

Figure H–3.—(**A**) Distribution of Berea Sandstone well locations used for kriging. The bedrock topography grid (Brockman and others, 2003) was used to sample elevations every 1,500 ft along the outcrop. (**B**) Standard error map for the Berea Sandstone; no compiling of surfaces or hand editing was necessary.

DMS)]: Columbus, Ohio Department of Natural Resources, Division of Geological Survey Digital Data File 2.

Patchen, D.G., Hickman, J.B., Harris, D.C., Drahovzal, J.A., Lake, P.D., Smith, L.B., Nyahay, Richard, Schulze, Rose, Riley, R.A., Baranoski, M.T., Wickstrom, L.H., Laughrey, C.D., Kostelnik, J., Harper, J.A., Avary, K.L., Bocan, J., Hohn, M.E., and McDowell, R., 2006, A Geologic play book for Trenton-Black River Appalachian Basin exploration: West Virginia Univertsity, Final report prepared for U.S. Department of Energy, contract no. DE-FC26-03NT41856, 601 p.

Riley, R.A., 2001, Mapping the deepest underground sources of drinking water in Ohio: Columbus, Ohio Department of Natural Resources, Division of Geological Survey final report to U.S. EPA on 319(h) grant, 5 p., 1 map (scale 1:500,000).

Slucher, E.R., Swinford, E.M., Larsen, G.E., Schumacher, G.A., Shrake, D.L., Rice, C.L., Caudill, M.R., and Rea, R.G., 2006, Bedrock geologic map of Ohio: Columbus, Ohio Department of Natural Resources Division of Geological Survey Map BG-1, scale 1:500,000.

Wickstrom, L.H., Venteris, E.R., Harper, J.A., McDonald, J., Slucher, E.R., Carter, K.M., Greb, S.F., Wells, J.G., Harrison, W.B., III, Nuttall, B.C., Riley, R.A., Drahovzal, J.A., Rupp, J.A., Avary, K.L., Lanham, S., Barnes, D.A., Gupta, N., Baranoski, M.A., Radhakkrishnan, P., Solis, M.P., Baum, G.R., Powers, D., Hohn, M.E., Parris, M.P., McCoy, K., Grammer, G.M., Pool, S., Luckhardt, C., and Kish, P., 2005, Characterization of geologic sequestration opportunities in the MRCSP region—Phase I task report perpared for U.S. DOE cooperative agreement No. DE-PS26-05NT42255: Columbus, Ohio Department of Natural Resources, Division of Geological Survey, OFR 2005-1, 153p.